[2014]

International Journal of Computational Engineering Research (IJCER)

Volume 4, Issue 4, April, 2014

A broad ranging open access journal Fast and efficient online submission Expert peer review, rapid publication High visibility

Editorial Board

Editor-In-Chief

Editorial Committees

Dr. José M. Merigó Lindahl
Qualification: Phd Business Administration
Affiliation: Department of Business Administration, University of Barcelona, Spain

Dr. Mohamed Shokry Nayle
Qualification: Phd, Engineering
Affiliation: faculty of engineering Tanta University Egypt

CONTENTS:

Artificial Neural Network: A Soft Computing Application In Biological Sequence Analysis

Rabi Narayan Behera
Institute of Engineering & Management, Salt Lake, Kolkata-700 091, India

ABSTRACT

The huge amount of available biological expression level data sets all over the world requires automated techniques that help scientists to analyze, understand, and cluster protein structure prediction, multiple alignment of sequences, phylogenic inferences etc. Major hurdles at this point include computational complexity and reliability of the searching algorithms. artificial neural networks a Soft Computing Paradigm widely used in analyzing gene expression level data produced by microarray technology on the genomic scale, sequencing genes on the genomic scale, sequencing proteins and amino acids, etc because of its features such as strong capacity of nonlinear mapping, high accuracy for learning, and good robustness. ANN be trained from examples without the need for a thorough understanding of the task in hand, and able to show surprising generalization performance and predicting power In this paper we review some of the artificial neural networks and related pattern recognition techniques that have been used in this area.

General Terms: *Artificial Neural Networks, Architectures, Learning Algorithms, Topologies, Biological Sequence.*

I. INTRODUCTION

Advancement in the genomics arena like The Human Genome Project (HGP), Microarray Data Analysis can produce large amounts of expression level data by parallel processing. Microarray Data Analysis aims to measure mRNA levels in particular cells or tissues for many genes at once that relies on the hybridization properties of nucleic acids *on a genomic scale*. Microarrays have given a new direction towards the study of genome by allowing researchers to study the expression of thousands of genes simultaneously for the first time. It is being predicted that this is essential to understanding the role of genes in various biological functions.

The action of discovering a motif (a short DNA or protein sequence) of gene expression is closely related to correlating sequences of genes to specific biological functions, helps in understanding the role of genes in biological functions.

The most challenging area of Computational Biology is to study thousands of genes across diverse conditions simultaneously. New computational and data mining techniques need to be developed for low-cost, low precision (approximate), good solutions in order to properly comprehend and interpret expression.

Gene Expression Analysis includes Differential analysis/marker selection for searching genes that are differentially expressed in distinct phenotypes, Class prediction (supervised learning), Class discovery (unsupervised learning), Pathway analysis(search for sets of genes differentially expressed in distinct phenotypes) and data conversion tasks, such as filtering and normalizing, which are standard prerequisites for genomic data analysis.

Artificial Neural Network (ANNs) inspired by Biological Neural Network (BNNs) and Statistical Learning are widely used pattern recognition techniques in microarray data analysis. ANN can be trained to identify the relevant genes that are used to make this distinction which is also distinguishing between *complementary DNA* (cDNA) microarray data of two types of colorectal lesions.

We have surveyed a number of Artificial Neural Network (ANNs), some important learning algorithms and related techniques that help (have been used) in discovering or correlating patterns of expression data (e.g. microarray data) to biological function. We have given a chronological survey of calculating number of hidden neurons in neural network. In this paper you will find a summary of our survey along with basic concepts of ANNs and some important learning algorithms.

Artificial Neural Networks (ANNs) is unlike traditional computing (algorithmic approach) which require prior instruction to solve a problem, belong to the adaptive class of techniques in the *machine learning* arena. ANNS are used as a solution to various nonlinear complex problems; however, their success as an intelligent pattern recognition methodology has been most prominently advertised.

ANNs were inspired by the biological neural networks, whose performance is analogous to the most basic functions of human brains. Most models of ANNs are organized in the form of a number of processing units (also called artificial neurons, or simply neurons [1]), and a number of weighted connections (artificial synapses) between the neurons.

Though artificial neural networks are not an exact copy of biological human brain, it is important to begin with understanding fundamental concepts of Organization of the Nervous System and Brain.

Nervous System:

The human nervous system can be broken down into three stages that may be represented in block diagram form as:

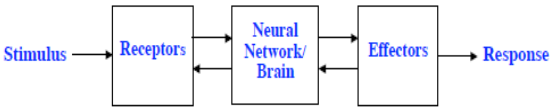

The receptors collect information from the environment (e.g. photons on the retina), The effectors generate interactions with the environment (e.g. activate muscles), The flow of information/activation is represented by arrows – feedforward and feedback. Naturally, this paper will be primarily concerned with how the neural network in the middle works.

Basic Components of Biological Neurons:

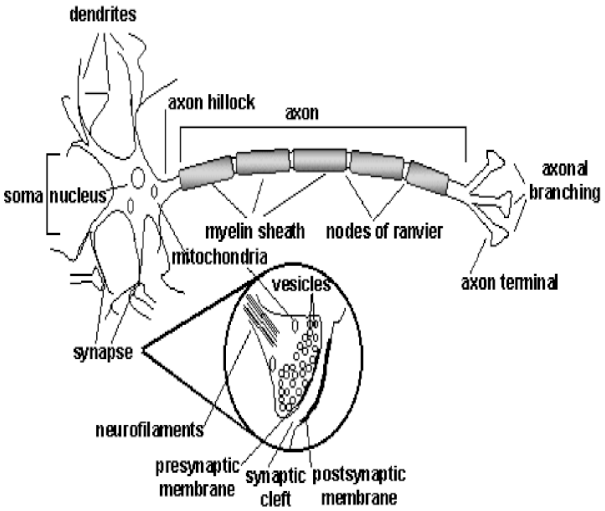

The majority of ***neurons*** encode their activations or outputs as a series of brief electrical pulses (i.e. spikes or action potentials). When sufficient input is received (i.e. a threshold is exceeded), the neuron generates an action potential or 'spike' (i.e. it 'fires').

That action potential is transmitted along the axon to other neurons, or to structures outside the nervous systems (e.g., muscles).

The neuron's ***cell body (soma)*** processes the incoming activations and converts them into output activations by summation of incoming signals (spatially and temporally).

The neuron's ***nucleus*** contains the genetic material in the form of DNA. This exists in most types of cells, not just neurons.

Dendrites are fibres which emanate from the cell body and provide the receptive zones that receive activation from other neurons. Signals from connected neurons are collected by the dendrites.

Axons are fibres acting as transmission lines that send activation to other neurons.

The junctions that allow signal transmission between the axons and dendrites are called ***synapses***. The process of transmission is by diffusion of chemicals called ***neurotransmitters*** across the synaptic cleft.

If sufficient input is not received (i.e. the threshold is not exceeded), the inputs quickly decay and no action potential is generated.

Timing is clearly important – input signals must arrive together strong inputs will generate more action potentials per unit time.

The process of building an ANN, similar to its biological inspiration, involves a learning episode (also called training). During learning episode, the Network requires a massive number of associative mappings to observe a sequence of recorded data, and adjusts the strength of its synapses according to a learning algorithm and based on the observed data, so that a particular input leads to a specific target output.

Training a neural network is the process of finding a set of weight and bias values so that for a given set of inputs, the outputs produced by the neural network are very close to some target values.

A neural network can be thought of as a complicated mathematical function that has various constants called weights and biases, which must be determined. The process of finding the set of weights and bias values that best match your existing data is called training the neural network. There are many ways to train a neural network.

Learning algorithms are generally divided into two types, supervised and unsupervised.

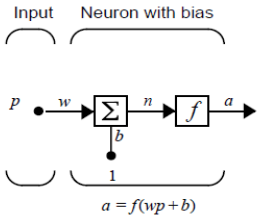

The scalar input *p* is transmitted through a connection that multiplies its strength by the scalar weight *w*, to form the product *wp*, again a scalar. *b* is a bias value allows you to shift the activation function to the left or right**,** which may be critical for successful learning. The activation function of a node defines the output of that node given an input or set of inputs. Neurons are "switches" that output a "1" when they are sufficiently Activated, and '0' when not. Here the weighted input *wp* + *b* is the argument of the activation function *f*, typically a step function or a sigmoid function, which takes the argument *n* and produces the scalar output *a*. The bias is much like a weight, except that it has a constant input of 1. [2]

Depending upon the problem variety of Activation function is used

1. Linear Activation function like step function
2. Nonlinear Activation function like sigmoid function

Using a nonlinear function which approximates a linear threshold allows a network to approximate nonlinear functions using only small number of nodes.

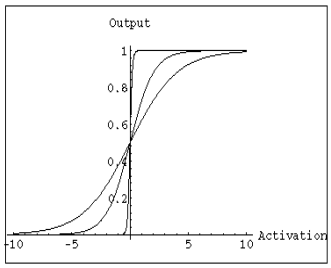

A list of common transfer function (activation functions) and their names can be found in following Table

Activation Functions	
Name	**Formula**
Identity	$f(x) = x$
Sigmoid	$f(x) = \frac{1}{1+e^{-x}}$
Tanh	$f(x) = \frac{e^{x}-e^{-x}}{e^{x}+e^{-x}}$
Step	$f(x) = \begin{matrix} -1 & if\ x < 0 \\ 1 & if\ x \geq 0 \end{matrix}$

Training the network nothing but adjusting both *w* and *b* scalar parameters of the neuron itself so that the cost functions is minimized and to exhibits some desired or interesting behavior.

Cost function:

$\hat{C} = (\sum (x_i - x_i')^2) / N$
Where x_i is desired output and x_i's are the output of the neural network.
The supervised algorithms require labelled number of hidden neurons in neural network number of hidden neurons in neural network training data and external agent for supervision. In other words, they require more a prior knowledge about the training set.

The most important, and attractive, feature of ANNs is their capability of learning (generalizing) from example (Extracting knowledge from data) and adapt dynamically to the changing system. ANNs can do this without any pre-specified rules that define intelligence or represent an expert's knowledge. This feature makes ANNs a very popular choice for gene expression analysis and sequencing.

ANNs can select its own relevant input variable from the available data, and the model is developed subsequently which can in turn greatly increase the expert's knowledge and understanding of the problem.

In this paper, we discuss some important ANN like Feedforward Neural Networks and Backpropagation Neural Networks.

Feedforward Neural Network – The feedforward neural network consist of a series of layers. In this network the information moves in only one direction — forwards: From the input layer data goes through the hidden layer (if any) and to the output layer. There are no cycles or loops in the network. Any finite input-output mapping is possible with one hidden layer and enough neurons in it.

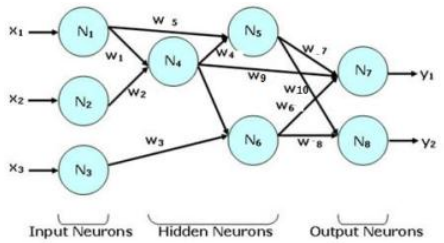

The network consists of **neurons** distributed in three different layers, each of which computes a function (called an **activation function**) of the inputs carried on the in-edges (edges pointing into the neuron) and sends the output on its out-edges (edges pointing out of the neuron). The inputs and outputs are weighed by **weights** W_i and shifted by **bias** factor specific to each neuron. It has been shown that for certain neural network topologies, any continuous function can be accurately approximated by some set of weights and biases. Therefore, we would like to have an algorithm which when given a function *f*, learns a set of weights and biases which accurately approximate the function. For **feed-forward neural networks** (artificial neural networks where the topology graph does not contain any directed cycles), the back-propagation algorithm described later does exactly that.

Output of a single neuron can be calculated as follows

Output = A ($\sum W_n * I_n$ + bias) where A is the activation function of the neuron, W_n is the weight of the n^{th} in-edge, In is the input carried across the n^{th} in-edge, and bias is the bias of the neuron.

Weight of a neuron can be calculated from the training data a pairs of sets of inputs and outputs (X_i,Y_i) where X_i is the input to all input neurons and Y_i is the output of the neural network after running the inputs in X_i.

The entire training dataset is D=Union $((X_i, Y_i))$

We need to find the weights of edges and biases of neurons in the network which minimize the sum of squares error (SSE) of the training data. The **SSE** of the network with respect to the training data D is computed using the formula,

$$SSE(D) = Sum((Y_i - Z_i)^2)$$

Feed-forward networks cannot perform temporal computation. More complex networks with internal feedback paths are required for temporal behavior.

Back propagation neural networks

The weights and biases are initially assigned to a random continuous (real) value between -1 and 1. The algorithm trains the neural network incrementally, meaning that each instance is considered independently, and after considering a training instance, the weights and biases are updated before considering another one. The update is done in a way that performs a gradient descent minimization of the error with respect to the weights and biases.

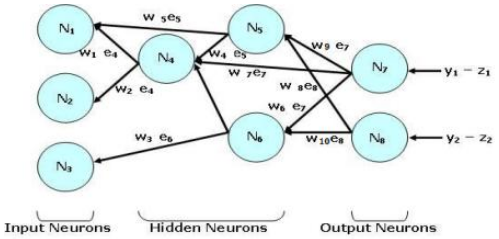

The learning algorithm can be split into three phases for an instance (X_i, Y_i) for i=1,2,3,….

Calculate Output - Calculate Z_i, the output of the network for the training instance's input set X_i.

Calculate Blame - Y_i is the desired value for Z_i, so when they are different, there is some error. From this error, we wish to compute a blame value for each neuron. Blames will later be used to decide by how much to adjust weights and biases. The blames are just the *linear* error. Blame can be shared with the help of Delta Rule.

$$\Delta W_{ji} = \eta * \delta_j * x_i$$

$$\delta_j = (t_j - y_j) * f'(h_j)$$

Where η is the learning rate of the neural network, t_j and y_j are targeted and actual output of the j^{th} neuron, h_j is the weighted sum of the neuron's inputs and f' is the derivate of the activation function f.

Problem with Multilayer Network is that we don't know the targeted output value for the Hidden layer neurons.

This can be solved by a trick:

$$\delta_i = \sum (\delta_k * W_{ki}) * f'(h_i)$$

The first factor in parenthesis involving the sum over k is an approximation to $(t_i - a_i)$ for the hidden layers when we don't know t_i.

Calculate Blame for Output Neurons - The blame of each output neuron is calculated as $Y_i - Z_i$. The blame should be proportional to partial derivatives for the gradient to minimize the sum *squared* error of the whole network.

Calculate Blame for Input and Hidden Neurons - The blame for an input or hidden neuron is calculated in terms of the blames of its out-neurons (the ones that it is pointing to). Because of this dependency, the blames need to be calculated in a topologically sorted order of the reverse of the network topology graph. This is similar to the order in which the outputs of neurons are calculated except that the topology graph must first be reversed before topologically sorting. The formula for the blame of an input or hidden neuron is $\sum W_k * E_k$ where E_k is the

blame of an out-neuron and W_k is the weight of the edge that connects to the out-neuron. This step of propagating the error backwards is why the learning algorithm is called back-propagation.

Adjust Weights and Biases – This last step performs the actual gradient descent by adjusting the weights with the formula: $W_{ij} = W_{ij} + r * E_j * A_j'(I_j) * O_i$ where r is the learning rate, E_j is the blame of neuron j, Aj' is the derivative of neuron j's activation function, I_j is the input fed to neuron j during calculation of the output in the first step, and O_i is the output of neuron i during the first step. The biases are similarly adjusted using the formula: $bias\_i = bias\_i + r*E_i$.

Learning completes with the all training instances are run. To achieve better accuracy, we may wish to run the training data multiple times through the learning algorithm without over fitting.

Neural networks need a lot of parameters like NN architecture, number of hidden neurons in hidden layer, activation function, inputs, and updating of weights etc and many of these parameters can significantly affect the accuracy, stability and runtime of neural networks. The backpropagation algorithm, one can only expect the algorithm to have good performance with a finite training set.

A fundamental question that is often raised in the applications of neural networks is *"how large does the net**work** have to be to perform a desired task?".* Answers to this question are directly related to the capability of neural networks, and should be given independently of the learning algorithms employed.

Number of Hidden Neurons

It is crucial to pick a proper neural network topology from infinite set of directed acyclic graphs before training with some restriction is that the number of input nodes must match the number of inputs to the function and the number of output nodes must match the number of outputs of the function. But we are free to choose any topology for the hidden neurons as long as there is a path from each input neuron to some output neuron and vice versa.

The fixing of the hidden neuron is an important for the designing of Neural Network model. The random selection of hidden neuron may cause over fitting and under fitting problem in the network. Several researchers tried and proposed many approach for fixing hidden neuron. The survey has been made to find the number of hidden neurons in neural network is and described in a chronological manner.

Year	Method/Concept	Reference
1991	exactly solves the multilayer neural network training problem, for any arbitrary training set with bounds on the size of a multilayer neural network to exactly implement an arbitrary training set;[3]	Michael A. Sartori and Panos J. Antsaklis
	Bounds on the Number of Hidden Neurons in Multilayer Perceptrons	Shih-Chi Huang and Yih-Fang Huang
1993	Proposed two parallel hyper plane methods for finding the number of hidden neurons. The 2^n / 3 hidden neurons are sufficient for this design of the network.[4]	Arai
1995	Investigated the estimation theory to find the number of hidden units in the higher order feedforward neural network. This theory is applied to the time series prediction. The determination of an optimal number of hidden neurons is obtained when the sufficient number of hidden neurons is assumed. According to the estimation theory, the sufficient number of hidden units in the second-order neural network and the first-order neural networks are 4 and 7, respectively. The simulation results show that the second-order neural network is better than the first-order in training convergence. According to that, the network with few nodes in the hidden layer will not be powerful for most applications. The drawback is long training and testing time.[5]	Li et al.
1996	presented another method to find an optimal number of hidden units. The drawback is that there is no guarantee that the network with a given number of hidden units will find the correct weights. According to the statistical behaviours of the output of the hidden units, if a network has large number of hidden nodes, a linear	Hagiwara

	relationship is obtained in the hidden nodes.[6]	
1997	Developed a method to fix hidden neuron with negligible error based on Akaike's information criteria. The number of hidden neurons in three layer neural network is N -1 and four-layer neural network is N/2 + 3 where N is the input-target relation[7]	Tamura and Tateishi
1998	Proposed a statistical estimation of number of hidden neurons. The merits are speed learning. The number of hidden neurons mainly depends on the output error. The estimation theory is constructed by adding hidden neurons one by one. The number of hidden neurons is formulated as N_h = K Log || P_cZ||/Log S, where S is total number of candidates that are randomly searched for optimum hidden unit c is allowable error.[8]	Fujita
1998	Upper bounds on the number of hidden neurons in feed forward networks with arbitrary bounded nonlinear activation functions- This paper used the fact what Sartori and Antsaklis pointed out in 1991, the sigmoid function is not necessary to be used as non-linearity of the neurons and . Huang and Babri showed that standard single-hidden layer feed forward networks (SLFN) with not more than N hidden neurons and with any bounded non linear activation function which has a limit at one infinity can learn these N distinct samples with zero error.	Guang-Bin Huang, Haroon A. Babri
1999	Presented a method to determine the number of hidden units which are applied in the prediction of cancer cells. Normally, training starts with many hidden units and then prune the network once it has trained. However pruning does not always improve generalization. The initial weights for input to hidden layer and the number of hidden units are determined automatically. The demerit is no optimal solution.[9]	Keeni et al
2001	Presented a statistical approach to find the optimal number of hidden units in prediction applications. The minimal errors are obtained by the increase of number of hidden units. Md. Islam and Murase proposed a large number of hidden nodes in weight freezing of single hidden layer networks. The generalization ability of network may be degraded when the number of hidden nodes(N_h) is large because N^{th} hidden node may have some spurious connections.[10]	Onoda, Md. Islam and Murase
2003	Implemented a set covering algorithm (SCA) in three-layer neural network. The SCA is based on unit sphere covering (USC) of hamming space. This methodology is based on the number of inputs. Theoretically the number of hidden neurons is estimated by random search. The output error decreases with N_h being added. The N_h is significant in characterizing the performance of the network. The number of hidden neurons should not be too large for heuristic learning system. The N_h found in set covering algorithm is 3L/2 hidden neurons where L is the number of unit spheres contained in N dimensional hidden space[11]	Zhang et al
2003	developed the model for learning and storage capacity of two-hidden-layer feedforward network. In 2003, Huang [12] formulated the following: in single hidden layer and in two hidden layer.	Huang
2004	A three-layer neural network (NN) with novel adaptive architecture has been developed. The hidden layer of the network consists of slabs of single neuron models, where neurons within a slab—but not between slabs— have the same type of activation function. The network activation functions in all three layers have adaptable parameters.	Panayiota Poirazi, Costas Neocleous, Costantinos S. Pattichis
2006	developed a separate learning algorithm which includes a deterministic and heuristic approach. In this algorithm, hidden-to-output and input-to-hidden nodes are separately trained. It solved the local minima in two-layered feedforward network. The achievement is best convergence speed[14]	Choi et al.
2006	Estimating the Number of Hidden Neurons in a Feedforward Network Using the Singular Value Decomposition - to quantify the significance of increasing the number of neurons in the hidden layer of a feedforward neural network architecture using the singular value decomposition (SVD).[15]	Eu Jin Teoh, Cheng Xiang, Kay Chen Tan

2007	Optimizing number of hidden neurons in neural networks - A method is proposed using, quantitative standard based on the Signal to Noise Ratio Figure (SNRF) to detect over fitting automatically using the training error only, to optimize the number of hidden neurons in Neural Network to avoid over fitting problem.[16]	Yinyin Liu, Janusz A. Starzyk, Zhen Zhu
2008	presented the lower bound on the number of hidden neurons. The number of hidden neurons is $N_h=q^n$ where q is valued upper bound function. The calculated values represent that the lower bound is tighter than the ones that has existed. The lower and upper bound on the number of hidden neurons help to design constructive learning algorithms. The lower bound can accelerate the learning speed, and the upper bound gives the stopping condition of constructive learning algorithms. It can be applied to the design of constructive learning algorithm with training set N numbers.[17]	Jiang et al
2009	investigated the effect of learning stability and hidden neuron in neural network. The simulation results show that the hidden output connection weight becomes small as number of hidden neurons N_h becomes large. This is implemented in random number mapping problems. The formula for hidden nodes is $N_h=\sqrt{N_iN_0}$ where N_i is the input neuron and N_0 is the output neuron. Since neural network has several assumptions which are given before starting the discussion to prevent divergent. In unstable models, number of hidden neurons becomes too large or too small. A trade-off is formed that if the number of hidden neurons becomes too large, output of neurons becomes unstable, and if the number of hidden neurons becomes too small, the hidden neurons becomes unstable again.[18]	Shibata and Ikeda
2009	Bernoulli Neural Network with Weights Directly Determined and with the Number of Hidden- Layer Neurons Automatically Determined Based upon polynomial interpolation and approximation theory, a special type of feedforward neural-network is constructed in this paper with hidden-layer neurons activated by Bernoulli polynomials to overcome the drawback of the conventional Back propagation neural network algorithm such as slow convergence and local minima existence. A weight detection algorithm is also proposed which detects weights of the neural network without the lengthy back propagation training procedures. More over a Structure Automatic Determination algorithm is proposed which can obtain the optimal number of hidden layers neurons in order of achieving the highest learning accuracy.[19]	Yunong Zhang, Gongqin Ruan
2010	proposed a technique to find the number of hidden neurons in MLP network using coarse-to-fine search technique which is applied in skin detection. This technique includes binary search and sequential search. This implementation is trained by 30 networks and searched for lowest mean squared error. The sequential search is performed in order to find the best number of hidden neurons[20]	Doukim et al.
2010	proposed the learning algorithms for determination of number of hidden neurons.[21]	Wu and Hong
2011	Panchal proposed a methodology to analyze the behavior of MLP. The number of hidden layers is inversely proportional to the minimal error.[22]	Panchal et al.
2011	Improving the character reorganization efficiency of feed forward BP Neural Network- Presented a method for improvement of character recognition capability of feed-forward back-propagation neural network by using one , two and three layers. Also it has been shown that with more hidden layers and modified momentum term a soft real time system can be introduced where performance is more critical. [23]	Amit Choudhary , Rahul Rishi
2011	A Clustering Based Method to Stipulate the Number of Hidden Neurons of MLP Neural Networks: Applications in Pattern Recognition we propose a clustering based method to state the number of hidden neurons that can produce good classification error rate. Our cluster based method uses much less CPU time consuming than method[24]	m.r. Silvestre, s.m. Oikawa2, f.h.t. Vieira, l.l. Ling
2012	Approximating Number of Hidden layer neurons in Multiple Hidden Layer BPNN Architecture --	Karsoliya Saurabh

	The process of deciding the number of hidden layers and number of neurons in each hidden layer is still confusing. In this paper, an survey is made in order to resolved the problem of number of neurons in each hidden layer and the number of hidden layers required.[25]	
2012	developed a method used in proper NN architectures. The advantages are the absence of trial-and-error method and preservation of the generalization ability. The three networks MLP, bridged MLP, and fully connected cascaded network are used. The implemented formula: as follows, $N_h=N+1$ for MLP Network, $N_h=2N+1$ for bridged MLP Network and $N_h=2^n-1$ for fully connected cascade NN. The experimental results show that the successive rate decreases with increasing parity number. The successive rate increases with number of neurons used. The result is obtained with 85% accuracy.[26]	Hunter et al

Some sources claim that one hidden layer of neurons between the input nodes and output nodes are enough to accurately approximate any continuous function.

This is an extremely important finding because the computational complexity of the learning algorithm increases quadratically with the number of neurons in the network and this experiment shows that only very few neurons are necessary for this dataset.

Comparison to Other Classifiers: Neural networks are even a good alternative to other classification algorithms such as decision trees, Bayesian network, Inductive logic programming and naïve Bayes. The chart below shows the classification accuracy of neural networks compared to that of decision trees and naïve Bayes. It seems that neural networks perform about the same as those two classifiers and often times produce a little better results than naïve Bayes. Neural networks Can model more arbitrary functions (nonlinear interactions, etc.) and therefore might be more accurate, provided there is enough training data. But it can be prone to over-fitting as well.

Layered, feed-forward, backpropagation neural networks: These are a class of ANNs whose neurons are organized in layers. The layers are normally fully connected, meaning that each element (neuron) of a layer is connected to each element of the next layer. However, self-organizing varieties also exist in which a network starts either with a minimal number of synaptic connections between the layers and adds to the number as training progresses (*constructive*), or starts as a fully connected network and prunes connections based on the data observed in training (*destructive*).
Backpropagation [27] is a learning algorithm that, in its original version, belongs to the gradient descent optimization methods [28]. The combination of backpropagation learning algorithm and the feed-forward, layered networks provide the most popular type of ANNS. These ANNS have been applied to virtually all pattern recognition problems, and are typically the first networks tried on a new problem. The reason for this is the simplicity of the algorithm, and the vast body of research that has studied these networks. As such, in sequencing, many researchers have also used this type of network as a first line of attack.
Examples can be mentioned in [29,30]. In [29] Wu has developed a system called gene classification artificial neural system (GenCANS), which is based on a three layered, feed-forward backpropagation network. GenCANS was designed to "classify new (unknown) sequences into predefined (known) classes. It involves two steps, sequence encoding and neural network classification, to map molecular sequences (input) into gene families (output)". In [30] the same type of network has been used to perform rapid searches for sequences of proteins.

Other examples can be mentioned in Snyder and Stormo's work in designing a system called *GeneParser*.[31] Here authors experimented with two variations of a single layer network (one fully connected, and one partially connected with an activation bios added to some inputs), as well as a partially connected two-layer network. The authors use dynamic programming as the learning algorithm in order to train the system for protein sequencing.
1 ANNS were the first group of machine learning algorithm to be used on a biological pattern recognition problem. [32]
2 Distinguish between sporadic colorectal adenomas and cancers (SAC), and inflammatory bowel disease (IBD)-associated dysplasias and cancers.

Self-organizing neural networks: These networks are a very large class of neural networks whose structure (number of neurons, number of synaptic connections, number of modules, or number of layers) changes during learning based on the observed data. There are two classes of this type of networks: destructive and constructive. Destructive networks are initially a fully connected topology and the learning algorithm prunes synapses (sometime entire neurons, modules, or layers) based on the observed data. The final remaining network after learning is complete, usually is a sparsely connected network. Constructive algorithms start with a minimally connected network, and gradually add synapses (neurons, modules, or layers) as training progresses, in order to accommodate for the complexity of the task at hand.
Self-organizing networks divide into some major and very well known groups. Bellow we summarize the application some of these major groups in sequencing and expression level data analys is **Self-Organizing Map**: A self-organizing map (SOM) [33] is a type of neural network approach first proposed by Kohonen [34]. SOMs have been used as a divisive clustering approach in many areas including genomics. Several groups have used SOMs to discover patterns in gene expression data. Among these Toronen et al. [35], Golub et al. [36], and Tamayo et al. [37] can be mentioned. Tamayo and colleagues [37] use self-organizing maps to explore patterns of gene expression generated using Affymetrix arrays, and provide the GENECLUSTER implementation of SOMs. Tamayo and his colleagues explain the implementation of SOM for expression level data as follows: **"**An SOM has a set of nodes with a simple topology and a distance function on the nodes. Nodes are iteratively mapped into k-dimensional "gene expression space" (in which the i^{th} coordinate represents the expression level in the i^{th} sample)" [38]. A SOM assigns genes to a series of partitions on the basis of the similarity of their expression vectors to reference vectors that are defined for each partition. The summary of the basic SOM algorithm is perhaps best described in Quackenbush's review [39]: "First, random vectors are constructed and assigned to each partition. Second, a gene is picked at random and, using a selected distance metric, the reference vector that is closest to the gene is identified. Third, the reference vector is then adjusted so that it is more similar to the vector of the assigned gene. The reference vectors that are nearly on the two-dimensional gird are also adjusted so that they are more similar to the vector of the assigned gene. Fourth, steps 2 and 3 are iterated several thousand times, decreasing the amount by which the reference vectors are adjusted and increasing the stringency used to define closeness in each step. As the process continues, the reference vectors converge to fixed values. Last, the genes are mapped to the relevant partitions depending on the reference vector to which they are most similar"**.**
SOMs, like the *gene shaving* approach[40], have the distinct advantage that they allow a priori knowledge to be included in the clustering process. Tamayo et. al. explain this and other advantages of the SOM approach as follows: "The SOM has a number of features that make them particularly well suited to
clustering and analyzing gene expression patterns. They are ideally suited to exploratory data analysis, allowing one to impose partial structure on the clusters (in contrast to the rigid structure of hierarchical clustering, the strong prior hypotheses used in Bayesian clustering, and the nonstructural of k-means clustering) facilitating easy visualization and interpretation. SOMs have good computational properties and are easy to implement, reasonably fast, and are scalable to large data sets".
The most prominent disadvantage of the SOM approach is that it is difficult to know when to stop the algorithm. If the map is allowed to grow indefinitely, the size of SOM is gradually increased to a point when clearly different sets of expression patterns are identified. Therefore, as with k-means clustering, the user has to rely on some other source of information, such as PCA, to determine the number of clusters that best represents the available data. For this reason, Sasik and his colleagues believe that "SOM, as implemented by Tamayo et al is essentially a restricted version of k-means: Here, the *k* clusters are linked by some arbitrary user-imposed topological constraints (e.g. a 3 x 2 grid), and as such suffers from all of the problems mentioned above for k-means (and more), except that the constraints expedites the optimization process". [37]
There are many varieties to SOM, among which the self-organizing feature maps (SOFM) should be mentioned. The *growing cell structure* (GCS) [41] is another derivative of SOFM. It is a self organizing and incremental (constructive) neural learning approach. The unsupervised variety of GCS was used by Azuaje [42] for discovery of gene expression patterns in B-cell lymphoma. Using cDNA microarray expression data, GCS was able to "identify normal and diffuse large B-cell lymphoma (DLBCL) patients. Furthermore, it distinguishes patients with molecularly distinct types of DLBCL without previous knowledge of those subclasses".

Self-organizing trees*:* Self-organizing trees are normally constructive neural network methods that develop into a tree (usually binary tree) topology during learning. Among examples of these networks applied to sequencing the work of Dopazo et al. [43], Wang et al. [44,45], and Herrero et al. [46] can be mentioned.
Dopazo and Carazo introduce the self-organizing tree algorithm (SOTA). [43] SOTA is a hierarchical neural network that grows into a binary tree topology. For this reason SOTA can be considered a hierarchical clustering algorithm [41]. SOTA is based on Kohonen's SOM discussed above and Fritzke's growing cell [34]. SOTA was originally designed to analyze pre-aligned sequences of genes (polygenetic reconstruction).

Wang and colleagues extended that work in [43,44] in order to classify protein sequences: "(SOTA) is now adapted to be able to analyze patterns associated to the frequency of residues along a sequence, such as protein dipeptide composition and other n-gram compositions". In [46], Herrero and colleagues demonstrate the application of SOTA to Microarray expression data. The show that SOTA's performance is superior to that of classical hierarchical clustering techniques. Among the advantages of SOTA as compared to hierarchical cluster algorithms, one can mention its time complexity, and its top-to-bottom hierarchical approach. SOTA's runtimes are approximately linear with the number of items to be classified, making it suitable for large datasets. Also, because SOTA forms higher clusters in the hierarchy before forming the lower clusters, it can be stopped at any level of hierarchy and still produce meaningful intermediate results.

There are many other types of self-organizing trees that for space considerations cannot be mentioned here.

SOTA was only chosen here to give a brief introduction to these types of networks, and not because we believe that these are the most common types of self-organizing trees.

***ART* and its derivatives:** *Adaptive Resonance Theory* was introduced by Stephen Grossberg [47] in

1976. Networks designed based on ART are unsupervised and self-organizing, and only learn in the socalled "resonant" state. ART can form (stable) clusters of arbitrary sequences of input patterns by learning (entering resonant states) and self-organizing. Since the inception, many derivatives of ART have emerged. Among these *ART-1* (the binary version of ART; forms clusters of binary input data) [48], *ART-2*(analog version of ART) [49], *ART-2A* (fast version of ART-2) [50], *ART-3* (includes "chemical transmitters" to control the search process in a hierarchical ART structure) [50], *ARTMAP* (supervised version of ART) [51] can be mentioned. Many hybrid varieties such as *Fuzzy–ART* [52], *Fuzzy-ARTMAP* (supervised Fuzzy-ART) [52] and *simplified Fuzzy-ARTMAP* (SFAM) [51] have also been developed.

The ART family of networks has a broad application in virtually all areas of pattern recognition. As such, they have also been applied in biological sequencing problems. In general, in problem settings where the number of clusters is not previously known, researchers tend to use unsupervised ART, where when number of clusters is known a priori, usually the supervised version, ARTMAP, is used.

Among the unsupervised implementations, the work of Tomida et al. [53] should be mentioned. Here the authors used Fuzzy ART for expression level data analysis. This study is significant in that it compares results of Fuzzy ART with those of hierarchical clustering, k-mean clustering, and SOMs in analyzing and sequencing expression level data on the genomic scale. In this study the authors consider a two dimensional problem space in which the first dimension is the expression level and the second dimension is time, in order to consider the variation of expression levels in time. In this study, the authors report the lowest gap index3 among the four algorithms considered for Fuzzy ART. In terms of robustness of clustering results, the authors report a robustness of 82.2% for Fuzzy ART versus 71.1%, 44.4% and 46.7%, for hierarchical clustering, *k*-means clustering, and SOMs respectively. As a result the authorsconclude that Fuzzy ART also performs best in noisy data.

Among supervised implementations, Azuaje's use of SFAM in cDNA data analysis with the purpose of discovery of gene function in cancer can be mentioned. [54] In this study the authors use a data set generated for a previous study [18] using SOFM. Here the authors were able to also distinguish between classes of cancer using SFAM instead of SOFM (reported earlier in this paper).

Other neural network techniques

***Molecular computers* and *molecular neural networks*:** The idea of molecular and cellular computing dates back to the late 1950's when Richard Feynman delivered his famous paper describing "sub-microscopic" computers. He suggested that living cells and molecules could be thought of as potential computational components. Along the same lines, a revolutionary form of computing was developed by Leonard

Aldeman in 1994, when he announced that he had been able to solve a small instance of a computationally intractable problem using a small vial of DNA. [55] Aldeman had accomplished this by representing information as sequences of bases in DNA molecules. He then showed how to exploit the self assembly property of DNA and use DNA-manipulation techniques to implement a simple but massively parallel random search.

As a result, it has been suggested byMills [56] (among others) that a "DNA computer using cDNA as input might be ideal for clinical cell discrimination". In particular, Mills recommends the neural networks version of Aldeman's DNA computing scheme developed also by Mills and his colleagues [56] to the classification and sequencing tasks involved in expression level profiling. Mills reports in [56] that his "preliminary experimental results suggest that expression profiling should be feasible using a DNA neural network that acts directly on cDNA".

The DNA neural networks are the most recent and innovative ANN solution suggested for expression data profiling and sequencing. Its massively parallel nature offers exceedingly fast computation. The method presents high potential in various aspects of the solution that it offers and should offer breakthrough advancement to the field.

Bayesian Neural Networks: There are a number of recent networks that have been suggested as solutions for sequencing and expression data analysis. For instance, Bayesian neural networks (BNNs), are another technique that has been recently used for gene expression analysis. Liang et al. [57] have used the BNNs with structural learning for exploring microarray data in gene expressions. The BNNs are an important addition to the host of ANN solutions that have been offered to the problem at hand, as they represent a
large group of hybrid ANNs that combine classical ANNs with statistical classification and prediction theories.

CONCLUSION

There are a number of ANN solutions that have been offered to the problem of biological sequencing and expression data analysis. While many researchers have applied "classical" ANN solutions to the problem and are reporting favorable results as compared to non-adaptive counter parts, others have suggested or developed pioneering and revolutionary ANNs. Many of these techniques offer feasible solutions to the
above mentioned problems, while some also offer significant speedup in achieving the solutions. We believe that the performance of a technique should ultimately be measured in the biological soundness and relevance of its results. As such, we believe that techniques that allow the incorporation of a priori biological knowledge show greater potential.

3 In this study, the authors use gap index to "evaluate the similarity of profiles as area between each profile and average profile during temporal phase". This review represents only a small part of the research being conducted in the area, and only is meant as a complementary/continuation of the survey that others have conducted in this area. It should in no way to be taken as a complete survey of all algorithms. If not for any other reason, for the reason of limited space, some significant developments in the area had to be left out. Furthermore, new techniques and algorithm are being proposed for microarray data analysis on a daily basis, making survey articles such as this highly time dependent.

REFERENCES

[1] McCulloch, W.S. and Pitts, W. 1943. A logical calculus of the ideas immanent in nervous activity. Bulletin of Mathematical Biophysics. 5: 115-133.

[2] MH Beale, 1992, Neural Network Toolbox - MathWorks.

[3] M. A. Sartori and P. J. Antsaklis, "A simple method to derive bounds on the size and to train multilayer neural networks," IEEE Transactions on Neural Networks, vol. 2, no. 4, pp. 467–471, 1991.

[4] M. Arai, "Bounds on the number of hidden units in binary-valued three-layer neural networks," Neural Networks, vol. 6, no. 6, pp. 855–860, 1993.

[5] J.Y. Li, T. W. S. Chow, and Y. L. Yu, "Estimation theory and optimization algorithm for the number of hidden units in the higher-order feedforward neural network," in Proceedings of the IEEE International Conference on Neural Networks, vol. 3, pp. 1229–1233, December 1995.

[6] M. Hagiwara, "A simple and effective method for removal of hidden units and weights," Neurocomputing, vol. 6, no. 2, pp. 207–218, 1994.

[7] S. Tamura and M. Tateishi, "Capabilities of a four-layered feedforward neural network: four layers versus three," IEEE Transactions on Neural Networks, vol. 8, no. 2, pp. 251–255, 1997.

[8] O. Fujita, "Statistical estimation of the number of hidden units for feedforward neural networks," Neural Networks, vol. 11, no. 5, pp. 851–859, 1998.

[9] K.Keeni, K. Nakayama, and H. Shimodaira, "Estimation of initial weights and hidden units for fast learning of multi-layer neural networks for pattern classification," in Proceedings of the International Joint Conference on Neural Networks (IJCNN '99), vol. 3, pp. 1652–1656, IEEE, July 1999.

[10] T. Onoda, "Neural network information criterion for the optimal number of hidden units," in Proceedings of the 1995 IEEE International Conference on Neural Networks, vol. 1, pp. 275–280, December 1995.

[11] M. M. Islam and K. Murase, "A new algorithm to design compact two-hidden-layer artificial neural networks," Neural Networks, vol. 14, no. 9, pp. 1265–1278, 2001

[12] Z. Zhang, X. Ma, and Y. Yang, "Bounds on the number of hidden neurons in three-layer binary neural networks," Neural Networks, vol. 16, no. 7, pp. 995–1002, 2003.

[13] G. B. Huang, "Learning capability and storage capacity of two-hidden-layer feedforward networks," IEEE Transactions on Neural Networks, vol. 14, no. 2, pp. 274–281, 2003. View at Publisher ·

[14] B. Choi, J. H. Lee, and D. H. Kim, "Solving local minima problem with large number of hidden nodes on two-layered feed-forward artificial neural networks," Neurocomputing, vol. 71, no. 16–18, pp. 3640–3643, 2008

[15] Teoh EJ, Tan KC, Xiang C., "Estimating the number of hidden neurons in a feedforward network using the singular value decomposition" IEEE Trans Neural Netw. 2006 Nov;17(6):1623-9.

[16] Yinyin Liu, Janusz A. Starzyk, Zhen Zhu. "optimizing number of hidden neurons in neural networks" 2007

[17]. N. Jiang, Z. Zhang, X. Ma, and J. Wang, "The lower bound on the number of hidden neurons in multi-valued multi-threshold neural networks," in Proceedings of the 2nd International Symposium on Intelligent Information Technology Application (IITA '08), pp. 103–107, December 2008

[17] K. Jinchuan and L. Xinzhe, "Empirical analysis of optimal hidden neurons in neural network modeling for stock prediction," in Proceedings of the Pacific-Asia Workshop on Computational Intelligence and Industrial Application, vol. 2, pp. 828–832, December 2008

[18]. K. Shibata and Y. Ikeda, "Effect of number of hidden neurons on learning in large-scale layered neural networks," in Proceedings of the ICROS-SICE International Joint Conference 2009 (ICCAS-SICE '09), pp. 5008–5013, August 2009.

[19] Y Zhang. "Bernoulli Neural Network with Weights Directly Determined and with the Number of Hidden- Layer Neurons Automatically Determined" ISNN '09 Proceedings of the 6th International Symposium on Neural Networks on Advances in Neural Networks Pages 36-45, 2009.

[20] C. A. Doukim, J. A. Dargham, and A. Chekima, "Finding the number of hidden neurons for an MLP neural network using coarse to fine search technique," in Proceedings of the 10th International Conference on Information Sciences, Signal Processing and Their Applications (ISSPA '10), pp. 606–609, May 2010.

[21]. Y. K. Wu and J. S. Hong, "A literature review of wind forecasting technology in the world," in Proceedings of the IEEE Lausanne Power Tech, pp. 504–509, July 2007.

[22]. G. Panchal, A. Ganatra, Y. P. Kosta, and D. Panchal, "Behaviour analysis of multilayer perceptrons with multiple hidden neurons and hidden layers," International Journal of Computer Theory and Engineeringvol, vol. 3, no. 2, pp. 332–337, 2011.

[23] Amit Choudhary, Rahul Rishi "Improving the character recognition efficiency of feed forward BP neural network"

[24] MR Silvestre "A Clustering Based Method to Stipulate the Number of Hidden Neurons of mlp Neural Networks: Applications in Pattern Recognition" TEMA Tend. Mat. Apl. Comput., 9, No. 2 (2011)

[25] *Saurabh Karsoliya* ," Approximating Number of Hidden layer neurons in Multiple Hidden Layer BPNN Architecture "International Journal of Engineering Trends and Technology , 2012,

[26] D. Hunter, H. Yu, M. S. Pukish III, J. Kolbusz, and B. M. Wilamowski, "Selection of proper neural network sizes and architectures: a comparative study," IEEE Transactions on Industrial Informatics, vol. 8, no. 2, pp. 228–240, 2012

[27]. M. H. Hassoun. *Fundamentals of Artificial Neural Networks*. MIT Press, March 1995.

[28] N LeRoux,"Using Gradient Descent for Optimization and Learning" 2009

[29] Wu, C. H. (1995) Chapter titled "Gene Classification Artificial Neural System" in *Methods In Enzymology: Computer Methods for Macromolecular Sequence Analysis*, Edited by Russell F. Doolittle, Academic Press, New York.

[30] Wu, Cathy, S. Zhao, H. L. Chen, C. J. Lo and J. McLarty. (1996). Motif identification neural design for rapid and sensitive protein family search. *CABIOS*, 12 (2), 109-118.

[31] Snyder, E. E., Stormo, G. D. (1995) Identification of Coding Regions in Genomic DNA. *J. Mol. Biol.* 248: 1-18.

[32] F Valafar. "Pattern Recognition Techniques in Microarray Data Analysis: A Survey", Special issue of Annals of New York Academy of Sciences, *Techniques in Bioinformatics and Medical Informatics*. (980) 41-64, December 2002.

[33] T. Kohonen, *Self-Organizing Maps*, Third Extended Edition. Springer, Berlin, Heidelberg, New York, 2001.

[34] Kohonen, T. "The Self-Organizing Map" (1991) *Proc. IEEE* 78, 1464–1480

[35] Toronen, P. *et al* Analysis of gene expression data using self organizing maps (1999) FEBS Letters, 451, 142-146

[36]. Golub, T. R. Molecular classification of cancer: class discovery and class prediction by gene expression monitoring (1999) Science, 286, 531-537

[37] Tamayo, P. *et al*. Interpreting patterns of gene expression with self-organizing maps: methods and application to hematopoietic differtiation (1999) Proc. Natl. Acad. Sci. USA 96, 2907-2912

[38] Pablo Tamayo"Interpreting patterns of gene expression with self-organizing maps: Methods and application to hematopoietic differentiation" Proc Natl Acad Sci U S A. Mar 16, 1999; 96(6): 2907–2912.

[39] Quackenbush, J. Computational Analysis of Microarray Data (2001) *Nature Genetics* 2, 418-427

[40] T Hastie" 'Gene shaving' as a method for identifying distinct sets of genes with similar expression patterns" Genome Biol. 2000; 1(2): research0003.1–research0003.21. Published online Aug 4, 2000.

[41] Fritzke B. 1994. Growing cell structures--A self-organizing network for unsupervised and supervised learning. *Neural Network 7*:1141-1160.

[42] Azuaje F, Unsupervised neural network for discovery of gene expression patterns in B-cell lymphoma. Online Journal of Bioinformatics 1:26-41, 2001

[43] Dopazo J. & Carazo J. M. (1997) Phylogenetic reconstruction using an unsupervised growing neural network that adopts the topology of a phylogenetic tree. *Journal of Molecular Evolution* 44, 226-233

[44] Wang HC, Dopazo J, Carazo JM (1998) Self-organizing tree growing network for classifying amino acids *Bioinformatics* 14(4): 376-377

[45] Wang HC, Dopazo J, de la Fraga LG, Zhu YP, Carazo JM (1998) Self-Organizing Tree-growing Network for the classification of Protein Sequences. *Protein Science* 7:2613-2622

[46] J. Herrero, A. Valencia, and J. Dopazo. *A hierarchical unsupervised growing neural network for clustering gene expression patterns*. Bioinformatics, 17:126--136, 2001

[47] Stephen Grossberg. Adaptive pattern classification and universal recoding: I. Parallel development and coding of neural feature detectors. *Biological Cybernetics*, 23:121-134, 1976. Reprinted in Anderson and Rosenfeld, 1988.

[48] Gail A. Carpenter and Stephen Grossberg. Art 2: Selforganisation of stable category recognition codes for analog input patterns. *Applied Optics*, 26:4919-4930, 1987

[49] Gail A. Carpenter, Stephen Grossberg, and D.B. Rosen. Art2-a: An adaptive resonance algorithm for rapid category learning and recognition. *Neural Networks*, 4:493-504, 1991.

[50] Gail A. Carpenter and Stephen Grossberg. Art3: Hierarchical search using chemical transmitters in self-organizing pattern recognition architectures. *Neural Networks*, 3:129-152, 1990.

[51] T. Kasuba, "Simplified fuzzy ARTMAP," AI Expert, November (1993)

[52] Gail A. Carpenter, Stephen Grossberg, and D.B. Rosen. Fuzzy art: Fast stable learning and categorization of analog patterns by an adaptive resonance system. *Neural Networks*, 4:759-771, 1991.

[53] S. Tomida, T. Hanai, H. Honda, and T. Kobayashi. Gene Expression Analysis Using Fuzzy ART *Genome Informatics* 12: 245–246 (2001) 245

[54] Azuaje, F. A computational neural approach to support the discovery of gene function and classes of cancer. IEEE Trans Biomed Eng 48:332-339, 2001.

[55] Adleman, L.M. (1994) Molecular computation of solutions to combinatorial problems. *Science* 266, November 11, 1021–1024.

[56] Mills, A.P. Jr. et al. (2000) DNA analog vector algebra and physical constraints on large-scale DNA-based neural network computation. In DNA Based Computers V, (Winfree, E. and Gifford, D.K., eds), pp. 65–73, American Mathematical Society

[57] Liang, Y. et al. Bayesian Neural Network for Microarray Data Proceedings of the IEEE International Joint Conference On Neural Network, Hawaii, (2002)

Automated Toll Collection Using Satellite Navigation

Ms.Kirti A.Lonkar [1], Ms. Pratibha P. Kulkarni [2], Ms Monalisha Dash [3], Mr.Abhishek Dhawan[4], Mr.Hemant R.Kumbhar[5], Mr.Monika P.Gagtap[6].
[1, 2, 3, 4, 5, 6,] *Student, Dept. Of Computer Engineering, S.V.P.M's COE Malegaon (Bk,) Tal: Baramati Dist: Pune, Maharashtra, India*

ABSTRACT:
Recently, most developments are done in the field of the Expressways Network Toll Collection. Most electronic toll collection are implemented by DSRC (dedicated short-range communication) technology .In recent years in ETC development GPS global positioning system technique took place DSRC (dedicated short-range communication) technique. However a new generation of electronic toll collection is rapidly developed to replace dedicated short-range communication based electronic toll collection system. Global positioning system technology has become the new trend for road charging system, which implements electronic toll collection system based on positioning and Global System for MCT(Mobile communication technologies). In this paper the flow of the system are described the design of GPS (Global positioning system) based ETC (Electronic toll collection) system are discussed.

Keywords: *Global positioning system, Dedicated short range communication, Electronic toll collection, Mobile communication*

I. INTRODUCTION

Since from decades maintain and cost of road-ways are collected in direct manner or indirect manner in the older era the cost incurred were compensated either by tax payment on fuel or by budget allocation from national income disadvantage of this tax collection was tax payers had to pay for roads which was not at all use by them that means they have to pay extra money. However in other method, tolls are directly taken from the drivers passing road/street. Many benefits are it is a source of the capital generation, then management of traffic jam problem, firm request management

II. EXISISTING SYSTEM

Since from decades cost of construction, extension, maintenance and, roads, bridges and tunnels were collected through tolls for Revenue Generation. In previous method RFID technology was used ,in this system sensors were placed above roads and vehicles get charged ,sensors identifies the chassis number & number plates of vehicle through sensors and details send to server after that server further processed and toll is collected but this technology has some risks. Basically RFID technology is based on image processing technique. in which number plates and chassis numbers are scanned as a image afterwards further processing on that image is done and remaining task get finished regarding toll collection of particular vehicle. but problem with this system is that if due to mud or any other reason number plate or chassis number of vehicle get covered and not visible properly then sensors cannot be detect it properly so that it rises a problem while identifying the vehicle and but oblivious toll collection also can not completed. In our proposed system we eliminate this problem by using GPS technology.

III. PROPOSED SYSTEM

Purpose of the proposed system is to do the tasks remotely on the client machine through server.The aim is to develop Toll Collection System on express highway in such a way that, so the user have no need to keep money with him to pay toll and without the vehicle even having to slow down or stop at a toll.

IV. SYSTEM ARCHITECTURE

The system architecture of GPS-based ETC system is illustrated in Fig. 1, which includes five key parts of unit: interfacing hardware device, manual toll collection team, control unit, Transaction management unit and the money Payment Center. The working process of GPS-based ETC system is described as follows procedure:

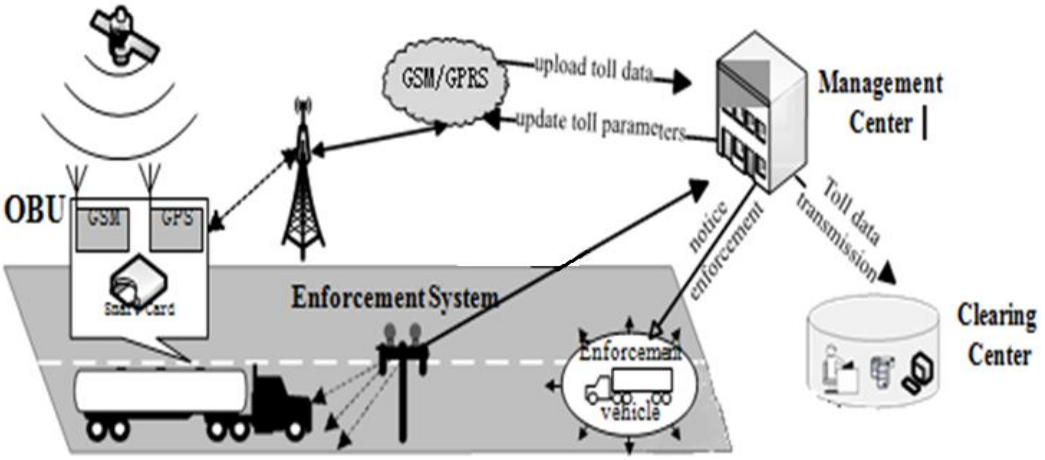

Fig. 1 Architecture of GPS-based ETC system.

Drivers goes to the money payment center registers and installs interfacing hardware device and applies for pre-paid card or post-paid card.

When vehicle moves into the toll area, interfacing hardware device checks current vehicle's position coordinate from GPS with the virtual toll node coordinate, kept in the storage of interfacing hardware device. After logistic determining, the interfacing hardware device sets up wireless communication channel through GSM module.

Interfacing hardware device sends transaction message to control system by the GSM module through mobile network.

After auditing to control system saves toll data and sends back transaction information to the Interfacing hardware device.

The Interfacing hardware device receives and displays the transaction result then it is working properly. If there is an error in transaction the result either there is a problem in the interfacing device or may be installation not properly done.

When the vehicle crosses the charging zone, if the Interfacing hardware device has abnormal state or the vehicle doesn't install an Interfacing hardware device the violation will be processed.

The transaction control unit clears all information according to toll data from control unit, and divides in road service providers.

The money Payment Center collects toll records and clearing data for account query.

Problem Setup and Notations

Input: Taking latitude and longitude through GPS

Output: Vehicle Location.

Result: Receiving message about deduction of balance.

I is a set of various vehicle types

I= {t1, t2... tn}

V is a set of individual vehicles

V= {v1, v2……, vn}

P is a set of prepaid account for different users.

P= {b1, b2… bn}

R is a set of fixed amount for different vehicles

R= {c1, c2... cn}

Then,

• ∀ I | V pay R cash from prepaid account P

V. MODULE DESCRIPTION

• **Interfacing hardware device**: it includes several components, GSM module, people interface

• **GSM Module**: The interfacing hardware device and control system communicate each other through the dedicated VPN (Virtual private network) based on GSM/GPRS mobile communication network.

• **Peoples Interface**: showing the interfacing hardware device status, vehicle information, card residual amount etc.The working rules and laws of the interfacing hardware device is described as follows: The highway network is divided into a number of independent sections by their arrival, leaving it and optional interchange. Some points in sections are defined as virtual toll node and their coordinate are stored in the interfacing hardware device memory.

Manual toll collection team: If in Travelers account doesn't have sufficient balance for paying toll then that vehicles are stop by manual toll collection team and toll will collect. And have lower priority but in case of insufficient balance in account of traveler it has higher priority.

• **Control unit**: The control unit is the core part of the system and its functions includes as follows:
• Can change the geographical scope of charging area like adds or deletes a toll road.
• Set up toll payment rate of the road and digital map information, etc.
• Collect and save toll information for clearing.
• Have extended function such as vehicle movement, traffic management, immediate assistance, etc.
• **Transaction management unit**: The Transaction management units do the transactions of the amount to be charged from the vehicle.
• **Payment Service Center**: This center takes ETC users registration, and provides customer service.

VI. CONCLUSION

So we concluded that the electronic automated toll collection technology idea of prepaying tolls having flexible features of charging zone and charging mode and also have better compatibility with intelligent transportation system ,Main objective of this electronic toll collection system are reduce traffic congestion, reduce waiting time, save fuel and increase highway capacity.

VII. ACKNOWLEDGEMENT

Our project is also an outcome of ideas contributed by many and we would like to gratefully acknowledge them here. We express our sincere thanks to all those who have provided us with valuable guidance towards the completion of this report as a part of the syllabus of the degree course.

We deeply thank our HOD Prof.Mrs.Varsha D.Mhaske for her useful guidance. We also thank our Project Guide Prof. Mr.Hemant R.Kumbhar and Co-Guide Prof.Ms. Monika P.Gagtap.without whom this project would have been a distant reality. We also thank them for giving us timely support in all phases of the project.We express our sincere thanks and gratitude to the project coordinator Prof.Mr.Yogesh R.Khalate for motivates us throughout the project. We also like to thanks to all teachers and staff for their valuable suggestions and feedback.

REFERENCES

[1] Saijie Lu, Tiejun He, Zhaohui Gao Intelligent Transportation System Research Center Southeast University Nanjing,
[2] Wei-Hsun Lee , Shian-Shyong Tseng , and Ching-Hung Wang, "design and implement of electronic toll collection system based on vehicle positioning system techniques," Computer Communications, vol. 31 ,2008,pp. 2925–2933.
[3] Wei-Hsun Lee, Shian-Shyong Tseng, and Bor-Shenn Jeng, "Electronic Toll Collection Based on Vehicle-Positioning system Techniques," proc. IEEE. International Conference on Networking, Sensing and Contro Taipei, Taiwan. March.2004,pp.643-648.
[4] Murphy T J, "Road user charging using satellite positioning technology," 12th IEE International Conference on Road Transport Information and Control (RTIC 2004), London, UK, 2004,pp,222-225.
[5] Juan Guillenno Jordan, etc., "A comparison of different technologies for EFC and other ITS applications" 2001 IEEE Intelligent Transportation System Conference, Aug. 2000

The Effect of Aluminum Waste on the Material Properties of Concrete

Elivs .M. Mbadike[1], N.N Osadebe[2]
[1] department Of Civil Engineering Department, Michael Okpara University Of Agriculture, Umudike, Nigeria.
[2] professor Of Civil Engineering, University Of Nigeria, Nsukka

ABSTRACT
The research investigated the density, Poisson ratio, young's modulus of Elasticity and modulus of Rigidity of aluminum waste concrete. Aluminum waste which was obtained from Aluminum Extrusion Industry (ALEX) Inyishi in Ikeduru local Government Area of State, Nigeria, was investigated. Concrete cubes with different ingredient components were cast and cured in water at room temperature for 28 days. Some selected mixes were used for the Poisson ratio test and control test respectively. A total of 66 concrete cubes were cast for the determination of density, Poisson ratio, young's modulus of elasticity and modulus of rigidity. The results of the density, poisson ratio, young's modulus of Elasticity and modulus of Rigidity ranges from 2.35-2.55kg/m^3, 0.38-153, 2.89 x 10^{-5} – 3.41 x 10$^{-5,}$ and o.56 x 10^{-5} -1.24x 10^{-5} respectively. The result of the control test of the density, Poisson ratio, young's modulus of Elasticity and modulus of Rigidity ranges from 2.41-2.56kg/m^3 0.53-2.01, 3.04 x 10^{-5} – 3.41 x 10^{-5} and 0.56 x 10^{-5} -1.38 x 10^{-5} respectively. Aluminum waste produces no significant effect on the density, Poisson ratio, young's modulus of Elasticity and modulus of Rigidity of the concrete.

Keywords: *Density, Poisson ratio, modulus of elasticity modulus of rigidity, aluminum waste.*

I. INTRODUCTION

Concrete is a mixture of cement, water, aggregates and admixtures (if any) in a given proportion. Aggregate represents some 60-80% of the concrete volume. They are inert grains bound by means of a blinder which is cement. Although inert, they introduce an important contribution to these major characteristics which make concrete the most favoured building materials [1]. Aggregates help to reduce shrinkage and heat dissipation during hardening and also contribute to the increase in the mechanical strength of concrete [2]. Cement generally represent 12-14% of concrete weight. During the hardening process, it generates shrinkage and heat dissipation phenomenon which leads to material cracking [3]. Water occupies 6-8% of the composition of fresh concrete. It provides for cement hydration and for the workability of fresh concrete mixture [4]. [5] reported that the standard workability tests are not suitable for aggregate concrete since they are sensitive to unit weight. [6] made similar observations when working with some materials. The incorporation of aluminum waste in concrete manufacture may provide a satisfactory solution to the problem posed by concrete production [7].

Finally the incorporation of aluminum waste in concrete should not impair concrete durability. Traditional assessment methods must therefore be adopted to evaluate this material [8]. This study contributes to the development of a methodology for assessing concrete manufactured from the aluminum waste. The methodology is based on the study of concrete containing this material. The durability and the environmental impact of concrete are closely connected to its transport properties which control the kinetics of the penetration of water and aggressive agent into concrete [9]. The movement of chemical species within the material and the leaching of certain chemicals are also closely linked to concrete to concrete diffusivity [10].
Finally, some selected mix ratios were used to determine density, poisson ratio, young's modulus of elasticity and modulus of rigidity of concrete produced with aluminum waste.

II. METHODOLOGY

Some selected mix ratios were used to cast concrete cubes for the determination of density, Poisson ratio, young's modulus of elasticity and moduluss of rigidity. Also, some selected mix ratios (control tests) were used to cast concrete cubes for the determination of the same properties. A total of forty five concrete cubes were cast and twenty one concrete cubes were also cast as control tests. The concrete cubes were cast and cured in water at room temperature for 28 days hydration period. At the end of the hydration period, the concrete cubes were tested for density, Poisson ratio, young's modulus of elasticity and modulus of rigidity.

The concrete cubes have the dimension of 150mm x 150mm x 150mm. The fine aggregate used was clean river sand, free from deleterious substances with a specific gravity of 2.62 and bulk density of 1533kg/m^3. The coarse aggregate was obtained from a local supplier with a maximum size of 20mm, specific gravity of 2.65 and bulk density of 1467kg/$m^{3.}$ Both aggregates conforms to [11] and. [12] respectively for coarse and fine aggregates. The cement used was Ordinary Portland Cement (Dangote) which conforms to [13]. The water used was a potable water. The aluminium waste used was obtained from Aluminum Extrusion industry (ALEX) Inyishi in Ikeduru Local Government Areas of Imo State, Nigeria. The waste was sieved with 150µm sieve size to obtain a finely divided material used for this work.

III. RESULT AND DISCUSSION

Table 1 shows the chemical analysis of aluminum waste while table 2 shows the chemical analysis of Ordinary Portland Cement used in this work.

Table 1 shows that aluminum waste contain mainly $S10_2$ (56.58%), Al_2O_3 (15.89%), and CaO (18,2%). The presence of calcium oxide constitutes about 11.30% of Ordinary Portland Cement (OPC). The presence of calcium in aluminum waste enhances the complete hydration of OPC and consequently the development of higher strength concrete. The setting and constituent hardening of paste- water and cement was directly responsible for the strength of the concrete. This was enhanced by the presence of calcium in aluminum waste. The mechanism is that in the presence of water the silicates and aluminates of OPC form products of hydration or hydrates which in time produce a hard mass. Table 1 also shows that aluminum waste contains 0.5% M_gO, of which 0.093% is present in OPC. Tables 3 and 4 shows the selected mixes used for the Poisson ratio test and the control mixes used for the Poisson ratio test respectively. Tables 5-8 described the effect of aluminum waste on the material properties of concrete. The result showed that there was no significant change in the density, Poisson ratio, young's modulus of elasticity and modulus of rigidity.

The results of density, Poisson ratio, young's modulus of elasticity and modulus of rigidity ranges from 2.35 - 2.55 kg/m^3, 0.38 - 1.53, 2.89 x 10^{-5} - 3.41 x 10^{-5} and 0.56 x 10^{-5}- 1.24 x 10^{-5} respectively; while the results of the control test ranges from 2.41 - 2.56kg/m^3, 0.53 - 2.01, 3.04 x 10^{-5} – 3.41 x 10^{-5}, and 0.56 x 10^{-5} – 1.38 x 10^{-5} respectively.

Table 1: Chemical Analysis of Aluminum Waste

Property	**Aluminum waste**
C_aO(%)	18.2
M_gO(%)	0.5
Fe_2O_3(%)	0.26
Na_2O(%)	0.36
Al_2O_3(%)	15.89
$S1O_2$(%)	56.58
Z_nO(%)	0.79
M_nO(%)	0.56
LO1(%)	6.4
SO_4(%)	Nil
CuO(%)	Trace
$T1O_2$(%)	Trace
C_dO(%)	Trace

Table 2: Chemical Analysis of Dangote cement

Oxide composition	**Percentage by weight (%)**
M_gO	0.093
Fe_2O_3(%)	6.405
C_aO	11.30
Al_2O_3	20.60
$S1O_2$	52.40
$T1O_2$	0.52
Na_2O	2.10
K_2O	2.60
L01	3.90

Table 3: Selected Mixes Used for the Poisson Ratio Test

S/No	Z_1	Z_2	Z_3	Z_4	Z_5
1	0.55	1.00	0.00	1.50	3.00
2	0.55	0.95	0.10	2.00	4.00
3	0.55	0.88	0.16	2.50	4.00
4	0.55	0.83	0.20	2.00	5.00
5	0.55	0.92	0.80	2.50	4.50
6	0.55	0.96	0.70	2.25	4.00
7	0.55	0.85	0.75	1.85	3.70
8	0.55	0.80	0.50	2.25	4.75
9	0.55	0.78	0.13	2.25	4.75
10	0.55	0.80	0.25	2.20	4.40
11	0.55	0.78	0.23	2.25	5.00
12	0.55	0.88	0.15	1.75	3.50
13	0.55	0.76	0.60	2.25	4.75
14	0.55	0.78	0.78	2.00	3.50
14	0.55	0.79	0.65	2.00	4.25

Z_1 = Water cement ratio
Z_2 = Fraction of Ordinary Portland Cement
Z_3 = Fraction of Aluminum Waste
Z_4 = Fraction of Fine Aggregates
Z_5 = Fraction of Coarse Aggregates

Table 4: Selected Control Mixes for the Poisson Ratio Test

S/No	Z_1	Z_2	Z_3	Z_4	Z_5
1	0.55	0.97	0.09	2.15	4.30
2	0.55	0.90	0.08	2.13	4.10
3	0.55	0.89	0.08	2.19	4.44
4	0.55	0.83	0.10	2.00	4.13
5	0.55	0.81	0.13	2.04	3.88
6	0.55	1.00	0.09	2.10	3.83
7	0.55	0.96	0.07	2.25	4.38

Table 5: Results of the determination Poisson ratio

S/No	Replications	Failure load (KN)	dy ($x10^{-2}$mm)	dx ($x10^{-2}$mm)	Wet weight (kg)	Dry weight (kg)
1	A	800	192	87	8.50	8.71
	B	732	176	30	8.00	8.05
	C	776	210	108	8.66	8.54
	A	750	130	410	8.41	8.44
2	B	510	120	98	8.10	8.11
	C	558	121	76	7.92	8.30
	A	630	250	110	8.80	8.84
3	B	667	200	230	8.15	8.18
	C	791	216	58	8.05	8.00
	A	660	180	80	8.90	8.91
4	B	700	189	66	8.55	8.53
	C	600	183	93	8.67	8.67
5	A	410	114	120	7.90	8.56
	B	720	155	130	7.65	8.20
	C	598	162	99	8.63	7.95
	A	655	100	90	8.11	7.15
6	B	582	105	162	8.70	8.81
	C	707	176	155	8.30	8.26
	A	490	108	102	8.25	8.34
7	B	761	140	116	8.70	8.77
	C	713	115	100	8.65	8.60
8	A	680	263	88	8.48	8.39
	B	796	161	106	7.94	8.08
	C	722	237	94	8.02	8.00
	A	715	112	46	8.55	8.52
9	B	820	171	230	8.61	8.65
	C	631	102	152	8.15	7.95

10	A B C	861 743 666	208 183 126	100 75 192	7.66 8.00 8.80	8.13 8.15 8.84
11	A B C	620 688 606	180 174 128	115 68 91	8.14 8.45 8.11	7.75 8.57 8.14
12	A B C	525 766 748	145 107 131	290 161 167	7.98 8.44 8.31	6.94 8.43 8.38
13	A B C	600 630 690	171 133 130	84 105 217	8.80 8.42 8.25	8.83 8.46 8.22
14	A B C	592 618 498	158 141 148	53 98 130	7.75 8.13 8.62	8.04 8.15 8.58
15	A B C	730 695 610	150 157 177	295 109 76	8.55 8.66 7.97	9.21 8.70 7.88

Table 6: Results of the Determination of Poisson Ratio (Control)

S/No	Replications	Facture load (KN)	dy ($x10^{-2}$mm)	dx ($x10^{-2}$mm)	Wet weight (kg)	Dry weight (kg)
1	A B C	702 776 615	110 202 210	60 140 91	8.12 7.62 8.00	8.16 8.04 8.20
2	A B C	535 708 762	150 158 140	10 30 66	8.77 8.61 8.30	8.81 8.68 8.41
3	A B C	697 620 609	176 131 157	84 52 112	8.33 8.10 8.46	8.42 8.11 8.55
4	A B C	598 701 646	196 182 128	280 38 74	8.22 8.18 8.00	8.25 8.19 8.08
5	A B C	750 800 708	163 177 93	100 600 190	7.60 8.82 8.70	8.01 8.70 8.55
6	A B C	724 521 689	149 137 132	58 121 97	8.65 8.35 8.41	8.66 8.27 8.58
7	A B C	664 840 780	98 116 103	200 133 109	8.20 8.00 8.70	8.30 8.67 8.08

Table 7: Results of the Determination of Density, Poisson Ratio, Young's Modulus of Elasticity and Modulus of Rigidity

S/No	Replications	Fc	Average Fc	ℓ	μ	E ($x10^{-5}$)	G ($x10^{-5}$)
1	A B C	35.56 32.53 34.49	34.19	2.50	0.38	3.41	1.24
2	A B C	33.33 22.67 24.80	26.93	2.45	1.53	3.03	0.60
3	A B C	28.00 29.64 35.16	30.93	2.47	0.62	3.22	0.99
4	A B C	29.33 31.11 26.67	29.04	2.55	0.43	3.15	1.10
5	A B C	18.22 32.00 26.58	25.60	2.44	0.83	2.95	0.81
6	A B C	29.11 25.87 26.58	28.80	2.39	1.11	2.94	0.70

7	A B C	21.78 33.82 31.69	29.09	2.54	0.88	2.95	0.78
8	A B C	30.22 35.38 32.09	32.56	2.42	0.46	3.14	1.08
9	A B C	31.78 36.44 28.04	32.09	2.48	1.08	3.28	0.79
10	A B C	38.27 33.02 29.60	33.63	2.48	0.47	3.34	1.44
11	A B C	27.56 30.58 26.93	28.36	2.42	0.58	3.00	0.95
12	A B C	23.33 34.04 33.24	30.19	2.35	1.59	2.89	0.56
13	A B C	26.67 28.00 30.67	28.45	2.52	0.98	3.26	0.82
14	A B C	26.31 27.47 22.13	25.30	2.45	0.64	2.96	0.90
15	A B C	32.44 30.89 27.11	30.15	2.55	1.04	3.40	0.83

Table 8: Results of the Determination of Density, Poisson Ratio, Young's Modulus of elasticity and Modulus of Rigidity (Control)

S/No	Replications	Fc	Average Fc	ℓ	μ	E ($x10^{-5}$)	G ($x10^{-5}$)
1	A B C	31.20 34.49 27.33	31.01	2.41	0.55	3.07	0.99
2	A B C	23.76 31.47 33.87	29.70	2.56	0.24	3.41	1.38
3	A B	30.97 27.56	28.53	2.48	0.53	3.16	1.03
	C	27.06					
4	A B C	26.58 31.16 28.71	28.82	2.43	0.74	3.04	0.87
5	A B C	33.33 35.56 31.47	33.45	2.49	2.01	3.36	0.56
6	A B C	32.18 23.16 30.62	28.65	2.52	0.67	3.27	0.98
7	A B C	29.51 37.33 34.67	33.84	2.47	1.42	3.32	0.69

CONCLUSION

The conclusion of the study can be summarized as follows:

a) Aluminum waste can be used as an admixture in concretes production.

b) Aluminum waste has no significant effect on the density, Poisson ratio, young's modulus of elasticity and modulus of rigidity of concrete.

c) Aluminum waste can also be used as a supplementary cementitious material in concrete production.

d) Curing is very necessary in concrete in order to ensure the complete hydration of cement.

REFERENCES

[1] Neville A.M. (1995): "Properties of Concrete" 4th edition, Pitman Publishing company Ltd, New York.

[2] He, C. Makovicky and Osbaeck, B. (1998): "Measurement of Acid Soluble silica in salt water" Journal of applied sciences, Vol. 8, pp 160-172.

[3] Machotra, V.M. (1988): A global Review with emphasis on durability and Innovation concrete". Journal of American concrete institute, Vol 30,pp 120-130.

[4] Neville, A.M and Brooks, J. (1995): "Concrete Technology"; 3rd Edition, Pearson publishers, India.

[5] Cook, D.J. (1997) "Coarse aggregate Polystyrene granules mixes for use is masonry unit, Building and Environment" 150-182.

[6] Sri Ravindrarajah, R (1999): "The use of Polystyrene aggregate granules in concrete" Journal of American concrete institute, Vol 30, pp 150-156.

[7] Basher M_cCabe, C.C. and Long, A (2005): "The influences of admixture on the properties of fresh and hardened concrete" Journal of scientific industrial Research Vol, 8, pp199-214.

[8] Chatterji, A.K. (1992): "Adsorption of lime and Pozzolanic activity" Journal of Scientific industry Research, Vol. 19B, pp 493-494.

[9] Pimienta P, Remond. S., Rodrigues, N.,and Bournazel, J.P. (1999): "Assessing the properties of mortar containing Municipal solid waste incineration fly ash". International congress creating with concrete, University of Dundee, pp 319-326.

[10] Remond, S, Pimienta, P and Bentz, D.P. (2002): "Effect of incorporation of Municipal solid waste fly ash in concrete". Journal of cement and concrete Research, Vol. 10, pp 12-14.

[11] British standards Institution, BS 877 (1967): Foamed or expanded blast furnace slag lightweight aggregates for concrete, London, pp8.

[12] British standards Institution, BS 3797 (1964): "Light weight aggregates for concrete". London, pp 8.

[13] British standards institution, BS 12 (1978): "Specifications for Ordinary and Rapid Hardening Portland Cement", London, pp 38.

Five Component Concrete Mix Optimization of Aluminum Waste Using Scheffe's Theory

Elivs .M. Mbadike[1], N.N Osadere[2]

[1]*Departemnt of Civil Engineering Department Michael Okpara University of Agriculture, Umudike Umuahia, Nigeria.*

[2]*Professor of Civil Engineering Department, University Of Nigeria, Nsukka*

ABSTRACT

The research investigated some mechanical properties of Aluminum Waste concrete to Harness its structural properties in the construction industry. Aluminum Waste which was obtained from Aluminum Extrusion Industry (ALEX) Inyishi in Ikeduru Local Government Area of Imo Sate, Nigeria was investigated. The work extended Scheffe's optimization techniques from fourth to fifth dimensions and obtained mathematical models for the optimization of the compressive and flexural strength of a five component concrete mix. A software for the Optimization of the mechanical properties of Aluminum Waste Concrete was developed. Seheffe's experimental design techniques was followed to produce concrete with different ingredient components which were used to cast cube and beam samples.

The cubes and beams have dimensions of 150mmx150mmx150mm and 100mmx100mmx500mm respectively. The samples were tested for 28 days hydration period. The developed software gave an optimum mix ratio of 1:1.1:1.75:1.15:0.7 (Cement, Fine Aggregate, Coarse Aggregate, Aluminum Waste, Water) which generated a compressive strength of 29.81N/mm^2, an increase of 14.35% in compressive strength over a standard mix. The result represented a saving of 16% by volume of concrete and a reduction of four thousand naira per cubic meter of concrete when compared with the standard mix. The software for the optimum mix ratio for flexural strength gave a value of 11.72N/mm^2. There was as increase in flexural strength of 9.46% of the standard mix. The research concludes that aluminum waste concrete is economical and produces high compressive and flexural strength and can be used in structural members such as beams and columns where high compressive strength concrete is needed.

KEYWORDS: compressive strength, flexural strength, scheffe's model, aluminum waste.

I. INTRODUCTION

Shelter is a serious problem in developing countries like Nigeria. As a result majority of the people in Nigeria especially those occupying the riverine areas are living in substandard house [1]. The major factor militating against the provision of affordable houses in Nigeria is high cost of ms.academicjournals.org/ building materials.

The materials commonly used in concrete construction industry include Water, Cement, Sand and Granite[2]. Water is always available in its natural state as Rainwater, River water, Fresh sea water and Borehole water. Sand is also available in its Natural state as River sand, Sea sand, Erosion sand and Desert dunes (sand from the desert). Cement and granite are not commonly available in their natural states. They are processed materials. In most cases the point of use is different from point of manufacture. According to [3], concrete is any product or mass made by the use of any cementing medium. Aggregates are defined as particles of rock which, when brought together in a bound or unbound conditions form part or whole of an engineering or building structure [4].

Concrete has been classified into two broad classes: Plan and reinforced [5].

Generally concrete is good in compression and poor in tension [6]. Modern research in concrete seeks to provide greater understanding of its constituent materials and possibilities of improving its desired qualities. For instance, cement has partially replaced with fuel ash [7]. The trend of cost of concrete products has led many researchers to go into the search for alternative and affordable materials for use in concrete. It is in the spirit of the search for alternative and affordable materials for concrete that this research work tried to see the applicability of aluminum waste in concrete production.

II. MATERIALS AND METHODS

Simplex design formulation: The relation between the actual components and pseudo components is according to [8].

Z = AX _____ (1)

Z and X are five element vectors where A is a five by five matrix. The value of matrix A will be obtained from the first five mix ratios. The mix ratios are:

Z_1[0.67:1:1.7:2:0.5],
Z_2[0.58:1:1.5:1.9:0.8],
Z_3[0.6:1:1.2:1.7:1],
Z_4[0.8:1:1:1.8:1.3],
Z_5[0.74:1:1.2:1.3:1.5],

The corresponding pseudo mix ratios are:

X_1[1:0:0:0:0], X_2[0:1:0:0:0],
X_3[0:0:1:0:0], X_4[0:0:0:1:0],
X_5[0:0:0:0:1]. Substitution of X_i and z into equation (1) gives the values of A as

$$A = \begin{Bmatrix} 0.67 & 0.58 & 0.6 & 0.8 & 0.74 \\ 1 & 1 & 1 & 1 & 1 \\ 1.7 & 1.5 & 1.2 & 1 & 1.2 \\ 2 & 1.9 & 1.7 & 1.8 & 1.3 \\ 0.5 & 0.8 & 1 & 1.3 & 1.5 \end{Bmatrix} \quad \text{-- (2)}$$

The first five mixture ratios are located at the vertices of the four dimensional factor space. Ten other pseudo mix ratios located at mid points of the lines joining the vertices of the factor space are:

Z_{12}[½ : ½ :0:0:0], X_{13}[½ :0: ½ :0:0],
Z_{14}[½ :0:0: ½ :0], X_{15}[½ :0:0:0: ½],
Z_{23}[0: ½ : ½ :0:0], X_{24}[0: ½ :0: ½ :0],
Z_{25}[0:0: ½ :0: ½], X_{34}[0:0: ½ : ½ :0],
Z_{35}[0:0: ½ :0: ½], X_{45}[0:0:0 ½ : ½].

Substituting these values into equation (1) will give the corresponding actual mix ratios, Z as;

Z_{12}[0.625:1:1.6:1.95:0.65],
Z_{13}[0.635:1 :1.45:1.85:0.75],
Z_{14}[0.735:1:1.35:1.90:0.90],
Z_{15}[0.705:1:1.45:1.65:1.],
Z_{23}[0.59:1:1.35:1.80:0.9],
Z_{24}[0.69:1:1.25:1.85:1.05],
Z_{25}[0.66:1:1.35:1.60:1.15],
Z_{34}[0.70:1:1.10:1.75:1.15],
Z_{35}[0.67:1:1.20:1.50:1.25],
Z_{45}[0.77:1:1.10:1.55:1.40].

No pseudo component according to [9] should be more than one or less than zero. The summation of all the pseudo components in a mix ratio must be equal to one [10,11].

That is

$0 \leq x_i \leq 1$ _____ (3)

$\sum X_i = 1$ _____ (4)

The general equation for regression is given as:

$Y = b_o + \sum b_i x_i + \sum b_{ij} x_i x_j + \sum b_{ii} x_i x_j x_k$
+…… + ∑bij, i2…… inxi, xi2…….xin + e
_____ (5)

Where i≤i1 ≤i2 ≤……≤ in ≤q respectively [12].

Expanding equation (5) up to second order Polynomial for five component mixture, we obtain:

$$\mathbf{Y} = b_o+b_1x_1 + b_2x_2 + b_3x_3 + b_4x_4 + b_5x_5 + b_{11}x_1^2 + b_{12}x_1x_2 + b_{13}x_1x_3 + b_{14}x_1x_4 + b_{15}x_1x_5 + b_{22}x_2^2 + b_{23}x_2x_3 + b_{24}x_2x_4 + b_{25}x_2x_5 + b_{33}x_3^2 + b_{34}x_3x_4 + b_{35}x_3x_5 + b_{44}x_4^2 + b_{45}x_4x_5 + b_{55}x_5^2 + e \quad (6)$$

But $\sum x_i = 1$

That is $X_1 + X_2 + X_3 + X_4 + X_5 = 1$ (7)

Multiplying equations (7) by bo will give

$box_1 + box_2 + box_3 + box_4 + box_5 = bo$ (8)

Multiplying equation (7) by x_1 will give

$X_1^2 + x_1x_2 + x_1x_3 + x_1x_4 + x_1x_5 = X_1$ (9)

Similarly multiplying equation (7) by x_2, x_3, x_4 and x_5 will respectively give:

$X_1x_2 + x_2^2 + x_2x_3 + x_2x_4 + x_2x_5 = X_3$ (10)

$X_1x_3 + x_2x_3 + x_3^2 + x_3x_4 + x_3x_5 = X_3$ (11)

$X_1x_4 + x_2x_4 + x_3x_4 + x_4^2 + x_4x_5 = X_4$ (12)

$X_1x_5 + x_2x_5 + x_3x_5 + x_4x_5 + x_5^2 = X_5$ (13)

Rearranging equations (9) to (13) in terms

of xi^2 will give respectively

$X_1^2 = x_1 - x_1x_2 - x_1x_3 - x_1x_4 - x_1x_5$ (14)

$X_2^2 = x_2 - x_1x_2 - x_2x_3 - x_2x_4 - x_2x_5$ (15)

$X_3^2 = x_3 - x_1x_3 - x_1x_3 - x_2x_3 - x_3x_4 - x_3x_5$ (16)

$X_4^2 = x_4 - x_1x_4 - x_1x_4 - x_2x_4 - x_3x_4 - x_4x_5$ (17)

$X_5^2 = x_5 - x_1x_5 - x_2x_5 - x_2x_5 - x_3x_5 - x_4x_5$ (18)

Substituting equation (8) into equations (14-18) and equation (6) and re-arranging and replacing with a constant α will yield.

$$Y = \alpha_1x_1 + \alpha_2x_2 + \alpha_3x_3 + \alpha_4x_4 + \alpha_5x_5 + \alpha_{12}x_1x_2 + \alpha_{13}x_1x_3 + \alpha_{14}x_1x_4 + \alpha_{15}x_1x_5 + \alpha_{23}x_2x_3 + \alpha_{24}x_2x_4 + \alpha_{25}x_2x_5 + \alpha_{34}x_3x_4 + \alpha_{35}x_3x_5 + \alpha_{45}x_4x_5 + e \quad (19)$$

Equation (19) can be re-written as $Y = y + e$ (20)

Where e = Standard error or standard deviation and

$$Y = \alpha_1x_1 + \alpha_2x_2 + \alpha_3x_3 + \alpha_4x_4 + \alpha_5x_5 + \alpha_{12}x_1x_2 + \alpha_{13}x_1x_3 + \alpha_{14}x_1x_4 + \alpha_{15}x_1x_5 + \alpha_{23}x_2x_3 + \alpha_{24}x_2x_4 + \alpha_{25}x_2x_5 + \alpha_{34}x_3x_4 + \alpha_{35}x_3x_5 + \alpha_{45}x_4x_5 \quad (21)$$

Equation (21) is the Scheffe's (5,2) Lattice Polynomial equation. These responses are constant and are determined by carrying out Laboratory practicals. A total of fifteen (15) such practical tests were carried out to correspond to the fifteen coefficients of equation (21).
To validate the model extra fifteen mix ratios (control) were determined and used in the Students T-test.

Table 1: Pseudo and Actual Mix Ratios for the Control Test

Points	Ratio of Materials									
	Water	Cement	Sand	Coarse aggregate	Aluminum waste	Water	Cement	Sand	Coarse aggregate	Aluminum waste
	X_1	X_2	X_3	X_4	X_5	Z_1	Z_2	Z_3	2_4	Z_5
C_1	0.25	0.25	0.25	0.25	0	0.6625	1	1.35	1.85	0.90
C_2	0.25	0.25	0.25	0	0.25	0.6475	1	1.40	1.725	0.95
C_3	0.25	0.25	0	0.25	0.25	0.6975	1	1.35	1.75	1.025
C_4	0.25	0	0.25	0.25	0.25	0.7025	1	1.275	1.70	1.075
C_5	0	0.25	0.25	0.25	0.25	0.68	1	1.225	1.675	1.15
C_6	0.2	0.2	0.2	0.2	0.2	0.678	1	1.32	1.74	1.02
C_7	0.3	0.3	0.3	0.1	0	0.635	1	1.42	1.86	0.82
C_8	0.3	0.3	0.3	0	0.1	0.629	1	1.44	1.81	0.84
C_9	0.3	0.3	0	0.3	0.1	0.689	1	1.38	1.84	0.93
C_{10}	0.3	0	0.3	0.3	0.1	0.695	1	1.29	1.78	0.99
C_{11}	0	0.3	0.3	0.3	0.1	0.668	1.	1.23	1.75	1.08
C_{12}	0.1	0.3	0.3	0.3	0	0.661	1	1.28	1.82	0.98
C_{13}	0.3	0.1	0.3	0.3	0	0.679	1	.132	1.84	0.92
C_{14}	0.3	0.3	0.1	0.3	0	0.675	1	1.38	1.88	0.88
C_{15}	0.1	0.2	0.3	0.4	0	0.683	1	1.23	1.81	1.03

COMPRESSIVE AND FLEXURAL STRENGTH TEST: THE MATERIAL USED INCLUDES:

- Granite which is free from deleterious material with a maximum size of 20mm.
- The cement used is Dangote cement which is a brand of Ordinary Portland cement and conform to [13].
- The water used is clean water from borehole.
- River sand used in this research work is free from deleterious material with a specific gravity of 2.62.
- Aluminum waste was obtained from the Aluminum Extrusion industry (ALEX) Inyishi in Ikeduru local Government of Imo State, Nigeria. The waste was sieved with 150µm sieve size in order to obtain a finely divided material.

The materials were batched by weight. Mixing was done manually using spade and hand trowel. 150mm x 150mm x 150mm concrete cube moulds were used for compressive strength test while 100mm x 100mm x 100mm x 500mm beam moulds were used for flexural strength. The concrete cubes and beams were cured for 28 days at room temperature. At the end of the hydration period the cubes and beams were crushed and the compressive and flexural strengths were determined according to the requirement of [14].

RESULTS AND DISCUSSION

The results of the compressive and flexural strength obtained by the optimization approach applied in the work are presented in table 2 and table 4.

The results of the experimental test and Simplex (Scheffe) Model are Presented in table 3 and 5 respectively. The proposed regression models for compressive and flexural strength were tested for adequacy using the Students' T-test. This is shown is table 7 for compressive strength and table 9 for flexural strength. Table 6 presents the results obtained from test carried out to experimentally check the outcome of the regression models. The experimental results agreed favorably with the software derived. The compressive strength gave 29.81 N/mm^2 and the flexural strength 11.72$N/mm^{2.}$

Table 6 showed that aluminum waste is not weak in flexure and will therefore be adequate in structural members where the concrete may be required to resist some measure of flexural stress such as in rigid pavements. The results of table 6 also showed that the use of the proposed optimized aluminum waste produced a saving of 16% in mass of concrete. The economic benefit analysis of the work showed that four thousand naira is saved per cubic meter of concrete when aluminum waste is used instead of a standard component 1:2:4 concrete mix.

Table 2: Compressive Strength Test Result

Points	Replicate 1 (N/mm^2)	Replicate 2 (N/mm^2)	Replicate 3 (N/mm^2)	Average Compressive strength (N/mm^2)
1	27.20	30.22	30.80	29.41
2	17.78	19.56	21.64	19.66
3	18.49	21.29	26.00	21.93
4	21.64	18.58	22.76	20.99
5	26.04	21.07	13.56	20.22
12	13.29	9.51	20.35	14.38
13	18.40	22.04	19.16	19.87
14	23.20	27.04	26.27	25.50
15	24.62	23.02	22.22	23.29
23	21.87	22.27	25.78	23.31
24	14.67	20.04	26.76	20.49
25	15.33	27.47	22.36	21.72
34	31.16	23.11	35.16	29.81
35	21.73	28.36	27.29	25.79
45	18.53	15.20	12.49	15.41
C_1	31.38	18.02	23.38	24.26
C_2	16.27	17.82	27.69	20.59
C_3	17.18	20.80	23.82	20.60
C_4	23.56	19.47	21.96	21.66
C_5	23.78	22.25	18.70	21.58
C_6	14.31	17.51	22.67	18.16
C_7	22.80	23.91	20.84	22.52
C_8	29.20	17.87	20.22	22.43
C_9	25.16	12.93	13.69	17.26
C_{10}	24.27	26.22	28..13	26.21
C_{11}	20.58	18.40	17.73	18.90
C_{12}	22.93	18.70	19.78	20.47
C_{13}	21.02	20.04	30.22	23.76
C_{14}	21.78	8.98	20.27	17.01
C_{15}	18.27	24.49	12.71	18.49

Table 3: Result of experimental test and simplex (Scheffe) model.

S/No	Experimental compressive test result (N/mm^2)	Scheffe's model compressive strength test result (N/mm^2)
1	29.41	29.41
2	19.66	19.66
3	21.93	21.93
4	20.99	20.99
5	20.22	20.22
6	14.38	14.38
7	19.87	19.87
8	25.50	25.50
9	23.29	23.29
10	23.31	23.31
11	20.49	20.49
12	21.72	21.72
13	29.81	29.81
14	25.79	25.79
15	15.41	15.41
16	24.26	21.841
17	20.59	20.688
18	20.60	18.913
19	21.66	23.349
20	21.58	23.783
21	18.16	21.666
22	22.52	19.618
23	22.43	19.08
24	17.26	18.959
25	26.21	24.506
26	18.90	24.923
27	20.47	23.807
28	23.76	23.794
29	17.01	20.33
30	18.49	25.052

Table 4: Flexural strength test result

Points	Replicate 1 (N/mm^2)	Replicate 2 (N/mm^2)	Replicate 3 (N/mm^2)	Average Compressive strength (N/mm^2)
1	5.80	6.05	7.60	6.48
2	7.45	9.85	9.30	8.87
3	8.95	9.90	10.60	9.82
4	5.65	6.95	6.60	6.40
5	10.45	12.90	11.80	11.72
12	6.60	7.60	7.90	7.37
13	7.00	9.00	8.50	8.17
14	5.90	6.20	9.00	7.03
15	7.75	8.10	11.00	8.95
23	8.70	9.60	10.50	9.60
24	7.00	8.00	10.00	8.33
25	9.50	12.00	10.10	10.53
34	7.45	9.55	8.90	8.63
35	9.95	12.50	10.90	11.12
45	8.74	10.45	8.65	9.28
C_1	8.48	8.00	8.25	8.24
C_2	8.20	10.55	8.75	9.17
C_3	9.00	7.90	7.00	7.97
C_4	9.50	9.98	7.50	8.99
C_5	15.63	14.55	8.10	12.76
C_6	8.96	13.35	8.90	10.40
C_7	10.00	8.70	9.00	9.23
C_8	9.30	9.20	9.30	9.27
C_9	11.00	7.90	8.50	9.13
C_{10}	9.11	14.00	6.95	10.02
C_{11}	8.95	9.68	6.70	8.44
C_{12}	8.45	11.04	6.25	8.58
C_{13}	11.70	8.15	7.60	9.15
C_{14}	12.95	10.68	9.85	11.16
C_{15}	14.00	10.00	8.10	10.70

Table 5: Result of Experimental Test and Simplex (Scheffe) Model

S/No	Experimental flexural strength test result (N/mm^2)	Scheffe's model flexural strength test result (N/mm^2)
1	6.48	6.48
2	8.87	8.87
3	9.82	9.82
4	6.40	6.40
5	11.72	11.72
6	7.37	7.37
7	8.17	8.17
8	7.03	7.03
9	8.95	8.95
10	9.60	9.60
11	8.33	8.33
12	10.53	10.53
13	8.63	8.63
14	11.12	11.12
15	9.28	9.28
16	11.47	8.336
17	9.17	9.324
18	7.97	8.689
19	8.99	8.993
20	12.76	9.771
21	11.38	9.047
22	9.23	8.397
23	9.27	8.764
24	9.13	8.086
25	11.32	8.439
26	8.44	9.325
27	8.58	8.741
28	9.15	8.181
29	11.16	7.955
30	10.70	8.534

Table 6: Mass and strength of standard and optimization mixes compared

Item	Cement (kg)	Fine aggregate (kg)	Aluminum waste (kg)	Coarse aggregate (kg)	Water (kg)	Compressive strength (N/mm^2)	Flexural Strength (N/mm^2)
Standard mix	**1**	**2.00**	**0.00**	**4.00**	**0.55**	**26.07**	**9.46**
optimized mix	**1**	**1.1**	**1.15**	**1.75**	**0.70**	**29.81**	**11.72**
Saving	**0**	**0.9**		**2.25**	**0.15**	**3.74**	

ECONOMIC BENEFITS

From table 6, saving in concrete mass per design mass.

= 0.9 + 2.25 + 0.15 = 3.3kg.

Mass of concrete in $1m^3$ concrete= 2400kg [15]

Hence mass of concrete saved in $1m^3$

= 3.3 x mass of concrete in $1m^3$/design unit mass

$= 3.3 \times \frac{2400}{20.5} = 386.34kg$

But density of concrete $= \frac{\text{mass}}{\text{Volume}} = 2400$

Hence volume of concrete saved

$= \frac{\text{Mass}}{\text{Density}} = \frac{386.35}{2400} = 0.16m^3$

Cost of $1m^3$ of concrete = #25,000

:. Cost of concrete saved per m^3

= #25000 x 0.16 = #4,000

:. Percentage volume of concrete saved per m^3

$= \frac{0.16m^3}{1m^3} \times \frac{100}{1} = 16\%$

Table 7: T-statistics for the Control Parts of Compressive Strength

Points	Method of Mixing/Test ye	ym	Difference d_1 = ye – ym
C_1	24.26	24.841	+2.419
C_2	20.59	20.688	-0.098
C_3	20.60	18.913	+1.687
C_4	21.66	23.349	-1.689
C_5	21.58	23.783	-2.203
C_6	18.16	21.666	-3.506
C_7	22.52	19.618	+2.902
C_8	22.43	19.08	+3.35
C_9	17.26	18.959	-1.699
C_{10}	26.21	24.506	+1.704
TOTAL			**2.867**

Average difference $d = \frac{\sum d_1}{n} = \frac{2.867}{10}$

$= 0.2867$

Variance, $\sum d^2 = \frac{\sum (d-d)^2}{n-1} = \frac{53.0318}{9}$

$= 5.892$

Standard deviation, Sd = 2.427

t-statistics, t = $\frac{d}{Sd/\sqrt{10}} = \frac{0.2867}{2.427/\sqrt{10}}$

$= 0.37$

For the case of two tailed test and for 5% level of significant and 9 degrees of freedom, we obtain $t_{0.975}$, 9 = 2.26.

Because the calculated t-value is less than that obtained from the table (i.e 2.26), we conclude that there is no significant difference in the two methods.
That is to say we accept null hypothesis.

Table 8: t- Statistics for the Control Points of Flexural strength

Points	**Method of Mixing/Test ye**	**ym**	**Difference d_1 = ye – ym**
C_1	8.24	8.336	-0.096
C_2	9.17	9.324	-0.154
C_3	7.97	8.689	-0.719
C_4	8.99	8.993	-0.003
C_5	8.20	8.771	-0.571
C_6	10.40	9.047	1.353
C_7	9.23	8.397	0.833
C_8	9.27	8.764	0.506
C_9	9.13	8.086	1.044
C_{10}	10.02	8.439	1.581
		TOTAL	**3.774**

ye = Experimental laboratory result
ym = model result.

Average difference, $d = \frac{\sum d_1}{n} = \frac{3.776}{10} = 0.3774$

Variance, $Sd^2 = \frac{\sum(d_1-d)^2}{n-1} = \frac{5.8218}{9} = 0.6460$

Standard deviation, Sd = 0.8043

t-statistics, $t = \frac{d}{sd/\sqrt{10}} = \frac{0.3774}{2.8043/\sqrt{10}}$

$= 1.484$

For the case of two tailed test and for 5% level significant and the degree of freedom of 9, we obtain $t_{0.975}$, 9 = 2.26. Because the calculated t, value is less than that obtained from the table (i.e 1.484 < 2.26), we concluded that the result is not significant at 5% level.
Therefore, we accept null hypothesis.

CONCLUSION

The research concludes that aluminum waste can be used in construction as an additive in concrete but should not exceed 16%. Aluminum waste can also be used as a fifth component in concrete production.

Aluminum waste has the advantage of high compressive strength material and cost saving over its standard counterpart.

REFERENCE

[1] Kashi, M.G, Malloy, R.A and Swan, C.W (2002); "Fly ash/Plastic synthetic aggregate for construction materials" Chelsea center for recycling and economic development, University of Massachustts Lowel, report 45.

[2] Neville, A.M. (1983): "Creep of Plan and structural concrete" Longman publishers Limited, London.

[3] Neville, A.M and Brooks, J.J (2002): "Concrete Technology". Pearson education pte Limited, India.

[4] Majid, N.Z.A (2002): "The Influence of aggregate properties on the strength of concrete". Civil and Structural Engineering works, Malaysia.

[5] Ghose, D.N. (1989): "Materials of construction" TATA McGraw-Hill publishing co-Ltd, New Delhi.

[6] Orie, O.U (2005); "Structural Engineering". History and philosophy science and Technology, University of Benin Press, Benin City, Nigeria.

[7] David J and Galliford, N. (2000): "Bridge construction at Huddersfield Canal". Concrete 34, Number 6.

[8] Scheffe, H, (1958): Experiments with Mixture. Journal of Royal Statistics society series B, 20:344-360.

[9] Scheffe, H. (1958): Experiments with mixtures, Journal of Royal Statistics Society series B, 344-360.

[10] Obam, S.A (1998): A Model for Optimization of Strength of Palm Kernel Shell Aggregate Concrete. A. M.Sc Thesis, University of Nigeria, Nsukka.

[11] Scheffe, H, (1958). Experiments with mixtures. Journal of Royal Statistics Society Series B, 344-360.

[12] Simon, M.J., Lagergreen, E.S and Synder, K.A (1997). Concrete Mixtures Optimization Using Statistics Mixture Design Methods. Proceedings of the PCI/FHWA International Symposium on high performance concrete, New Orieans, PP 230-244.

[13] British Standards Institution, BS 12 (1978): "Ordinary and Rapid Hardening Portland cement: London, pp8.

[14] British Standard Institution, BS 1881 (1986): Methods of Testing concrete, London.

[15] Oyenuga, V.O (2001): "Reinforced Concrete Design". Asros Limited, Lagos, Nigeria.

Simulation of Photon and Electron dose distributions by MCNP5 code for the treatment area using the linear electron accelerator (LINAC) in Dongnai General Hospital, Vietnam

Nguyen Van Hai[1], Nguyen Van Hung[2], Dinh Thanh Binh[3], Duong Thanh Tai[3]
[1]Dalat Vocational Training College, [2]Center for Nuclear Techniques in Hochiminh city,
[3]Dongnai General Hopital, Vietnam

ABSTRACT:
Nowadays, radiotherapy by linear electron accelerators (LINAC) has became popular and given high effects for cancer treatment in hospitals of Vietnam. The paper presents simulation for distribution of radiation dose fields by MCNP5 code for electron and photon radiations inside and outside the treatment room in Dongnai General Hospital. From that, it could carry out comparision between the results of calculation and those of experimental measurements at Dongnai General Hospital.

The calculation results described the distributions of radiation dose fields at some positions of inside and outside the treatment room. This is one of the important basises for calculating radiation safety in radiotherapy as well as construction and setup of rooms.

Keywords: *Radiotherapy, Linear electron accelerator (LINAC), Radiation safety, Dose field, MCNP5 code*

I. INTRODUCTION

The LINACs can emit one of two types of radiation which are photons, electrons with high dose, so the dose distribution in the treatment area is relatively complex. From receiving the dose distribution results fully and accurately, we will to have recommendations about radiation safety for healthcare facilities using the LINACs. MCNP5 code is used to calculate the simulated distribution of photon and electron doses inside and outside the treatment room. Subject of simulations in this report is available at Primus machines Cancer Center, Dongnai General Hospital, Vietnam.

II. EXPERIMENTAL

Radiation therapy in a hospital room built is set up according to the general regulations of production [1] with machine room dimensions shown in Figure 1.

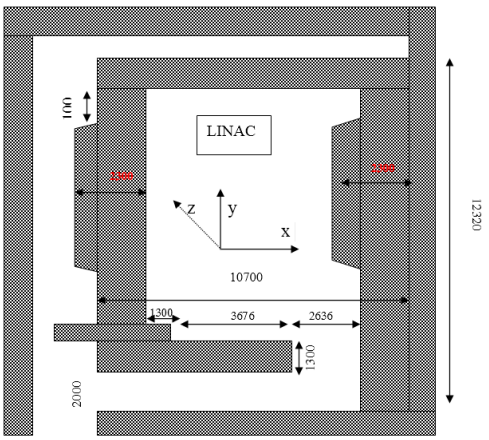

Figure 1. Radiation model room at Dongnai General Hospital.

The internal and external walls were made by concrete with density of 2.5 g/cm^3. Radiation therapy room door was made by lead together on / off semi-automatic control system.

Configuration and parameters of LINAC:

Configuration and specifications of the LINAC [2] are as follows:

Brand: Primus; Manufacturer: Simien (Germany); radiation type: single-energy electrons with energies of 5, 7, 8, 10, 12, 14 MeV; photons with energies of 6 and 15 MeV.

The probability distribution of the corresponding photons is outlined in Table 1 and 2.

Table 1. Distribution of photon beam with energy of 6 MeV.

Energy (MeV)	Relative probabilities (%)	Energy (MeV)	Relative probabilities (%)	Energy (MeV)	Relative probabilities (%)	Energy (MeV)	Relative probabilities (%)
0.10	0.05	0.40	0.80	1.00	11.80	3.00	9.60
0.15	0.10	0.50	1.60	1.25	14.40	4.00	8.10
0.20	0.20	0.60	3.20	1.50	12.80	5.00	6.40
0.30	0.60	0.80	9.00	2.00	14.40	6.00	0.80

Table 2. Distribution of photon beam with energy of 15 MeV.

Energy (MeV)	Relative probabilities (%)	Energy (MeV)	Relative probabilities (%)	Energy (MeV)	Relative probabilities (%)	Energy (MeV)	Relative probabilities (%)
0.10	0.06	0.50	2.28	1.50	4.86	6.00	7.17
0.15	0.73	0.60	2.35	2.00	10.18	8.00	0.72
0.20	0.89	0.80	4.69	3.00	16.98	10.00	4.19
0.30	1.98	1.00	4.65	4.00	13.48	15.00	1.00
0.40	2.19	1.25	5.42	5.00	9.08	20.00	0.00

Note: Refer to this values when performing QA at Dongnai General Hospital.

Set the input file:

File input is a description of all the parameters of the problem, including materials, resources, computational requirements [3].

The geometry of the problem consists of two components: fixed and radiotherapy room accelerator can shoot many different angles around the axis of the machine.

- Radiotherapy room consists of 4 walls around the room, inner room walls, hallways, patient bed and doors lead.

- Accelerator consists of body, locomotives, cones, waveguides, beer Tungstens, sad ion, the collimator and jaws with aperture of 1.83x83 cm^2 (corresponding to the projection 40x40 cm^2).

Source with disc-shape, isotropic toward the patient's bed with a distance of 224 cm from the ground. Photon and electron energy levels listed above.

Requirements are calculated dose rate in air and concrete blocks shaped 1.5 cm diameter, 5 cm length at the following locations:

+Direction -$\vec{y}$: the cell with coordinates of (0,-5,120), (0,-10,120)... (0,-400,120), respectively.

+ Direction -$\vec{x}$: the cell with coordinates of (-5,0,120), (-10,0,120) ... (-590,0,120), respectively; co-ordinate origin is from the ground, and the central axis of the source.

III. RESULTS AND DISCUSSION

After using the software simulation mode and calculated by the Visual Editor executable (command form), the results are as follows:

Structure radiation therapy room

Observed system accomodations in 3-dimensional space with multiple viewing angles and different sizes are presented in Figure 2.

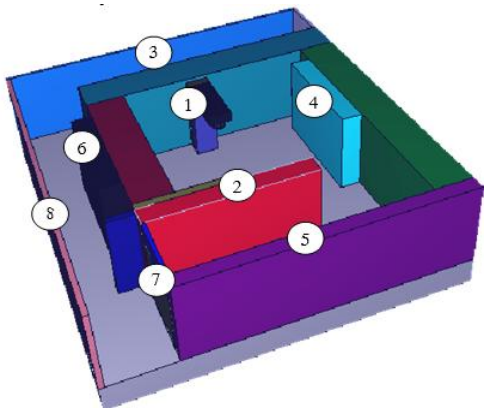

Figure 2. Radiotherapy Department in Dongnai General Hospital (1: Accelerator; 2: inside walls; 3, 4, 5, 6: concrete walls; 7: doors lead; 8: corridor).

Scattering of photons and electrons in the room

Implementation of particle display functions of the software requirements for a simulation, scattering processes of photons and electrons in the treatment room are presented in Figures 3, 4 and 5.

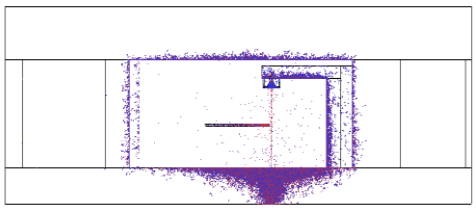

Figure 3. Scattering of 15 MeV energy photons (plane y, z).

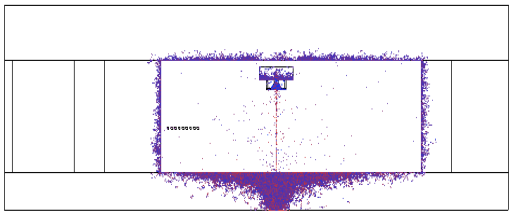

Figure 4. Scattering of 15 MeV energy photons (plane x, z).

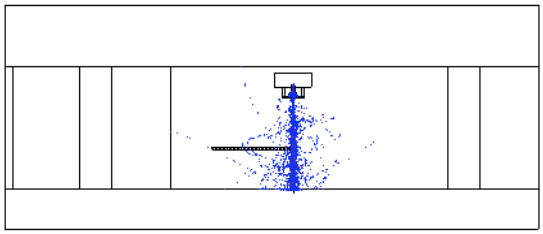

Figure 5. Scattering of 10 MeV energy electrons (plane x, z).

From the scattering images, they are shown: range of photon scattering is very large and complex distribution in the case of large particles made with range spread throughout the room, including locomotives. In the case of plant at 0^o location, primarily scattering direction is toward the patient's bed. For the case of plant at 90^o location, the scattering direction is toward the operators with relatively high quantity, and the range of electron scattering has tendency for concentrating in the direction from the source to the patient's bed.

Results of calculating dose rate

From calculating the dose rate for each position, we obtain the dose distribution with distances from the source (and compared with experimental results measured by the portable photon dose-rate meter of Inspector, USA).

Table 3. The dose distribution of 15 MeV energy photon in the direction of -$\vec{y}$.

Distance from source (cm)	Dose rate calculated by MCNP (μSv/h)	Experimentally measured dose rate (μSv/h)	Relative error in MCNP (%)	Distance from source (cm)	Dose rate calculated by MCNP (μSv/h)	Experimentally measured dose rate (μSv/h)	Relative error in MCNP (%)
5	110,343.21	110,344.00	0.37	90	1,410.20	1,413.41	1.97
10	56,315.60	56,315.89	0.52	95	1,237.54	1,240.13	2.03
15	37,842.31	37,845.24	0.63	100	944.82	945.81	2.27
20	27,793.53	27,794.47	0.71	105	860.35	864.17	2.35
25	21,688,57	21,691.88	0.79	110	795.35	797.90	2.41
30	17,070,34	17,073.75	0.86	115	640.53	641.63	2.58
35	13,876.84	13,877.02	0.92	120	568.07	570.43	2.67
40	11,231.65	11,232.15	0.99	125	520.31	522.81	2.79
45	9,372.82	9,375.81	1.05	130	455.17	456.79	2.87
50	7,717.94	7,718.87	1.11	135	397.94	398.64	3.02
55	6,527.46	6,528.24	1.18	140	373.94	377.40	3.15
60	5,527.14	5,,528.20	1.26	145	377.38	378.99	3.14
65	4,547.03	4,549.12	1.32	150	355.54	356.46	3.20
70	3,937.05	3,940.90	1.44	155	318.78	321.93	3.34
75	3,375.22	3,378.23	1.47	160	286.74	287.32	3.48
80	2,466.32	2,466.40	1.63	165	263.33	266.98	3.57
85	1,820.14	1,821.40	1.83	170	260.43	261.37	3.63

Calculation and simulation results showed consistent ones with experimental values. The measured experimentally values are negligible higher due to environmental background.

Table 4. The dose distribution of 15 MeV enery photon in the direction of -$\vec{x}$.

Distance from source (cm)	Dose rate calculated by MCNP (μSv/h)	Experimentally measured dose rate (μSv/h)	Relative error in MCNP (%)	Distance from source (cm)	Dose rate calculated by MCNP (μSv/h)	Experimentally measured dose rate (μSv/h)	Relative error in MCNP (%)
5	112,343.21	112,389.92	0.37	135	468.60	469.73	2.79
10	56,473.80	56,474.19	0.52	140	390.10	462.55	2.87
15	37,921.36	37,622.24	0.63	145	373.43	474.00	3.02
20	27,806.78	27,809.45	0.71	150	367.18	368.33	3.15
25	21,762.22	21,765.35	0.79	155	345.35	365.67	3.14
30	17,454.36	17,554.47	0.86	160	318.42	350.07	3.20
35	13,910.33	14,113.49	0.92	165	302.98	305.77	3.34
40	11,371.63	11,375.34	0.99	170	271.12	273.91	3.48
50	7,856.20	8,257.71	1.05	175	205.08	205.32	3.57
55	6,641.05	6,743.94	1.11	180	178.19	179.46	3.63
60	5,,805.07	6,307.25	1.18	185	179.83	179.88	3.80
65	5,906.42	6,008.09	1.26	190	135.90	137.90	6.96
75	3,677.65	3,681.49	1.32	195	106.56	106.67	3.81

Distance from source (cm)	Dose rate calculated by MCNP (μSv/h)	Experimentally measured dose rate (μSv/h)	Relative error in MCNP (%)	Distance from source (cm)	Dose rate calculated by MCNP (μSv/h)	Experimentally measured dose rate (μSv/h)	Relative error in MCNP (%)
80	2,918.09	3,021.71	1.40	200	113.50	113.58	3.81
85	2,033.92	2,335.25	1.47	205	112.95	112.02	3.80
90	1,873.05	1,673.97	1.63	210	108.36	108.37	4.00
95	1,532.98	1,533.65	1.83	220	106.79	106.90	4.10
100	1,184.36	1,187.53	1.97	230	98.22	98.29	4.13
105	899.28	972.56	2.03	240	90.28	90.42	4.15
110	821.45	825.15	2.27	250	81.56	81.60	4.16
115	726.86	728.32	2.35	260	69.63	69.73	5.00
120	677.42	698.95	2.41	270	53.09	53.19	5.00
125	603.71	618.96	2.58	280	43.52	43.53	5.00
130	540.37	581.54	2.67	290	26.85	26.91	5.00

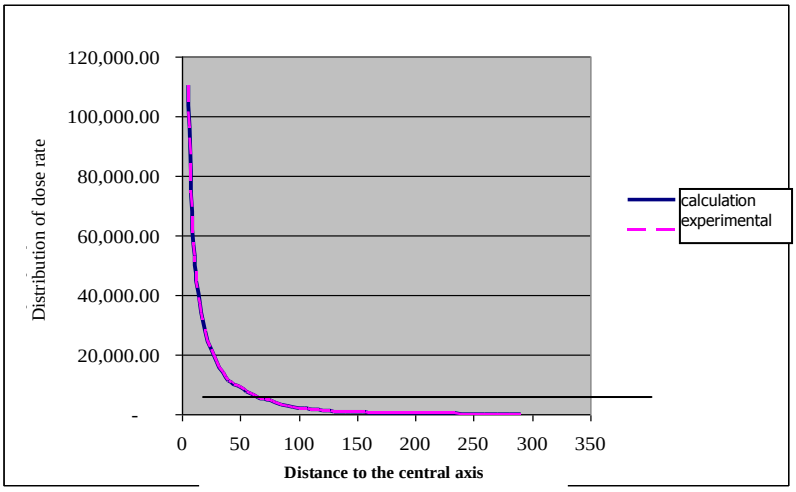

Figure 8. Graph comparison between the calculated results and experimental measurements (interpolation from Table 4).

Table 5. The dose distribution of 15 MeV energy photon in the direction of $-\vec{x}$ (in concrete).

Distances from the source (cm)	Dose rate calculations MCNP (μSv/h)	Distances from the source (cm)	Dose rate calculations MCNP (μSv/h)
300	17.3910	360	0.0094
310	12.0100	370	0.0033
320	1.0190	380	0.0021
330	0.7180	390	0.0010
340	0.0528	400	0.0007
350	0.0187	410	0.0003

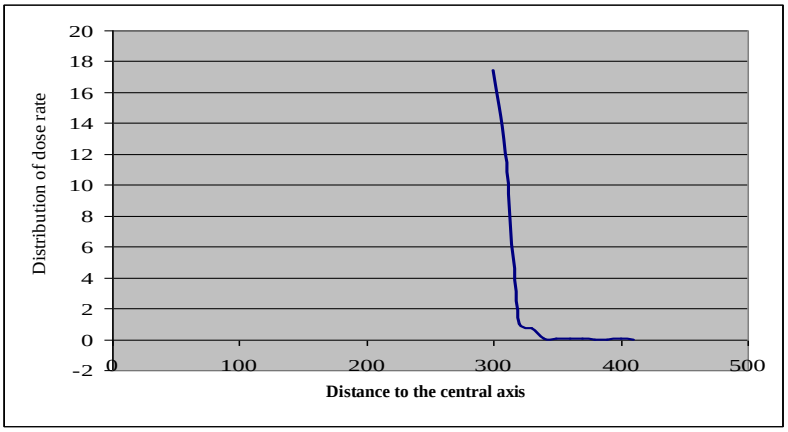

Figure 8. Graph comparison between the calculated results and experimental measurements (interpolation from Table 5).

Radiation is decreased rapidly in the concrete wall, so that the concrete shielding is in a match. The simulation of radiation and dose rate measurements can help for getting optimal shielding.

Table 6. The dose distribution of 10 MeV enery electron in the direction of $-\vec{x}$ (in concrete).

Distance from source (cm)	Dose rate calculated by MCNP (μSv/h)	Relative error in MCNP (%)	Distance from source (cm)	Dose rate calculated by MCNP (μSv/h)	Relative error in MCNP (%)	Distance from source (cm)	Dose rate calculated by MCNP (μSv/h)	Relative error in MCNP (%)
5	110,343.21	0.54	70	315.30	3.75	135	50.51	4.46
10	10,584.36	0.65	75	238.65	3.81	140	45.13	4.51
15	4,301.56	0.95	80	226.22	3.97	145	36.60	4.53
20	2,428.68	1.12	85	196.75	3.99	150	45.79	4.57
25	1,713.48	2.12	90	152.66	4.10	155	45.14	4.58
30	1,247.11	2.90	95	169.23	4.16	169	42.98	4.61
35	858.82	2.95	100	135.26	4.19	165	33.64	4.64
40	793.20	2.99	105	110.87	4.23	170	21.83	4.72
45	637.62	3.12	110	71.10	4.25	175	19.50	4.79
50	650.96	3.13	115	78.93	4.27	180	19.42	4.81
55	506.20	3.41	120	74.60	4.28	185	18.41	4.82
60	458.73	3.52	125	56.88	4.30	190	14.26	4.83
65	302.26	3.67	130	53.41	4.42	195	11.53	4.87

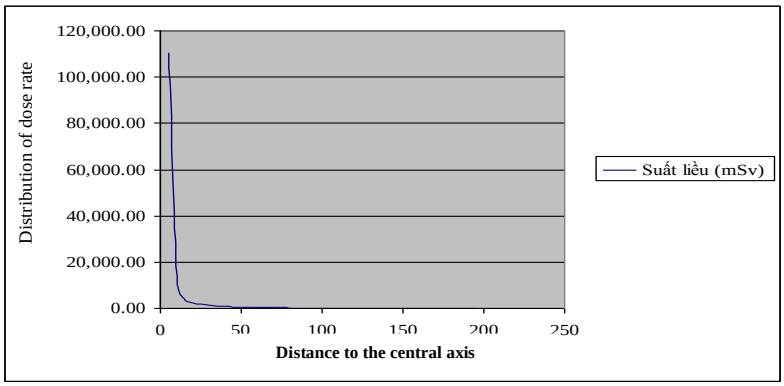

Figure 9. Graph comparison between the calculated results and experimental measurements (interpolation from Table 6).

From Figure 9 it is shown that electron dose rates are decreased rapidly with distance, due to the stronger absorption of photons..

IV. CONCLUSION

From independently simulation by the MCNP software, we obtained the results that are quite consistent with experimental measurements. This allows the user to confirm that the simulation method of calculating dose distribution for all radiation at different energy levels in all positions of inside and outside the radiation room. From that, it could establish a 3-dimension map on dose field distribution inside and outside the treatment room.

One of the important goals of our research is directed toward safety shielding calculations for radiation treatment room just to ensure radiation safety and efficiency in the highest stage of economic development, by changing thicknesses of the concrete as well as the size and structure of the room.

REFERENCES

[1]. MED AID, Inc Vietnam (2010), *Requirement of preparing Siemens Primus machine room*, 12-BT1-X2 Bac Linh Dam, Hoang Mai, Hanoi, Vietnam.
[2]. Siemens Medical Solutions USA (2003), *PRIMUS Linear Accelerator*, Ins., Siemens AG.
[3]. Los Alamos National Laboratory (2006), *MCNP/MCNPX*, Los Alamos, New Mexico.

Experimental investigation of crack in aluminum cantilever beam using vibration monitoring technique

[1,] Akhilesh Kumar, & [2,] J. N. Mahto
[1,] *(Department of Mechanical Engineering, B.I.T. Sindri)*
[2,] *(Assistant Professor, Department of Mechanical Engineering, B.I.T. Sindri)*
V. B. U. Hazaribag

ABTRACT:
It has been observed that the dynamic behaviour of a structure changes due to the presence of a crack. Analysis of such phenomena is useful for fault diagnosis and the detection of cracks in structures. An experimental setup is designed in which an aluminium cantilever beam with cracks is excited by a power exciter and accelerometer attached to the beam provides the response. The cracks are assumed to be open to avoid non-linearity. The effects of crack and positions on the fundamental frequencies of slender cantilever beams with edge cracks are investigated experimentally. The experiments are conducted using specimens having edge cracks of different depths at different positions to validate the numerical results obtained. The experimental results of frequencies can be obtained from digital storage oscilloscope (DSO).

The first three natural frequencies were considered as basic criterion for crack detection. To locate the crack, 3D graphs of the normalized frequency in terms of the crack depth and location are plotted. The intersection of these three contours gives crack location and crack depth. Out of several case studies conducted the results of one of the case study is presented to demonstrate the applicability and efficiency of the method suggested.

Index term: - *Cantilever Beam, Oscilloscope, Power Oscillator, Vibration Exciter, Accelerometer etc.*

I. INTRODUCTION

The interest in the ability to monitor a structure and detect damage at the earliest possible stage is pervasive throughout the civil, mechanical and aerospace engineering communities. Current damage-detection methods are either visual or localized experimental methods such as acoustic or ultrasonic methods, magnet field methods, radiographs, eddy-current methods or thermal field methods. All of these experimental techniques require that the vicinity of the damage is known a priori and that the portion of the structure being inspected is readily accessible. Subjected to these limitations, these experimental methods can detect damage on or near the surface of the structure. The need for additional global damage detection methods that can be applied to complex structures has led to the development of methods that examine changes in the vibration characteristics of the structure. Damage or fault detection, as determined by changes in the dynamic properties or response of structures, is a subject that has received considerable attention in the literature. The basic idea is that modal parameters (notably frequencies and mode shapes) are functions of the physical properties of the structure. Therefore, changes in the physical properties will cause changes in the modal properties. Ideally, a robust damage detection scheme will be able to identify that damage has occurred at a very early stage, locate the damage within the sensor resolution being used, provide some estimate of the severity of the damage, and predict the remaining useful life of the structure. The method should also be well-suited to automation. To the greatest extent possible, the method should not rely on the engineering judgment of the user or an analytical model of the structure. A less ambitious, but more attainable, goal would be to develop a method that has the features listed above, but that uses an initial measurement of an undamaged structure as the baseline for future comparisons of measured response. Also, the methods should be able to take into account operational constraints. For example, a common assumption with most damage- identification methods reported in the technical literature to date is that the mass of the structure does not change appreciably as a result of the damage. However, there are certain types of structures such as offshore oil platforms where this assumption is not valid. Another important feature of damage-identification methods, and specifically those methods which use prior models, is their ability to discriminate between the model/data discrepancies caused by modeling errors and the discrepancies that are a result of structural damage. The effects of damage on a structure can be classified as

linear or nonlinear. A linear damage situation is defined as the case when the initially linear-elastic structure remains linear-elastic after damage. The changes in modal properties are a result of changes in the geometry and/or the material properties of the structure, but the structural response can still be modeled using a linear equation of motion. Nonlinear damage is defined as the case when the initially linear-elastic structure behaves in a nonlinear manner after the damage has been introduced. One example of nonlinear damage is the formation of a fatigue crack that subsequently opens and closes under the normal operating vibration environment. Other examples include loose connections that rattle and nonlinear material behavior. A robust damage-detection method will be applicable to both of these general types of damage. The majority of the papers summarized in this review address only the problem of linear damage detection.

1.1 PRESENT AIM OF WORK

For conducting the experiment, first of all we will be preparing the machine setup. This machine is already available in the market, but our aim is to prepare this machine using some conventional machining methods, so that we can have a machine at a cheap rate. The machine will be measuring the vibration response of the aluminum solid beam. Vibration response will be taken through beam with the help of oscilloscope.

II. LITERATURE REVIEW

2.1 PRESENT WORK

For the literature review primarily various journals selected. The brief reviews of these papers are as follow.

Scott W. et. al.[1] Studied this report contained a review of the technical literature concerning the detection, location, and characterization of structural damage via techniques that examine changes in measured structural vibration response. The report was first categorizes the methods according to required measured data and analysis technique. The analysis categorized includes changes in modal frequencies, changes in measured mode shapes and changes in measured flexibility coefficients. Methods that use property (stiffness, mass, damping) matrix updating, detection of nonlinear response, and damage detection via neural networks are also summarized.

Prasad Ramchandra Baviskar et. al.[2] This paper addressed the method of multiple cracks detection in moving parts or beams by monitoring the natural frequency and prediction of crack location and depth using Artificial Neural Networks (ANN). Determination of crack properties like depth and location is vital in the fault diagnosis of rotating machine equipments. For the theoretical analysis, Finite Element Method (FEM) is used wherein the natural frequency of beam is calculated whereas the experimentation is performed using Fast Fourier Transform (FFT) analyzer. In experimentation, simply supported beam with single crack and cantilever beam with two cracks are considered. The experimental results are validated with the results of FEM (ANSYSTM) software. This formulation can be extended for various boundary conditions as well as varying cross sectional areas. The database obtained by FEM is used for prediction of crack location and depth using Artificial Neural Network (ANN). To investigate the validity of the proposed method, some predictions by ANN are compared with the results given by FEM. It is found that the method is capable of predicting the crack location and depth for single as well as two cracks. This work may be useful for improving online conditioning and monitoring of machine components and integrity assessment of the structures.

Lee et. al.[3] presented a method to detect a crack in a beam. The crack was not modeled as a mass less rotational spring, and the forward problem was solved for the natural frequencies using the boundary element method. The inverse problem was solved iteratively for the crack location and the crack size by the Newton-Raphson method. The present crack identification procedure was applied to the simulation cases which use the experimentally measured natural frequencies as inputs, and the detected crack parameters are in good agreements with the actual ones. The present method enables one to detect a crack in a beam without the help of the mass less rotational spring model.

Rizos et. al.[4] Modeled the crack as a mass less rotational spring, whose stiffness was calculated using fractures mechanics. He also conducted experiments to detect crack depth and location from changes in the mode shapes of cantilever beams. A major disadvantage of using mode shape based technique is that obtaining accurate mode shapes involves arduous and meticulous measurement of displacement or acceleration over a large number of points on the structure before and after damage. The accuracy in measurement of mode shapes is highly dependent on the number and distribution of sensors employed.

Owolabi et. al.[5] used natural frequency as the basic criterion for crack detection in simply supported and fixed-fixed beams. The method suggested has been extended to cantilever beams to check the capability and efficiency. There is need to see if this approach can be used for fixed-free beams.

Kisa et. al.[6] The vibration characteristics of a cracked Timoshenko beam are analyzed. The study integrates the FEM and component mode synthesis. The beam divided into two components related by a flexibility matrix which incorporates the interaction forces. The forces were derived from fracture mechanics

expressions as the inverse of the compliance matrix is calculated using stress intensity factors and strain energy release rate expressions.

III. EXPERIMENTAL SETUP

3.1 MODEL DESCRIPTION

Aluminum beams were used for this experimental investigation. The setup consisted of 64 beam models with the fixed-free ends. Each beam model was of cross-sectional area 16mm X 16 mm with a length of 450 mm from fixed end. It had the following material properties: Young's modulus, E=70GPa, density, ρ=2700Kg/m 3, the Poisson ratio, μ=0.33.

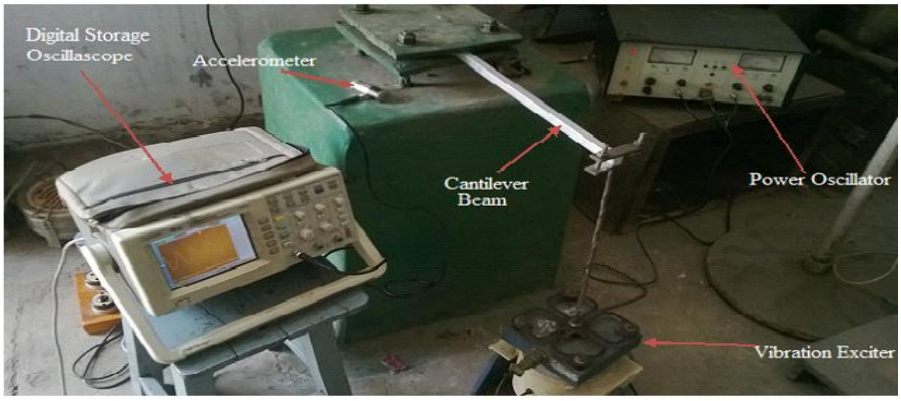

Fig: - 1. Experimental Setup

3.2 METHODOLOGY

The fixed–free beam model was clamped at one end, between two thick rectangular steel plates. The beam was excited with a vibration exciter. The first three natural frequencies of the un-cracked beam were measured. Then, cracks were generated to the desired depth using hexa blade. The crack always remained open during dynamic testing total 64 beam models were tested with cracks at different locations starting from a location near to fixed end. The crack depth varied from 2mm to 10mm at each crack position. Each model was excited by vibration exciter. This served as the input to the system. It is to be noted that the model was excited at a point, which was a few millimeters away from the center of the model. This was done to avoid exciting the beam at a nodal point. Since the beam would not respond for that mode at that point. The dynamic responses of the beam model were measured by using accelerometer placed on the model as indicated in Fig. 1. The response measurements were acquired, one at a time, using the digital storage oscilloscope (DSO).

IV. RESULTS AND DISCUSSION

4.1 RESULTS

The experimental data from the curve-fitted results were tabulated, and plotted (in a three dimensional plot) in the form of frequency ratio (ω_c/ω) (ratio of the natural frequency of the cracked beam to that of the un-cracked beam) versus the crack depth (a) for various crack location (X). Tables 1-3 show the variation of the frequency ratio as a function of the crack depth and crack location for beams with fixed-free ends.

4.2 CHANGES IN NATURAL FREQUENCY

Fig. 2 to 4 shows the plots of the first three frequency ratios as a function of crack depths for some of the crack positions. Fig.5 to Fig.7 shows the frequency ratio variation of three modes in terms of crack position for various crack depths respectively. From Fig.2 it is observed that, for the cases considered, the fundamental natural frequency was least affected when the crack was located at 360mm from fixed end. The crack was mostly affected when the crack was located at 40mm from the fixed end. Hence for a cantilever beam, it could be inferred that the fundamental frequency decreases significantly as the crack location moves towards the fixed end of the beam. This could be explained by the fact that the decrease in frequencies is greatest for a crack located where the bending moment is greatest. It appears therefore that the change in frequencies is a function of crack location. From Fig.3 it is observed that the second natural frequency was mostly affected for a crack located at the center for all crack depths of a beam due to the fact that at that location the bending moment is having large value. The second natural frequency was least affected when the crack was located at 360mm from fixed end. From Fig.4 it is observed that the third natural frequency of beam changed rapidly for a crack located at 250 mm. The third natural frequency was almost unaffected for a crack located at the center of a cantilever beam; the reason for this zero influence was that the nodal point for the third mode was located at the center of beam

TABLE: - 1 Fundamental Natural Frequency Ratio (Ω_c/Ω) As A Function Of Crack Location (X) And Crack Depth (A)

x	a=2mm	a=4mm	a=5mm	a=6mm	a=7mm	a=8mm	a=9mm	a=10mm
40mm	0.9859	0.9286	0.8998	0.8699	0.8232	0.7736	0.7214	0.6725
100mm	0.9862	0.9325	0.9101	0.8778	0.8465	0.7863	0.7446	0.6969
150mm	0.9911	0.9621	0.9326	0.8998	0.8665	0.8126	0.7864	0.75
200mm	0.9925	0.9587	0.9262	0.9046	0.8821	0.8629	0.8156	0.7956
220mm	0.983	0.97	0.9565	0.9256	0.9121	0.8956	0.8524	0.8259
250mm	0.9962	0.9762	0.9746	0.9598	0.9498	0.9356	0.9021	0.8835
300mm	0.9991	0.9897	0.9762	0.9746	0.9729	0.9721	0.9682	0.9571
360mm	1	1	1	1	1	1	1	1

TABLE:-2 Second Natural Frequency Ratio (ω_c/ω) As A Function Of Crack Location (X) And Crack Depth (a)

x	a=2mm	a=4mm	a=5mm	a=6mm	a=7mm	a=8mm	a=9mm	a=10mm
40mm	0.9911	0.9452	0.9125	0.8878	0.8489	0.8056	0.7582	0.7102
100mm	0.9931	0.9685	0.9425	0.9285	0.9189	0.9111	0.9052	0.8954
150mm	1	0.9512	0.9256	0.918	0.8803	0.8214	0.7689	0.7123
200mm	0.9937	0.9568	0.9365	0.921	0.8956	0.8521	0.7925	0.7532
220mm	0.9869	0.9765	0.971	0.9536	0.9214	0.8654	0.8452	0.8215
250mm	0.9978	0.9834	0.9705	0.9612	0.9622	0.9478	0.9389	0.9245
300mm	0.9998	0.987	0.9756	0.9702	0.9635	0.9486	0.9325	0.9246
360mm	0.9989	0.9986	0.9889	0.9898	0.9863	0.9721	0.9598	0.9563

TABLE:-3 Third Natural Frequency Ratio (ω_c/ω) As A Function Of Crack Location (X) And Crack Depth (a)

x	a=2mm	a=4mm	a=5mm	a=6mm	a=7mm	a=8mm	a=9mm	a=10mm
40 mm	0.9989	0.9465	0.9045	0.8756	0.8256	0.7732	0.6987	0.6423
100 mm	0.9931	0.9563	0.9456	0.9178	0.8849	0.8598	0.8127	0.7896
150 mm	0.991	0.9512	0.9298	0.9056	0.8569	0.8026	0.7258	0.6489
200 mm	0.9921	0.9789	0.9569	0.9365	0.8951	0.8465	0.8024	0.7598
220 mm	0.9927	0.9751	0.9632	0.9421	0.9287	0.8961	0.8365	0.7893
250 mm	0.9997	0.9758	0.9711	0.9589	0.9425	0.9245	0.8869	0.8456
300 mm	0.9982	0.9863	0.9681	0.9427	0.9156	0.8879	0.8462	0.8169
360 mm	0.9961	0.9911	0.9724	0.9568	0.9398	0.9285	0.9153	0.8896

From Fig.5 it is observed that, for the cases considered, the fundamental natural frequency was least affected when the crack depth was 6mm. The crack was mostly affected when the crack depth was 10mm. Hence for a cantilever beam, it could be inferred that the fundamental frequency decreases significantly as the crack depth increase to 61% of beam depth. This could be explained by the fact that the decrease in frequencies is greatest for a more crack depth because as more material gets removed the stiffness of the beam decrease and hence the natural frequency. It appears therefore that the change in frequencies is a function of crack depth also.

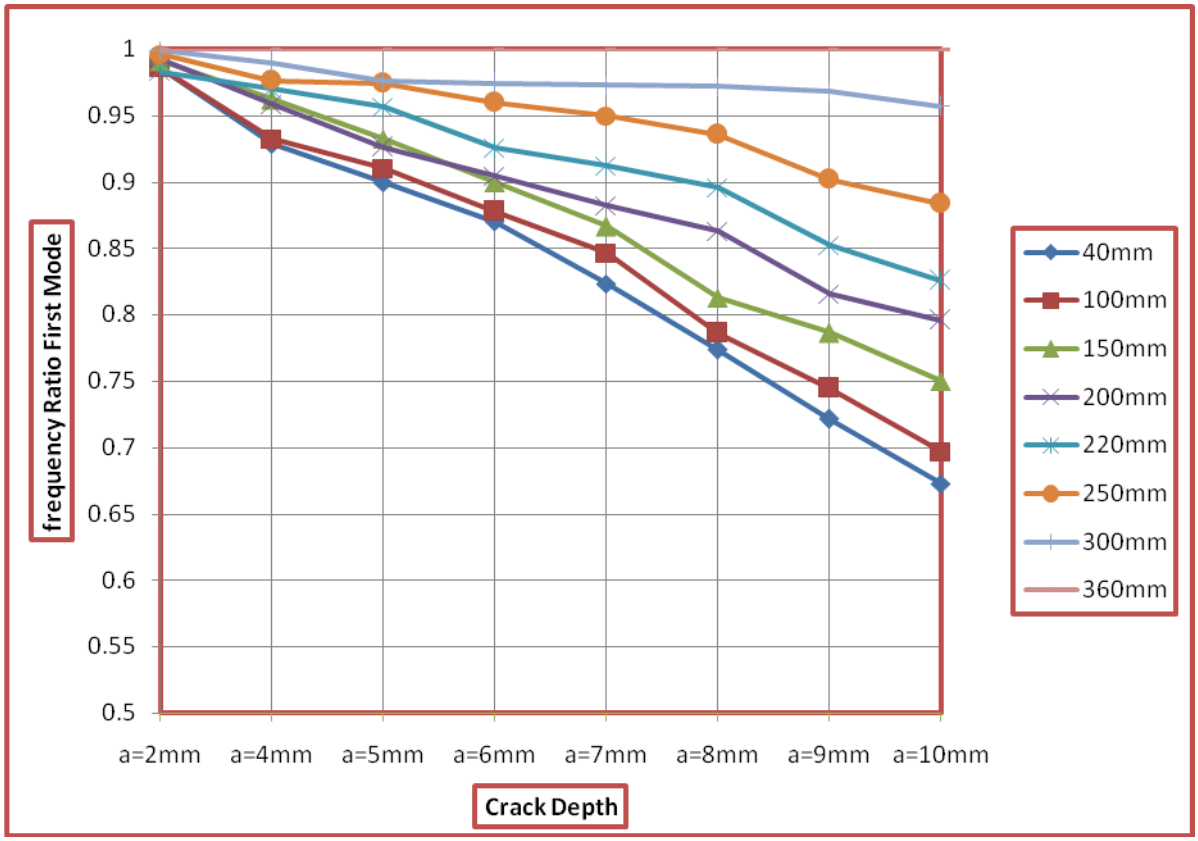

Fig.2. Fundamental natural frequency ratio in terms of crack depth for various crack positions

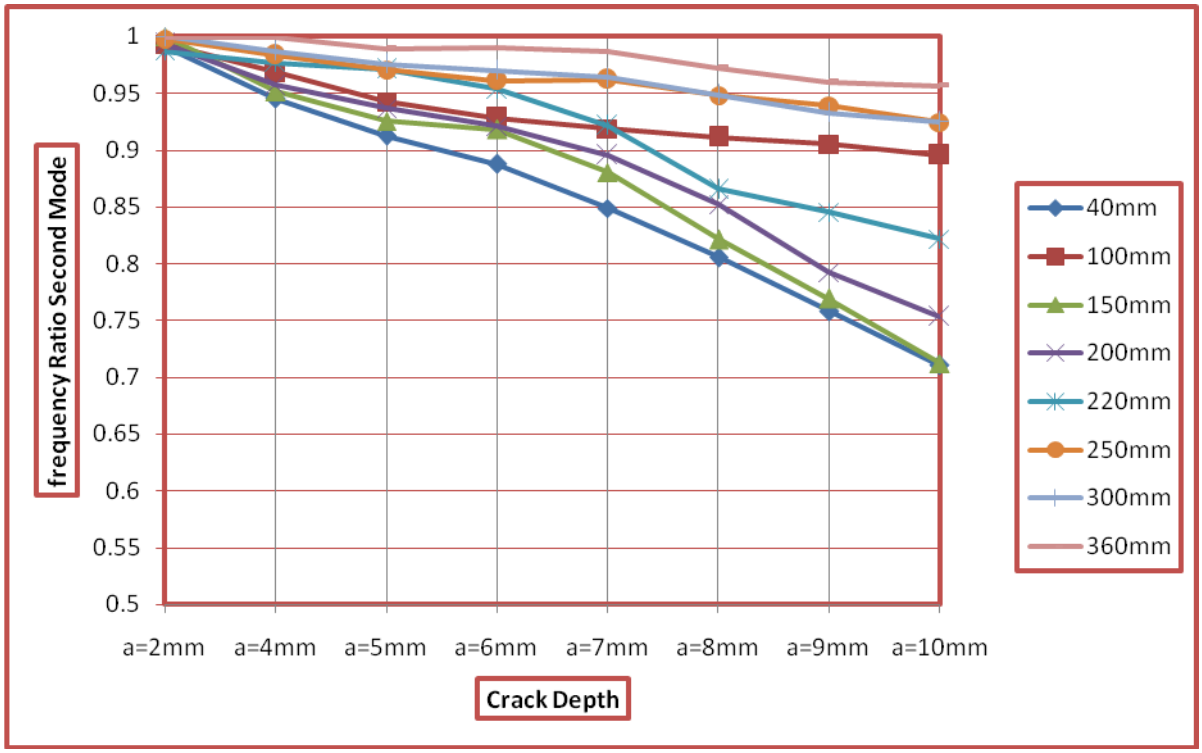

Fig.3. Second natural frequency ratio in terms of crack depth for various crack positions

From Fig.6 it is observed that the second natural frequency was mostly affected for a crack depth of 10mm at the crack location 150mm. The second natural frequency was least affected when the crack depth was 10mm. From Fig.7 it is observed that the third natural frequency of beam changed rapidly for a crack depth of 10mm. Third natural frequency was remained unaffected when crack depth was 6mm. Third natural frequency was remained unchanged at crack locations 55mm, 220mm, and 300mm due to the presence of node point at that position. Fig.8 to Fig.10 show the three dimensional plots of Normalized Frequency versus Crack Location and Crack Depth for first, second and third mode respectively for crack location of 250mm and crack depth of 6mm. To get these three dimensional plots. In Fig.8 to Fig.10, the contour line is not present due to the presence of node points.

4.3 CRACK IDENTIFICATION TECHNIQUE USING CHANGES IN NATURAL FREQUENCIES

As stated earlier, both the crack location and the crack depth influence the changes in the natural frequencies of a cracked beam. Consequently, a particular frequency could correspond to different crack locations and crack depths. This can be observed from the three-dimensional plots of the first three natural frequencies of cantilever beams as shown in Fig.8 to Fig.10. On this basis, a contour line, which has the same normalized frequency change resulting from a combination of different crack depths and crack locations (for a particular mode) could be plotted in a curve with crack location and crack depth as its axes.

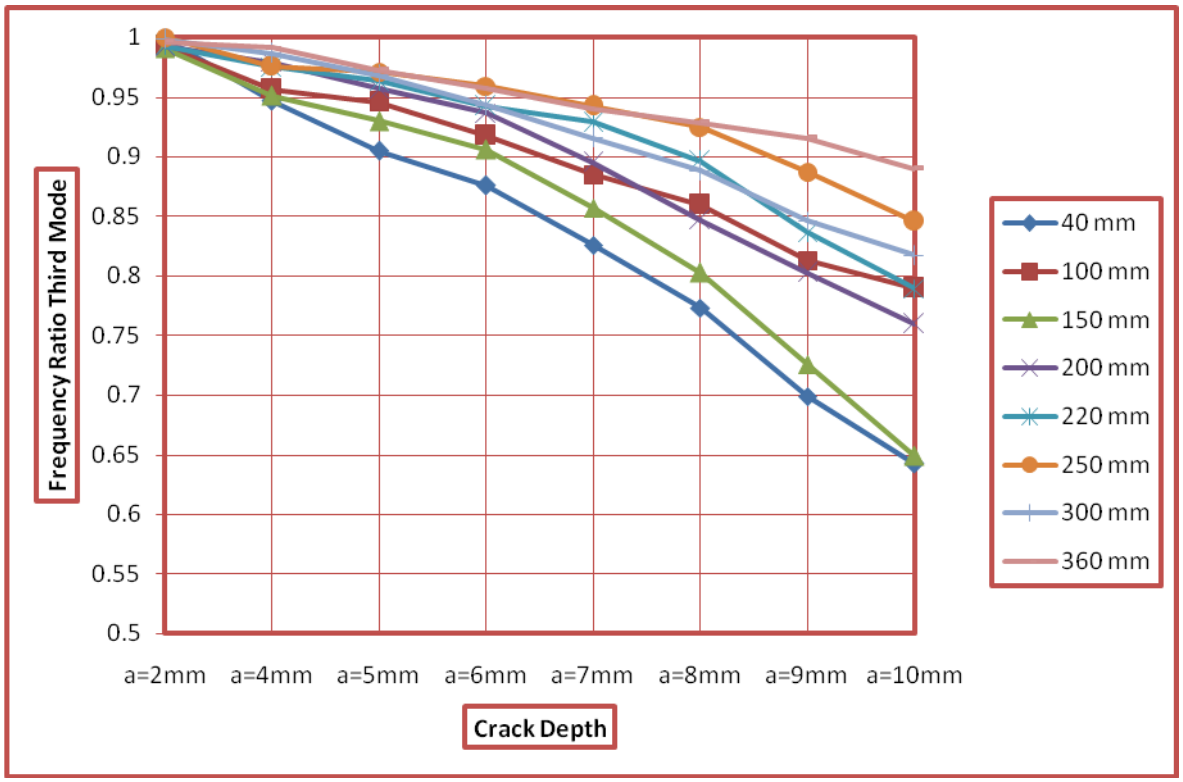

Fig.4. Third natural frequency ratio in terms of crack depth for various crack positions

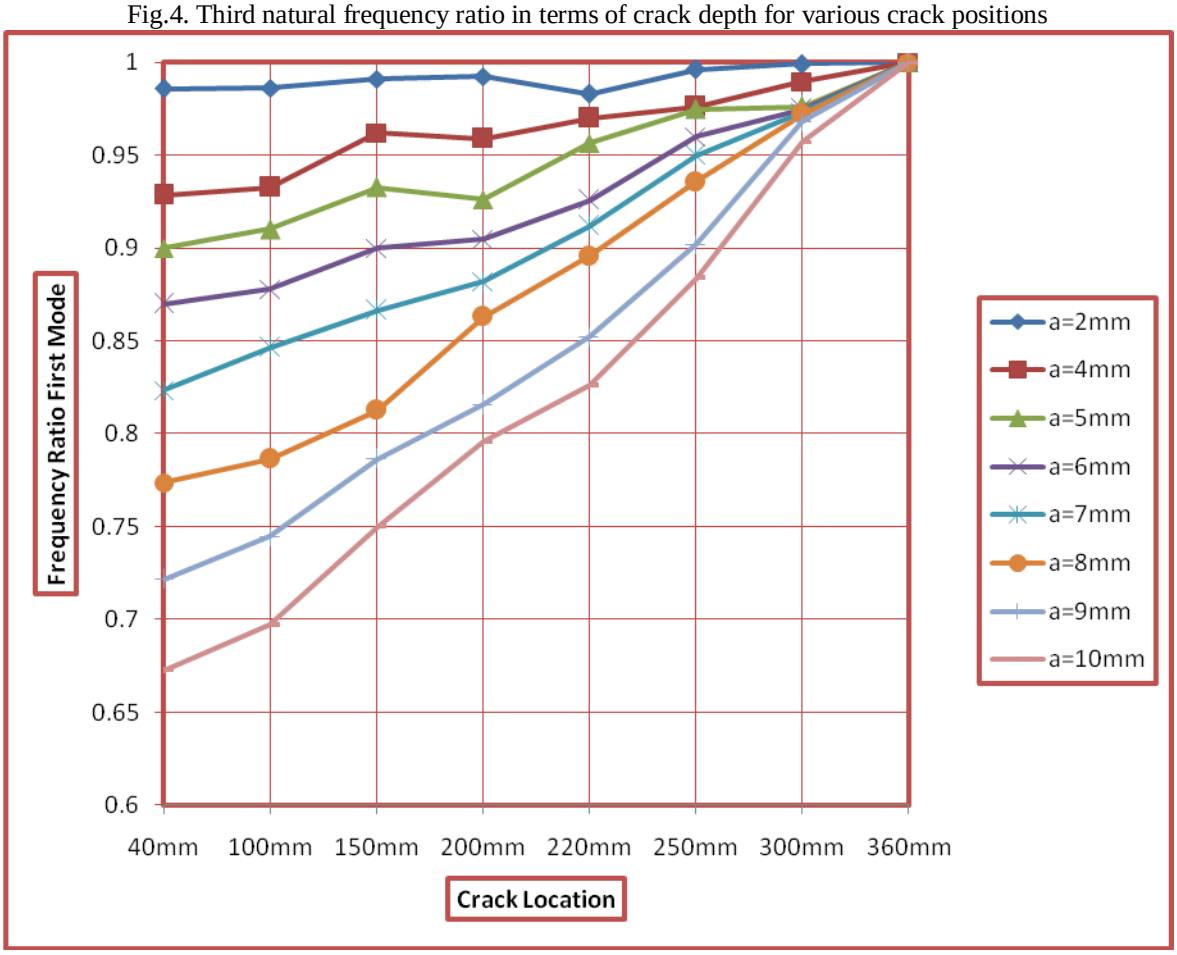

Fig.5. First Mode Frequency Ratio in Terms of Crack Position for Various Crack Depths

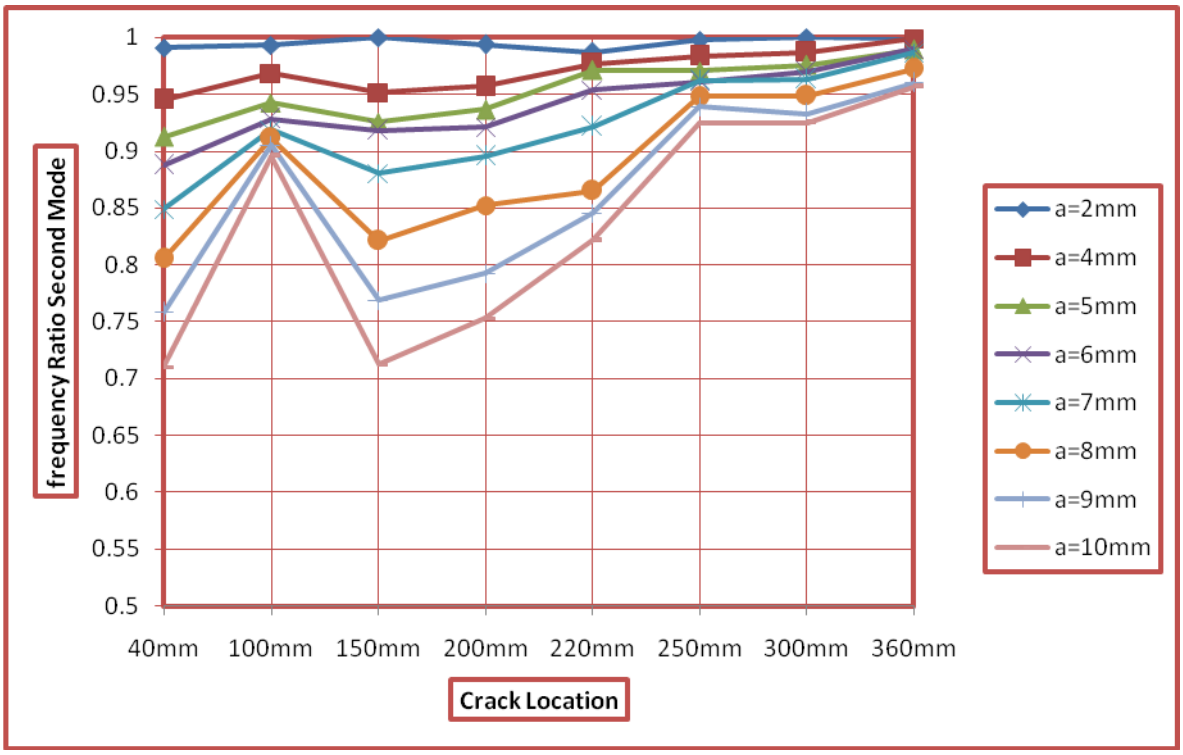

Fig.6. Second Mode Frequency Ratio in Terms of Crack Position for Various Crack Depths

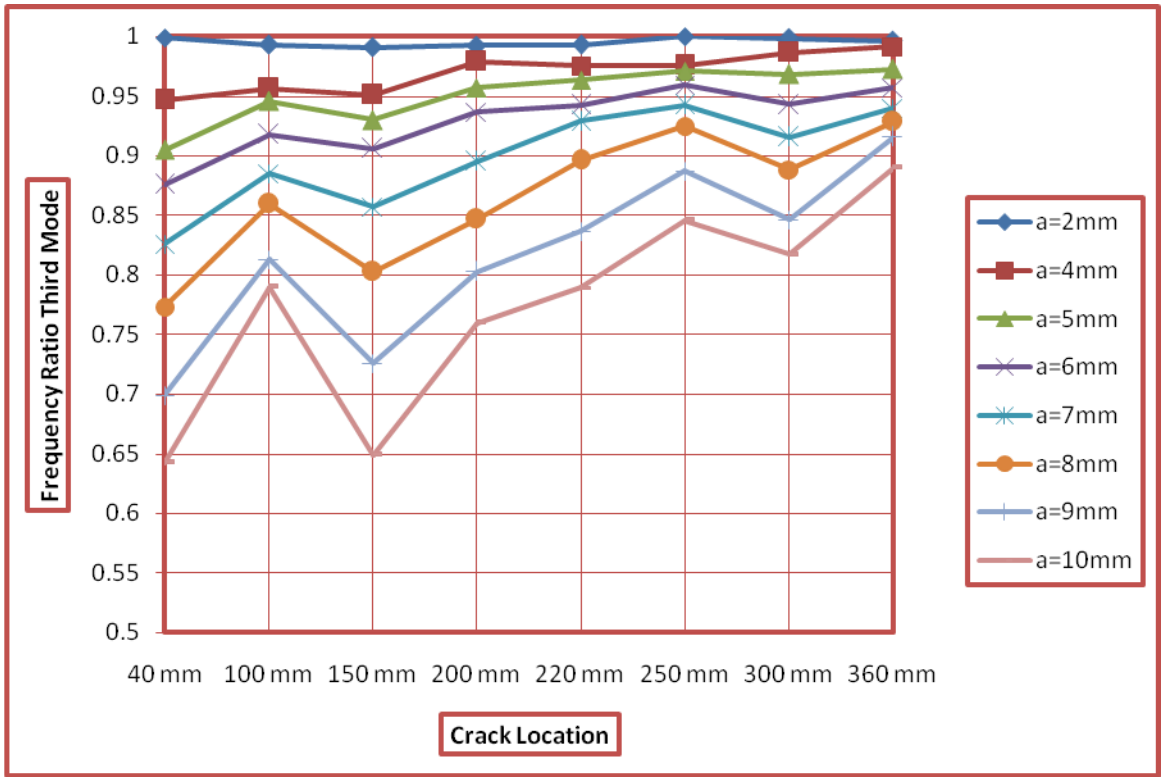

Fig.7. Third Mode Frequency Ratio in Terms of Crack Position for Various Crack Depths

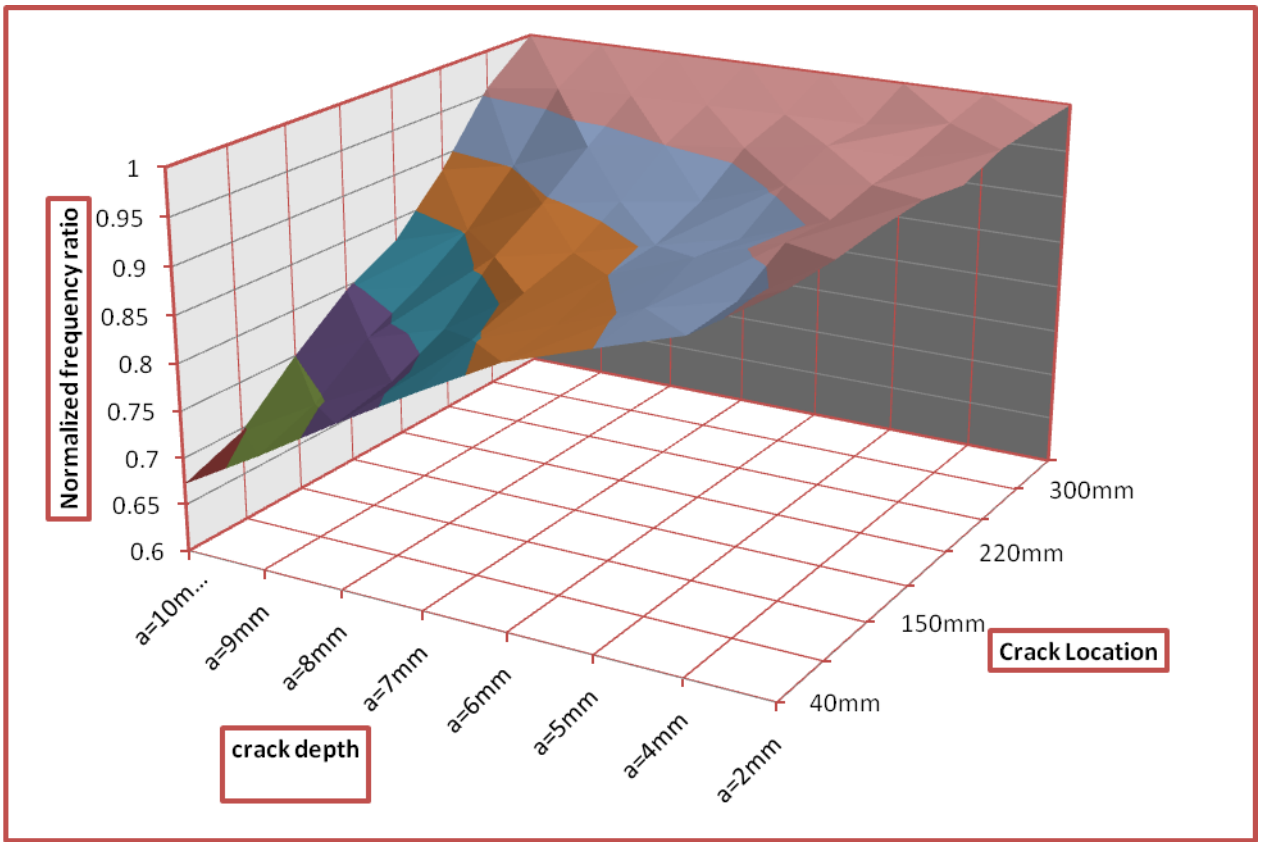

Fig.8. Three-dimensional plot with contour lines of normalized natural frequency versus crack location and crack depth for first mode for crack location of 250mm and crack depth of 6mm

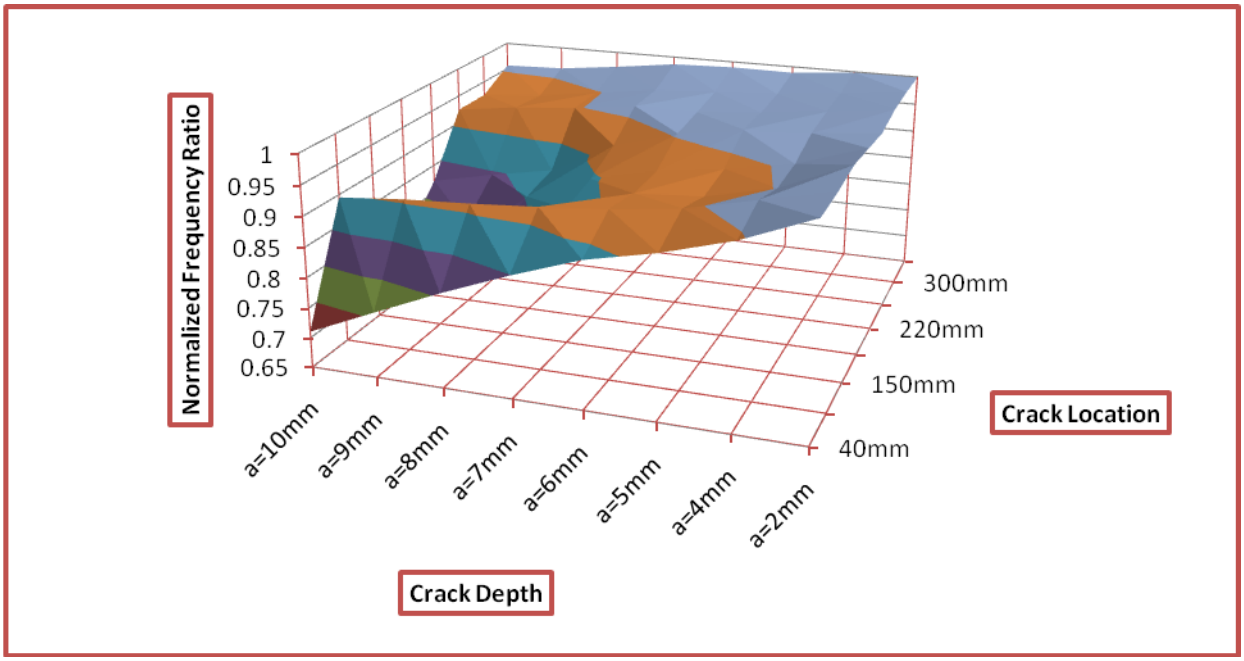

Fig.9. Three-dimensional plot with contour lines of normalized natural frequency versus crack location and crack depth for second mode for crack location of 250mm and crack depth of 6mm

For a beam with a single crack with unknown parameters, the following steps are required to predict the crack location, and depth, namely, (1) measurements of the first three natural frequencies; (2) normalization of the measured frequencies; (3) plotting of contour lines from different modes on the same axes; and (4) location of the point(s) of intersection of the different contour lines. The point(s) of intersection, common to all the three modes, indicate(s) the crack location, and crack depth. This intersection will be unique due to the fact that any normalized crack frequency can be represented by a governing equation that is dependent on crack depth (a), crack location (X). Therefore a minimum of three curves is required to identify the two unknown parameters of crack location and crack depth.

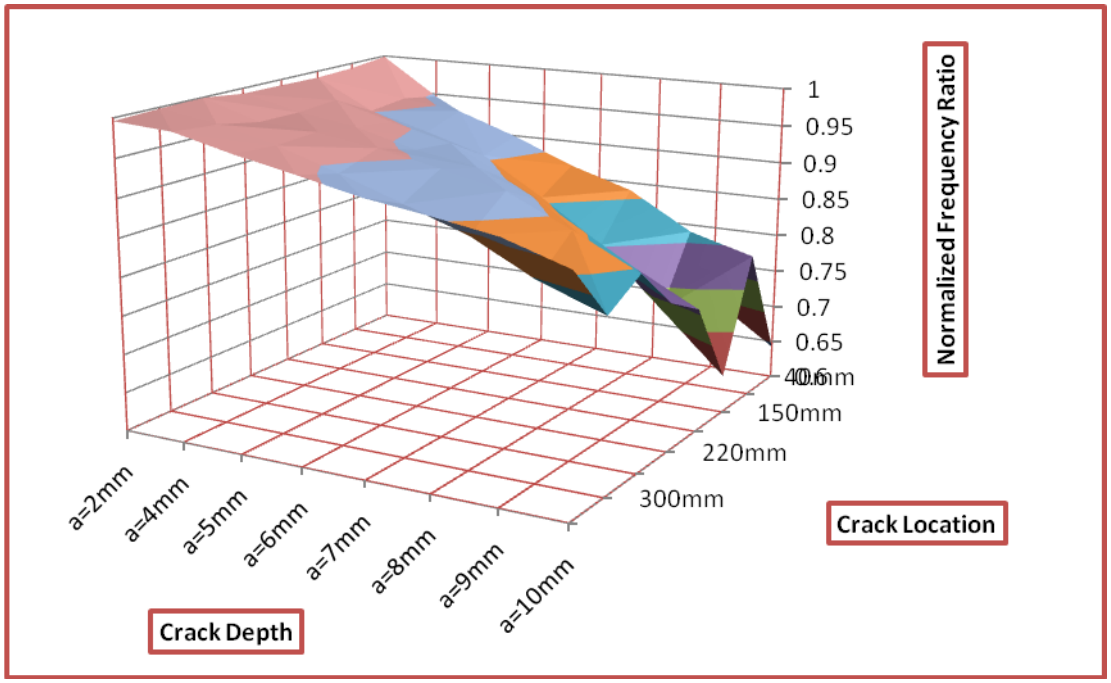

Fig.10. Three-dimensional plot with contour lines of normalized natural frequency versus crack location and crack depth for third mode for crack location of 250mm and crack depth of 6mm

From Tables 1-3, it is observed that for a crack depth of 6mm located at a distance of 250mm from fixed end of the beam, the normalized frequencies are 0.9598 for the first mode, 0.9612 for the second mode and 0.9589 for the third mode. The contour lines with the values of 0.9598, 0.9612 and 0.9589 were retrieved from the first three modes with the help of MINITAB software as shown in Fig.11 to Fig.13 and plotted on the same axes as shown in Fig.14. From the Fig.14 it could be observed that there are two intersection points in the contour lines of the first and the second modes. Consequently the contour of the third mode is used to identify the crack location (X=250mm) and the crack depth (a=6mm), uniquely. The three contour lines gave just one common point of intersection, which indicates the crack location and the crack depth. Since the frequencies depend on the crack depth and location, these values can be uniquely determined by the solution of a function having solutions one order higher (in this case, three) than the number of unknowns (in this case, two, namely crack depth and location) to be determined. This is the reason for the requirement of three modes. If there were more parameters that influence the response (besides the crack depth and location), then one will require more modes to identify the unknown crack depth and crack location.

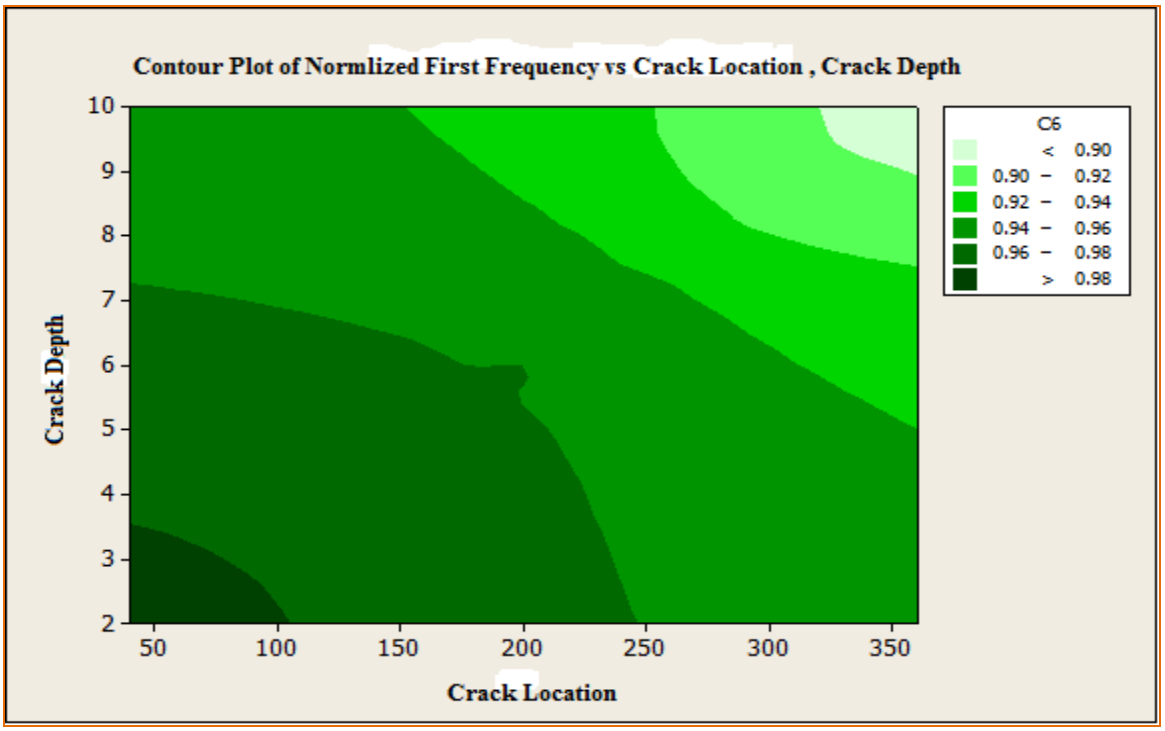

Fig.11. Frequency contour plot of mode-1 for normalized frequency 0.9598

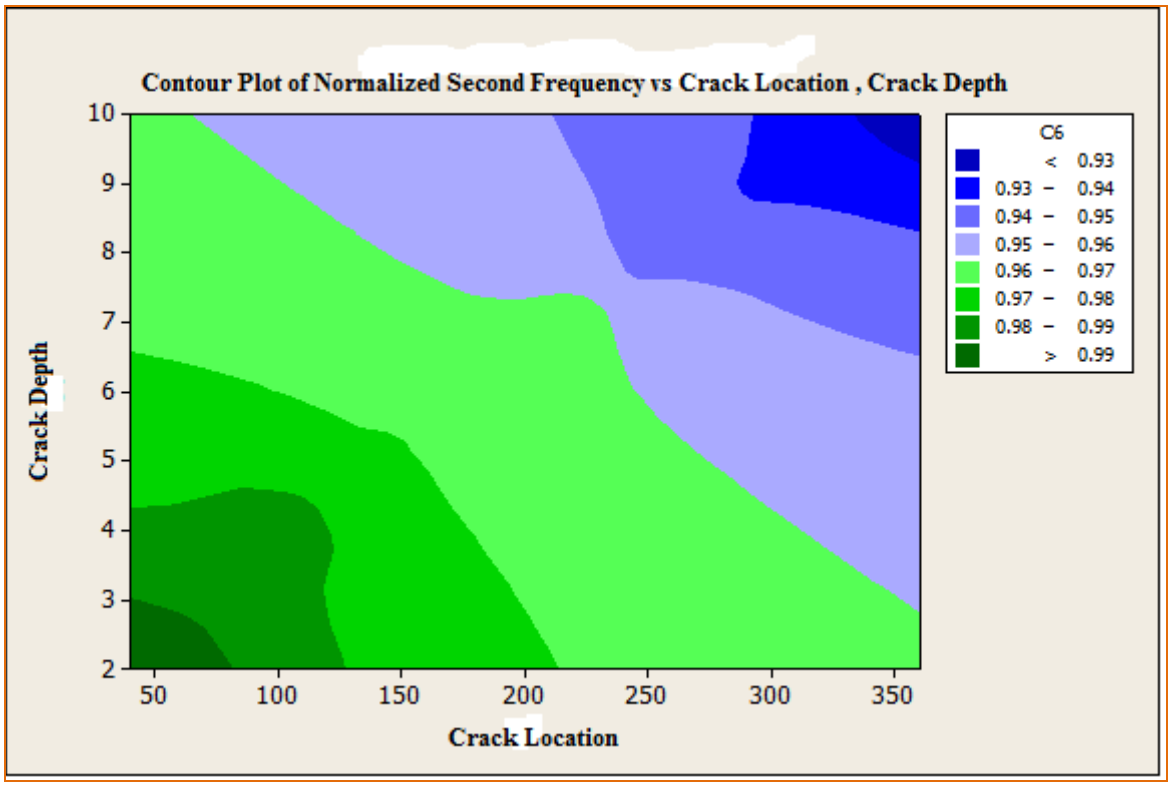

Fig.12. Frequency contour plot of mode-2 for normalized frequency 0.9612

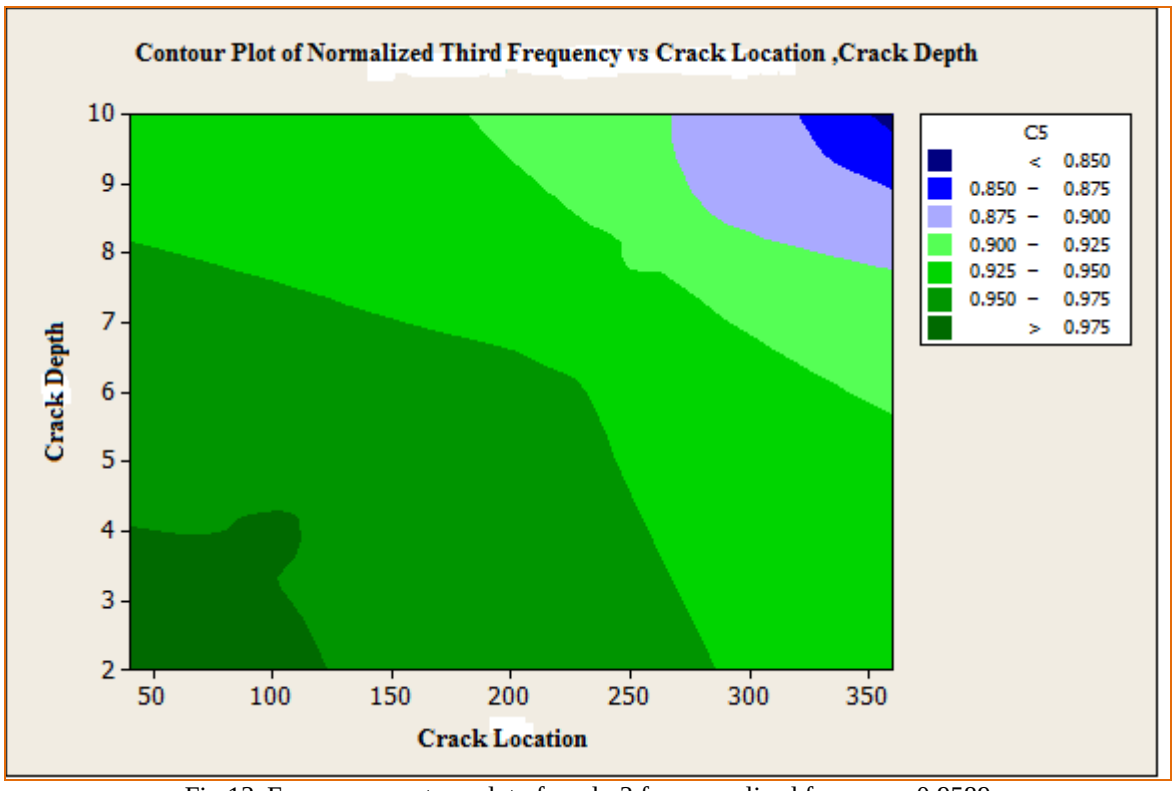

Fig.13. Frequency contour plot of mode-3 for normalized frequency 0.9589

V. CONCLUSIONS

Detailed experimental investigations of the effects of crack on the first three modes of vibrating cantilever beams have been presented in this paper. From the results it is evident that the vibration behavior of the beams is very sensitive to the crack location, crack depth and mode number. A simple method for predicting the location and depth of the crack based on changes in the natural frequencies of the beam is also presented, and discussed. This procedure becomes feasible due to the fact that under robust test and measurement conditions, the measured parameters of frequencies are unique values, which will remain the same (within a tolerance level), wherever similar beams are tested and responses measured. The experimental identification of crack location and crack depth is very close to the actual crack size and location on the corresponding test specimen.

The following conclusions were drawn:-

1. With the presence of crack in the beam the frequency of vibration decreases.
2. The above information can be used to predict the failure of beam as well as shaft and preventive steps can be taken.

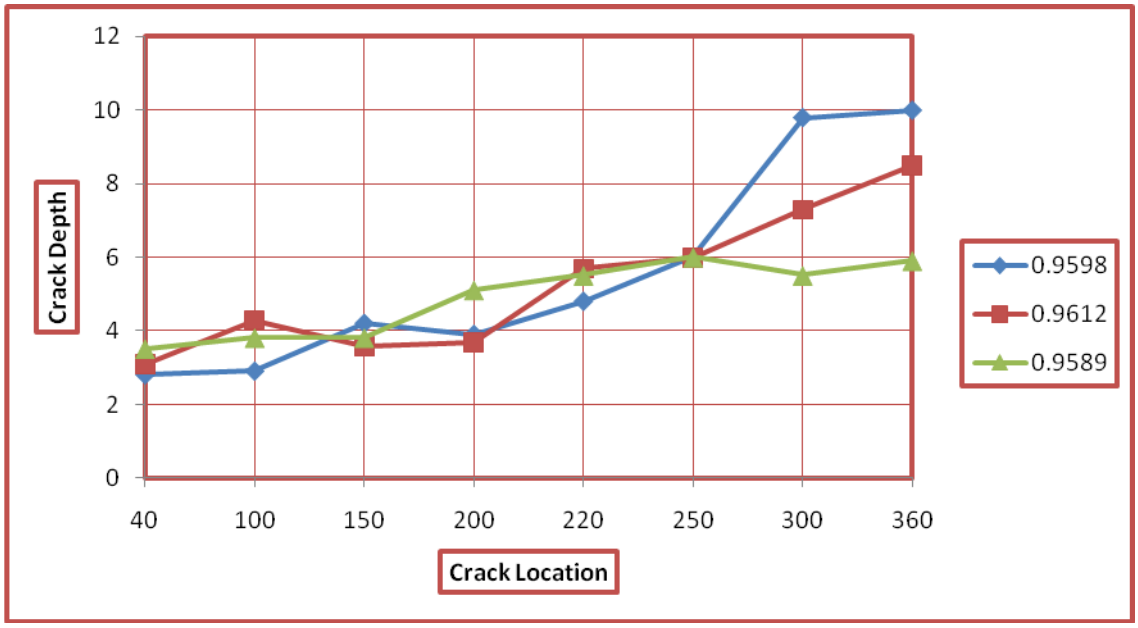

Fig.14. Crack identification technique by using frequency contours of the first three modes of beam (mode 1, normalized frequency (0.9598); mode 2, normalized frequency (0.9612); and 3: mode 3, normalized frequency (0.9589).

REFERENCE:-

[1]. *Scott W "Damage Identification and Health Monitoring of Structural and Mechanical Systems from Changes in Their Vibration Characteristics" A Literature Review LA-13070-MS UC-900 Issued: May 1996.*

[2]. *Prasad Ramchandra Baviskar, "Multiple Cracks Assessment using Natural Frequency Measurement and Prediction of Crack Properties by Artificial Neural Network" International Journal of Advanced Science and Technology Vol. 54, May, 2013.*

[3]. *J. Lee, "Identification of a crack in a beam by the boundary element method", Journal of Mechanical Science and Technology, vol. 24 (3), pp. 801-804, 2010.*

[4]. *Rizos R.F., N.Aspragathos, A.D.Dimarogonas, (1990), Identification of crack location and magnitude in a cantilever beam from the vibration modes, Journal of Sound and Vibration 138(3) 381–388.*

[5]. *G.M. Owolabi, A.S.J. Swamidas, R. Seshadri, "Crack detection in beams using changes in frequencies and amplitudes of frequency response functions", Journal of Sound and Vibration, vol. 265 (1), pp. 1–22, 2003.*

[6]. *M. Kisa, J. Brandon and M. Topcu, Free vibration analysis of cracked beams by a combination of finite elements and component mode synthesis methods, Computers and Structures, 67, (1998), 215-223.*

[7]. *A.D.Dimarogonas, "Vibration of cracked structures: a state of the art review", Engineering Fracture Mechanics, vol. 55, pp. 831-857, 1996.*

[8]. *A.V.Deokar, V.D.Wachaure, ", Experimental Investigation of Crack Detection in Cantilever Beam Using Natural Frequency as Basic Criterion", 08-10 DECEMBER, 2011.*

[9]. *H. Nahvi, M. Jabbari, "Crack detection in beams using experimental modal data and finite element model", International Journal of Mechanical Sciences 47 (2005) 1477–149.*

Inter-image Anatomical Correspondence and Automatic Segmentation of bones by Volumetric Statistical Modelling of knee MRI

Meenaz H. Shaikh
Electronics & Telecommunication
VIT, Mumbai University

Anuradha Joshi
Electronics & Telecommunication
VIT, Mumbai University

Shraddha Panbude
Electronics & Telecommunication
VIT, Mumbai University

Abstract:
One of the challenging problem in Osteoarthritis is detecting the cartilage loss due to the disease progression. The sensitivity of detection from 3D MR images can be improved significantly by focusing on regions of 'at risk' cartilage has been shown, defined consistently across subjects and time-points. We define these regions in a frame of reference based on the bones, which requires that the bone surfaces are segmented in each image, and that anatomical correspondence is established between these surfaces. Results have shown that this can be achieved automatically using surface-based Active Appearance Models (AAMs) of the bones. In this paper, by building a volumetric (set of surface) appearance model, we are describing a method of refining the segmentations and correspondences with the help of flowcharts and algorithms. We present results from the experiments carried out from this method on MRI knee images using surface AAM which comes out to be more precise for the volumetric AM for the bones than that of the single surface model.

Keywords: *Active Appearance Model (AAM), Active Contour Model, MRI, Search Model, Osteoarthritis, Segmentation.*

I. INTRODUCTION

Segmentation of anatomical objects from large three dimensional (3-D) medical data sets, obtained from routine Magnetic Resonance Imaging (MRI) examinations, for example, represents a necessary yet difficult issue in medical image analysis. With the steady increase of routine use of 3-D imaging methods such as MRI, computer tomography (CT), and 3-D ultrasound in radiological diagnosis, monitoring, radiotherapy, and surgical planning, for example, there is a clear need for improved and efficient methods for the extraction of anatomical structures and for a description by morphometric analysis [1]. In some limited applications, segmentation can be achieved with minimal user interaction by applying simple and efficient image processing methods, which can be applied routinely.

Quantitative analysis of cartilage from high field strength MR images is recognised as a potential biomarker for measuring Osteoarthritis (OA) disease progression and efficacy of disease modifying treatments. OA is a slowly progressing disease and loss of cartilage is difficult to detect over reasonably short timescales. Sensitivity to cartilage loss can be achieved in cohort studies by focusing on 'at risk' regions which are consistent between time-points and across subjects.

In this paper we present an improvement on the surface AAM approach for automatically segmenting the bones and establishing anatomical correspondence between images. The method constructs an Appearance Model of the whole image volume (*Volumetric AM*) which provides a mean reference image and a mapping of correspondence points from the mean image to each of the study images. The volumetric AM approach offers operational advantages compared to the surface AAMs, and possible performance benefits. Unlike the surface AM, the method does not require a training set of manual segmentations of the bones in order to construct the model – just one manual bone segmentation is required, for the mean model image. Identifying the regions of high stress, likely to experience changes in cartilage thickness, is simplified, because reference can be made to the both the mean bone shape and to soft tissue landmarks which are also visible in the mean model image [2].

Our results demonstrate that the volumetric AM provides more accurate segmentations of the bones, as assessed by applying this technique to the set of surfaces obtained from 3d MR images on MRI knee images using surface AAM.

II. METHOD

This section describes an efficient method for generating maps of cartilage thickness and volume for the tibia and the femur. Fig. 1 gives a schematic description of the steps involved in tracking cartilage changes over time.

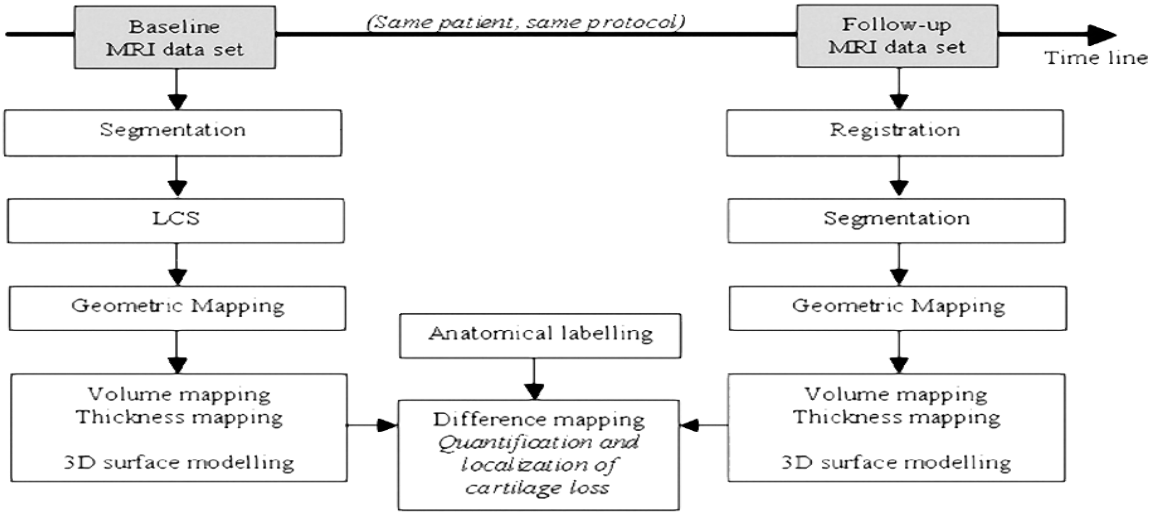

Fig. 1. Schematic Representation

2.1. Active Contour Models

Describe flexible contour models which are attracted to image features. These energy minimizing spline curves are modeled as having stiffness and elasticity and are attracted toward features such as lines and edges. Constraints can be applied to ensure that they remain smooth and to limit the degree to which they can be bent. Snakes can be considered as parameterized models, the parameters being the spline control points. They are usually free to take almost any smooth boundary with few constraints on their overall shapes. The idea of fitting by using image evidence to apply forces to the model and minimizing an energy function is effective.

2.2. Piecewise Linear Image Transformation

A function or operator that takes an image as its input and produces an image as its output. Depending on the transform chosen, the input and output images may appear entirely different and have different interpretations.

2.3. Shape of Model

Make the Shape model, which finds the variations between contours in the training data sets. Computing a shape model from the position of the correspondences in all of the images performing piece-wise affine warping of all of the images to the mean shape and computing a texture model for the registered images computing the best-fit of the shape model to each of the example images and modifying the positions of the correspondences in each example image to minimize the cost of encoding the image using the current model The optimization strategy used three levels of image resolution and employed a course-to-fine regime for manipulating the correspondences at each resolution. The patella, distal femur and proximal tibia bones were segmented in each slice of the mean model image using the End Point software package. In addition, the location of other image landmarks, such as the bones' contact points and extent of the maniacal windows, were marked on the slice segmentations. Closed surface triangular mesh representations of the mean bones were constructed from the parallel slice segmentations providing 60,456 39,238 and 11,808 points on the femur, tibia and patella surfaces respectively. Anatomical regions of interest were drawn on the mean bone shapes using a 3D annotation tool, using both shape and image landmark cues, following the definitions suggested by Eckstein:

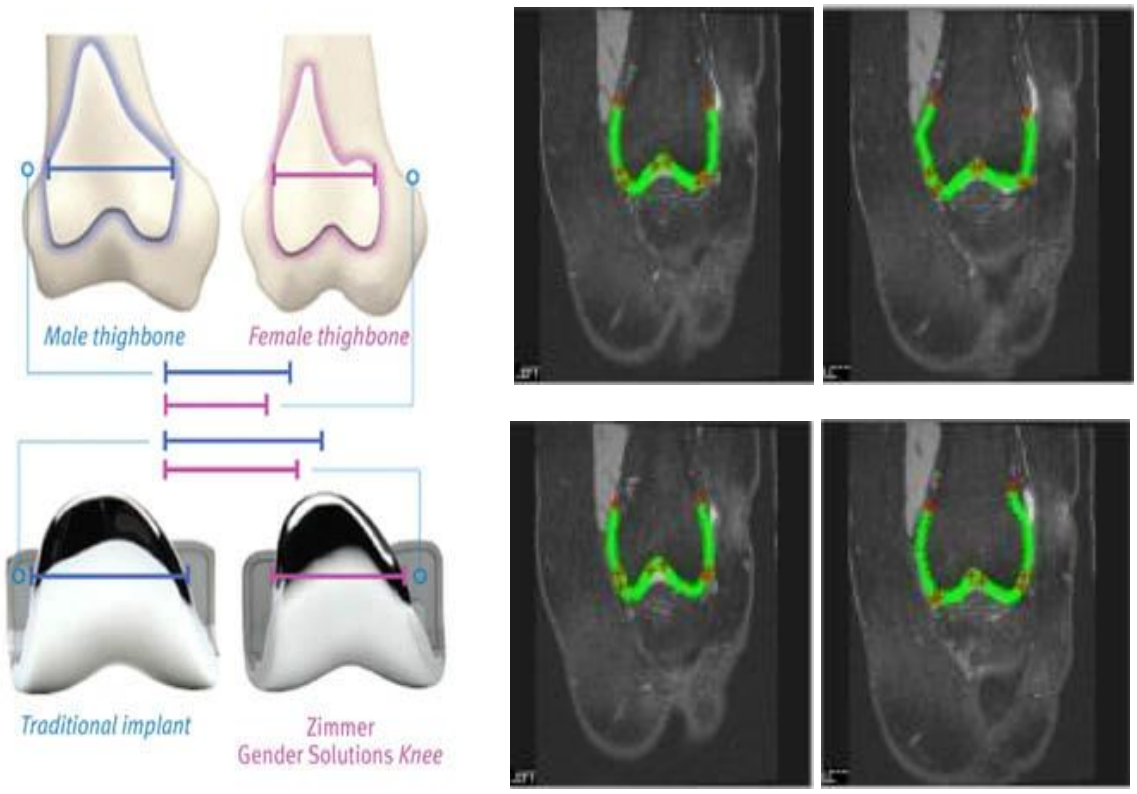

Fig. 2. Shape of the Model

2.4. Search Model

The Search Model is used to find the object location and shape-appearance parameters, in a test set. Training is done by displacing the Model and translation parameters with a known amount, and measuring the error, between the intensities form the real image, and those intensities described by the model.

The found error correlations are used to make the inverse model which gives the optimal parameter update and new location when you input the error vector with difference between model and real intensities.

The objective of knee joint arthroplasty is to eliminate pain and to maintain or restore knee stability and the best possible joint mobility. Until recently, it has often proved difficult to attain these goals, above all to retain them over a long period of time. However, to preserve or restore normal kinematics, the tensioning of the ligaments should be coordinated, and as little bone as possible should be resected; thus, knee joint arthroplasty has become even more elaborate in terms of surgical techniques and requires increasingly sophisticated instruments.

2.5. Combined Model

Often Shape and Texture are correlated in some way. Thus we can use PCA to get a combined Shape-Appearance model.

Principal component analysis (Karhunen-Loeve or Hotelling transform) - PCA belongs to linear transforms based on the statistical techniques. This method provides a powerful tool for data analysis and pattern recognition which is often used in signal and image processing as a technique for data compression, data dimension reduction or their decorrelation as well. There are various algorithms based on multivariate analysis or neural networks that can perform PCA on a given data set. Presented paper introduces PCA as a possible tool in image enhancement and analysis.

Following are the flowcharts (Fig. 3 and Fig. 4) depicting the subdivision process for total area and femoral area of subchondral bone (tAB) and cartilage surface area (AC) in the tibia [3], [4].

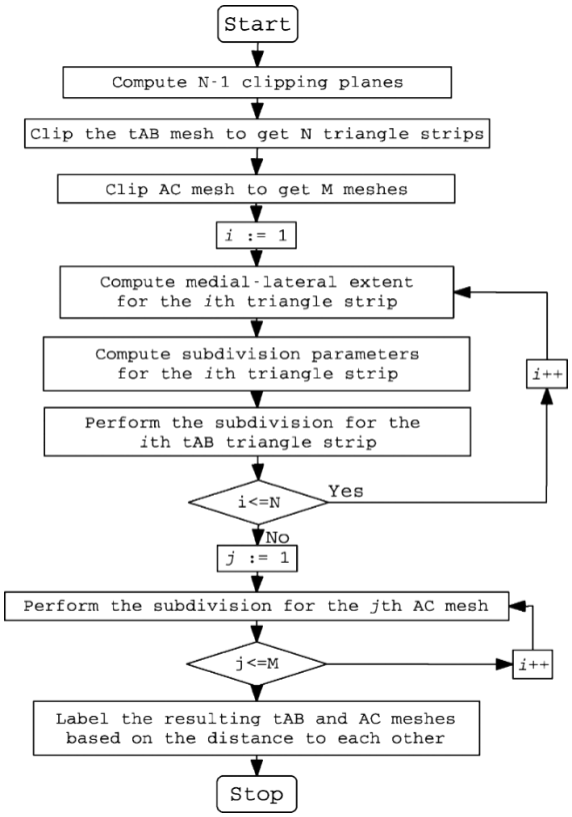

Fig. 3. Flowchart depicting the subdivision process for total area of subchondral bone (tAB) and cartilage surface area (AC) in the tibia.

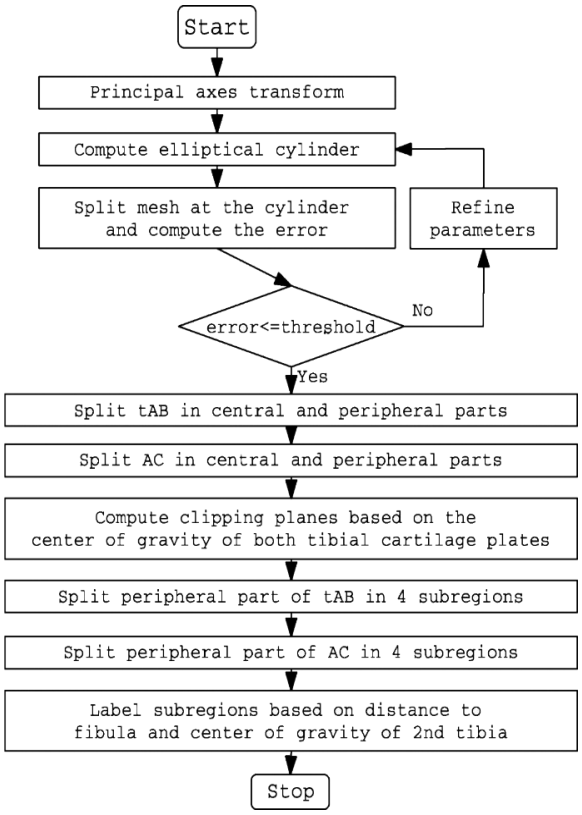

Fig. 4. Flowchart depicting the subdivision process for femoral area of subchondral bone (tAB) and cartilage surface area (AC).

III. RESULTS

The techniques described above were used in application of medical. Here we show results using the Knee models described earlier. Fig. 5 shows the four images which has been used as input. Fig. 6 shows the images for detection of knee bones and after analyzing those images and combining the models we get the concluding results as shown in fig. 7.

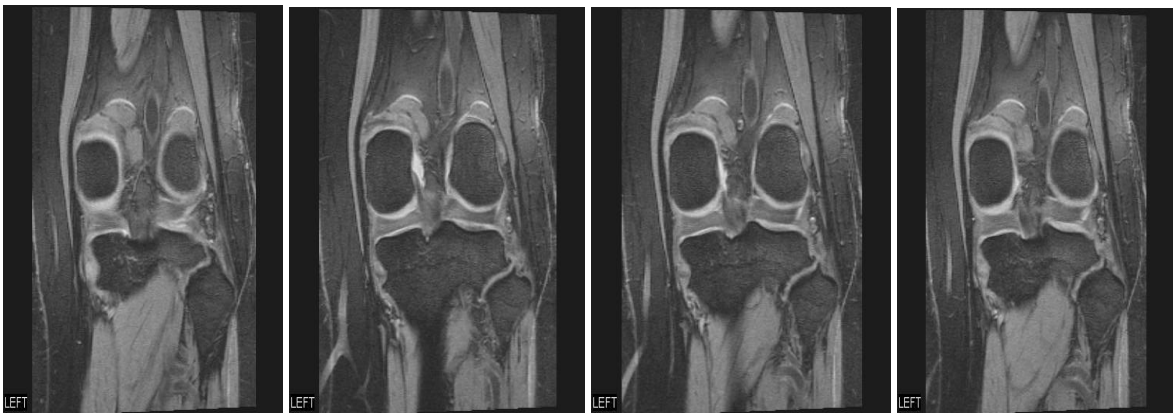

Fig. 5.

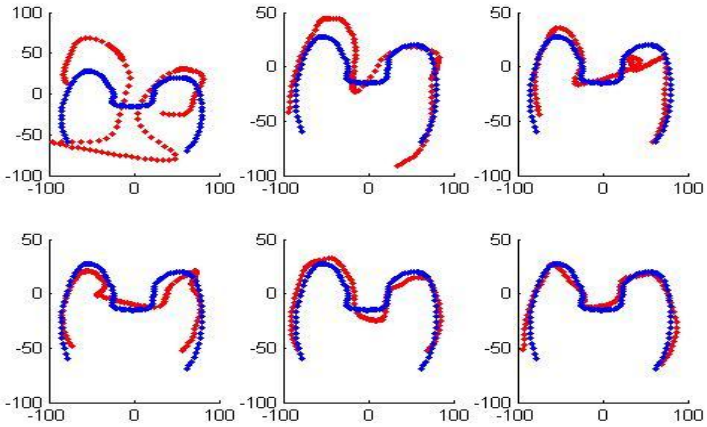

Fig. 6.

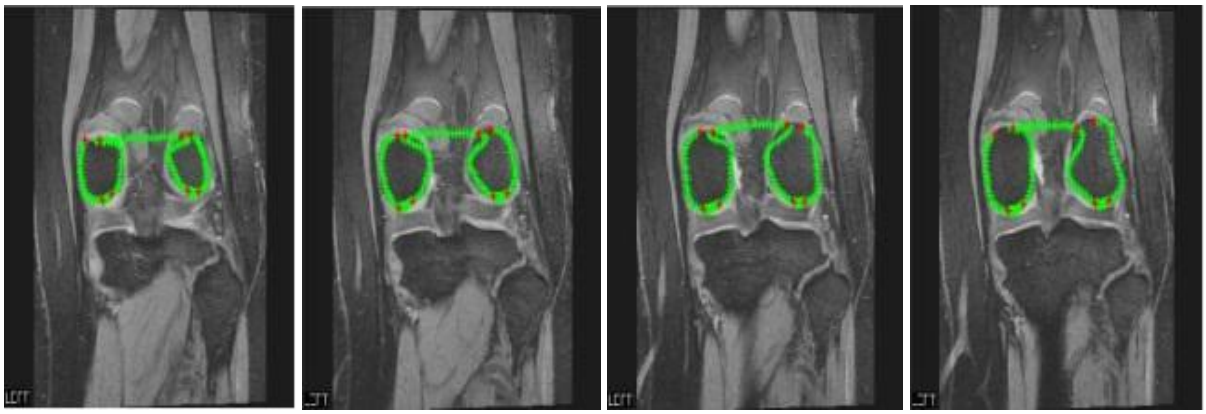

Fig. 7.

IV. CONCLUSION

In this paper we described the construction of a volumetric AM to refine the inter-image correspondence provided by surface AAMs. Finding and describing the object in a test image, using the multi scale model. We start with the mean shape on the location, and use the search model to find the Knee location, shape and appearance.

The results demonstrate that the volumetric AM approach improves the accuracy of the bone segmentations, compared to the surface AAM. Moreover, the volumetric AM also provides robustness and is able to segment smaller structures, such as the patella bone, which was not possible using the surface-based AAM approach. This is due to the volumetric AM's ability to locate the patella in relation to the other structures within the image. Results on reproducibility of regional mean thickness measures indicate that the volumetric AM provides better intra-subject reproducibility across multiple images, indicating that longitudinal measures of change in cartilage thickness are likely to be more sensitive.

REFERENCES

[1] Robert Toth; Anant Madabhushi, "Multifeature Landmark-Free Active Appearance Models: Application to Prostate MRI Segmentation", IEEE Transactions on Medical Imaging, vol. 31, no. 8, August 2012.

[2] Martin A. Lindquist; Cun-Hui Zhang; Gary Glover; Lawrence Shepp; Qing X. Yang, "A Generalization of the Two-Dimensional Prolate Spheroidal Wave Function Method for Nonrectilinear MRI Data Acquisition Methods", IEEE Transactions on Image Processing, vol. 15, no. 9, September 2006.

[3] Wolfgang Wirth; Felix Eckstein, "A Technique for Regional Analysis of Femorotibial Cartilage Thickness Based on Quantitative Magnetic Resonance Imaging", IEEE Transactions on Medical Imaging, vol. 27, no. 6, June 2008.

[4] Tomos G. Williams; "Automatic Segmentation of Bones and Inter-Image Anatomical Correspondence by Volumetric Statistical Modelling of Knee MRI", IEEE ISBI 2010.

An Experimental Investigation on the Effect of Ggbs & Steel Fibre in High Performance Concrete

M. Adams Joe[1], A. Maria Rajesh[2]

[1]Associate Professor, Dept. of Civil Engineering, TREC, Nagercoil, Tamilnadu, India
[2]Assistant Professor, Dept. of Civil Engineering, ACEW, Nagercoil, Tamilnadu, India

ABSTRACT

The present paper focuses on investigating characteristics of M40 concrete with Various propotional of replacement of cement with Ground Granulated Blast furnace Slag (GGBS) and adding 1% of steelfibre. High Performance Concrete (HPC) is a concrete meeting special combinations of performance and uniformity requirements that cannot be always achieved routinely by using conventional constituent sand normal mixing. This leads toexamine the admixtures to improve the performance of the concrete. Considering costof construction also drawn the attention of investigators to explore new replacements of ingredients of concrete. Ten mixes were studied with GGBS & Steel Fibre using a water binder ratio of 0.35 and super plasticizer CONPLAST SP-430. The cubes, cylinders and prisms were tested for both Compressive, Split tensile, Flexural and Pull out strengths GGBS can enhance the durability aspects of HPC compared to control mix. Among the mixes the mix with replacement level as 0%,10%,20%,30%,40% & 50% of GGBS and 1% steel fibre is better with respect to strength and durability. Concrete is a mixture of cement, fine aggregate, coarse aggregate and water. It is found that by the 40% replacement of cement with GGBS and steel fibre helped in improving the strength of the concrete substantially compared to Control concrete.

Keywords: *High Performance Concrete (HPC), Ground Granulated Blast furnace Slag (GGBS), Steel Fibre.*

I. INTRODUCTION

Concrete has been the major instrument for providing stable and reliable infrastructure since the days of the Greek and roman civilization. Concrete is a mixture of cement, water, and aggregates, with or without admixtures. Only for special applications the concrete grade can be increased to 40 Mpa and above. These special applications of high performance concrete (HPC) cannot be achieved by Ordinary Portland Cement (OPC). It is achieved not only by reducing water cement ratio but also by replacement of cement with some mineral admixture like Silica fume, Ground Granulated Blast Furnace Slag (GGBS), Metakaolin and Fly ash etc with chemical admixtures.

II. EXPERIMENTAL INVESTIGATION

2.1 Materials used

Ordinary Portland cement, 43 Grade conforming to IS:8112-1989[4].The specific gravity of cement was **3.15.**

2.1.1 Fine aggregate

Locally available river sand conforming to Grading zone II of IS: 383 1970[5].Its specific gravity was 2.56.

2.1.2 Coarse aggregate

Locally available crushed blue granite stones conforming to graded aggregate of nominal size 20 mm as per IS: 383 – 1970

2.1.3 Ground Granulated Blast Slag (GGBS)

Ground granulated blast furnace slag obtained from Nandi Steel, Bangulore . Ground granulatedblast-furnace slag is the granular material formed when molten iron blast furnace slag is rapidlychilled (quenched) by immersion in water. It is a granular product with very limited crystalformation, is highly cementitious in nature and, ground to cement fineness, and hydrates like portland cement.

2.1.4 Super Plasticizer

A commercially available sulphonated naphthalene formaldehyde based super plasticizer (CONPLAST SP 430) was used as chemical admixture to enhance the workability of the concrete.

2.1.5 Steel fiber (SF)

Corrugated steel fibres of aspect ratio 100:1 is used.

2.2Mix Proportion and Mix details

In this investigations IS Mix Design is adopted for Proportioning of Concrete Mix M40.This code presents a generally applicable method for selecting mixture proportion for high strength concrete and optimizing this mixture proportion on basis of trial

Adopting mix proportional are 1 : 1.09 : 1.89 : 0.35

2.3Test Specimens and Test procedure

The concrete cubes of 150mm size, cylinders of size 150mm diameter and 300mm length and prism 500 X 100 X 100 mm size were used as test specimens to determine the compressive strength of concrete and split tensile strength and Flexural strength of concrete for the both cases i.e. normal concrete and modified concrete. The ingredients of concrete were thoroughly mixed till uniform consistency was achieved. The cubes and cylinders were properly compacted. All the mixes were prepared by mixing the concrete in laboratory mixer along with water and super plasticizer

III. RESULTS AND DISCUSSIONS

The compressive strength of concrete was determined at the age of 28 days. The specimens were cast and tested as per IS: 516-1959.

Table: 1 Comp. Strength @ 28 days

Mix	% of GGBS	% of Cement	Steel Fibre	% of Super plasticizer	Comp. Strength @ 28 days
M1	0	100	1	2	41.55
M2	10	90	1	2	42.60
M3	20	80	1	2	45.85
M4	30	70	1	2	50.45
M5	40	60	1	2	56.85
M6	50	50	1	2	52.7

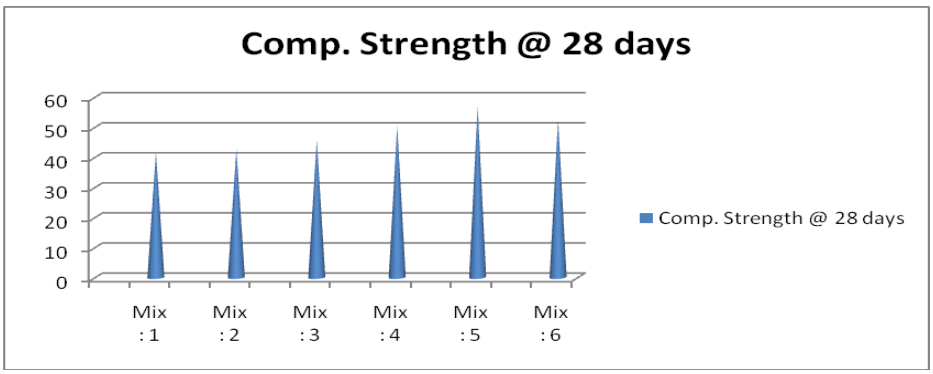

The splitting tensile strength of concrete cylinder was determined based on IS: 516-1959. Load is applied until the specimen fails, along the vertical diameter.

Table: 2 Split Tensile Strength @ 28 days

Mix	% of GGBS	% of Cement	Steel Fibre	% of Super plasticizer	Split Tensile Strength @ 28 days
M1	0	100	1	2	6.10
M2	10	90	1	2	6.25
M3	20	80	1	2	6.55
M4	30	70	1	2	7.90
M5	40	60	1	2	8.95
M6	50	50	1	2	8.10

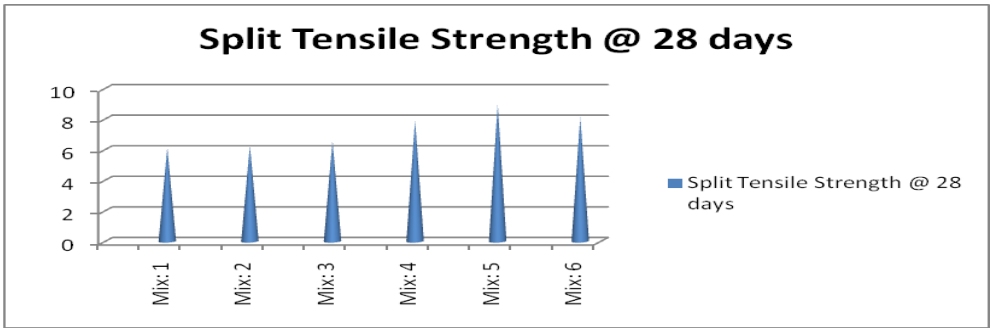

The Flexural strength of concrete was determined at the age of 28 days. The specimens were cast and tested as per IS: 516-1959.

Table: 3 Flexural Strength @ 28 days

Mix	% of GGBS	% of Cement	Steel Fibre	% of Super plasticizer	Flexural Strength @ 28 days
M1	0	100	1	2	9.20
M2	10	90	1	2	9.85
M3	20	80	1	2	10.50
M4	30	70	1	2	11.20
M5	40	60	1	2	12.6
M6	50	50	1	2	11.5

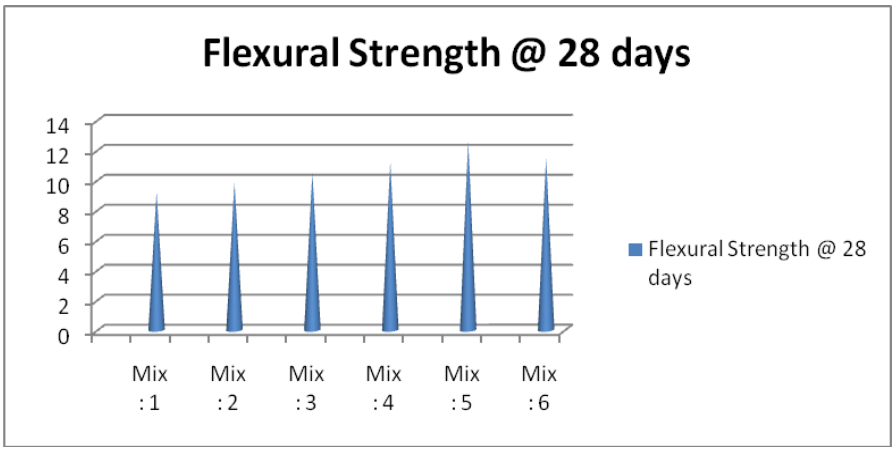

The Pull out strength of concrete was determined at the age of 28 days. The specimens were cast and tested as per IS: 516-1959.

Table: 4 Pull out Strength @ 28 days

Mix	% of GGBS	% of Cement	Steel Fibre	% of Super plasticizer	Pull Out Strength @ 28 days
M1	0	100	1	2	9.50
M2	10	90	1	2	10.78
M3	20	80	1	2	11.76
M4	30	70	1	2	12.55
M5	40	60	1	2	13.5
M6	50	50	1	2	12.85

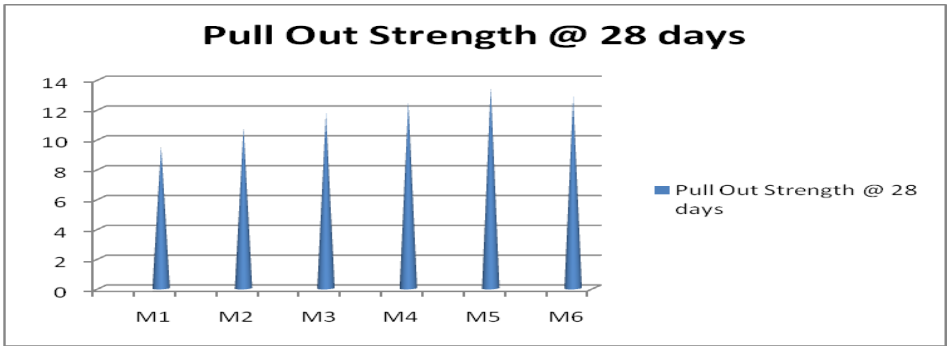

The optimum percentage levels of 40% GGBS and 1% Steel fibre replacement to the weight of the cement is taken with the HPC M40 mix ratio of 1 : 1.09 : 1.89 : 0.35 which gave the better results. In order to increase the workability, Superplasticizer is used. The Compressive strength of 56.85 N/mm2 is achieved in the HPC mix due to the presence of GGBS which exhibits more filler effect. Graph 1, 2,3 and 4 represents the compressive strength, split tensile strength, flexural strength Pull out strength of various mixes with different replacement level of GGBS and steel fibre at the age of 28 days.As there was an appreciable increase in the workability of concrete with increasing percent replacement of cement with GGBS, therefore wlc ratio can be reduced keeping the slump constant, which will result in an increase in compressive strength. The Split tensile strength of 8.95N/mm2 , Flexural strength of 12.6 N/mm2 and Pull out strength of 13.5 N/mm^2 is achieved by the usage of Superplasticizer and properties of steel fibre in the HPC mix.

IV. CONCLUSION

[1]. It is observed that the Optimum Compressive Strength of High Performance Concrete is obtained replacement of 40 % Cement by GGBS
[2]. From the above experimental results it is proved that, GGBS can be used as alternative material for the cement. Based on the results the compressive , split tensile, flexural and Pull out strengths are increased as the percentage of ggbs increased upto 40 % and above decrease.
[3]. Higher strength development is due to filler effect of GGBS and properties of steel fiibre
[4]. GGBS can be used as one of the alternative material for the cement.
[5]. From the experimental results 40% of cement can be replaced with GGBS.

REFERENCES

[1]. D.Neeraja "International Journal of scientific & Engineering research" Volume 4, issue2, Feb 2013
[2]. Dr.P.Muthupriya"International Journal of civil Engineering & Technology" Volume 4, issue4, july - aug 2013,PP No. 29 – 35
[3]. Prashant Y.Pawade[1], Nagarnaik P.B[2], Pande A.M[3] "International Journal Of Civil And Structural Engineering "Volume 2, No 2, 2011
[4]. Elavenil S. and Samuel Knight G.M (2007), "Behavior of steer fiber reinforced concrete beams and plates under static load", Journal of Research in Science, Computing, and Engineering, pp 11-28
[5]. P.Ramadoss,V.Prabakaran, K.Nagamani, "Dynamic mechanical performance of high-performance fiber reinforced concrete" International conference on recent developments instructural Engineering, Manipal (RDSE-2010)

E-IDOL: E-way of Issuing Document Online

[1,] Amitesh Dongre, [2,] Ankit Sahay, [3,] Ketan Chirde, [4,] Onkar Telang, [5,] Rasika Ingle

#Dept. of Computer Technology, Yeshwantrao chavan college of Engineering, Nagpur, India

ABSTRACT

Online Document Issuance Systemwill ensure that everyone will have access to various documents orcertificatesone needs from the government on the click of web page button on any computational electronic device.We aim to transform conventional administrative setup to more efficient and transparent organizationremovedelays and huge amount of paper work with reliable fast service electronically. Our Online Document Issuance System support governance of collector office by using more effective and transparent document issuing System, thereby improving the old governance methods and the services. This improved way of issuing document guaranteesthe fast delivery and stability of electronic documents. When using storage and issuance services online which are one of core services, users register their electronic documents and they are issued electronically in standard PDF format on their mail.

KEYWORD: *E-Governance, Electronic Document Issuance, Interdepartmental Verification, Unique Identification Number, MD5 Checksum.*

I. INTRODUCTION

The document is required by Every Indian at almost every step—for admission or for joining a professional course, for participating in a government auction or availing of government welfare schemes like subsidized public . In a move that could well breed more corruption, Every Indian has the right to issue various documents from the collector office, which is issued more than three lakh certificates annually. Certificates and Documents will be issued by the overburdened and short-staffed deputy collector's office. In addition, there is an involvement of agents, lack of transparency, prolonged process with lengthy queues and overwhelm requirement of documents leads to inefficient and hectic document issuing system in India

The purpose of the online web Service is to make the entire process transparent so that any layman can easily follow the step-by-step instructions to get the desired certificate hassle-free and on time. This service ensures the process is convenient, faster and fully beneficial to the common man.

II. CURRENT SCENARIO

When we went to the local office for survey by creating a document we found that the process was very time consuming and there are lots of issues for creation of any document the first is we were not able to find the proper place for receiving of application forms then when we found it there was a very large queue of people and there was only two queue for this office which was unable to handle such a large amount of people it took about an hour to receive an application form and after that we have to fill the details and stand in another queue which was also crowded for submission of our application form it also took long time to fill the form and then we were told that it would take about a month for the document to be created or the other option was bribing the babu so that he could do the work quickly.

From our survey we found that the process of document issuance is very hectic, time consuming and it encourages corruption. It is very difficult for a common man to issue a document and wait till his document is deliver in this process he becomes helpless and frustrated because his lots of useful time is lost and he has no other option for document creation. We also found that the government employees has to face over burden of office task because of lack of employees in front of such a large population and also they are not trained properly and over all they have a hectic schedule so they are not able to do their work more efficiently.

We also found that there is lots of corruption in system from small clerks to big officers maximum of them accept bribe. The low salaries of people made them susceptible, bringing with it more inefficiencies and the easy way of making money with less or no accountability. The crime of corruption is easily forgotten, the law offers easy way back into the mainstream and acceptance by the society. In addition to that it is the lure of luxury, personal status enhancement and the false sense of elitism that makes the corrupt vulnerable to illegal and unethical means of acquiring wealth.

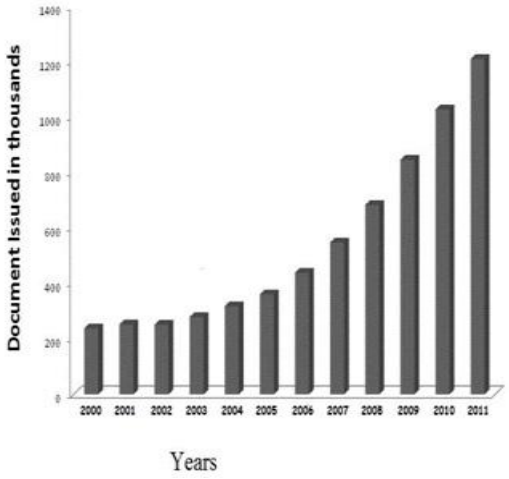

Fig 1: Documents issuance year's wise statistics

As per the survey we have done at Nagpur collector office,wefound that the documents issued every year in INDIA are drastically growing as shown in the graph. As Indian population is expanding at a very high rate so the requirement for the documents are dramatically increasing to improvegovernment. After collecting the data and carefully examining it we found out that the number of certificates created in year of 2000 was around 2 lakh and reaching till the year of 2011 it was about 14 lakh which was a great increase. We also found out that for doing such a huge amount of work the employee were not adequate which increases load of work on them and so they are not able to work properly and efficiently . The result of this is that documents issuance time and corruption increases.

The reason behind introducing novel e-governance system is to mini work load on government employees will decrease, the issuing time of document will get decreased and this will definitely help to reduce corruption in government office.

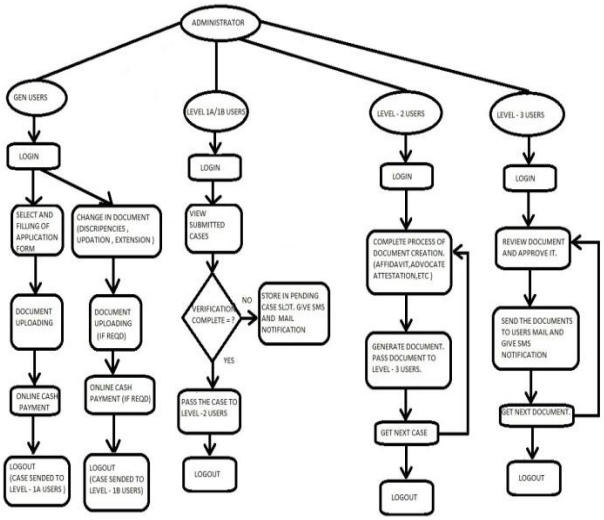

Fig2: High Level Diagram

III. OUR IMPLEMENTATION

We have come up with an idea to issue the documents online this will help to reduce the time, corruption, reduce the burden of staff and it could be applied from anywhere so we have implemented our project in different phases.

A. Phase (1):-

In phase 1 we have done a detailed background survey in Collector office (NAGPUR) and Social Welfare Justice Department (NAGPUR). We decided that first we will create five documents (Cast certificate, Cast validity, Income certificate, Domicile certificate, Non creamy Layer). Then we have done a survey on how these documents are created, authenticated and what time is required for the same.

In phase1 there will be general user who can login after registration, can view different type of documents which are available for him/her toissue, can request for a document by filling application form, can request for change in issued document from EIDOL and can pay online when it is required.

B. Phase (2):-

The work of level 1A/1B Employer of EIDOL in phase 2 will be that he will login then view the submitted cases and verify their documents.if there would be any document missing he will alert the user by e-mail and text message and give a limit of 15 days to submit the document or will discard the case if the user is not able to submit the document in allotted time. If the user have submitted required documents correctly then he/she will pass the case to level 2 Employer of EIDOL.

C. Phase (3):-

In phase 3 the level 2 Employer of EIDOL will login first then perform the full procedure of document creation.when the document will ready he/she will check it and will pass it to level 3 Employer of EIDOL for approval.

D. Phase (4):-

When the level 2 Employer of E-IDOL will forward a case to level 3 Employer of E-IDOL. The level 3 user will view it and approve it and send the document to user through mail and will also give user a sms notification. The document generated will be stored in database and user can view it in future in their profile's document box.

IV. SNAPSHOT

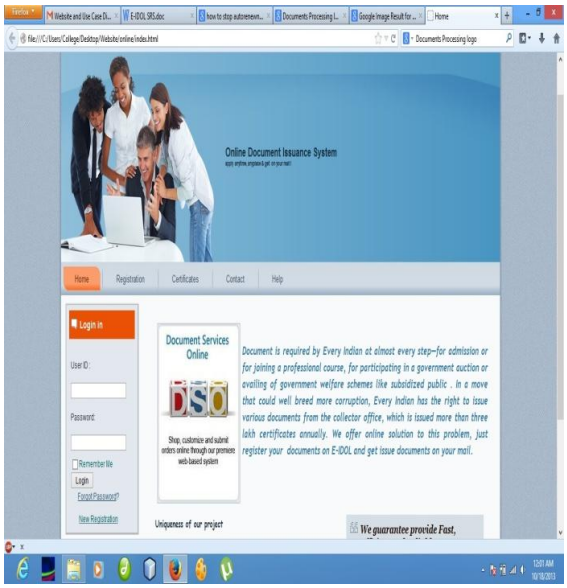

Figure 3: home page

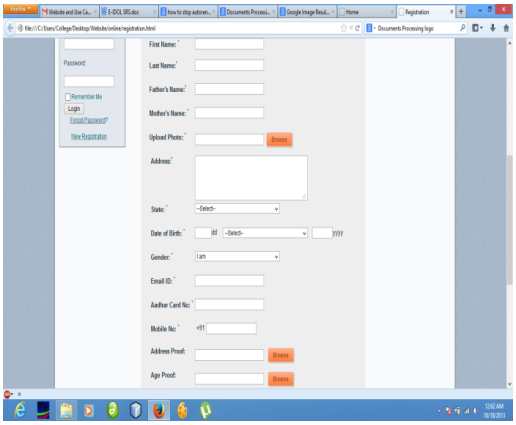

Figure 4: Registration page

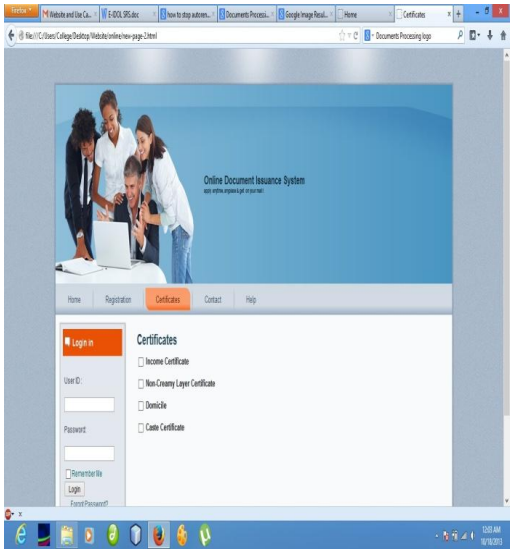

Figure5: Certificates Offered

V. SECURITY

Security plays a very important role in any online process. *Security*is probably one of the most significant concerns for us so we have used various steps to make our online process secure by using appropriate protocols and algorithms to make our process secure.

MD5 Algorithm:-

The MD5 message-digest algorithm is a widely used cryptographic hash function producing a 128-bit (16-byte) hash value, typically expressed in text format as a 32 digit hexadecimal number. MD5 has been utilized in a wide variety of cryptographic applications, and is also commonly used to verify data integrity.

MD5 processes a variable-length message into a fixed-length output of 128 bits. The input message is broken up into chunks of 512-bit blocks (sixteen 32-bit words); the message is padded so that its length is divisible by 512. The padding works as follows: first a single bit, 1, is appended to the end of the message. This is followed by as many zeros as are required to bring the length of the message up to 64 bits less than a multiple of 512. The remaining bits are filled up with 64 bits representing the length of the original message, modulo 2^{64}.

The main MD5 algorithm operates on a 128-bit state, divided into four 32-bit words, denoted *A*, *B*, *C* and *D*. These are initialized to certain fixed constants. The main algorithm then uses each 512-bit message block in turn to modify the state. The processing of a message block consists of four similar stages, termed *rounds*; each round is composed of 16 similar operations based on a non-linear function *F*, modular addition, and left rotation. Figure 1 illustrates one operation within a round. There are four possible functions *F*; a different one is used in each round:

$$F(B,C,D) = (B \wedge C) \vee (\neg B \wedge D)$$
$$G(B,C,D) = (B \wedge D) \vee (C \wedge \neg D)$$
$$H(B,C,D) = B \oplus C \oplus D$$
$$I(B,C,D) = C \oplus (B \vee \neg D)$$

$\oplus, \wedge, \vee, \neg$Denote the XOR, AND, OR and NOT operations respectively.

B. Securing SQL Server:-

Surface area reduction is a security measure that involves stopping or disabling unused components. Surface-area reduction helps improve security by providing fewer avenues for potential attacks on a system. The key to limiting the surface area of SQL Server includes running required services that have "least privilege" by granting services and users only the appropriate rights.

Principals are the individuals, groups, and processes granted access to SQL Server. "Securable" are the server, database, and objects the database contains. Each has a set of permissions that can be configured to help reduce the SQL Server surface area.Securing SQL Server can be viewed as a series of steps, involving four areas: the platform, authentication, objects (including data), and applications that access the system.The platform for SQL Server includes the physical hardware and networking systems connecting clients to the database servers and the binary files that are used to process database requests.

VI. PHYSICAL SECURITY

Best practices for physical security strictly limit access to the physical server and hardware components. For example, use locked rooms with restricted access for the database server hardware and networking devices. In addition, limit access to backup media by storing it at a secure off-site location. Implementing physical network security starts with keeping unauthorized users off the network.

VII. SYSTEM SECURITY

Operating system security packs and upgrades include important security enhancements. Apply all updates and upgrades to the operating system after you test them with the database applications.

Firewalls also provide effective ways to implement security. Logically, a firewall is a separator or restrictor of network traffic, which can be configured to enforce your organization's data security policy. If you use a firewall, you increase security at the operating system level by providing a chokepoint where your security measures can be focused.

C. SSL Certificate:-

SSL (Secure Sockets Layer) is a standard security technology for establishing an encrypted links between a server and a client typically a web server and a browser or a mail server and a mail client. SSL allows sensitive information such as credit card numbers, social security numbers, and login credentials to be transmitted securely. Normally, data sent between browsers and web servers is sent in plain text leaving you vulnerable to eavesdropping. If an attacker is able to intercept all data being sent between a browser and a web server they can see and use that information. More specifically, SSL is a security protocol. Protocols describe how algorithms should be used; in this case, the SSL protocol determines variables of the encryption for both the link and the data being transmitted.

SSL Certificates have a key pair a public and a private key. These keys work together to establish an encrypted connection. The certificate also contains what is called the "subject," which is the identity of the certificate/website owner. To get a certificate, you must create a Certificate Signing Request (CSR) on your server. This CSR creates the private key and a CSR data file that you send to the SSL Certificate issuer (called a Certificate Authority or CA). The CA uses the CSR data file to create a public key to match your private key without compromising the key itself. The CA never sees the private key. Once you receive the SSL Certificate, you install it on your server. You also install a pair of intermediate certificates that establish the credibility of your SSL Certificate by tying it to your CA's root certificate. The instructions for installing and testing your certificate will be different depending on your server.

VIII. CONCLUSIONS

In this paper, we considered the problem of offline document issuance system of INDIA, in order to maximize the efficiency, security and ease of this system. We developed an efficient Online Document Issuance System making ADHAAR as the base of the system. This system essentially gives the best possible performance for generation, processing and delivering the documents to the actual destined user. In addition most of the drawbacks of offline system are minimized taking only relevant facts into consideration. We believe that our results provide an interesting step towards a principled study of document generation of INDIA and information gathering.

IX. ACKNOWLEDGMENT

The major project described here was a collaborative effort between Engineering students of Yeshwantrao Chavan College of Engineering, University of Nagpur; the project ran from mid-September of 2013 to mid-march of 2014.The authors wish to acknowledge sincere thanks to Miss. Rasika Ingle for their efforts and support in project development,.

REFERENCES

[1] Shailendra C Jain Palvia , Sushil S Sharma ,"E-Government and E-Governance:Definations/Domains status around the world"2007

[2] P-Sharma,"E-Governance by p.sharma-A P H Publishers_Edition-01"2001

[3] Sharma, S.K. (2004) Assessing E-government Implementations, *Electronic Government Journal*, 1(2), 2004, pp. 198-212

[4] Sharma, S. K. (2006) An E-Government Services Framework, Encyclopedia of Commerce, E-Government and Mobile Commerce, Mehdi Khosrow-Pour, Information Resources Management Association, Idea Group Reference, INDIA, pp. 373-378. 2006.

[5] National Commission for BackwardClasses2010-2011website http://www.ncbc.nic.in/Organisationalsetup.html.

[6] Mumbai city setu 2011 website http://mumbaicitysetu.org/Certificates.html.

[7] Delhi government website 2007-2008 http://www.delhi.gov.in/wps/wcm/connect/doit_revenue/Revenue/Home/Services/Certificates/OBC+Certificate.

[8] http://www.delhi.gov.in/wps/wcm/connect/doit_revenue/Revenue/Home/Services/Certificates/

[9] Delhi government website 2008 http://dcnortheast.delhigovt.nic.in/issue_of_certificate.htm

[10] http://obcreservation.net/ver2/reservation-mainmenu-9/25-user-article/142-caste-validity-a-verification-certificate.html

[11] Government of Maharashtra 2005https://barti.maharashtra.gov.in/ecastevalidation/ccvis/index.html

[12] The times of India website 2009 http://timesofindia.indiatimes.com/city/kolhapur/BARTI-to-distribute-caste-validity-certificates-from-November-28-to-December-1/articleshow/26487317.cms

Real Time Identification of Toxic Gases Based on Artificial Neural Networks

Slimane Ouhmad [1,] Ahmed Roukhe [1,] Hassane Roukhe[2]

[1] *LAMPE Laboratory, Department of Physics, Faculty of Sciences, Moulay Ismail University, Bp 11201, Zitoune, Meknes –Morocco .*

[2]*Higher Institute of Trades Audiovisual and Cinema (ISMAC), Mohamed V University, Rabat, Morocco.*

ABSTRACT

The assessment of air pollution using sensors is yet widespread, especially indoor air quality. Artificial Neural Networks (ANNs) constitutes a commonly used approach for the identification of air pollutants. In this paper, we propose the development of Multi-Layer Perceptron (MLP) Neural Network on-line type for the real time identification. For this reason, we used the data base obtained from the multi-sensor system designed for detection of three toxic gases. Compared with some previous research which used multiple linear regression methods and MLP off-line type , our model is proved to be much more successful in terms of the correct identification in real time even with low concentration (one part per million) with better mean square errors (MSE $< 4.10^{-04}$ *) .*

Keywords: *Toxic gases, Artificial Neural Networks, Multi-Layer Perceptron, On-line learning, Real Time Identification.*

I. INTRODUCTION

In recent years, Neural Network models have been developed and successfully applied to atmospheric pollution modeling in general [1-2] and air quality problems in particular [2-8]. Unlike other modeling techniques, Artificial Neural Networks (ANN) is capable of modeling highly non-linear relationships [9-10].The ANNs performance is superior when compared to statistical methods such as multiple linear regression [11,12]. Among the various NN-based models, the feed-forward Neural Network, also known as the Multi Layer Perceptron type Neural Network (MLPNN), is the most commonly used and has been applied to solve many difficult and diverse problems [13–17].

Our approach in this paper consists of training a MLPNN for the identification of toxic gases in a real time manner. For this, we used a database obtained from a multi-sensor system which consists of six chemical sensors of type TGS (called electronic noses) based on metal oxide [18]. Each sensor emits an electrical signal characterized by three variables: Accordingly, a) the initial conductance (G0), b) the dynamic slope of the conductance (dGS/dt) , and c) the steady-state conductance GS [2, 18-20].

The first step consists of a careful selection of adequate parameters of the structure, namely architecture, functions activation, and weights of the neurons by our developed method of neural network (MLP) to find out the right settings for each implementation of these networks. The second step is meant to examine the performance of this model which allows us to compare it with previously developed models [21-22] in terms of correct identification.

The present study aims at developing a quick and easily reliable method to classify and identify the low concentration toxic gases, in real time.The study is significant by virtue of three major benefits: The first is that the application of the on-line learning can be used for the security of air quality in real-time. The second is to select a stable optimum design with a minimum of hidden layers and the neurons in each layer. The last advantage is to prove the power of odor evaluation system (electronic nose) even with low concentration (one Part per Million).

The rest of the paper is organized as follows: The second section is called Materials and Methods. It deals mainly with feature extraction and artificial neural networks. This latter is about the general properties of the trained ANNs consisting of developed MLP algorithm. The third part is devoted to the results and discussions of the performance of our model during learning and testing phases. In the last section, we will draw some conclusions and suggest future research.

II. MATERIAL AND METHODS

2.1. Feature extraction

The features obtained for data analysis were extracted from the temporal responses of the sensor array realized by [18] for the detection of the toxic gases H2S (hydrogen sulfide), NO2 (nitrogen dioxide) and their mixture (H2S- NO2).

The sensor array comprised six TGS-XX (with XX = 800, 813, 822, 825, 832 and 2105),Taguchi Gas Sensor obtained from Figaro Engineering, Incorporation [23]. We want to better exploit the information obtained from each experiment.

To achieve this aim, both the traditional steady state response but also additional features that can better characterize the sensor and analysis system were used. For every sensor within the array and measurement performed, three representative features from the response signal were extracted:

• G0: the initial conductance of a sensor calculated as the average value of its conductance during the first minute of the measurement.

• Gs: the steady-state conductance calculated as the average value of its conductance during the latest minute of a measurement.

• dG/dt: the dynamic slope of the conductance calculated between 2 and 50 min of a measurement. This corresponds to a phase where a fast increase of sensor conductance is observed [24].

These three features were extracted from the response of each sensor. Given the fact that there were 6 sensors within the array, each measurement was described by 18 features.

2.2. Artificial neural networks (ANNs)

Artificial Neural Networks (ANNs) are a set of mathematical, statistical and computational methods inspired by nerve cells (neurons) [24-25].Then emergent properties to solve problems once described as complex.ANNs use a high number of units (neurons) interconnected among them by using a connectionist approach to computation. They are needed sets of data, which are differenced in inputs and outputs [26], Figure.1.

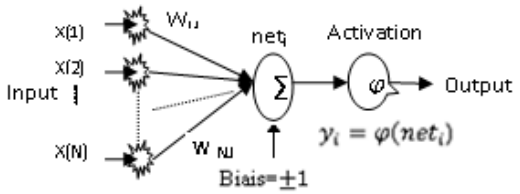

Figure 1: Neural network model

The way of using ANNs has two parts. One is called "training", and as the own word says, it consists on a process where the system is able to identify the different inputs with the outputs, and their relations. It is said that the system is, in certain way, "learning". In the second part, (testing), the ANN provides an output when new inputs are introduced. This answer is based on the information that the own system was able to catch in training part. New outputs will be correct if the inputs used for training and testing are similar [27 -28].

2.2.1 Multi-layer perception (MLP) neural network.

The MLP is the most frequently used neural network technique, which makes it possible to carry out the most various applications. The identification of the MLP neural networks requires two types of stages. The first is the determination of the network structure. Different networks with one layer hidden have been tried, and the activation function used in this study is the sigmoid function describedas: $\varphi_i(x) = \frac{1}{1+e^{-\alpha_i x}}$ (1), with $\alpha_i = \alpha_1, \alpha_2$ and α_3(see Table 1.and Figure 2.).

The second stage is the identification (testing) of the three toxic gases, by using back-propagation neural networks (a Matlab based algorithm was developed in our laboratory), [29].

2.2.2 Training algorithm

The MLP network training can be viewed as a function approximation problem in which the network parameters (weights and biases) are adjusted, during the training, in an effort to minimize error function between the network output and the desired output [30-31]. Among these, the most popular and widely used ANNs training algorithm is the Back Propagation (BP) [32, 33]. The BP method, also known as the error back propagation algorithm, is based on the error correlation learning rule [34]. The BP neural networks are trained with different training algorithms. In this section we describe one of these algorithms. The BP algorithm uses the gradients of the activation functions of neurons in order to back-propagate the error that is measured at the output of a neural network and calculate the gradients of the output error over each weight in the network. Subsequently, these gradients are used in updating the ANN weights [35].

The algorithm is described by following rules:

1. Initialization: Set all the weights and biases to small real random values.
2. Presentation of input and desired outputs: Present the Input matrix, x(1), .,x(N) and corresponding desired response d(1),d(2),.,d(N), one pair at a time, where N is the number of training patterns.
3.Calculation of actual outputs: Use Eq. (2) to calculate the output signals $y_1; y_2 \; ; \; ; y_{N_M}$

$$y_i = \varphi\left(\sum_{j=1}^{N_M-1} W_{ij}\, x_j^{M-1} + b_j^{M-1}\right), i = 1,..N_{M-1}\,. \tag{2}$$

4. Adaptation of weights (w_{ij}) and biases (b_i):

$$W_{ij}^{l-1}(n+1) = W(n) + \Delta W_{ij}^{l-1}(n). \tag{3}$$

$$b_i^{l-1}(n+1) = b_i^{l-1}(n) + \Delta b_i^{l-1}(n) \tag{4}$$

Where $\Delta W_{ij}^{l-1}(n) = \mu x_j(n)\delta_i^{l-1}(n)$. and (5)

$$\Delta b_i^{l-1}(n) = \mu\delta_i^{l-1}(n)\,. \tag{6}$$

and $\boldsymbol{\delta}$ is the derivative of error function with respect to the weight.

$$\delta = \left(\partial E/_{\partial W}\right) = \left(\frac{\partial E_{MSE}}{\partial W}\right). \tag{7}$$

Where $E_{MSE} = \frac{1}{2}\sum_{i=1}^{k}\left(d_i - y_i(n)\right)^2$, "Learning on line ". (8)

With

$$\delta = \delta_i^{l-1}(n)\begin{cases}\varphi'\left(net_i^{l-1}\right)[d_i - y_i(n)] & ,l=M\\ \varphi'\left(net_i^{l-1}\right)\sum_k W_{ki}\,.\,\delta_k^l\,, 1 \le l \le M-1\end{cases} \tag{9}$$

$$net_i^{l-1} = \sum_{j=1}^{N_M-1} W_{ij}\, x_j^{M-1} + b_j^{M-1}\quad . \tag{10}$$

in which $x_j(n)$ = output of node j at iteration n , l is layer, k is the number of output nodes of neural network, M is output layer, and $\boldsymbol{\varphi}$ is the activation function. The learning rate is represented by $\boldsymbol{\mu}$, with $\mathbf{0} < \boldsymbol{\mu} < \mathbf{1}$, [36-37].

2.2.3. The model and parameters used in the study.

Our choice is focused on a multi-layer non-recurring network, based on the learning algorithm of back propagation. The purpose of this learning algorithm is to minimize the mean square errors (MSEs). The network consists of two hidden layers of neurons. The first hidden layer contains 36 neurons. To increase the accuracy, we chose a second hidden layer in which we varied the number of neurons from 1 to 18. We retain the essential elements in Table 1.

Table.1. Architectures and parameters of ANN used in this study

Neural NetWork	MLP (MULTILAYER PERCEPTRON)Feed Forever, fully Connected (Learning on- line).	
Input (I)	I: (matrix of (6x3), 6 sensors each with three variables : G0, dG/dt, Gs.	
Output (O)	O (3x1), classification and identification three gases:NO_2 ,H_2S and NO_2-H_2S	
Architectures of Hidden Layers (Hi)	-36 neurons in First hidden layer (H1),and from 12 to 18 neurons in Seconde hidden layer (H2).	Does not Reach the result
	-36 neurons in H1,and from 1 to 11 neurons in H2	Achieved the result only in 3 neurons
Activation Functions	I-H1: sigmoid,(represented by blue color). H1-H2: sigmoid (represented by red color). H2-O: sigmoid (represented by green color).	Fig.2.
Encoding of classe (Output)	Classes can also be encoded as follows:	[1,-1,-1]=NO_2, [-1,1,-1]=H_2S, [-1,-1,1]=NO_2-H_2S .
Statistical results of our model	standard statistical measures: Accuracy= ($\frac{\text{Number of correctly classified data}}{\text{Total number of data}}$) * 100 Accuracy (classification) = ($\frac{50+50+50}{150}$ * 100) =100% Accuracy (Identification) = ($\frac{10+9+10}{30}$) * 100 = 96,6%	Fig.5 and Fig.6.
Learning Errors, Test Errors ,and Number of Iterations(N) respectively	MSE s < 10^{-05} , MSEs < 4.10^{-04} , N< 200 .	
Previous research in brief	-Accuracy (classification) = 86%. And Accuracy (Identification) = 74% -Number of Iterations (N) = 1200. -Great Architecture : I(18),H1(36 neurons),H2(3 neurons) H3(3 neurons) H4(2 neurons H5(3 neurons) ,and O(3 neurons) , that **used learning bach** [22].	

III. RESULTS AND DISCUSSION

In this part, the MLP is used to develop a model able to classify and identify toxic gases. The considered database is composed of 180 samples distributed in three classes (NO_2, H_2S and NO_2- H_2S(mixture)). The database is divided in two parts: 80 % used for the learning step, and 20 % are used for testing. The selection of samples used in learning and testing is done randomly.

The testing subset was used to assess the classification accuracy of the MLP after the training process [39, 40]. The error analysis was used to examine the developed of the designed model.

The criterion exploited in this study was the Mean Square Error (MSE). To be concise and straight forward only the results corresponding to the architecture (I/36 Neurons in -H1 / 3 neurons in-H2 / O), as discussed in Table 1 above, are shown. Figure 2 shows the activation functions used in the hidden layers of our selected architecture. Figure 3 shows the on-line training process MSE evolution in terms of training individuals. As we can see, the MSE is very small. The MSE in terms of testing individuals is illustrated in Figure 4 and it takes small values; this shows the efficiency of our neural model.

The results of classification (training individuals) and identification (testing individuals) are shown in Figure 5, and Figure 6. We can easily notice that all individuals are affected to their correct groups.

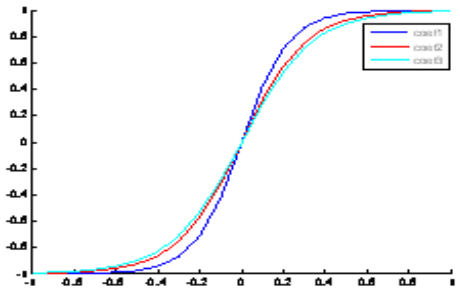

Fig.2.Activation functions used in this study

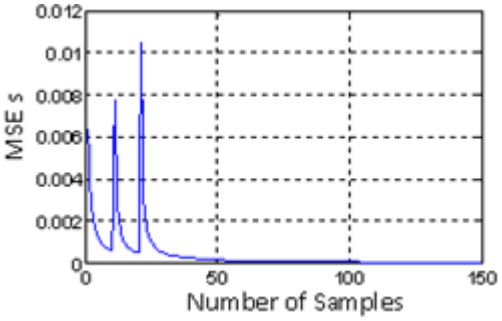

Fig.3. Evolution of the minimums MSEs during learning

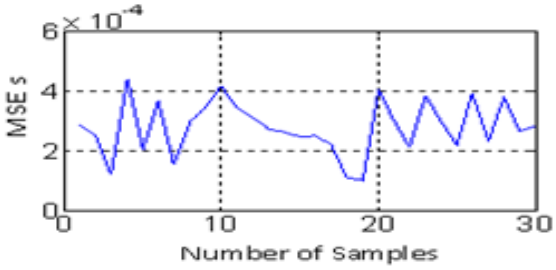

Fig .4.Evolution of the minimums MSEs the during testing

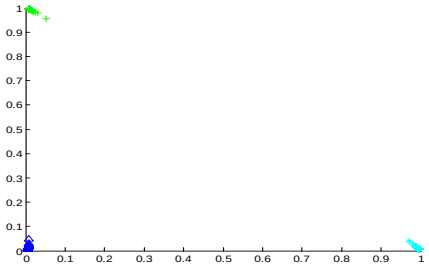

Fig.5.Classification of three toxic gases(learning)

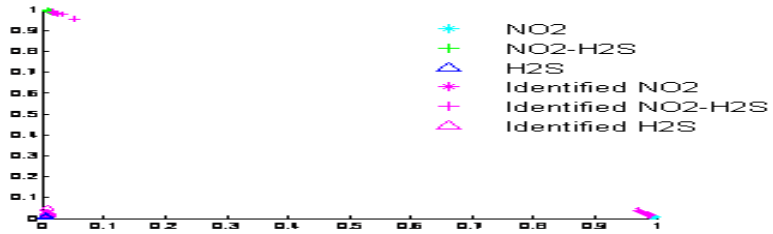

Fig.6.Classification and identification of three toxic gases (testing)

The results obtained have given a better classification and identification. In comparison to previous research which has been effected by great architecture that used learning bach (off-line) toolbox. [21,22].

IV. CONCLUSION AND FUTURE WORK

In this paper, we have studied different architectures to better optimize our design MLP neural network. We have also presented the results of the optimal design. According to these results, our classification reached the rate of 100%, and excellent identification.

The results are very encouraging and show that the smart multisensory systems have a discriminating power of toxic gases at low concentration (1ppm) in real time. This system can be very applicable when there is a danger that cannot be alarmed by human smell sense. The next work will be devoted to the use of an unsupervised neural network model based on the self-organizing map and comparison of performances.

REFERENCES

[1] M.W Gardner, SR Dorling. Artificial neural networks (the multilayer perceptron, Review of Applications in the Atmospheric Sciences.Atmos Environ, Volume. 32, No. 14/15, pp.2627–2636, 1998,

[2] K.D.Karatzas,S.Kaltsatos, Air pollution modelling with the aid of computational intelligence methods in Thessaloniki, Greece,Simulation Modeling Practice and Theory ,vol .15,pp 1310–1319 , 2007

[3] M Boznar, M Lesjack, P Mlakar.A neural network based method for short-term predictions of ambient SO2 concentrations in highly polluted industrial areas of complex Terrain, Atmospheric Environment ,vol, B 27,No.2,pp 221–230, 1993

[4] MW Gardner, SR Dorling. Neural network modelling and prediction of hourly NOx and NO2 concentrations in urban air in London .Atmospheric Environment, vol 33, No 5, pp.709–719, 1999.

[5] MW Gardner, SR Dorling. Statistical surface ozone models: an improved methodology to account for non-linear behaviour. Atmospheric Environment, vol B 34, No.1, pp, 21–34, 1999.

[6] A .Chaloulakou , M Saisana , N Spyrellis. Comparative assessment of neural networks and regression models for forecasting summertime ozone in Athens.Sci Total Environ, vol, 313, No.1-3,pp1-13, 2003.

[7] F Karaca, O Alagha, F Ertürk. Application of inductive learning: air pollution forecast in Istanbul, Turkey. Intell Autom Soft Co2005,vol 11,No 4, ,pp 207–216, 2005.

[8] F Karaca, A Nikov, O Alagha. NN-AirPol: a neural-network-based method for air pollution evaluation and control. Int J Environ Pollut 2006a, vol 28,No(3/4), pp 310–325, 2006.

[9] U.Brunelli, V.Piazza, L., Pignato , F Sorbello, S.Vitabile. Two-day ahead prediction of daily maximum concentrations of SO2, O3, PM10, NO2, CO in the urban area of Palermo, Italy. Atmospheric Environment, vol.41, 2967–2995, 2007.

[10] S.Palani et al .Ann application for prediction atmospheric nitrogen deposition to aquatic ecosystems.Marine Pollution Bulletin, vol .62.pp,1198-1206, 2011 . doi :10.1016/j .marpolbul .2011.03.033.

[11] D.-C. Park,Structure optimization of Bi-Linear Recur-rent Neural Networks and its application to Ethernet net-work traffic prediction, Information Sciences,vol.22 No.10,pp 1448-1462, December, 2009. , doi:10.1016/j.ins.2009

[12] J. Yi, V.R. Prybutok,A neural network model forecasting for prediction of daily maximum ozone concentration in an industrialized urban area, Environmental Pollution, vol. 92. Pp , 349–357, 1996.

[13] I. Athanasiadis, K. Karatzas, P.Mitkas, Contemporary air quality forecasting methods: a comparative analysis between statistical methods and classification algorithms, in: R. Sokhi, J. Brexhler (Eds.) , Proceedings of the 5th International Conference on Urban Air Quality Measurement, Modelling and Management, (Spain) Valencia, 29–31 March 2005.

[14] E. I. Vlahogianni, M. G. Karlaftis, J. C. Golias, Optimized and meta-optimized neural networks for short-term traffic flow prediction: A genetic approach, Transportation Research Part C, vol. 1,pp, 211–234, 2005.

[15] A. Eswaradass, X.-H. Sun, M. Wu,A neural network based predictive mechanism for available bandwidth", proceeding of 19th IEEE International Conference on Parallel and Distributed Proceeding Symposium, , Workshop 10,vol 11, 228, 2005 . doi>10.1109/IPDPS.2005.234

[16] H. Yousefi zadeh, E.A. Jonckheere, J.A. Silvester, Utilizing neural networks to reduce packet loss in self-similar tele traffic, proceeding of IEEE International. Conference on Communications, vol.3.pp,1942–1946, 2003.

[17] M. Badura et al, Statistical assessment of quantification methods used in gas sensor system", Sensors and Actuators B: Chemical vol.188, pp,815– 823, November 2013.

[18] B.W. Licznerski, K. Nitsch, H. Teterycz, T. Sobanski, K. Wisniewski, "Characterisation of electrical parameters for multilayer SnO2gas sensors", Sensors and Actuators B: Chemical vol.103, No, (1–2),pp. 69–75, 2004..

[19] O.Helli ."Multicapteurs de gaz pour la conception d'un nez électronique de surveillance de la pollution atmosphérique", thèse d'Université Metz (2003).

[20] K An ngo, "Etude d'un système multiplicateur pour la détection sélective des gaz", thèse d'Université, université paul cesanne Aix Marseille III , 2006.

[21] A .Lfakir , "Identification et Quantification d'une atmosphère gazeuse complexe à l'aide d'un système multicapteures intelligent . Application La détectionde mélanges composés de H_2S ,NO_2,SO_2 en atmosphère humide variable", thèse d'Université Metz, 2006.

[22] N. El Barbri , O.Helli , M. Lumbreras, M. Sidt, B. Bouchikhi , et A. Roukhe, "Analyse Qualitative et Quantitative des gaz polluants H2S, NO2 et leur melange, par les reseaux de neurones artificiels", IXèmes Journées Maghrébines des Sciences des Matériaux JMSM'2004, Tome 3, Oran 8-11,Mai (2004),pp 867-873

[23] T.Seiyama,N.Yamazoe,S.Yamauchi ,"Chemical Sensor Technology" Vol. 1, 2, 3 et 4. Elsevier Science Ltd, 1988.

[24] W.S. McCulloch, W.H. Pitts, "A logical calculus of the ideas immanent in nervous activity", Bulletin of Mathematical Biophysics, vol. 5 ,pp115–133, 1943.

[25] Bishop, C. M. Neural networks for pattern recognition.NY: Oxford University Press, 1995.

[26] S.Haykin. Neural Networks and Learning Machines; Pearson Prentice Hall: New Jersey, 2009

[27] J. R. Hilera, V.J. Martíne. Redes neuronales artificiales. Fundamentos, modelos y aplicaciones, Addison-Wesley Ibero Americana S.A. Madrid , Spain, 1995.

[28] S. Haykin, Neural Networks: A comprehensive foundation Prentice Hall: New Jersey, 2008.

[29] S.Ouhmad ,A .Roukhe, Classification of toxic pollutant gases by the use of artificial neural networks type multilayer perceptron,XI the International Symposium on Environment, Catalysis and Process Engineering (ECGP'11) France, Villeneuve, d'Ascq, pp. 27, 26-28 June, 2013.

[30] R. Pasti, L. N. de Castro, Bio-inspired and gradient-based algorithms to train MLPs: The influence of diversity, Information Sciences, vol. 179, pp. 1441–1453, 2009.

[31] . E. Rumelhart, G.E. Hinton, All, Learning representations by back-propagating errors,Nature ,vol .322,pp533–536, 1986.

[32] D.E.Rumelhart,J.L.McClelland, Parallel Distributed Processing.Foundations, Cambridge, MA ,vol.1, 1986,MIT Press,

[33] Y. Chauvin, D. E.Rumelhart (Eds.), Back propagation:Theory, Architectures, and Applications, Lawrence Erlbaum Associates, 1995.

[34] J. Ramesh,P.T.Vanathi,K.Gunavathi, Fault classification in phase-locked loops using back-propagation neural networks, ETRI journal,vol. 30, pp.546-553, 2008.

[35] D.Panagiotopoulos, C.Orovas, D.Syndoukas, A heuristically enhanced gradient approximation (HEGA) algorithm for training neural networks, Neurocomputing, Vol. 73, pp.1303-1323, 2010.

[36] R. Ceylan, Y. O¨ zbay ,Comparison of FCM, PCA and WT techniques for classification ECG arrhythmias using artificial neural network, Expert Systems with Applications, vol 33,pp.286–295, 2007.

[37] Y. Kutlu and all, Optimizing the performance of an MLP classifier for the automatic detection of epileptic spikes, Expert Systems with Applications , vol. 36, pp7567–7575, 2009.

[39] M. M. Mostafa, Profiling blood donors in Egypt: A neural network analysis, Expert Systems with Applications, vol .36, 5031–5038, 2009.

[40] S.Chabaa , A. Zeroual, J.Antari, MLP Neural Networks for Modeling non Gaussian Signal, Workshop STIC Wotic 09 in Agadir,(Morocco) 24-25, December, ,pp.58, 2009.

ISSN (e): 2250 – 3005 || Vol, 04 || Issue, 4 || April – 2014 ||
International Journal of Computational Engineering Research (IJCER)

Effect of First Order Chemical Reaction on Free Convection in a Vertical Double Passage Channel for Conducting Fluid

J. Prathap Kumar[1], J.C. Umavathi[2], Deena Sunil Sharanappa[3]
[1, 2, 3] *Department of Mathematics, Gulbarga University, Gulbarga-585 106, Karnataka, India*

ABSTRACT:
This paper reports investigation on laminar free convection in a vertical double passage channel for electrically conducting fluid in the presence of first order chemical reaction. The channel is divided into two passages by inserting a thin plane conducting baffle. After placing the baffle one of the passage is concentrated. An analytical solution has been developed for the coupled nonlinear ordinary differential equations using regular perturbation method. The results show that the thermal and mass Grashof number and Brinkman number enhances the flow where as Hartmann number and first order chemical reaction parameter suppresses the flow at all the baffle positions in both the streams.

Keywords: *Baffle, conducting fluid, first order chemical reaction, free convection, perturbation method.*

I. INTRODUCTION

The study of heat and mass transfer for an electrically conducting fluid under the influence of transverse magnetic field has attracted researchers in the recent past due to its relevance in many engineering problems such as MHD generators, heat exchangers, thermal processing, gas-cooled nuclear reactors and others. In the absence of magnetic field, references [1-3] will give some ideas about fluid flow and thermal characteristics inside a vertical channel with symmetric or asymmetric thermal boundary conditions. For an infinite vertical plate, Raptis and Kafoussias [4] studied the flow and heat transfer characteristics in the presence of magnetic field. Later Raptis [5] extended the vertical plate problem to a vertical channel problem in the presence of magnetic field. Malashetty et al. [6, 7, 8], Umavathi et al. [9], and Prathap Kumar et al., [10] studied mixed convection in a vertical channel for one and two fluid models. Umavathi et al. [11] analyzed magneto hydrodynamic free convection flow in a vertical rectangular duct for laminar, fully developed regime taking into consideration the effect of Ohmic heating and viscous dissipation. Umavathi and Sridhar [12] studied the Hartmann two-fluid Poiseuille-Couette flow in an inclined channel. Shah and London [13] have summarized the laminar forced convection heat transfer results for various channel cross sections, which were reported in the literature until 1970.

In particular process involving the mass transfer effects has been considered to be important precisely in chemical engineering equipments. The other applications include solidification of binary alloys and crystal growth dispersion of dissolved materials or particulate water in flows, drying and dehydration operations in chemical and food processing plants, evaporation at the surface of water body. The order of the chemical reaction depends on several factors. One of the simplest chemical reactions is the first order reaction in which rate of reaction is directly proportional to the species concentration. Das et al. [14] have studied the effect of mass transfer on the flow started impulsively past an infinite vertical plate in the presence of wall heat flux and chemical reaction. Muthucumaraswamy and Ganeshan [15, 16] have studied the impulsive motion of a vertical plate with heat flux/mass flux/suction and diffusion of chemically reactive species. Seddeek [17] has studied the finite element method for the effect of chemical reaction, variable viscosity, thermophoresis, and heat generation/absorption on a boundary layer hydro magnetic flow with heat and mass transfer over a heat surface. Kandasamy et al. [18, 19] have examined the effects of chemical reaction, heat and mass transfer with or without MHD flow with heat source/suction. The rate of heat transfer in a vertical channel could be enhanced by using special inserts. These inserts can be specially designed to increase the included angle between the velocity vector and the temperature gradient vector, rather than to promote turbulence. This increases the rate of heat transfer without a considerable drop in the pressure by Guo et al. [20]. A plane baffle may be used as an insert to enhance the rate of heat transfer in the channel. To avoid a considerable increase in the transverse thermal resistance into the channel, a thin and perfectly conductive baffle is used. The effect of such baffle on the laminar fully developed combined convection in a vertical channel with different uniform wall temperatures has been studied analytically by Salah El-Din [21]. Their study showed that for mixed convection the heat transfer between the walls and fluid can be significantly enhanced according to the baffle position and higher values of Nusselt number can be obtained when the baffle become as near the wall as possible.

Keeping in view the applications of chemical reaction and the increase of rate of heat transfer by introducing a baffle, motivated to investigate the effect of first order chemical reaction for electrically conducting fluid in a vertical channel. After inserting the baffle the fluid in stream-I is concentrated.

II. MATHEMATICAL FORMULATION

Consider a steady, two-dimensional laminar fully developed free convection flow in an open ended vertical channel filled with purely viscous conducting fluid. The *X*-axis is taken vertically upward, and parallel to the direction of buoyancy, and the *Y*-axis is normal to it as seen in Fig. 1. The channel walls are maintained at a constant temperature and the fluid properties are assumed to be constant. The channel is divided into two passages by means of thin, perfectly conducting plane baffle and each stream will have its own pressure gradient and hence the velocity will be individual in each stream.

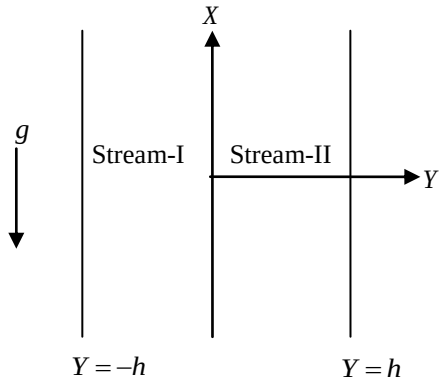

Figure1. Physical configuration.

The governing equations for velocity, temperature and concentrations are

Stream-I

$$\rho g \beta_T (T_1 - Tw_2) + \rho g \beta_C (C - C_{W2}) - \frac{dP}{dX} + \mu \frac{d^2U_1}{dY^2} - \sigma_e B_o^2 U_1 = 0 \quad (1)$$

$$\frac{d^2T_1}{dY^2} + \frac{\mu}{k}\left(\frac{dU_1}{dY}\right)^2 + \frac{\sigma_e}{k} B_o^2 U_1^2 = 0 \quad (2)$$

$$D\frac{d^2C}{dY^2} - KC = 0 \quad (3)$$

Stream-II

$$\rho g \beta_T (T_2 - Tw_2) - \frac{dP}{dX} + \mu \frac{d^2U_2}{dY^2} - \sigma_e B_o^2 U_2 = 0 \quad (4)$$

$$\frac{d^2T_2}{dY^2} + \frac{\mu}{k}\left(\frac{dU_2}{dY}\right)^2 + \frac{\sigma_e}{k} B_o^2 U_2^2 = 0 \quad (5)$$

Subject to the boundary and interface conditions on velocity, temperature and concentration as

$U_1 = 0$, $T_1 = T_{W_1}$, $C = C_{W1}$ at $Y = -h$

$U_2 = 0$, $T_2 = T_{W_2}$ at $Y = h$

$$U_1 = 0,\ U_2 = 0,\ T_1 = T_2,\ \frac{dT_1}{dY} = \frac{dT_2}{dY},\ C = C_{W2} \quad \text{at } Y = h^* \quad (6)$$

Introducing the following non-dimensional variables,

$$u_i = \frac{U_i}{\overline{U}_1},\ \theta_i = \frac{T_i - T_{W_2}}{T_{W_1} - T_{W_2}},\ Gr = \frac{g\beta_T \Delta T h^3}{\upsilon^2},\ Gc = \frac{g\beta_C \Delta C h^3}{\upsilon^2},\ \phi = \frac{C - C_{W2}}{C_{W1} - C_{W2}},\ \mathrm{Re} = \frac{\overline{U}_1 h}{\upsilon},\ Br = \frac{\overline{U}_1^2 \mu}{k\Delta T},\ Y^* = \frac{y^*}{h}$$

$$p = \frac{h^2}{\mu \overline{U}_1}\frac{dp}{dX},\ \Delta T = T_{W_2} - T_{W_1},\ \Delta C = C_{W_2} - C_{W_1},\ Y = \frac{y}{h},\ M^2 = \frac{\sigma_e B_0^{\,2} h^2}{\mu}. \tag{7}$$

One obtains the non-dimensional momentum, energy and concentration equations corresponding to stream-I and stream-II as

Stream-I

$$\frac{d^2 u_1}{dy^2} + GR_T\,\theta_1 + GR_C\,\phi - p - M^2 u_1 = 0 \tag{8}$$

$$\frac{d^2\theta_1}{dy^2} + Br\left(\left(\frac{du_1}{dy}\right)^2 + M^2\ u_1^2\right) = 0 \tag{9}$$

$$\frac{d^2\phi}{dy^2} - \alpha^2\phi = 0 \tag{10}$$

Stream-II

$$\frac{d^2 u_2}{dy^2} + GR_T\,\theta_2 - p - M^2\,u_2 = 0 \tag{11}$$

$$\frac{d^2\theta_2}{dy^2} + Br\left(\left(\frac{du_2}{dy}\right)^2 + M^2\,u_2^2\right) = 0 \tag{12}$$

Subject to the boundary conditions,

$$u_1 = 0,\ \theta_1 = 1,\ \phi = 1, \text{ at } y = -1$$
$$u_2 = 0,\ \theta_2 = 0, \text{ at } y = 1$$
$$u_1 = 0,\ u_2 = 0,\ \theta_1 = \theta_2,\ \frac{d\theta_1}{dy} = \frac{d\theta_2}{dy},\ \phi = n, \text{ at } y = y^*, \tag{13}$$

where $GR_T = \frac{Gr}{\mathrm{Re}}, GR_C = \frac{Gc}{\mathrm{Re}}, \alpha = \frac{kh^2}{D},\ n = \frac{C_2 - C_{W2}}{C_1 - C_{W2}}$.

III. SOLUTIONS

Solution of equation (10) can be obtained directly using boundary condition (13) and is given by

$$\phi = B_1 Cosh(\alpha y) + B_2 Sinh(\alpha y) \tag{14}$$

Equations (8), (9), (11) and (12) are coupled non-linear differential equations. Approximate solutions can be found by using the regular perturbation method. The perturbation parameter Br is usually small and hence regular perturbation method can be strongly justified. Adopting this technique, solutions for velocity, temperature and concentration are assumed in the form

$$u_i(y) = u_{i0}(y) + Br\,u_{i1}(y) + Br^2\,u_{i2}(y) + \ldots \tag{15}$$
$$\theta_i(y) = \theta_{i0}(y) + Br\,\theta_{i1}(y) + Br^2\,\theta_{i2}(y) + \ldots \tag{16}$$

Substituting equations (15) and (16) in equations (8), (9), (11) and (12) and equating the coefficients of like power of Br to zero and one, we obtain the zero and first order equations as

Stream-I
Zeroth order equations

$$\frac{d^2u_{10}}{dy^2}+GR_T\ \theta_{10}+GR_C\ \phi-p-M^2\,u_{10}=0 \tag{17}$$

$$\frac{d^2\theta_{10}}{dy^2}=0 \tag{18}$$

First order equations

$$\frac{d^2u_{11}}{dy^2}+GR_T\ \theta_{11}-M^2\ u_{11}=0 \tag{19}$$

$$\frac{d^2\theta_{11}}{dy^2}+\left(\left(\frac{du_{10}}{dy}\right)^2+M^2\ {u_{10}}^2\right)=0 \tag{20}$$

Stream-II
Zeroth order equations

$$\frac{d^2u_{20}}{dy^2}+GR_T\ \theta_{20}-p-M^2\ u_{20}=0 \tag{21}$$

$$\frac{d^2\theta_{20}}{dy^2}=0 \tag{22}$$

First order equations

$$\frac{d^2u_{21}}{dy^2}+GR_T\ \theta_{21}-p-M^2\ u_{21}=0 \tag{23}$$

$$\frac{d^2\theta_{21}}{dy^2}+\left(\left(\frac{du_{20}}{dy}\right)^2+M^2{u_{20}}^2\right)=0 \tag{24}$$

The corresponding boundary conditions reduces to
Zeroth-order

$u_{10}=0,\ \theta_{10}=1,\ \phi=1$, at $y=-1$

$u_{20}=0,\ \theta_{20}=0,$ at $y=1$

$$u_{10}=0,\ \ u_{20}=0,\ \theta_{10}=\theta_{20},\ \ \frac{d\theta_{10}}{dy}=\frac{d\theta_{20}}{dy},\ \phi=n,\text{ at } y=y^* \tag{25}$$

First order

$u_{11}=0,\ \theta_{11}=0$ at $y=-1$

$u_{21}=0,\ \theta_{21}=0$ at $y=1$

$$u_{11}=0,\ u_{21}=0,\ \theta_{11}=\theta_{21},\ \ \frac{d\theta_{11}}{dy}=\frac{d\theta_{21}}{dy}\ \text{ at } y=y^* \tag{26}$$

The solutions of zeroth and first order equations (17) to (24) using the boundary conditions as in equations (25) and (26) are
Zeroth order
Stream-I

$$\theta_{10}=z_1y+z_2 \tag{27}$$

$$u_{10}=A_1Cosh(My)+A_2Sinh(My)+r_1+r_2y+r_3Cosh(\alpha y)+r_4Sinh(\alpha y) \tag{28}$$

Stream-II

$$\theta_{20}=z_3y+z_4 \tag{29}$$

$$u_{20}=A_3Cosh(My)+A_4Sinh(My)+r_5+r_6y \tag{30}$$

First order
Stream-I

$$\theta_{11} = E_2 + E_1 y + q_1 y^2 + q_2 y^3 + q_3 y^4 + q_4 Cosh(\alpha y) + q_5 Sinh(\alpha y) + q_6 Cosh(2\alpha y) + q_7 Sinh(2\alpha y) + q_8 Cosh(2My) + q_9 Sinh(2My) + q_{10} Cosh(My) + q_{11} Sinh(My) + q_{12} y Cosh(My) + q_{13} y Sinh(My) + q_{14} y Cosh(\alpha y) + q_{15} y Sinh(\alpha y) + q_{16} Cosh(\alpha + M) y + q_{17} Cosh(\alpha - M) y + q_{18} Sinh(\alpha + M) y + q_{19} Sinh(\alpha - M) y \quad (31)$$

$$u_{11} = E_5 Cosh(My) + E_6 Sinh(My) + H_1 + H_2 y + H_3 y^2 + H_4 y^3 + H_5 y^4 + H_6 Cosh(\alpha y) + H_7 Sinh(\alpha y) + H_8 Cosh(2\alpha y) + H_9 Sinh(2\alpha y) + H_{10} Cosh(2My) + H_{11} Sinh(2My) + H_{12} y Cosh(My) + H_{13} y Sinh(My) + H_{14} y \cosh(\alpha y) + H_{15} y Sinh(\alpha y) + H_{16} Cosh(\alpha + M) y + H_{17} Cosh(\alpha - M) y + H_{18} Sinh(\alpha + M) y + H_{19} Sinh(\alpha - M) y + H_{20} y^2 Cosh(My) + H_{21} y^2 Sinh(My) \quad (32)$$

Stream-II

$$\theta_{21} = E_4 + E_3 y + F_1 y^2 + F_2 y^3 + F_3 y^4 + F_4 Cosh(2My) + F_5 Sinh(2My) + F_6 Cosh(My) + F_7 Sinh(My) + F_8 y Cosh(My) + F_9 y Sinh(My) \quad (33)$$

$$u_{21} = E_7 Cosh(My) + E_8 \sinh(My) + H_{22} + H_{23} y + H_{24} y^2 + H_{25} y^3 + H_{26} y^4 + H_{27} Cosh(2My) + H_{28} Sinh(2My) + H_{29} y Cosh(My) + H_{30} y Sinh(My) + H_{31} y^2 Cosh(My) + H_{32} y^2 Sinh(My) \quad (34)$$

The constants appeared in the above equations are presented in the Appendix.

IV. RESULTS AND DISCUSSIONS

The problem of free convective heat and mass transfer in a vertical double passage channel filled with electrically conducting fluid is investigated. The analytical solutions are found using regular perturbation method considering Brinkman number as the perturbation parameter. The effects of governing parameters such as Hartmann number, thermal Grashof number, mass Grashof number, Brinkman number and first order chemical reaction parameter on the velocity, temperature and concentration are shown graphically.

The effect of Hartmann number on the flow is shown in Figs. 2a,b,c and 3a,b,c. As the Hartmann number increases, the velocity and temperature decreases in both the streams at all the baffle positions. As the Hartmann number increases the fluid decreases which is the classical Hartmann result. When the baffle is near the hot wall the maximum velocity is in stream-II, when the baffle is near the cold wall the maximum velocity is seen in stream-I and when the baffle is in the center of the channel the maximum velocity is seen in stream-I.

The effect of thermal Grashof number on the velocity and temperature field is shown in Figs. 4a,b,c and 5a,b,c at all three different baffle positions. As the thermal Grashof number increases, the velocity and temperature increases in both the streams at all the baffle positions. This is an expected result because increase in thermal Grashof number results in increase of bouncy force and hence increases the flow in both the streams at all the baffle positions.

The effect of mass Grashof number on the velocity and temperature field is shown in Figs. 6a,b,c and 7a,b,c respectively. As the mass Grashof number increases the flow is enhanced in both the streams at all the baffle positions. The enhancement on velocity is significant in stream-I when compared to stream-II .This is due to the fact that the fluid is concentrated only in stream-I. Though the fluid is not concentrated in stream-II still its effect is observed in stream-II when the baffle position is in the center of the channel, this is due to the reason that we have considered the baffle to be conducting. That is say that, there is heat transfer from stream-I to stream-II but there is no mass transfer from stream-I to stream-II. Due to transfer of heat from stream-I to stream-II results in increase of both thermal buoyancy force and concentration buoyancy force and hence velocity increase in stream-II slightly as mass Grashof number increases as seen in Fig. 6. As mass Grashof number increases the temperature increases significantly in stream-I when the baffle position is at the center of the cold wall. There is no much variation on the temperature field when the baffle position is near the hot wall.

The effect of Brinkman number is shown in Figs. 8a,b,c and 9a,b,c on the velocity and temperature fields respectively. As the Brinkman number increase both the velocity and temperature increases in both the streams at all the baffle positions. This is due to the fact that increase in Brinkman number increases the viscous dissipation and hence the flow is enhanced.

The effect of first order chemical reaction parameter on the velocity, temperature and concentration fields are displayed in Figs. 10a,b,c, 11a,b,c and 12a,b,c respectively. As α increases the velocity, temperature and concentration decreases in stream-I, and remains constant in stream-II. The similar result was also obtained by Srinivas and Muturajan [22] for mixed convective flow in a vertical channel. This is due to the fact that the fluid in stream-I is concentrated. The maximum value of velocity and temperature is seen in stream-II for the baffle position at $y^* = -0.8$ and in stream-I for the baffle position at $y^* = 0$ and 0.8.

V. CONCLUSIONS

The effect of first order chemical reaction in a vertical double passage channel filled with electrically conducting fluid by inserting a thin baffle is investigated. The following conclusions were drawn:

.

1. Increasing the values of Hartmann number reduces the flow field where as increase in the thermal Grashof number and mass Grashof number enhance the flow in both the streams at different baffle positions.
2. Increase in the perturbation parameter (Brinkman number) enhances the velocity and temperature in both the streams.
3. Increase in the chemical reaction parameter suppresses the velocity, temperature and concentration in stream-I and remains invariant in stream-II.

REFERENCES

[1] S. Habchi and Archarya. Laminar mixed convection in a symmetrically or asymmetrically heated vertical channel. Numer. Heat Transfer, 9:605-618, 1986.

[2] W. Aung and G. Worku. Developing flow and reversal in a vertical channel with asymmetric wall temperatures. J. Heat Transfer, 108:299-304, 1986.

[3] M. Iqbal, B.D. Aggarwala and A.G. Fowlere. Laminar combined free and forced convection in a vertical non-circular ducts under uniform heat flux. Int. J. Heat Mass Transfer, 12:1123-1139, 1969.

[4] N. Raptis, Kafoussias. Heat transfer in a flow through a porous medium bounded by an infinite vertical plane under the action of magnetic field, Energy Res., 6:241-245, 1982.

[5] Raptis. Flow through a porous medium in the presence of magnetic field. Energy Res., 10:97-100, 1986.

[6] M.S. Malashetty, J.C. Umavathi and J. Prathap Kumar. Two fluid magnetoconvection flow in an inclined channel. Int. J. Transport Phenomena, 3:73-84, 2000.

[7] M.S. Malashetty, J.C. Umavathi and J. Prathap Kumar. Convective magnetohydrodynamic two fluid flow and heat transfer in an inclined channel. Heat and Mass Transfer, 37:259-264, 2001.

[8] M.S. Malashetty, J.C. Umavathi and J. Prathap Kumar. Magnetoconvection of two immiscible fluids in a vertical enclosure, Heat and Mass Transfer, 42:977-993, 2006

[9] J.C. Umavathi, B. Mallikarjun Patil and I. Pop. On laminar mixed convection flow in a vertical porous stratum with symmetric wall heating conditions. Int. J. Transport Phenomena, 8:1-14, 2006.

[10] J. Prathap Kumar, J.C. Umavathi and Basavaraj M Biradar. Mixed convection of composite porous medium in a vertical channel with asymmetric wall heating conditions. J. Porous Medium, 13:271-285, 2010.

[11] J.C. Umavathi, I.C. Liu, J. Prathap Kumar and I. Pop. Fully developed magneto convection flow in a vertical rectangular duct. Heat and Mass Transfer, 47:1-11, 2011.

[12] J.C. Umavathi and K.S.R. Sridhr. Hartmann two fluid Poisulle-Couette flow in an inclined channel, Int. J. Appl. Mech. Engg., 14:539-557, 2009.

[13] R.K. Shah and A. London. Laminar flow forced convection heat transfer and flow friction in straight and curved ducts-A summary of analytical solutions. Stanford University, Stanford, California, USA, Tech. Rep.vol. 75, 1971.

[14] U.N. Das, R.K. Deka and V.M. Soundalgekar. Effects of mass transfer on the flow past an impulsively started infinite vertical plate with constant heat flux and chemical reaction. Forsch Ingenieurwes, 60:284-287, 1994.

[15] R. Muthucumaraswamy and P. Ganesan. On impulsive motion of a vertical plate with heat flux and diffusion of chemically reactive species. Forsch Ingenieurwes, 66:17-23, 2000.

[16] R. Muthucumaraswamy and P. Ganesan. First order chemical reaction on flow past impulsively stratified vertical plate with uniform heat and mass flux. Acta Mech., 147:45-57, 2001.

[17] M.A. Seddek. Finite element method for the effects of chemical reaction, variable viscosity, thermophoresis and heat generation/absorption on a boundary layer hydro magnetic flow with heat and mass transfer over a heat surface. Acta Mech., 177:1-18, 2005.

[18] R. Kandasamy, K. Perisamy and K.K. Sivagnana Prabhu. Effects of chemical reaction, heat and mass transfer along a wedge with heat source and concentration in the presence of suction or injection. Int. J. Heat Mass Transfer, 48:1388-1394, 2005.

[19] R. Kandasamy, K. Perisamy and K.K. Sivagnana Prabhu. Chemical reaction, heat and mass transfer on MHD flow over a vertical stretching surface with heat source and thermal stratification effects. Int. J. Heat Mass Transfer, 48:4557-4561, 2005.

[20] Z.Y. Guo, D.Y. Li and B.X. Wang. A novel concept for convective heat transfer enhancement. Int. J. Heat Mass Transfer,.41:2221-2225, 1998.

[21] M.M. Salah El-Din. Fully developed laminar convection in a vertical double-passage channel. Appl Energy, 47:69-75, 1994.

[22] S. Srinivas, R. Muthuraj. Effect of chemical reaction and space porosity on MHD mixed convective flow in a vertical asymmetric channel with peristalsis. Mathematical and Computer Modeling, 54:1213-1227, 2011.

NOMENCLATURE

B_0	magnetic field
Br	Brinkman number
C_1	concentration in Stream-I
C_0	reference concentration
C_p	specific heat at constant pressure
c_p	dimensionless specific heat at constant pressure
D	diffusion coefficients
E_0	applied electric field
E	electric field load parameter
h	channel width
h^*	width of passage
g	acceleration due to gravity
Gr	Grashoff number
Gr	Grashoff number
G_c	modified Grashoff Number
GR_T, GR_C	dimensionless parameters
k	thermal conductivity of fluid
M	Hartmann number
p	nondimensional pressure gradient
Re	Reynolds number
T_1, T_2	dimensional temperature distributions
T_{w_1}, T_{w_2}	temperatures of the boundaries
$\overline{U_1}$	reference velocity
u_1, u_2	nondimensional velocities in Stream-I, Stream-II
U_1, U_2	dimensional velocity distributions
y^*	baffle position

GREEK SYMBOLS

α	chemical reaction parameters
β_T	coefficients of thermal expansion
β_C	coefficients of concentration expansion
σ_e	electrical conductivity
$\Delta T, \Delta C$	difference in temperatures & concentration
θ_i	non-dimensional temperature
γ	kinematics viscosity
ϕ	non-dimensional concentrations
ρ	density
μ	viscosity

SUBSCRIPTS

i refer quantities for the fluids in Stream-I and Stream-II, respectively.

VI. ACKNOWLEDGEMENTS

The authors greatly acknowledge the funding support from the Major Research project supported by University Grants Commission India (Grant No. 41-774/2012 (SR)).

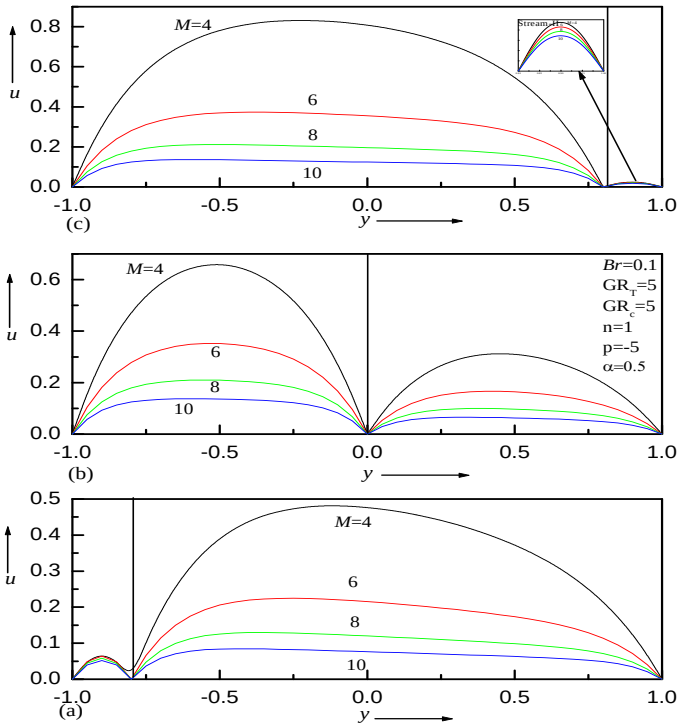

Figure2.Velocity profiles for differnt values of Hartmann number *M*
(a) *y**=-0.8 (b) *y**=0 (c) *y**=0.8

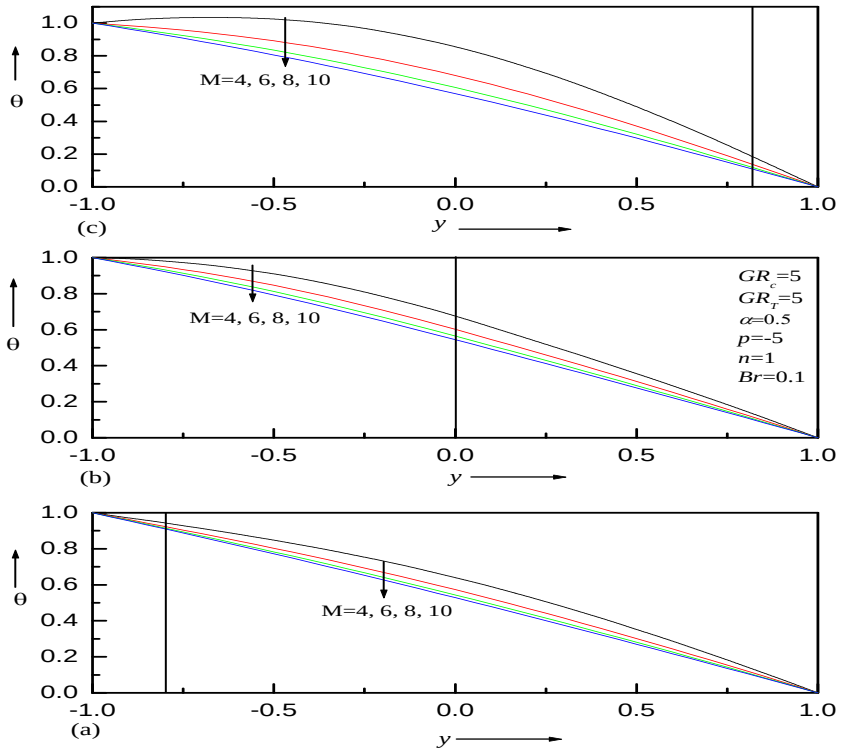

Figure3.Temperature profiles for differnt values of Hartmann number *M*
(a) *y**=-0.8 (b) *y**=0 (c) *y**=0.8

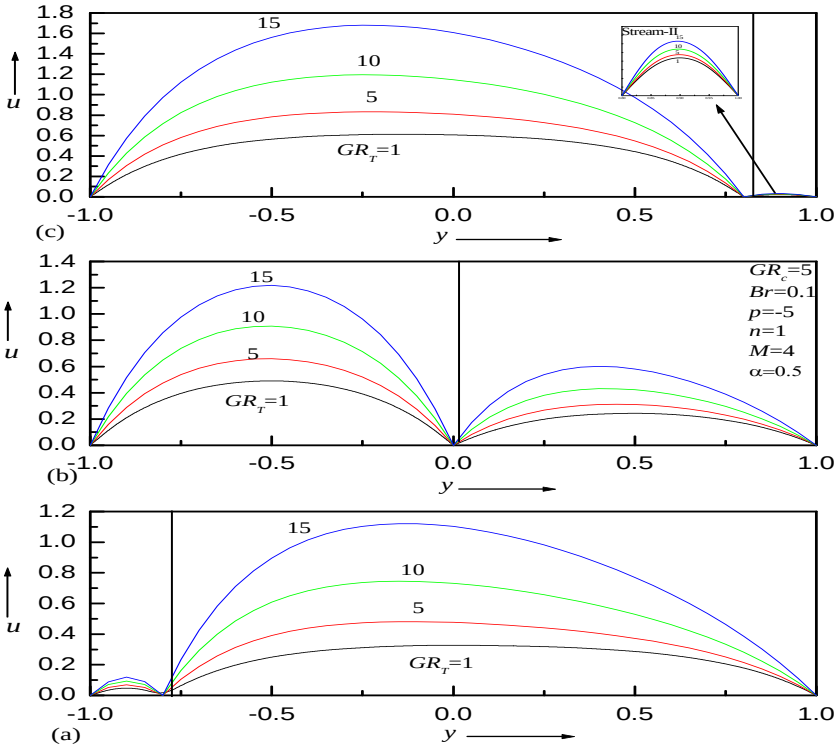

Figure4. Velocity profiles for different values of thermal Grashoff number GR_T at (a) y^*=-0.8 (b) y^*=0.0 (c) y^*=0.8

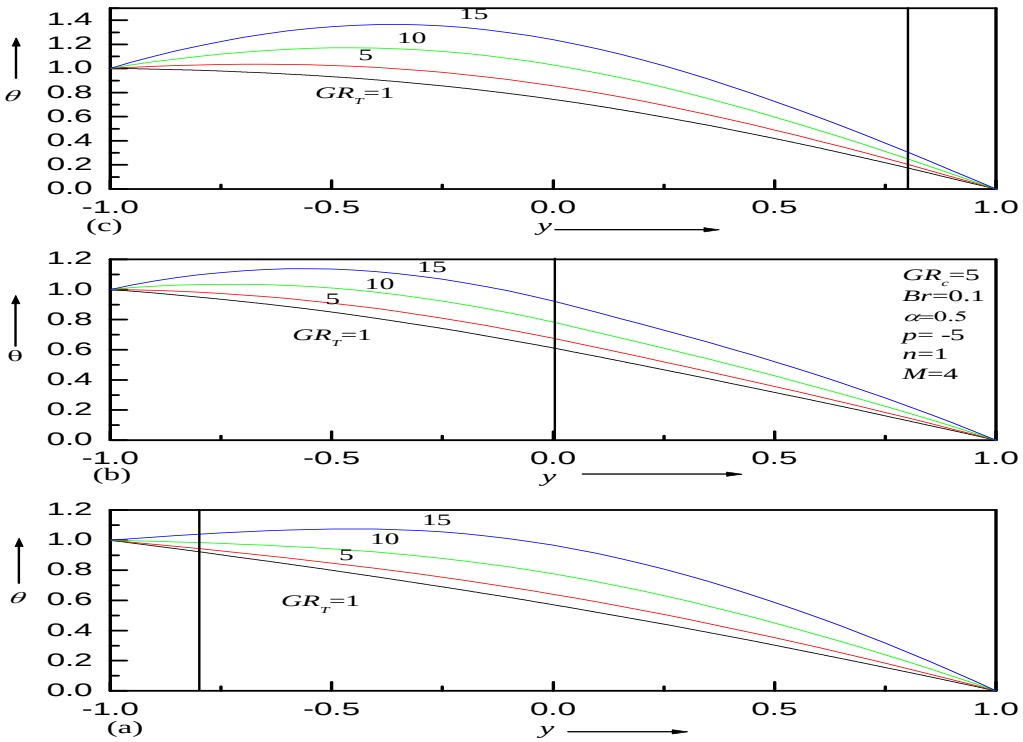

Figure5.Temperature profiles for different values of thermal Grashof number GR_T at (a) y^*=-0.8 (b) y^*=0 (c) y^*=0.8

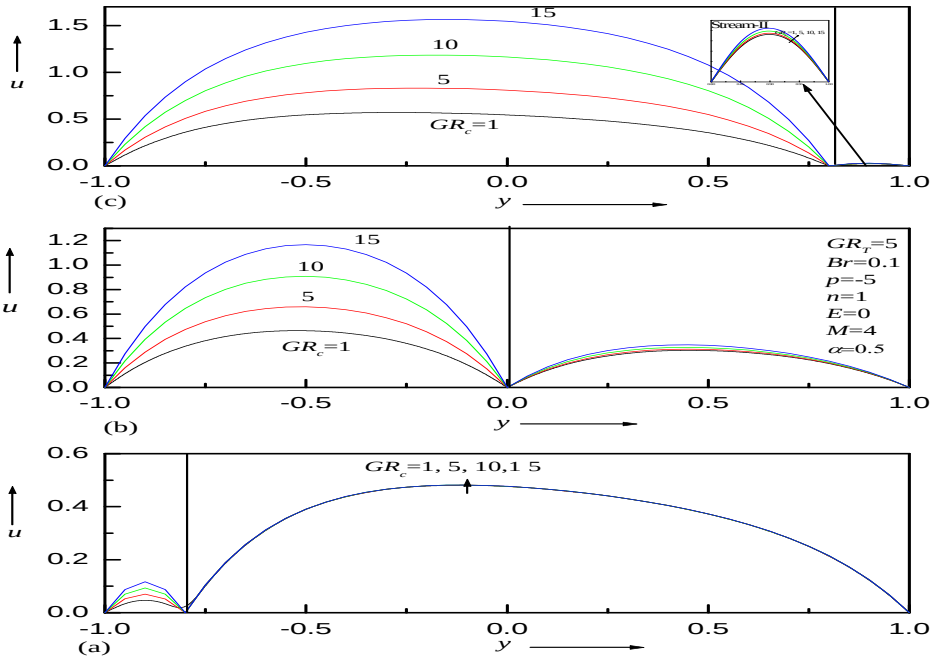

Figure6.Velocity profiles for different values of concentration Grashof number GR_C at (a) y^*=-0.8 (b) y^*=0 (c) y^*=0.8

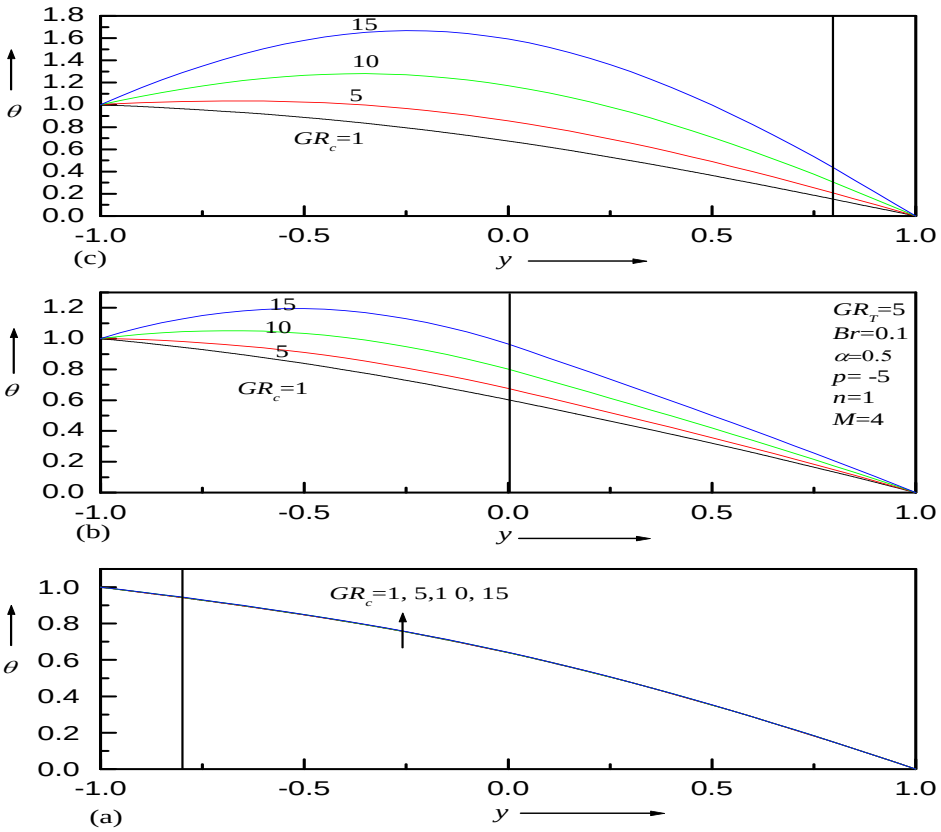

Figure7.Temperature profiles for different values of concentration Grashoff number GR_C at (a) y^*=-0.8 (b) y^*=0 (c) y^*=0.8

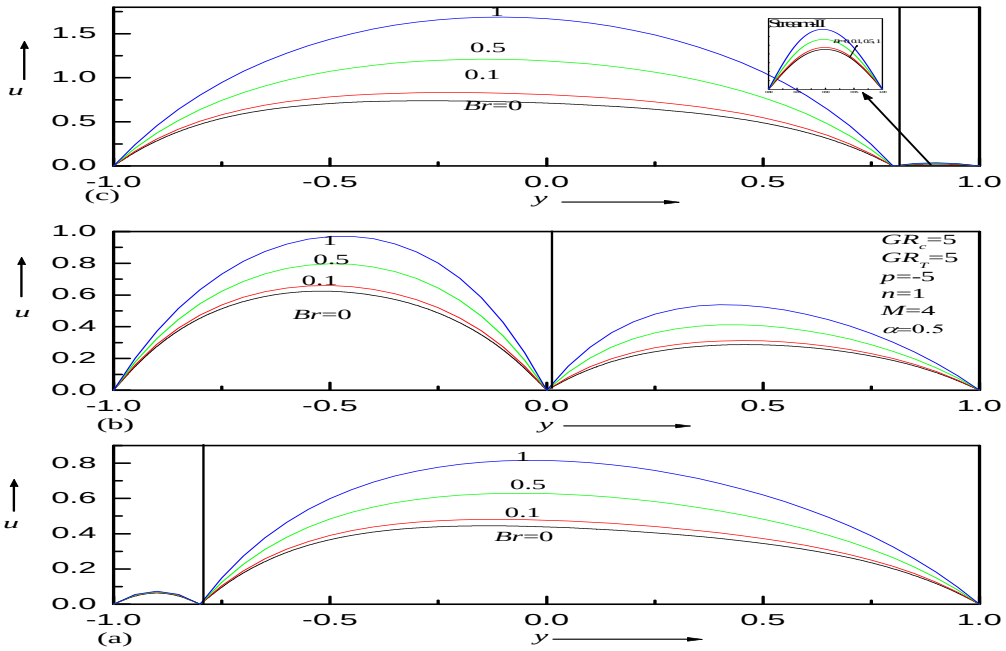

Figure8.Velocity profiles for different values of Brinkman number Br (a) y^*=-0.8 (b) y^*=0 (c) y^*=0.8

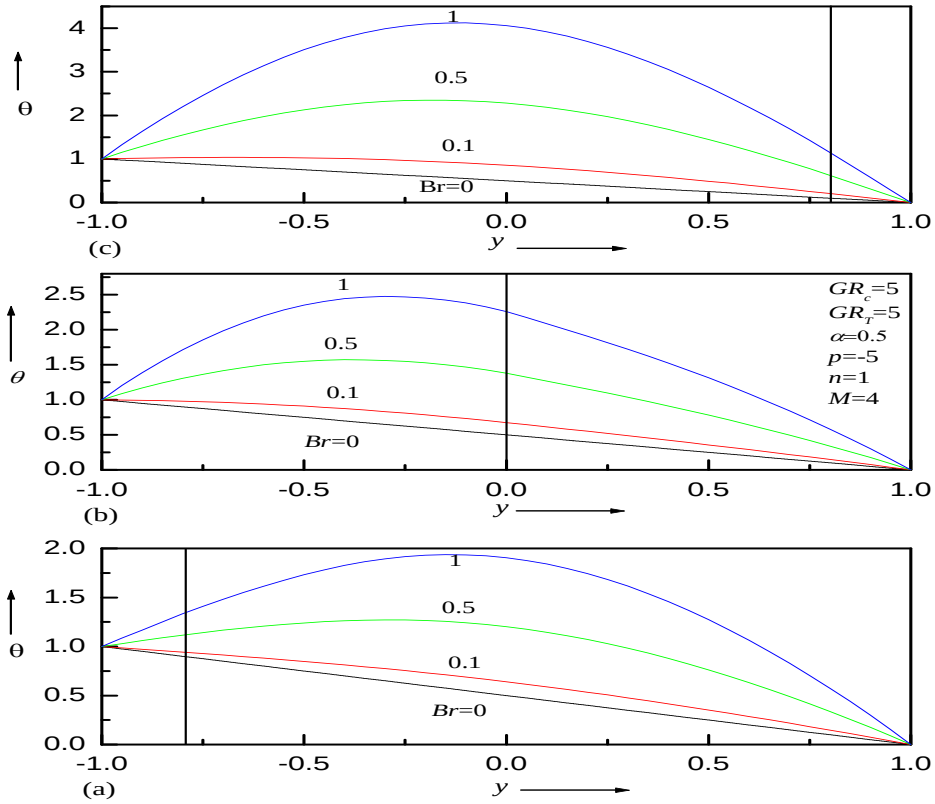

Figure9.Temperature profiles for differeent values of Brinkman number Br (a) y^*=-0.8 (b) y^*=0 (c) y^*=0.8

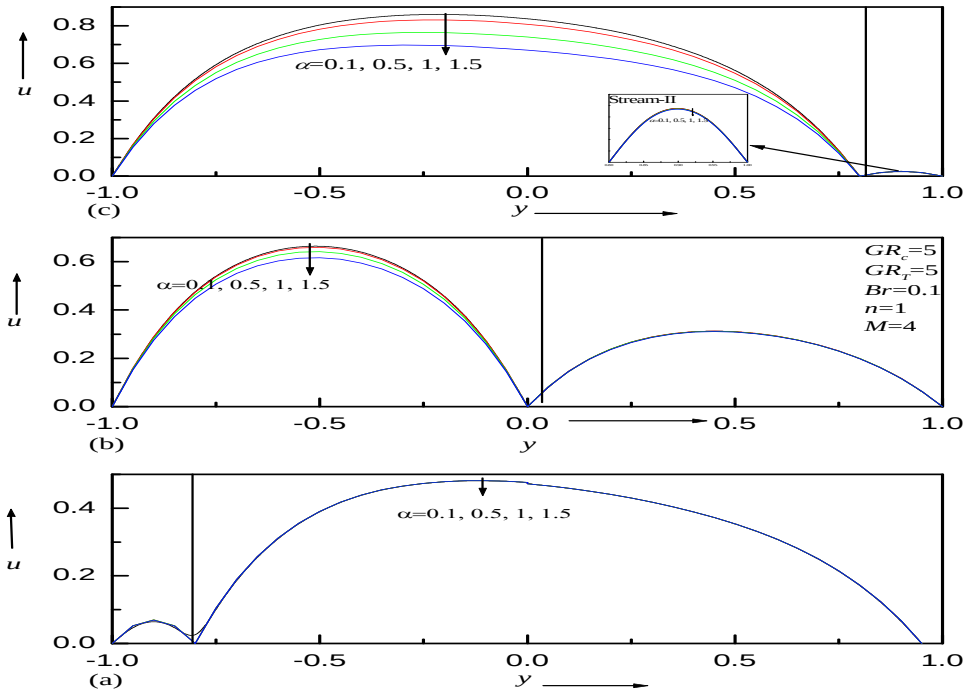

Figure10.Velocity profiles for different values of chemical reaction parameter α (a) y^*=-0.8 (b) y^*=0 (c) y^*=0.8

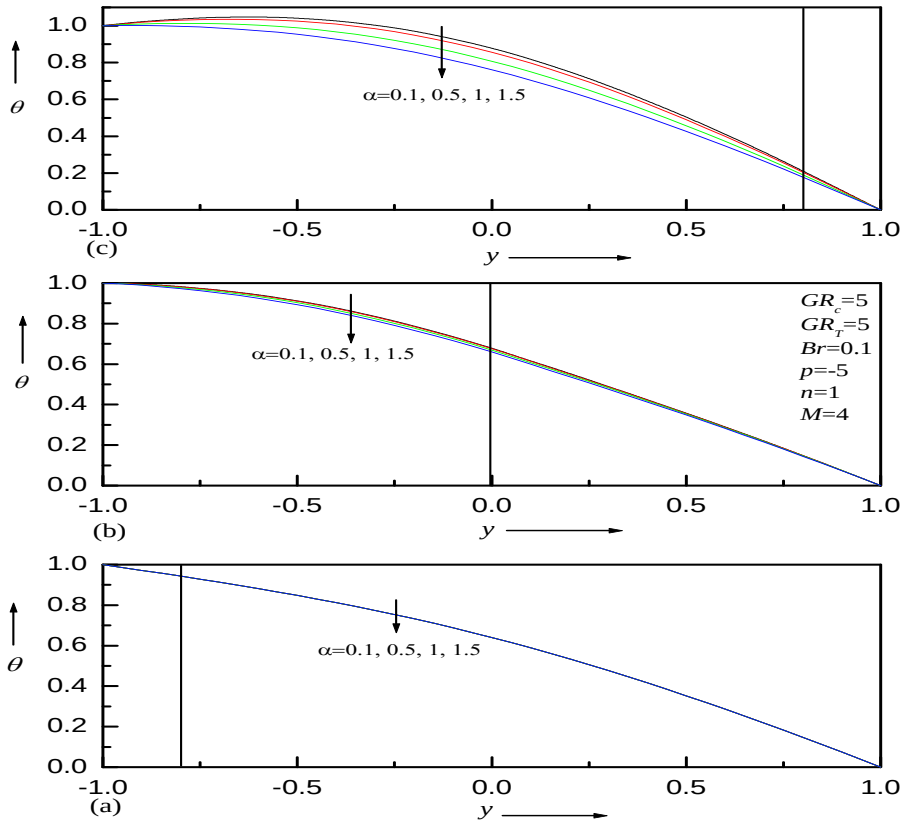

Figure11.Temperature profiles for different values of chemical reaction parameter α (a) y^*=-0.8 (b) y^*=0 (c) y^*=0.8

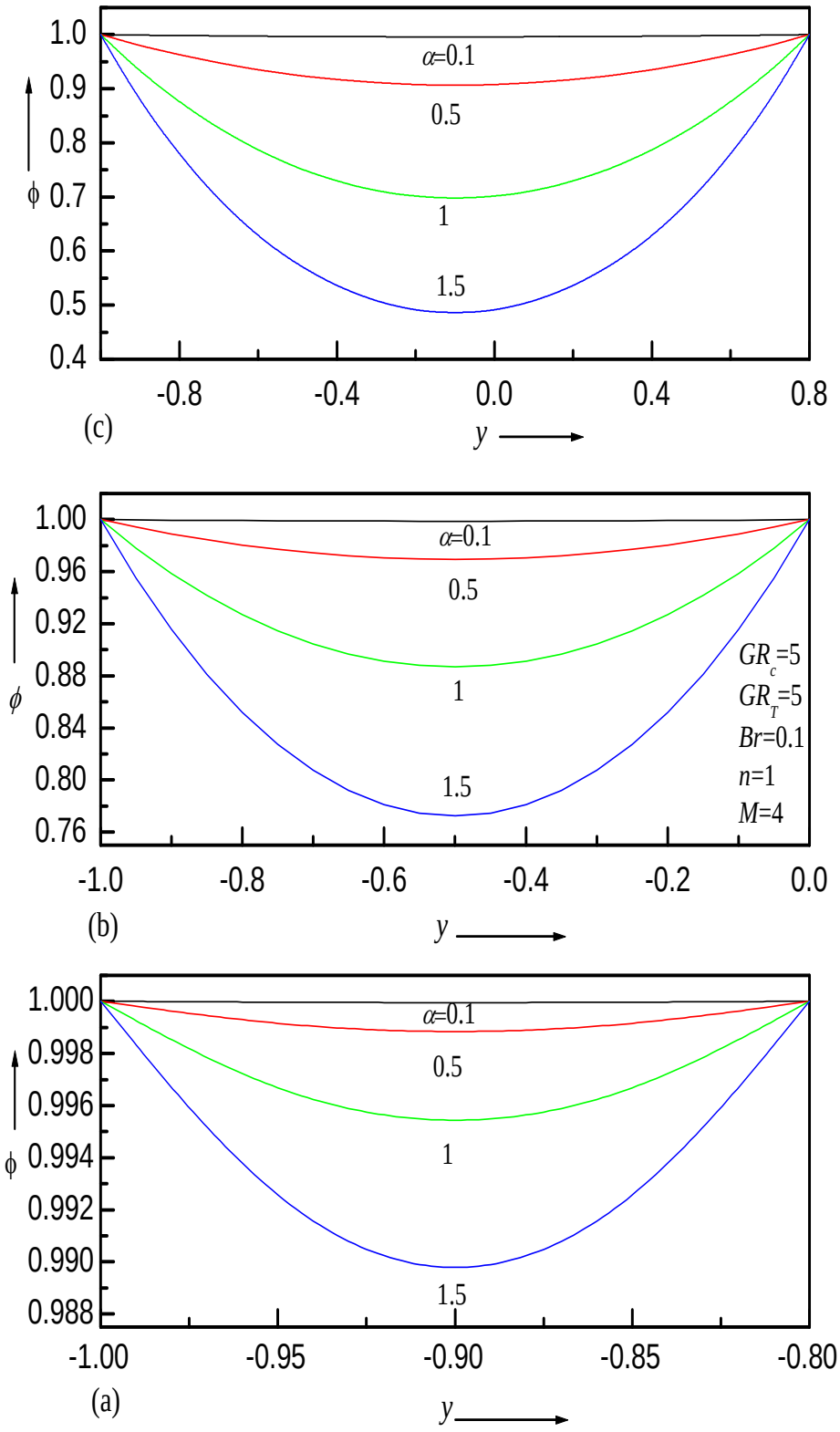

Figure12. Concentration profiles for different values of chemical reaction parameter α at (a) y*=-0.8 (b)y*=0 (c) y*=0.8

Appendix

$$B_1=\frac{Sinh(\alpha y^*)+nSinh(\alpha)}{Cosh(\alpha)Sinh(\alpha y^*)+Cosh(\alpha y^*)Sinh(\alpha y^*)},\ B_2=\frac{nCosh(\alpha y^*)-Cosh(\alpha y^*)}{Cosh(\alpha)Sinh(\alpha y^*)+Cosh(\alpha y^*)Sinh(\alpha y^*)},\ z_1=-\frac{1}{2},$$

$$z_2=\frac{1}{2},\ z_3=\frac{1}{2},\ z_4=\frac{-1}{2},\ r_1=\frac{GR_TC_2-P}{M^2},\ r_2=\frac{GR_TC_1}{M^2},\ r_3=-\frac{GR_CB_1}{\alpha^2-M^2},\ r_4=-\frac{GR_CB_2}{\alpha^2-M^2},\ r_5=\frac{GR_TC_4-P}{M^2},$$

$$r_6=\frac{GR_TC_3}{M^2},\ T_1=-r_1+r_2-r_3\cosh(\alpha)+r_4\sinh(\alpha),\ T_3=-r_5-r_6,\ T_4=-r_5-r_6y^*,$$

$$T_2=-(r_1+r_2y^*+r_3\cosh(\alpha y^*)+r_4\sinh(\alpha y^*)),\quad A_1=\frac{T_1Sinh(My^*)+T_2Sinh(M)}{Cosh(M)Sinh(My^*)+Cosh(My^*)Sinh(M)},$$

$$A_2=\frac{T_2Cosh(M)-T_1Cosh(My^*)}{Cosh(M)Sinh(My^*)+Cosh(My^*)Sinh(M)},\ A_3=\frac{T_3Sinh(My^*)-T_4Sinh(M)}{Cosh(M)Sinh(My^*)-Cosh(My^*)Sinh(M)},$$

$$A_4=\frac{T_3-A_3Cosh(M)}{Sinh(M)},\ p_1=-\frac{2M^2r_1^2+2r_2^2+\left(r_3^2-r_4^2\right)\left(M^2-\alpha^2\right)}{2},\ p_2=-2M^2r_1r_2,\ p_3=-M^2r_2^2,$$

$$p_4=-\left(2M^2r_1r_3+2r_2r_4\alpha\right),\ p_5=2M^2r_1r_4+2r_2r_3\alpha,\ p_6=-\frac{\left(r_3^2+r_4^2\right)\left(\alpha^2+M^2\right)}{2},\ p_7=-\left(M^2r_3r_4+r_3r_4\alpha^2\right),$$

$$p_8=-\left(A_1^2M^2+A_2^2M^2\right),\ p_9=-2A_1A_2M^2,\ p_{10}=-\left(2A_1M^2r_1+2A_2Mr_2\right),\ p_{11}=-\left(2A_2M^2r_1+2A_1Mr_2\right),$$

$$p_{12}=-2A_1r_2M^2,\ p_{13}=-2A_2M^2r_2,\ p_{14}=-2M^2r_2r_3,\ p_{15}=-2M^2r_2r_4,$$

$$p_{16}=-\left(A_1r_3M^2+A_2Mr_4\alpha+A_2M^2r_4+A_1M\alpha r_3\right),\ p_{17}=-\left(A_1M^2r_3+A_2M\alpha r_4-A_2M^2r_4-A_1M\alpha r_3\right),$$

$$p_{18}=-\left(A_2r_3M^2+A_1Mr_4\alpha+A_1M^2r_4+A_2M\alpha r_3\right),\ p_{19}=-\left(A_1M^2r_4+A_2M\alpha r_3-A_2M^2r_3-A_1M\alpha r_4\right),\ q_1=\frac{p_1}{2},$$

$$q_2=\frac{p_2}{6},\ q_3=\frac{p_3}{12},\ q_4=\frac{p_4\alpha-2p_{15}}{\alpha^3},\ q_5=\frac{p_5\alpha-2p_{14}}{\alpha^3},\ q_6=\frac{p_6}{4\alpha^2},\ q_7=\frac{p_7}{4\alpha^2},\ q_8=\frac{p_8}{4M^2},\ q_9=\frac{p_9}{4M^2},$$

$$q_{10}=\frac{p_{10}M-2p_{13}}{M^3},\ q_{11}=\frac{p_{11}M-2p_{12}}{M^3},\ q_{12}=\frac{p_{12}}{M^2},\ q_{13}=\frac{p_{13}}{M^2},\ q_{14}=\frac{p_{14}}{\alpha^2},\ q_{15}=\frac{p_{15}}{\alpha^2},\ q_{16}=\frac{p_{16}}{\left(\alpha+M\right)^2},$$

$$q_{17}=\frac{p_{17}}{\left(\alpha-M\right)^2},\ q_{18}=\frac{p_{18}}{\left(\alpha+M\right)^2},\ q_{19}=\frac{p_{19}}{\left(\alpha-M\right)^2},\ R_1=-\left(M^2r_5^2+M^2r_6^2\right),\ R_2=-2M^2r_5r_6,\ R_3=-M^2r_6^2,$$

$$R_4=-A_3^2M^2-A_4^2M^2,\ R_5=-2A_3A_4M^2,\ R_6=-\left(2A_3M^2r_5+2A_4M^2r_6\right),\ R_7=-\left(2A_4M^2r_5+2A_3M^2r_6\right),$$

$$F_1=\frac{R_1}{2},F_2=\frac{R_2}{6},F_3=\frac{R_3}{12},\ F_4=\frac{R_4}{4M^2},\ F_5=\frac{R_5}{4M^2},\ F_6=\frac{R_6M-2R_9}{M^3},\ F_7=\frac{R_7M-2R_8}{M^3},\ F_8=\frac{R_8}{M^2},\ F_9=\frac{R_9}{M^2},$$

$$T_5=-\begin{pmatrix}q_1-q_2+q_3+q_4Cosh(\alpha)-q_5Sinh(\alpha)+q_6Cosh(2\alpha)-q_7Sinh(2\alpha)+q_8Cosh(2M)-q_9Sinh(2M)\\+q_{10}Cosh(M)-q_{11}Sinh(M)-q_{12}Cosh(M)+q_{13}Sinh(M)-q_{14}Cosh(\alpha)+q_{15}Sinh(\alpha)\\+q_{16}Cosh\left(\alpha+M\right)+q_{17}Cosh\left(\alpha-M\right)-q_{18}Sinh\left(\alpha+M\right)-q_{19}Sinh\left(\alpha-M\right)\end{pmatrix},$$

$$T_6=-\left(F_1+F_2+F_3+F_4Cosh(2M)+F_5Sinh(2M)+F_6Cosh(M)+F_7Sinh(M)+F_8Cosh(M)+F_9Sinh(M)\right),$$

$$\begin{aligned}T_7=\ &F_1y^{*2}+F_2y^{*3}+F_3y^{*4}+F_4\cosh(2My^*)+F_5Sinh(2My^*)+F_6Cosh(My^*)+F_7Sinh(My^*)+F_8y^*Cosh(My^*)\\&+F_9y^*Sinh(my^*)-(q_1y^{*2}+q_2y^{*3}+q_3y^{*4}+q_4Cosh(\alpha y^*)+q_5Sinh(\alpha y^*)+q_6Cosh(2\alpha y^*)+q_7Sinh(2\alpha y^*)\\&+q_8Cosh(2My^*)+q_9Sinh(2My^*)+q_{10}Cosh(My^*)+q_{11}Sinh(My^*)+q_{12}y^*Cosh(My^*)+q_{13}ySinh(My^*)\\&+q_{14}yCosh(\alpha y^*)+q_{15}ySinh(\alpha y^*)+q_{16}Cosh\left(\alpha+M\right)y^*+q_{17}Cosh\left(\alpha-M\right)y^*\\&+q_{18}Sinh\left(\alpha+M\right)y^*+q_{19}Sinh\left(\alpha-M\right)y^*)\end{aligned},$$

$$\begin{aligned}T_8=\ &2F_1y^*+3F_2y^{*2}+4F_3y^{*3}+2MF_4Sinh(2My^*)+2MF_5Cosh(2My^*)+F_6MSinh(My^*)+F_7MCosh(My^*)\\&+F_8(y^*MSinh(My^*)+Cosh(My^*))+F_9(y^*MCosh(My^*)+Sinh(My^*))-(2q_1y^*+3q_2y^{*2}+4q_3y^{*3}\\&+q_4\alpha Sinh(\alpha y^*)+q_5\alpha Cosh(\alpha y^*)+2\alpha q_6Sinh(2\alpha y^*)+2q_7\alpha Cosh(2\alpha y^*)+2Mq_8Sinh(2My^*)\\&+2Mq_9Cosh(2My^*)+q_{10}MSinh(My^*)+q_{11}MCosh(My^*)+q_{12}(y^*MSinh(My^*)+Cosh(My^*))\\&+q_{13}(y^*MCosh(My^*)+Sinh(My^*))+q_{14}(y^*\alpha Sinh(\alpha y^*)+Cosh(\alpha y^*))+q_{15}(y^*\alpha Cosh(\alpha y^*)\\&+Sinh(\alpha y^*))+q_{16}(\alpha+M)Sinh(\alpha+M)y^*+q_{17}(\alpha-M)Sinh(\alpha-M)y^*+q_{18}(\alpha+M)Cosh(\alpha+M)y^*\\&+q_{19}(\alpha-M)Cosh(\alpha-M)y^*)\end{aligned},$$

$$E_1=\frac{\left(-T_5+T_6+T_7+T_8-T_8y^*\right)}{2},\ E_2=\frac{\left(T_5+T_6+T_7+T_8-T_8y^*\right)}{2},\ E_3=\frac{\left(-T_5+T_6+T_7-T_8-T_8y^*\right)}{2},$$

$$E_4=\frac{\left(T_5+T_6-T_7+T_8+T_8y^*\right)}{2},\ H_1=\frac{GR_T\left(E_2M^4+2q_1M^2+24q_3\right)}{M^6},\ H_2=\frac{GR_T\left(E_1M^2+6q_2\right)}{M^4},$$

$$H_3=\frac{GR_T\left(q_1M^2+12q_3\right)}{M^4},\ H_4=\frac{GR_Tq_2}{M^2},\ H_5=\frac{GR_Tq_3}{M^2},\ H_6=\frac{2\alpha q_{15}GR_T-q_4GR_T\left(\alpha^2-M^2\right)}{\left(\alpha^2-M^2\right)^2},$$

$$H_7=\frac{2q_{14}\alpha GR_T-q_5GR_T\left(\alpha^2-M^2\right)}{\left(\alpha^2-M^2\right)^2},\ H_8=-\frac{q_6GR_T}{4\alpha^2-M^2},\ H_9=-\frac{q_7GR_T}{4\alpha^2-M^2},\ H_{10}=-\frac{q_8GR_T}{3M^2},\ H_{11}=-\frac{q_9GR_T}{3M^2},$$

$$H_{12}=\frac{q_{12}GR_T-2q_{11}GR_TM}{4M^2},\ H_{13}=\frac{q_{13}GR_T-2q_{10}GR_TM}{4M^2},\ H_{14}=-\frac{q_{14}GR_T}{\alpha^2-M^2},\ H_{15}=-\frac{q_{15}GR_T}{\alpha^2-M^2},$$

$$H_{16}=-\frac{q_{16}GR_T}{\left(\alpha+M\right)^2-M^2},\ H_{17}=-\frac{q_{17}GR_T}{\left(\alpha-M\right)^2-M^2},\ H_{18}=-\frac{q_{18}GR_T}{\left(\alpha+M\right)^2-M^2},\ H_{19}=-\frac{q_{19}GR_T}{\left(\alpha-M\right)^2-M^2},$$

$$H_{20}=-\frac{q_{13}GR_T}{4M},\ H_{21}=-\frac{q_{12}GR_T}{4M},\ H_{22}=\frac{GR_T\left(E_4M^4+2F_1M^2+24F_3\right)}{M^6},\ H_{23}=\frac{GR_T\left(E_3M^2+6F_2\right)}{M^4},$$

$$H_{24}=\frac{GR_T\left(F_1M^2+12F_3\right)}{M^4},\ H_{25}=\frac{GR_TF_2}{M^2},\ H_{26}=\frac{GR_TF_3}{M^2},\ H_{27}=-\frac{GR_TF_4}{3M^2},\ H_{28}=-\frac{GR_TF_5}{3M^2},$$

$$H_{29}=\frac{F_8GR_T-2F_7GR_TM}{4M^2},\ H_{30}=\frac{F_9GR_T-2F_6GR_TM}{4M^2},\ H_{31}=-\frac{F_9GR_T}{4M},\ H_{32}=-\frac{F_8GR_T}{4M},$$

$$\begin{aligned}T_9=&H_1-H_2+H_3-H_4+H_5+H_6Cosh(\alpha)-H_7Sinh(\alpha)+H_8Cosh(2\alpha)-H_9Sinh(2\alpha)+H_{10}\cosh(2M)\\&-H_{11}Sinh(2M)-H_{12}Cosh(M)+H_{13}Sinh(M)-H_{14}Cosh(\alpha)+H_{15}Sinh(\alpha)+H_{16}Cosh\left(\alpha+M\right)\\&+H_{17}Cosh\left(\alpha-M\right)-H_{18}Sinh\left(\alpha+M\right)-H_{19}Sinh\left(\alpha-M\right)+H_{20}Cosh(M)-H_{21}Sinh(M)\end{aligned},$$

$$\begin{aligned}T_{10}=&H_1+H_2y^*+H_3y^{*2}+H_4y^{*3}+H_5y^{*4}+H_6Cosh(\alpha y^*)+H_7Sinh(\alpha y^*)+H_8Cosh(2\alpha y^*)+H_9Sinh(2\alpha y^*)\\&+H_{10}Cosh(2My^*)+H_{11}Sinh(2My^*)+H_{12}y^*Cosh(My^*)+H_{13}y^*Sinh(My^*)+H_{14}y^*Cosh(\alpha y^*)\\&+H_{15}y^*Sinh(\alpha y^*)+H_{16}Cosh\left(\alpha+M\right)y^*+H_{17}Cosh\left(\alpha-M\right)y^*+H_{18}Sinh\left(\alpha+M\right)y^*+H_{19}Sinh\left(\alpha-M\right)y^*,\\&+H_{20}y^{*2}Sinh(My^*)+H_{21}y^{*2}Sinh(My^*)\end{aligned}$$

$$\begin{aligned}T_{11}=&H_{22}+H_{23}y^*+H_{24}y^{*2}+H_{25}y^{*3}+H_{26}y^{*4}+H_{27}Cosh(2My^*)+H_{28}Sinh(2My^*)+H_{29}y^*Cosh(My^*)\\&+H_{30}y^*Sinh(My^*)+H_{31}y^{*2}Cosh(My^*)+H_{32}y^{*2}Sinh(My^*)\end{aligned},$$

$$\begin{aligned}T_{12}=&H_{22}+H_{23}+H_{24}+H_{25}+H_{26}+H_{27}Cosh(2M)+H_{28}Sinh(2M)+H_{29}Cosh(M)+H_{30}Sinh(M)\\&+H_{31}Cosh(M)+H_{32}Sinh(M)\end{aligned},$$

$$E_5=\frac{\left(T_9Sinh(My^*)+T_{10}Sinh(M)\right)}{Cosh(M)Sinh(My^*)+Cosh(My^*)Sinh(M)},\ E_6=\frac{\left(T_{10}Cosh(M)-T_9Cosh(My^*)\right)}{Cosh(M)Sinh(My^*)+Cosh(My^*)Sinh(M)},$$

$$E_7=\frac{\left(T_{12}Sinh(My^*)-T_{11}Sinh(M)\right)}{Cosh(M)Sinh(My^*)-Cosh(My^*)Sinh(M)},\ E_8=\frac{\left(T_{11}Cosh(M)-T_{12}Cosh(My^*)\right)}{Cosh(M)Sinh(My^*)-Cosh(My^*)Sinh(M)}.$$

ISSN (e): 2250 – 3005 || Vol, 04 || Issue, 4 || April – 2014 ||
International Journal of Computational Engineering Research (IJCER)

Extended Kalman Filter based Missile Tracking

Yassir Obeid Mohammed[1], Dr. Abdelrasoul Jabar Alzubaidi[2]
[1] Sudan Academy of Sciences (SAS); Council of Engineering Researches & Industrial Technologies,
[2] Electronics Dept- Engineering College –Sudan University of science and Technology

ABSTRACT:
kalman filter has been successfully used as an estimator in recursive linear systems. For nonlinear systems extended kalman filter is more suitable for use.In case the target trajectory is steady, tracking can be achieved by Kalman filte. But target maneuvering makes tracking process more complicated. Extended kalman filter gives real time tracking for such targets, provided we have high speed processor. This work describes and examines the use of this algorithm in missile and target tracking.
KEYWORDS: nonlinear, non-Gaussian, missile, tracking, estimator, extended kalman filter, Algorithm.

I. INTRODUCTION:

The kalman filter is an algorithm which uses a series of measurements observed over time, containing noise (random variations) and other inaccuracies, and produces estimates of unknown variables that tend to be more precise than those that would be based on a single measurement alone [1]. In tracking problems for example, with the assumption that the system parameters change linearly, Kalman filter equations operate properly as has been shown in a previous work [2]. Many practical systems have non-linear state update or measurement equations. The Kalman filter can be applied to a linearised version of these equations with loss of optimality [4]. In this research extended Kalman filter is used to estimate the position of a missile without losing optimality if the system is nonlinear. A simulation is conduct to test assumptions made.

II. KALMAN FILTER METHOD AND PHASES:

The Kalman filter estimates a process by using a form of feedback control: the filter estimates the process state at some time and then obtains feedback in the form of (noisy) measurements. Equations for the Kalman filter fall into two phases: time update and measurement update [3].
The Kalman filter model assumes the true state at time k is evolved from the state at (k − 1) according to

$$\mathbf{x}_k = \mathbf{F}_k\mathbf{x}_{k-1} + \mathbf{B}_k\mathbf{u}_k + \mathbf{w}_k \quad \text{..... [1]}$$

where

- $\mathbf{F}_k$ is the state transition model which is applied to the previous state $\mathbf{x}_{k-1}$;
- $\mathbf{B}_k$ is the control-input model which is applied to the control vector $\mathbf{u}_k$;
- $\mathbf{w}_k$ is the process noise which is assumed to be drawn from a zero mean multivariate normal distribution with covariance Q_k.

$$\mathbf{w}_k \sim N(0, \mathbf{Q}_k) \quad \text{..... [2]}$$

At time *k* an observation (or measurement) $\mathbf{z}_k$ of the true state $\mathbf{x}_k$ is made according to

$$\mathbf{z}_k = \mathbf{H}_k\mathbf{x}_k + \mathbf{v}_k \quad \text{..... [3]}$$

where $\mathbf{H}_k$ is the observation model which maps the true state space into the observed space and $\mathbf{v}_k$ is the observation noise which is assumed to be zero mean Gaussian white noise with covariance $\mathbf{R}_k$.

$$\mathbf{v}_k \sim N(0, \mathbf{R}_k) \quad \text{..... [4]}$$

The initial state, and the noise vectors at each step $\{\mathbf{x}_0, \mathbf{w}_1, ..., \mathbf{w}_k, \mathbf{v}_1 ... \mathbf{v}_k\}$ are all assumed to be mutually independent. In practice, their matrices might change with each time step or measurement, however sometimes, as it is considered in this case, they are assumed to be constant.

The time update equations are responsible for projecting forward (in time) the current state and error covariance estimates to obtain the a priori estimates for the next time step. The measurement update equations are responsible for the feedback—i.e. for incorporating a new measurement into the a priori estimate to obtain an improved a posteriori estimate.
In short the time update projects the current state estimate ahead in time. The measurement update adjusts the projected estimate by an actual measurement at that time.
After each time and measurement update pair, the process is repeated with the previous a posteriori estimates used to project or predict the new a priori estimates. This recursive nature is one of the very appealing features of the Kalman filter.

III. EXTENDED KALMAN FILTER IMPLEMENTATION:

If the process to be estimated and (or) the measurement relationship to the process is non-linear then a Kalman filter that linearizes about the current mean and covariance is referred to as an extended Kalman filter or EKF [4]. The EKF utilizes the first term in a Taylor expansion of the nonlinear function [5].
The approach adopted for implementing Kalman Filter is also valid in the case of extended Kalman Filter ie.,the two phases: Time Update ("Predict") and Measurement Update ("Correct") [2] are the same the difference will be in the equations. For the extended Kalman Filter the equations obtained are as follows:

$$X_k = f(x_{k-1}, u_{k-1}, w_{k-1}) \quad \text{[5]}$$

with a measurement z that is

$$z_k = h(x_k, v_k) \quad \text{[6]}$$

where the random variables w_k and v_k again represent the process and measurement noise. In this case the non-linear function f in the difference equation [1] relates the state at the previous time step k-1 to the state at the current time step k. It includes as parameters any driving function u_{k-1} and the zero-mean process noise w_k. The non-linear function *h* in the measurement equation [2] relates the state *Xk* to the measurement z_k.
In practice of course one does not know the individual values of the noise w_k and v_k at each time step. However, one can approximate the state and measurement vector without them as

$$\tilde{x}_k = f(\tilde{x}_{k-1}, u_{k-1}, 0) \quad \text{[7]}$$

and

$$\tilde{z}_k = h(\tilde{x}_k, 0) \quad \text{[8]}$$

where $\tilde{x}_k$ is some a posteriori estimate of the state (from a previous time step k) [4].

IV. ALGORITHM:

The algorithm used in Kalman filter approach and Radar detection with a little modification is valid for the Extended Kalman Filter implementation, the new algorithm is as follows:
Start
--- generate a hypothetical target .
(azimuth = 45 degrees, range = 200 km., height = 4000meter, heading = 90 degrees east, speed = 800 km/hr).
--- generate a tracker aircraft (or missile).
(azimuth = 45 digress, range = 70 km., heading = 90 degrees east, speed = 1200 km/hr).
(The tracker height should follow the data acquired from the height finder Radar in order to Approximate the real height of the target.)
--- asuuume that both the target and the tracker are detected by three dimensional Radar or azimth and range Radar plus height finder Radar..
--- apply Extended Kalman filter prediction formula to give the estimated target position.
--- maneuver the heading of the tracker based on the estimated coordinates of the target.
--- if the distance between the target and the tracker approaches zero is true.
then collision is assumed.
otherwise the target and the tracker are in visual contact.
end

V. RESULTS:

With the assumptions made above and values of F, G, H are known the Kalman filter equations resulted in values presented in table 1. Estimated values are a bit far from the measured values at the beginning of the observation but they are very close to the measured values when the object is close to the target. The implementation of the extended kalman Filter equations produced a more accurate values specially at the early stages of the process.

Table 1: results

	True Values			Estimates		Errors in Estimates	
	Position	**Velocity**	**Meas.**	**Position**	**Velocity**	**Position**	**Velocity**
T=Kt	X_1	X_2	**Z(k)**	$X_1(K)$	$X_2(k)$	$P_{11}(k)$	$P_{22}(k)$
0	**100**	**0**		**95**	**1**	**10**	**1**
1	**99.5**	**- 1**	**100**	**99.6**	**0.4**	**0.9**	**0.9**
2	**97.0**	**- 2.4**	**96.4**	**97.2**	**- 2.1**	**0.7**	**0.6**
3	**95.0**	**- 3.2**	**94.0**	**94.8**	**- 3.0**	**0.7**	**0.3**
4	**92.0**	**- 4**	**92.7**	**92.4**	**- 3.7**	**0.6**	**0.2**
5	**89.0**	**- 4.8**	**89.2**	**89.4**	**- 4.6**	**0.5**	**0.1**

The results shown in Table 1 assumes that both target and the tracker are approximately close in height.

VI. CONCLUSION:

Kalman Filters and Extended Kalmn Filter (EKF) produce estimates that are very near to measured values which means both can be used for the estimation of the position of an attacking missile. The EKF implementation results in values that are much close to the real values than those produced by KF estimates and hence more reliable positioning and tracking can be achieved.

REFERENCES:

[1] Kalman Filter – Wikipedia – the free encyclopedia, march, 2013.
[2] Missile Position Tracking using Kalman Filter, Yassir Obeid Mohammed and Dr. Abdelrasoul Jabar Alzubaidi, Electronics Dept-Engineering College, Sudan University of science and Technology.
[3] Understanding and Applying Kalman Filtering, *Lindsay Kleeman, Department of Electrical and Computer Systems Engineering, Monash University, Clayton.*
[4] An Introduction to the Kalman Filter, Greg Welch and Gary Bishop, department of Computer Science, University of North Carolina at Chapel Hill
[5] Tutorial on Particle Filters for Online Nonlinear/Non-Gaussian Bayesian Tracking, M. Sanjeev Arulampalam, Simon Maskell, Neil Gordon, and Tim Clapp.

ISSN (e): 2250 – 3005 || Vol, 04 || Issue, 4 || April – 2014 ||
International Journal of Computational Engineering Research (IJCER)

Development of the theoretical bases of logical domain modeling of a complex software system

Oleksandr Dorensky[1], Alexey Smirnov[2]
1 Lecturer, Department of Software, Kirovohrad National Technical University, Kirovohrad, Ukraine
2 Professor, Department of Software, Kirovohrad National Technical University, Kirovohrad, Ukraine

ABSTRACT
Software of modern information and telecommunications systems, as well as of automated control systems is characterized by complexity. Therefore, in the initial stages of the life cycle of complex software systems there exists an actual problem of the application of effective technologies decomposition and logical domain modeling, as well as of software design. The paper proposes a mathematical formulation of the definition of the basic conceptual units of logical domain model for the creation of complex software systems. The proposed mathematical formalization of the logical structure of the domain model in terms of objects, relationships, attributes and states is the theoretical basis of mathematical formalization of techniques of logical domain modeling using object-oriented technology.

Keywords: *software, object-oriented technology, modeling, data domain, logical model, object, link, attribute, condition.*

I. INTRODUCTION

Currently, information systems and technologies allow providing the automation of practically all the areas of human activity. This has become a consequence of the need to process considerably greater amounts of accumulated information and complexity of managing technologies of complex systems that ensure the functioning of many industries and activities of mankind. One of the main factors underlying this process is the rapid development of digital and computer technology, universal informatization and globalization of society. Thus, the development and implementation of complex software systems is one of the most important tasks of our time.

Modern information systems and automated control systems are characterized by being multicomponent, having many interactions of functional elements, processing and exchange of large amounts of data, having elements of competition while using of the system resources and, consequently, by the complexity of the design and development of software. The complexity of software systems is caused by the complexity of the real domain, the difficulties of managing the development process, the need to provide sufficient flexibility to a program, as well as by an unsatisfactory ways of behavior of large discrete systems [1]. Thus, currently, a scientific and technical challenge of designing, developing new and improving existing software complex systems is important.

Software implementation of any complex system requires the use of the domain decomposition, which is represented as its partition into constituent elements. Thus, the domain refers to a part of the real world, which is a medium definition and implementation of a specific automated process or a group of processes [2].

The domain decomposition is performed by one of the common schemes: structural (algorithmic) decomposition and object-oriented decomposition [3]. The basis of the first scheme is the partition by actions (algorithms) and is used in the development of simple software. Structural technology of the software considers the entire system as the function, which is parted into sub-functions (procedures), then on sub-sub-functions etc. Object-oriented decomposition provides decomposition into autonomous objects. Thus, in object-oriented technology, unlike in the structural, the basic unit is not a function, but a class of objects, each of which consists of methods (actions) and the data [3.5].

Application of object-oriented technology in the stages of analysis and design of complex software systems (CSS) allows offering a wide range of logic models, based on a unified notation. This approach to programming and maintenance stages is developed in detail in the form of object-oriented programming concept, which is displayed in the topology of modern languages and integrated systems [6-8].

However, the effective application of technology of creation of complex software systems (automated control systems, information and telecommunication systems, etc.) on an industrial scale may be achieved subject to the development of software tools software of supporting technological methodology development. The creation of such a software tools determines nontrivial tasks reflecting the objectively existing contradiction between the high level of the declarative language used by a person in the process of software development on the one hand, and the need for low-level of language of machine realization of the programs on the other hand.

One of the ways to solve this contradiction is a mathematical formalization of the logical methods of modeling the domain of complex software systems.

II. MATHEMATICAL FORMALIZATION OF THE DEFINITION OF BASIC CONCEPTUAL UNITS OF LOGICAL DOMAIN MODEL FOR CREATING SOFTWARE

On a conceptual level, the domain is represented by a logical model that describes the key abstractions of the domain. The basic conceptual units of a logical model are objects [1, 2, 4].

Object is an abstraction of a set of elements of the domain that are related by common structure and behavior [3, 4]. As elements of the domain can act as real world objects, aims and destination of the objects, incidents in the domain, the relationship between objects that have the dynamics of behavior, rules or standards specified in the domain, etc. [3, 5, 9].

Because the logical domain model (LDM) is the image of a part of the real world, the definition of the basic abstractions of a logic model is a gnoseological process based on dialectical categories of unitary, special and general.

The category of the unitary displays the domain elements that are given to the analyst in the feeling. Feeling is the first stage of learning, reflection of individual properties, features, parties of a domain. Lets denote the set of such properties allocated by the analyst in the process of cognition, P_Ω. These properties are the properties of the domain elements allocated by the analyst, which we denote as Ω. Thus, the result of the feeling is also the function of identification of the domain

$$\chi_p : \Omega \times P_\Omega \to \{0,1\},$$

where

$$\chi_p(\omega, p) = \begin{cases} 1, \text{ if the condition is performed } p-\text{element property } \omega, \\ 0, \text{ if the condition is not performed .} \end{cases} \quad (1)$$

The next stage of learning is the representation by the analyst of a category of special as playing in the minds previously perceived properties of features, sides of the domain P_Ω. This process is abstracting of the important, from the viewpoint of the analyst, characteristics of the domain elements, the set of which lets denote as C. The result of a presentation of the category of special may be formalized as a surjective representation $F_p : P_\Omega \to C$, which defines a partition of a set $P_\Omega\{P^C\}$, $c \in C$, where

$$\forall p \in P^C \quad F_p(P) = c; \quad (2)$$

$$\forall p \notin P^C \quad F_p(P) \neq c. \quad (3)$$

The next stage of learning is a synthesis based on the analysis of the unitary and, especially, general – of LDM objects. Based on the dialectical relationship of a unitary, specific and general, the process of such a synthesis may be formalized as an injective reflection $F_O : O \to \sigma(\Omega)$, where $\sigma(\Omega)$ - a set of all subsets of a set Ω, O – a set of objects of LDM, thus, that

$$[F_O(o) = \Omega_o] \Leftrightarrow [\exists \gamma \subseteq C((\forall \omega \in \Omega_o \forall c \in \gamma(\forall p \in P^c \chi_p(\omega, p) = 1)) \& (\forall \omega \in \Omega_o \exists c \in \gamma(\forall p \in P^c \chi_p(\omega, p) = 0)))], \quad (4)$$

$$\bigcup_{o \in O} F_O(o) = \Omega. \quad (5)$$

A subset Ω_o of a set of elements of the domain is abstracted as an object o if and only if there exists a set of abstractions of characteristics of the elements of the domain γ, common to all elements of the set Ω_o, and for each element of the domain that does not belong to the set Ω_o, in the set γ there is an abstraction of the characteristic which is not inherent to this element. Each element of the domain is included in a set, abstracted as an object of LDM.

Display F_O (formulas 4-5) defines a partial order on the set O by the following:

$$[o' \le o''] \Leftrightarrow [F_O(o') \supseteq F_O(o'')]. \quad (6)$$

The next important conceptual units of LDM are communications. Communication is an abstraction of the set of relationships that systematically occur between different elements of the domain [1, 2, 4]. That the element of the domain is associated by a certain relationship with another element of the domain, and must be displayed on the stage of presentation of the category of special by an abstraction of the characteristics depending on another element. Thus, we define a certain set of dependencies D, where $D \subset C$. Lets define the set of connections of LDM through R. Then, if we define a surjective display $F_R : D \to R$ so, that

$$D^r = \bigcup_{F_R(d)=r} \{d\}, \quad (7)$$

is based on the definition of communication [1, 4, 9]

$$\forall r \in R \left| D^r \right| = 2, \quad (8)$$

$$\forall r' \in R,$$
$$\forall r'' \in R(r' \ne r'') \Rightarrow$$
$$\left(D^{r'} \bigcap D^{r''} = \varnothing\right). \quad (9)$$

Thus, abstracting by the analyst of communication r between the objects o' and o'' the LDM may be formalized as the statement:

$$\exists d' \in D \exists d'' \in D(d' \ne d'') \&$$
$$(F_R(d') = F_R(d'') = r) \&$$
$$(\forall \omega \in F_O(o') \exists p \in P^{d'} \chi_p(\omega, p) = 1) \&$$
$$(\forall \omega \in F_O(o'') \exists p \in P^{d''} \chi_p(\omega, p) = 1). \quad (10)$$

Theorem 1. If o', o'', o'^*, o''^* belong to the set as the object of LDM, and there if a connection $r \in R$ exists between the objects o' and o'', then from the conditions $o' \le o'^*$ and $o'' \le o''^*$ there follows that relationship r exists between the objects o'^* and o''^*.

Proof. A proof of the theorem is trivial and follows the determination of the relationship (formula 10) and definition of a partial order on the set O (formula 6). At the stage of submission of the category of special two kinds of conceptual units of LDM are defined: state and attributes [1, 2, 4].

State is an abstraction of a characteristic of the element's position in its life cycle, which uses a specific set of rules, behavior patterns, and physical requirements and physical law. Attribute is an abstraction of a certain characteristic, which have all the elements abstracted as an object domain, which is not a dependence or condition [1, 4, 9]. Let's define through A a set of attributes of LDM, through S - a set of states of LDM. Thus,

$$C = A \bigcup S \bigcup D; \quad (11)$$
$$A \bigcap S = \varnothing; \quad (12)$$
$$A \bigcap D = \varnothing; \quad (13)$$
$$S \bigcap D = \varnothing. \quad (14)$$

Lemma 1. Let's define Z_o as the set of such $\gamma \subset C$, for which the following is performed:

$$(\forall \omega \in \Omega_o \forall c \in \gamma(\exists p \in P^c \chi_p(\omega, p) = 1)) \&$$
$$(\forall \omega \notin \Omega_o \forall c \in \gamma(\exists p \in P^c \chi_p(\omega, p) = 1)). \quad (15)$$

Then Z_o forms a semilattice under the operation of the sets merge.

Proof. Since the merge operation has the properties of associative, commutative and idempotent, to prove the lemma we must prove that for any γ_1 and γ_2, which belong to Z_o, the condition $\gamma_1 \bigcup \gamma_2 \in Z_o$ is fulfilled:

$$[\gamma_1 \in Z_o \& \gamma_2 \in Z_o] \overset{(15)}{\Rightarrow}$$
$$[\forall \omega \in \Omega_o (\exists c \in \gamma_1 (\forall p \in P^c \chi_p(\omega, p) = 1)) \&$$
$$(\exists c \in \gamma_2 (\forall p \in P^c \chi_p(\omega, p) = 1)) \&$$

$$\left(\forall\omega\notin\Omega_o\left(\exists c'\in\gamma_1\left(\forall p\in P^{c'}\chi_p(\omega,p)=0\right)\right)\&\right.$$
$$\left.\left(\exists c''\in\gamma_2\left(\forall p\in P^{c''}\chi_p(\omega,p)=0\right)\right)\right]\Rightarrow$$
$$\left[\left(\forall\omega\in\Omega_o\forall c\in\gamma_1\cup\gamma_2\left(\exists p\in P^{c}\chi_p(\omega,p)=1\right)\right)\&\right.$$
$$\left.\left(\forall\omega\notin\Omega_o\forall c\in\gamma_1\cup\gamma_2\left(\forall p\in P^{c}\chi_p(\omega,p)=0\right)\right)\right]\overset{(15)}{\Rightarrow}$$
$$\left[\gamma_1\cup\gamma_2\in Z_o\right].$$

The lemma is proved.

Consequence. For any object of LDM o there exists the largest element in the set Z_o

$$C_o=\max_{\gamma\in Z_o}\gamma, \tag{16}$$

if the order is defined as follows:

$$\left[\gamma_i\le\gamma_j\right]\Leftrightarrow\left[\gamma_i\cup\gamma_j=\gamma_j\right]. \tag{17}$$

The assertion of Lemma 1 allows determining the sets of attributes and states by the object of LDM as an injective display $F_A:O\to\sigma(A)$ and $F_S:O\to\sigma(S)$ where $\sigma(A)$ is the set of all subsets A, $\sigma(S)$ - the set of all subsets S, as follows:

$$F_A(o)=A\cap C_o, \tag{18}$$
$$F_S(o)=S\cap C_o. \tag{19}$$

Lemma 2. Combining the range of the display F_O – $\Phi_O=\{F_O(o)\}$, $o\in O$, - and the empty set $\varnothing$ forms a semilattice under the operation of the intersection of sets.

Proof. Since the operation of the intersection has the properties of associativity, idempotency and communicativeness, to prove the lemma we must prove that for any Ω' and Ω'', belonging to Φ_O, the condition $\Omega'\cap\Omega''\in\Phi_O$ or $\Omega'\cap\Omega''=\varnothing$ is fulfilled:

$$\left[\Omega'\in\Phi_O\ \&\ \Omega''\in\Phi_O\right]\overset{(4,16)}{\Rightarrow}$$
$$\left[\exists o'=F_O^{-1}(\Omega')\left(\left(\forall\omega\in\Omega'\forall c\in C_{o'}\left(\exists p\in P^{c}\chi_p(\omega,p)=1\right)\right)\&\right.\right.$$
$$\left.\left(\forall\omega\notin\Omega'\forall c'\in C_{o'}\left(\exists p\in P^{c'}\chi_p(\omega,p)=0\right)\right)\right)\&$$
$$\exists o''=F_O^{-1}(\Omega'')\left(\left(\forall\omega\in\Omega''\forall c\in C_{o''}\left(\exists p\in P^{c}\chi_p(\omega,p)=1\right)\right)\&\right.$$
$$\left.\left.\left(\forall\omega\notin\Omega''\forall c''\in C_{o''}\left(\forall p\in P^{c''}\chi_p(\omega,p)=0\right)\right)\right)\right]\Rightarrow$$
$$\left[\left(\Omega'\cap\Omega''=\varnothing\right)\ \text{or}\ \left(\exists o'=F_O^{-1}(\Omega')\exists o''=F_O^{-1}(\Omega'')\right.\right.$$
$$\left(\left(\forall\omega\in\Omega'\cap\Omega''\forall c\in C_{o'}\cup C_{o''}\left(\exists p\in P^{c}\chi_p(\omega,p)=1\right)\right)\&\right.$$
$$\left.\left.\left.\left(\forall\omega\in\Omega'\cap\Omega''\forall c\in C_{o'}\cup C_{o''}\left(\exists p\in P^{c}\chi_p(\omega,p)=0\right)\right)\right)\right)\right]\overset{(4)}{\Rightarrow}$$
$$\left[\left(\Omega'\cap\Omega''=\varnothing\right)\ \text{or}\ \left(\Omega'\cap\Omega''=\Phi_O\right)\right].$$

The lemma is proved.

Lemma 3. If o' and o'' belong to the set of objects of LDM, then from the condition $o'\le o''$ it follows, that $C_{o'}\subseteq C_{o''}$.

Proof.

$$\left[o'\le o''\right]\overset{(6)}{\Rightarrow}\left[F_O(o')\supseteq F_O(o'')\right]\Rightarrow$$
$$F_O(o')\cap F_O(o'')=F_O(o''). \tag{20}$$

From the lemma 2 it follows: or $F_O(o')\cap F_O(o'')=\varnothing$, but this contradicts (20), or

$$\left(\left(\forall\omega\in F_O(o')\cap F_O(o'')\forall c\in C_{o'}\cup C_{o''}\left(\exists p\in P^{c}\chi_p(\omega,p)=1\right)\right)\&\right.$$
$$\left.\left(\forall\omega\notin F_O(o')\cap F_O(o'')\exists c\in C_{o'}\cup C_{o''}\left(\forall p\in P^{c}\chi_p(\omega,p)=0\right)\right)\right.\overset{(20)}{\Rightarrow}$$
$$\left(\left(\forall\omega\in F_O(o'')\forall c\in C_{o'}\cup C_{o''}\left(\forall p\in P^{c}\chi_p(\omega,p)=1\right)\right)\&\right.$$

$$\left(\forall \omega \notin F_O(o'')\exists c \in C_{o'} \bigcup C_{o''}\left(\forall p \in P^c \chi_p(\omega, p) = 0\right)\right) \Rightarrow$$
$$C_{o''} \supseteq \left(C_{o'} \bigcup C_{o''}\right) \Rightarrow C_{o'} \subseteq C_{o''}.$$

The lemma is proved.

Theorem 2. If o' and o'' belong to the set of objects of LDM, then from the condition $o' \leq o''$ it follows, that $F_A(o') \subseteq F_A(o'')$.

Proof. Following the formula (18),

$$F_A(o'') = A \bigcap C_{o''} \overset{\text{lemma 3}}{\Rightarrow}$$
$$A \bigcap C_{o'} \subseteq A \bigcap C_{o''} \Rightarrow F_A(o') \subseteq F_A(o'').$$

The theorem is proved.

Theorem 3. If o' and o'' belong to the set of objects of LDM, then from the condition $o' \leq o''$ it follows, that $F_S(o') \subseteq F_S(o'')$.

Proof. Following the formula (19),

$$F_S(o'') = S \bigcap C_{o''} \overset{\text{lemma 3}}{\Rightarrow}$$
$$S \bigcap C_{o'} \subseteq S \bigcap C_{o''} \Rightarrow F_S(o') \subseteq F_S(o'').$$

The theorem is proved.

III. CONCLUSIONS

The proposed mathematical formalization of the structure of a logical model of the domain in terms of objects, relationships, attributes and states is the theoretical basis of mathematical formalization of techniques of logical domain modeling using an object-oriented approach. Formulated and proved assertions may be used to construct the algorithms for automated libraries of domain objects for developing object-oriented software of information and communication systems, as well as of automated control systems.

REFERENCES

[1] G. Booch. Object-Oriented Analysis and Design with Applications, 3rd edition. Addison-Wesley Professional publisher, 534 p., 2007.
[2] O.A. Smirnov , O.V. Kovalenko, Y.V. Meleshko. Software Engineering. EPL of KNTU, Kirovograd, 409 p., 2013.
[3] M. Glasser. Open Verification Methodology Cookbook. Springer, 290 p., 2009.
[4] S. Orlov. Technology creation software. Piter, SpB, 464 p., 2002.
[5] W.V. Siricharoen. Ontologies and Object Models in Object Oriented Software Engineering. IAENG International Journal of Computer Science, Volume 33, Issue 1, pp. 25-30, 2007.
[6] S. Swart, M. Cashman, P. Gustavson, J. Hollingworth. Borland C++ Builder Developer's Guide. Sams Publishing, 1128 p., 2003.
[7] S. Teixeira, X. Pacheco. Borland Delphi Developer's Guide. Sams Publishing, 1169 p., 2002.
[8] R. Lafore. Object-Oriented Programming in C++, Fourth Edition. Sams Publishing, 1012 p., 2002.
[9] A. Pillay. Object-Oriented Programming. School of Computer Science University of KwaZulu-Natal, Durban, 221 p., 2007.

ISSN (e): 2250 – 3005 || Vol, 04 || Issue, 4 || April – 2014 ||
International Journal of Computational Engineering Research (IJCER)

Performance Evaluation of the Masking Based Watershed Segmentation

Inderpal Singh[1], Dinesh Kumar[2]
Research Scholar in Computer Science and Engineering Department[1],
Faculty of IT Department[2],
Author Correspondence: DAV Institute of Engineering and Technology [1, 2,] Jalandhar (Punjab), India,

Abstract:
This paper has presented a performance evaluation of different image segmentation techniques. The image segmentation; segments a given image into separate regions and objects. It is widely used in various vision applications like face detections, motion detection etc. The overall objective of this paper is to design and implement various techniques of image segmentation. The shortcomings of image segmentation techniques will also be evaluated. This paper ends up with the performance evaluation of the over-segmentation, watershed segmentation using masking and also effect of the noise on the masking based watershed segmentation techniques. It has been shown that the noise has affected the segmentation at a great extent.

Keywords: *Image segmentation, Watershed, Clustering, Thresholding.*

I. INTRODUCTION

The purpose of image segmentation is to partition an image into meaningful regions with respect to a particular application. The segmentation is based on quantities taken from the image and might be colour, texture, grey level, depth or motion.

Applications of image segmentation range from filtering of noisy images, medical imaging, locating objects in satellite images (roads, forests, etc.), automatic traffic controlling systems, machine vision to problems of feature extraction and recognition [8]. Image segmentation means assigning a label to each pixel in the image such that pixels with same labels share common visual appearances. It makes an image easier to analyze in the image processing tasks.

There are many different methods available to implement image segmentation. There are many approaches available for the image segmentation. Examples are, edge based segmentation, region based segmentation, threshold based segmentation, markov random field based segmentation, hybrid techniques and clustering based image segmentation [12]. These segmentation methods differ from their computation complexity and segmentation quality.

II. IMAGE SEGMENTATION TECHNIQUES

Most segmentation techniques are either region-based or edge based.

1. Region-based techniques rely on common patterns in intensity values within a cluster of neighboring pixels. The cluster is referred to as the region, and the goal of the segmentation algorithm is to group regions according to their anatomical or functional roles [11].

2. Edge-based techniques rely on discontinuities in image values between distinct regions, and the goal of the segmentation algorithm is to accurately demarcate the boundary separating these regions [11].

III. MASKING BASED WATERSHED TRANSFORM

Watershed transform has concerned with great attention in recent years as an efficient morphological image segmentation tool. It is similar to region-based approach; it begins the growing process from every regional minimum point, each of which creates a single region after the transform. Watershed algorithm combines both the discontinuity and similarity properties successfully [5][16]. It performs well when it can distinguish the background location and the foreground object. It is based on grayscale mathematical

morphology. The main drawback of watershed transform is over-segmentation, sensitive to noise and high computational complexity those make it unsuitable for real-time process [6][17].

The masking operations are divided into two stages: cell and nucleus making. The better cell-mask and nucleus- mask value are determined by Eq. 3 and Eq. 4.The adaptive masking operations are used image normalization (N) and adaptive thresholding (T1 and T2) on the R, G and B color channels.

The adaptive threshold, we have used a dynamic threshold selection process (T1 and T2) by Eq. 1 and Eq. 2 based on Gray-threshold function.

$$T_1 = G_t(n) \tag{1}$$

Where, Gray threshold is calculated by Gt.

$$T_2 = G_t(N(N > T_1)) \tag{2}$$

$$M_1 = N > T_1 \tag{3}$$

Where, cell-mask and nucleus-mask are denoted by M1 and M2 respectively.

$$M_2 = N > T_2 \tag{4}$$

An image can have several regional maxima or minima but only one global maxima or minima. We have used Impose Minima to create new minima in the mask image at certain desired location by adaptively selecting threshold operation (T1 and T2) for morphological reconstruction to eliminate all minima from the image except the minima we specified. For morphological processing, we have applied Impose Minima function to create morphological process image using nucleus-masking (M2) and adaptive mask image on three-color channels

IV. LITERATURE SURVEY

Liu et al. (2008) [1] has discussed watershed transformation based on opening-closing operation and distance transform. Opening-closing operation is a kind of iterative calculation of erosion and dilation. It reflects the location feature of pixels in the image. It also overcame over-segmentation existed in traditional watershed segmentation preserving the original edges of the image.

Shan et al. (2010) [2] presented the improved watershed image segmentation method. The morphological opening/closing reconstruction filter is applied to remove the image noise. It keeps the information of object outlines when filtering the image.

Kumar et al. (2011) [3] has studied a color image segmentation method of automatic seed region growing on basis of the region with the grouping of the watershed algorithm. Texture Gradient is used for the extraction of the connected components of the image. Final Gradient image is input for the watershed algorithm.

Bala et al. (2012) [4] has described paper a novel method of image segmentation that includes image enhancement and noise removal techniques with the Prewitt's edge detection operator. It effectively reduce the over segmentation effect and achieve more accurate segmentation results than the existing method.

Ren et al. (2012) [5] has studied improved watershed segmentation method is used to raise the segmentation correctness of rock particles image. The new method used the qualities of mathematical morphology algorithm. Conventional watershed algorithm is too sensitive to noise. If it is use directly in the extraction of the rock particles, it often result is "over segment".

Chen et al. (2012) [6] authors discuss image reconstruction and segmentation in an improved watershed algorithm by using a plug-in function in flooding process. This method shows very low error rates compared with other approaches. Size filter is used to get the better result for image segmentation.

Zhang et al. (2012) [7] has demonstrated the adaptive marker extraction-based watershed algorithm is used to overcome the over-segmentation problem.

Rahman et al. (2013) [8] has discussed object counting in an image is one of the main challenges in image processing. Image segmentation is used to separate similar particles, which help calculating estimated total number of particles. Thresholding technique is desirable for counting objects in an image. It used the marker controlled watershed segmentation along with thresholding technique provides suitable result.

Fu et al. (2012) [9] presented the fast two-step marker-controlled watershed image segmentation method in CIELAB color space to resolve the over-segmentation problem, which saves a lot of execution time. The watershed super pixels segmentation technique produces over-segmented regions efficiently which adhere well to the real object boundaries

Ghoshale et al. (2013) [10] has described the several edge sharpening filters and to find the effect on the output image using watershed algorithm. A spatial sharpening filter on the performance of the segmented images and mathematical morphology plays a very important role.

Rahman et al. (2013) [11] present, a novel image segmentation method based on adaptive threshold and masking operation with watershed algorithm. Whose objective is to overcome over-segmentation problem of the traditional watershed algorithm.

V. GAPS IN EARLIER WORK

By conducting the literature survey it has been found that the most of the existing literature has neglected one of the following:

1. The over-segmentation problem is ignored i.e. as over segmentation degrades the performance or accuracy of the segmentation results by a lot; so it become an critical issue to reduce the effect of the over-segmentation by introducing some pre-processing operations.

2. The effect of the noise, dust, haze etc. is also ignored by the most of the researchers. It also degrades the performance of the over segmentation.

3. The computation time is still an issue for the most of the cases. As any enhancement on the existing method comes up with some potential overheads so it is required to reduce this time.

VI. PERFORMANCE EVALUATION

6.1. Evaluation of Over Segmentation

The watersheds transformation makes a number of regions as an output. The over-segmentation problem comes mostly from the noise and quantization error [11]. To eliminate the effect of local minima from noise or quantization error on the final results. First, the gradient of the original image is computed as a pre-processing and then the watersheds transformation is applied on the gradient of image[12][15]. Another approach is to apply a post-processing where a large number of regions are merged until the output meets a given criteria which can be the number of regions or a dissimilarity value between homogeneous regions. Figure 6.1(a) has shown the original image going to be segment. It is color image, which can be easily split, or segment into various parts.

Figure 6.1(a)

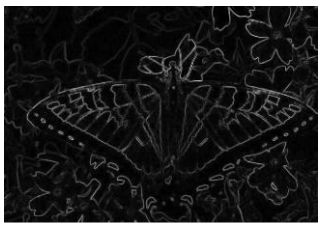

Figure 6.1(b)

(a) Original image (b) Gradient image

Figure 6.1(a) has shown the gradient image for the image shown in Figure 6.1(a). It is clearly shown that the Figure 6.1(a) shows the sharp changes areas in efficient manner.

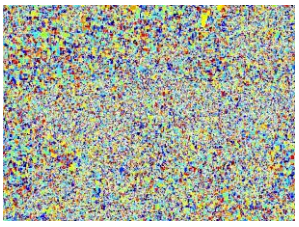

Figure 6.2(a)

Figure 6.2(b)

(a) Watershed Transform (b) Segmented output

Figure 6.2(a) has shown the watershed of the image shown in Figure 6.1(a). It is clearly shown that the watershed has been over segmented while segmenting the Figure 6.1(a) so will produce poor results as shown in Figure 6.2(b). Therefore some special aid likes masking or markers are required while using the watershed transform.

6.2. Analysis of Masking Based Watershed Algorithm for Noise Free Image.

The Watershed method, also called the watershed transform, is an image segmentation approach based on gray-scale mathematical morphology, to the case of color or, more generally speaking, multi component images. Different strategies are presented and a special attention is paid to the "bit mixing approach". This method objectively maps multi-dimensional data into a mono-dimensional space [13]. In geography, a watershed is the ridge that divides areas drained by different river systems. By viewing an image as a geological landscape, the watershed lines determine the boundaries that separate image regions. In the topographic representation of an image *I*, the numerical value (i.e., the gray tone) of each pixel stands for the evolution at this point. The watershed transform computes the catchments basins and ridgelines, with catchment basins corresponding to image regions and ridgelines relating to region boundaries.

Figure 6.3 Red, Green and Blue Channel output

Figure 6.3 has shown the red channel of the image, Green channel of the image and the blue channel of the image.

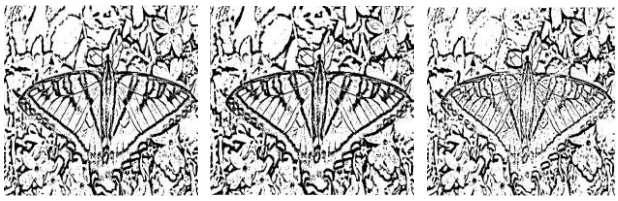

Figure 6.4 Red, Green and Blue Adaptive Mask Output

Figure 6.4 has shown the output of the masked images of each color channel shown in Figure 6.3.

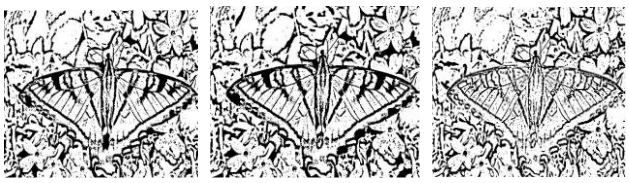

Figure 6.5 Smoothed Red, Green and Blue Segmented Image

Figure 6.5 has shown the morphological outputs of the Figure 6.4 respectively i.e. of each channel of RGB.

Figure 6.6 Red, Green and Blue Channel Segmented Image

Figure 6.6 has shown the final segmented outputs of the Figure 6.5 respectively i.e. of each channel of RGB.

Figure 6.7 has shown the final segmented image which concatenation of the Figure 6.6. The image very clearly segmented and showing the each segmented plane separately.

Figure 6.7 Segmented Output

6.3. Analysis of Masking Based Watershed Algorithm For Noisy Image.

Digital image noise may come from various sources. The acquisition process for digital images converts optical signals into electrical signals and then into digital signals and is one process by which the noise is introduced in digital images[14]. Each step in the conversion process experiences fluctuations, caused by natural phenomena, and each of these steps adds a random value to the resulting intensity of a given pixel.

A. Noise Density: .1

Figure 6.8(a) has shown the salt and pepper noise effected image with 10 % noise. Whereas the Figure 6.8(b) has sown the segmented image. It is clearly shown that the results are not much accurate than without noisy image.

Figure 6.8(a)

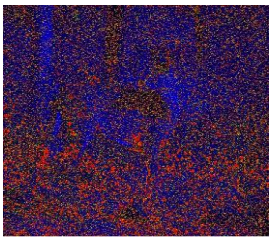

Figure 6.8 (b)

(a) Noisy image (b) Segmented image

B. Noise Density: .5

Figure 6.9(a) has shown the salt and pepper noise effected image with 50 % noise of the Figure 6.1(a). Whereas the Figure 6.9(b) has sown the segmented image. It is clearly shown that the results are not much accurate than without noisy image.

Figure 6.9(a)

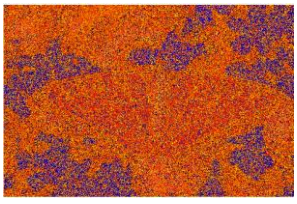

Figure 6.9(b)

(a) Noisy image (b) Segmented image

VII. CONCLUSION

The literature review has shown that the over-segmentation problem has been ignored in the most of existing work. The noise has also found to be critical issue for image segmentation techniques. So it is required to modify the existing methods in such a way that the modified technique will work better for noisy images as well and also overcome the problem of over segmentation. This performance evaluation of the over-segmentation, watershed segmentation using masking and also effect of the noise on the masking based watershed segmentation techniques have been shown. It has been proved that the noise has affected the segmentation at a great extent.

In near future we will extend this work to propose a new technique, which will modify the image watershed based segmentation using switching median filter and dynamic thresholding to improve the segmentation area even in case of noisy images.

REFERENCES

[1] Yuqian Zhao, Jianxin Liu, Huifen Li, and Guiyuan Li,“ Improved watershed algorithm for dowels image segmentation,” 7th IEEE World Congress on Intelligent Control and Automation, 2008. pp. 7644-7648.

[2] Xiaoyan Zhang, Yong Shan, Wei Wei, and Zijian Zhu, “An image segmentation method based on improved watershed algorithm,” IEEE International Conference on Computational and Information Sciences (ICCIS), 2010,pp.258-261.

[3] Ashwin Kumar and Pradeep Kumar, “A New Framework for Color Image Segmentation Using Watershed Algorithm”, Computer Engineering and Intelligent Systems, Vol. 2, No.3 pp.41-46, 2011.

[4] Anju Bala, “An Improved Watershed Image Segmentation Technique using MATLAB,” International Journal of Scientific & Engineering Research Vol.3, No.6, pp.1-4, June 2012.

[5] Yuncai Zhou and Hui Ren,“Segmentation Method for Rock Particles Image Based on Improved Watershed Algorithm,” IEEE International Conference on Computer Science & Service System (CSSS), 2012, pp.347-349.

[6] Jie Chen, Meng Lei, Yao Fan, and Yi Gao,“Research on an improved watershed algorithm to image segmentation,” 7th International Conference on Computer Science & Education (ICCSE), 2012, pp.1917-1919.

[7] Changmin Zhang, Shuaiqi Zhang, Junxia Wu and Shaoxiong Han, “An improved watershed algorithm for color image segmentation,”2012 International Conference on Computer Science and Electronics Engineering (ICCSEE), 2012, pp.69-72.

[8] Md. Sharifur Rahman and Md. Rafiqual Islam, “Counting objects in an image by marker controlled watershed segmentation and thresholding,” 3rd IEEE International on Advance Computing Conference (IACC), 2013, pp.1251-1256.

[9] Xianwei Han, Yili Fu and Haifeng Zhang,“A fast two-step marker-controlled watershed image segmentation method,” International Conference on Mechatronics and Automation (ICMA),2012, pp.1375-1380.

[10] Boren Li, Mao Pan, and Zixing Wu, “An improved segmentation of high spatial res- olution remote sensing image using Marker-based Watershed Algorithm,” 20th IEEE International Conference on Geoinformatics, 2012, pp.1-5.

[11] Farheen K. Siddiqui and Vineet Richhariya,“An Efficient Image Segmentation Approach through Enhanced Watershed Algorithm,” Computer Engineering and Intel- ligent Systems, Vol.4, No.6, pp 1-7,2013.

[12] P.P. Acharjya, A. Sinha, S. Sarkar, S. Dey and S. Ghosh,“A New Approach Of Watershed Algorithm Using Distance Transform Applied To Image Segmentation,” International Journal of Innovative Research in Computer and Communication Engineering, Vol.1, No.2, pp 185-189, April 2013.

[13] Dibyendu Ghoshal and Pinaki Pratim Acharjya,“Effect of Various Spatial Sharpening Filters on the Performance of the Segmented Images using Watershed Approach based on Image Gradient Magnitude and Direction,” International Journal of Computer Applications, Vol. 82, No.6, pp 19-25, November 2013.

[14] Md.Habibur Rahman and Md.Rafiqual Islam,“Segmentation of color image using adaptive thresholding and masking with watershed algorithm,” IEEE International Conference on Informatics, Electronics & Vision (ICIEV), 2013, pp.1-6.

[15] Rabul H Laskar, Kalyan Banerjee and Debajit Basak,“Removal of High Density Salt and Pepper Noise from Color Images through Variable Window Size,” IEEE International Conference on Circuits, Power and Computing Technologies, 2013, pp. 1132-1136.

[16] S. Beucher, F. Meyer, “The morphological approach to segmentation: The water- shed transformation, Mathematical Morphology in Image processing, Marcel Dekker Inc”, New York, pp.433-481, 1993.

[17] M.Sonka, V.Hlavac, and R.Boyle, Image Processing, Analysis, and Machine Vision, PWS Publishing, 1999.

ISSN (e): 2250 – 3005 || Vol, 04 || Issue, 4 || April – 2014 ||
International Journal of Computational Engineering Research (IJCER)

Performance Evaluation of Energy Consumption of Ad hoc Routing Protocols

Mohamed Otmani[1], Abdellah Ezzati [2]
[1] PhD student, Faculty of Science and Technology Settat, Morocco
[2] Asst. Professors, Faculty of Science and Technology Settat, Morocco

Abstract:
In wired networks there are different physical devices routing the traffic centrally, by consequence we can create paths in the network by using multiple management rules, but in Ad-Hoc network nodes must do this work in an autonomous way. For that there are three types of routing protocol proactive, reactive and hybrid. The first one continuously calculates the possible paths to be available at the time of transmission. The second one create the roads only when are needed. And the last one is a combination between the two methods. In this study we will focus on three routing protocols AODV, OLSR and ZRP; and compare their performance in terms of Routing Power, Throughput, Energy Consumed in Transmit mode, Energy Consumed in Receive Mode, End-to-End Delay..

Keywords: *AODV; OLSR; ZRP; ADHOC*

I. INTRODUCTION

Mobile ad-hoc network (MANET) is the network of mobile nodes that requires no infrastructure or centralized management in order to communicate. This type of network allows to create and deploy a wide field of communication quickly, and that's what we need in several cases such as a natural disaster or battlefield surveillance where there is no centralized infrastructure and all nodes are capable of movement and must be connected to each other dynamically and arbitrary. However, due to distributed nature of the wireless nodes and lack of energy resource this type of network must have specifics protocols.

In MANET network the nodes must the routing in an autonomous way, in this order there are three types of routing protocol proactive, reactive and hybrid. Every type of architecture or protocol has some advantages and disadvantages in this paper we will put this three types in test.

II. PROTOCOLS ANALYSED

The following protocols are considered for analysis:
• AODV
• OLSR
• ZRP

A. Overview Of OLSR Protocol

The basic principal of link-state routing is the complete knowledge of the network topology; each node performs a discovery of its neighbors and informs the others. To do that several messages are exchanged and different types of link are established.

1) Messages
- ✓ HELLO: Allows the discovering of the network and sends the information about the state and the type of link between the sender and each neighboring node.
- ✓ Topology Control: Allows determining the routing table by forwarding the list of the neighbors who has been selected as MPR by another MPR.
- ✓ Multiple Interface Declaration: Declare the presence of more than one interface in the node.
- ✓ Host and Network Association: To announce the gateway to a specific network like an Ethernet network.

2) Links

- ✓ UNSPEC link: A link with no specific information about his current state.
- ✓ Asymmetrical link: We say that a link is asymmetric if a node receives a message from another but there is no confirmation that the first one has been heard. It can be called unidirectional link.
- ✓ Symmetrical link: A link is called Symetric if the two nodes hear each other.
- ✓ Lost link: When a link has been reported as symmetrical or asymmetrical, but there is no message received for the momment from the node; we say is a lost link or a dead link.

3) Neighbors

In order to discover the neighbors, each node periodically sends in the HELLO messages information about neighboring, the nodes that are selected as MPR and the list nodes that are declared by that node as asymmetric. We can say that there are three types of neighbors, and two different sets.

a) Types of neighbors

- ✓ Not Neighbor: the node has no Symmetrical link.
- ✓ Symmetrical Neighbor: The node has at least one Symetrical link.
- ✓ MPR Neighbor: the node has been selected as an MPR by the sender neighbor.

b) Sets

The first set contains the one-hop neighbors of a node S, which having a symmetrical link with S denoted N1(s). The two-hop neighbors of a node S are defined as the following set: $N2(s) = \{y | y \neq s \wedge y \notin N1(s) \wedge (\exists x \in N1(s))\ [y \in N1(x)]\}$. These two sets N1(s) and N2(s) of each node S are built by the trading of HELLO messages. This allows all nodes to have a vision for 1-hop and 2-hop topology of the network and have all the information needed to build paths between a source and a destination.

c) Multipoint relays (MPR)

Even that all neighbors can read the packet already sent by a node; however in order to minimize retransmissions of packets, OLSR introduces the principle of MPR. Every node can choose from its neighbors a set of MPR, these MPR are the only ones can retransmit the broadcast packets. Each node S selects a subset of MPR from N1(s) that allows it to be joined by all nodes in N2(s).

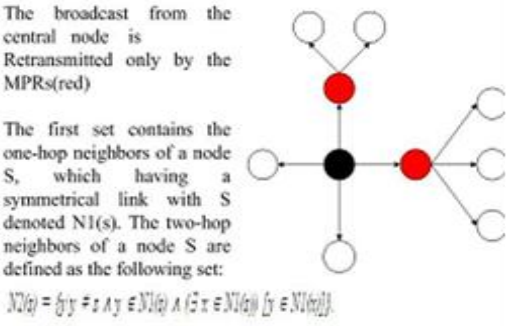

Figure 1. OLSR MPR

B. Overview of ZRP Protocol

The ZRP protocol [9] implements simultaneously, a proactive routing and reactive routing, in order to combine the advantages of both approaches. To do so, it passes through a cutting concept network into different zones, called "routing areas". A routing area for a node is defined by its "radius zone". This radius corresponds to the maximum number of hops that can exist between two nodes.

1) Architecture ZRP

An example of area is given in Fig. We note that for a radius of area equal to two, the routing area of the node S is constituted by all the nodes around the node S is a maximum of two hops between them. Are included in the routing area, all the neighbors of node S and all the neighbors of these neighbors.

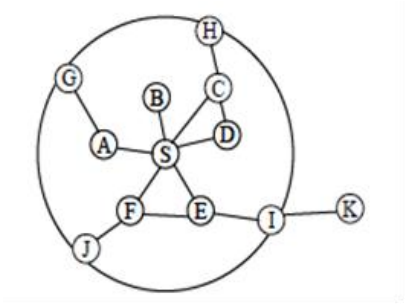

Figure 2. Example zones

2) Routing within ZRP

Routing within a zone is proactively via IARP protocol (intra-zone Routing Protocol) routing to external nodes of the zone is reactively through the IERP (Interzone Routing Protocol). In addition to these two protocols, ZRP uses the BRP (bordercast Routing Protocol). To build the list of devices nodes it is to an area and roads to reach them, using data provided by the topology IARP protocol. It is used to propagate search queries IERP roads in the network. Figure illustrates the necessary implementation of ZRP protocol network components.

A search path is as follows: we first checks if the destination node is in the area of the source node, in which case the path is already known. Otherwise, a request is initiated route RREQ to all peripheral nodes. These check if the destination exists in their areas. In the case of an affirmative answer, then the source will receive a RREP packet containing the path to the destination. Otherwise, the edge nodes broadcast the request to its own edge nodes which, in turn, perform the same processing.

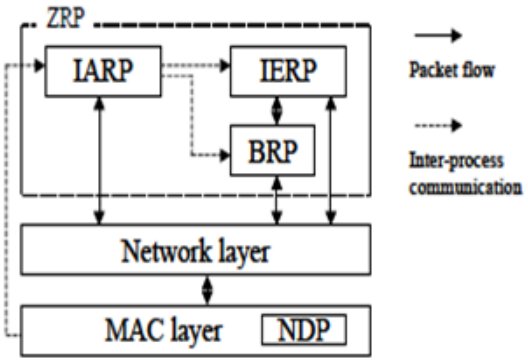

Figure 3. Components

- ✓ The routing protocol IERP: IERP is respondable management hosts that are present beyond the routing area. IERP collecting routing information reactively through bordercast queries that contain accumulations of routes from the source. When receives an IP data packet for an unknown destination (that is to say that it is not listed in the routing table in the interzone or intra-area routing table), is interrupted IERP. He responds by initiating a search for a solution ("route discovery") and bordercast a route request.

- ✓ The routing protocol IARP: IARP depends on the services of a separate protocol (referred to herein as the "Neighbor Discovery / Maintenance Protocol) to provide information about the neighbors of the host. At a minimum, this information contains the IP addresses of all neighbors. IARP can be configured to support additional information on neighbors, such as the cost of a link.

- ✓ The routing protocol BRP: The interface of the upper layer of BRP is implemented to be compatible with any IP-based application. However, we assume that the hierarchy of the routing area is visible only to entities ZRP protocol.

C. Overview Of AODV Protocol

AODV (Ad hoc On-Demand Distance Vector) is a reactive routing protocol used to find a route between a source and a destination, and allows mobile nodes to obtain new routes for new destinations in order to establish an ad hoc network. In this order several messages are exchanged, different types of link are established, and many information can be shared between the participants nodes. In AODV protocol we find hello message and three others significant type of messages, route request RREQ, route reply RREP and route error RERR. The Hello messages are used to monitor and detect links to neighbors, every node send periodically a broadcast to neighbors advertising it existent ,if a node fails to receive an hello message from neighbor a link down is declared. In order to communicate every node must create routes to the destinations, to achieve that the source node send a request message RREQ to collect information about the route state; if the source receives the RREP message the route up is declared and data can be sent and if many RREP are received by the source the shortest route will be chosen. Any nodes have a routing table so if a route is not used for some period of time the node drop the route from its routing table and if data is sent and a the route down is detected another message (Route Error RERR) will be sent to the source to inform that data not received.

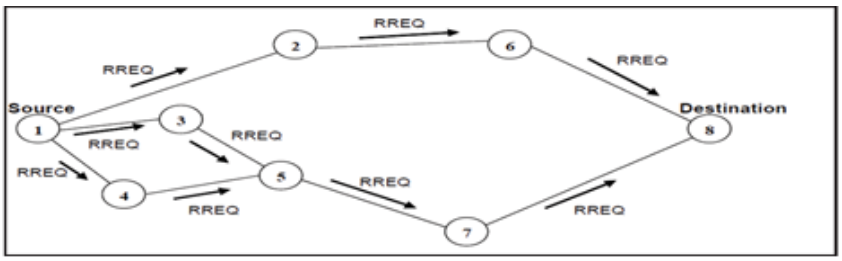

Figure 4. RREQ message

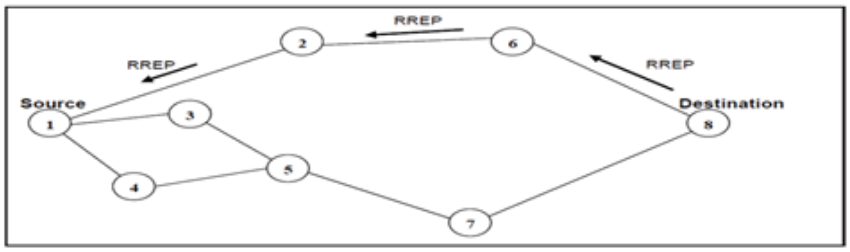

Figure 5. RREP message

1) Messages

a) Route Request (RREQ) Message. This type of message is used by AODV at first in order to locate a destination; this message contains identification of request, sequence number, destination address and also a count of hop started by zero.

b) Route Reply (RREP) Message. This type of message contains the same fields like Route Request (RREQ) Message, and it sent in the same route of reception of RREQ message. When the source received this message it mean that the destination is ready to accept information and the rout is working correctly.

c) Route Error (RERR) Message. Sometimes a node detect a destination node that not exists in network, in this scenario another message (Route Error RERR) is sent to the source informing that the data is not received. RERR is like an alert message used to secure table of routing.

III. SIMULATION ENVIRONMENT

The simulation process of MANET is implemented using simulator Qualnet. QualNet is network simulation and modelling software that predicts performance of networks through simulation and emulation. QualNet run on a vast array of platforms, including Linux, Windows XP, and Mac operating systems, it can run both 32- and 64-bit computing environments.

Table 1.Simulation Parameters

Simulator Parameters	
Mac Type	IEEE 802.11
Protocols under studied	AODV,OLSR,ZRP
Node movement model	Random
Traffic type	CBR
Node Speed	10m/s
Scenario Parameters	
Topology area	1000x1000
Simulation time	30 Seconds
Packet Size	256 bytes
Generic energy model Parameters	
Energy Model	Generic
Energy Supply Voltage	6.5 Volt
Transmit Circuitry Power Consumption	100.0 mW
Receive Circuitry Power Consumption	130.0 mW
Idle Circuitry Power Consumption	120.0 mW
Sleep Circuitry Power Consumption	0.0 mW

A. Snapshot of Simulation

The simulations of energy model were performed using QualNet Simulator 5.0.1. The traffic sources are CBR. The source-destination pairs are multiplying randomly over the network. The mobility model uses random waypoint model in a rectangular filed of 1000m x 1000m and deploys 50 nodes. During the simulation, each node starts its journey from a source node to destination node. This process repeats throughout the simulation, causing continuous changes in the topology of the underlying network. Fig.6 Shows the running simulation of snapshot when we applying CBR (1- 40) nodes and AODV routing protocol.

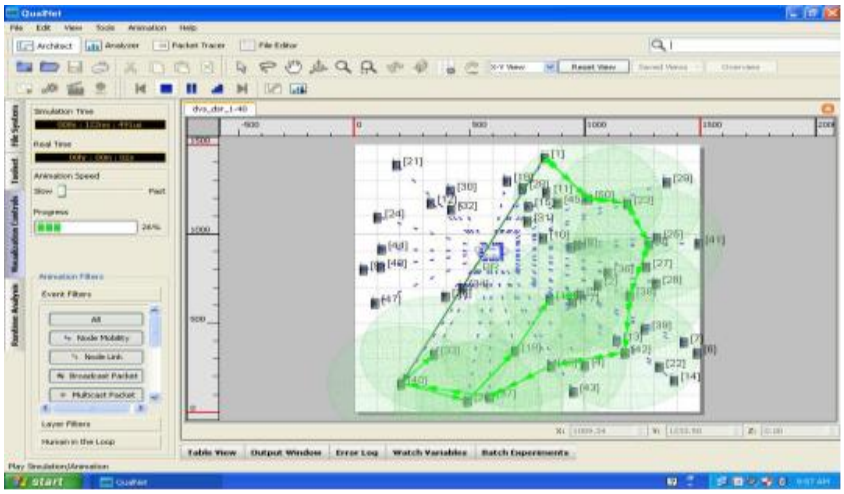

Figure 6.Snap shot of Qualnet Animator in Action

We obtained the number of scenarios in QualNet simulator with varying 10, 20, 30, 40 and 50 nodes selected randomly over a 1000X1000 topology area and taking different routing protocols which we are consider in our simulation. These protocols are AODV, OLSR and ZRP. The node speed is 10 m/sec and each simulation lasted 30 seconds simulation. We evaluate the performances metrics in Application and Physical layers of designed scenarios. The performance matrices are given below.

- Routing Power
- Throughput
- Energy Consumed in Transmit mode
- Energy Consumed in Receive Mode
- End-to-End Delay

IV. RESULT ANALYSIS

A. Throughput

The throughput of the protocols can be defined as percentage of the packets received by the destination among the packets sent by the source .The throughput is measured in bits per second (bit/s or bps).

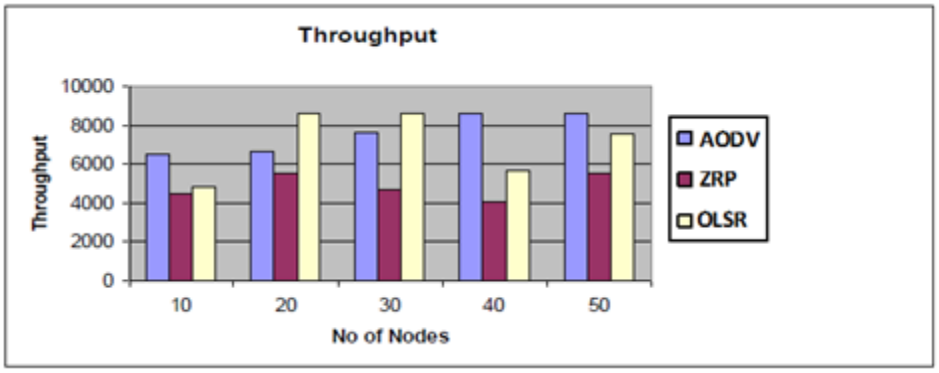

Figure 7.Throughput

Impact on Throughput: Throughput performance is high for AODV and OLSR. ZRP performance is very poor.

B. End-to-End delay

This metric is calculated by subtracting time at which first packet was transmitted by source from time at which first data packet arrived to destination.

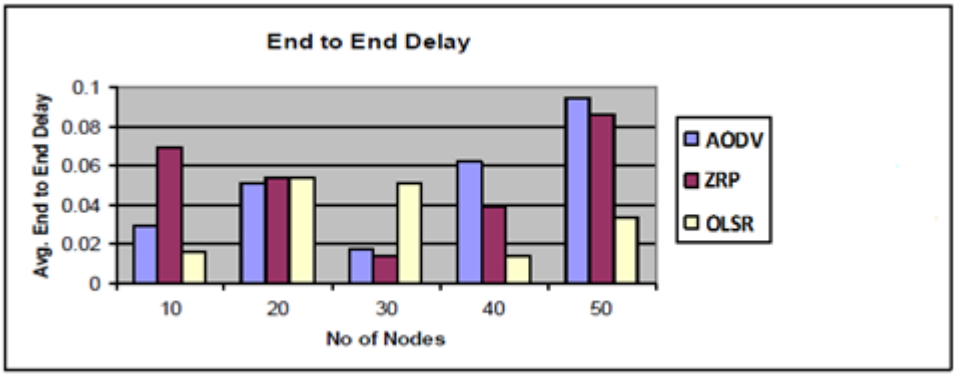

Figure 8. End-to-End delay

Impact on Average End to End delay: From the graph the average End to End delay is low for OLSR while using less nodes as well as more nodes. AODV has high.

C. Data packet delivery ratio

The data packet delivery ratio is the ratio of the number of packets generated at the source to the number of packets received by the destination.

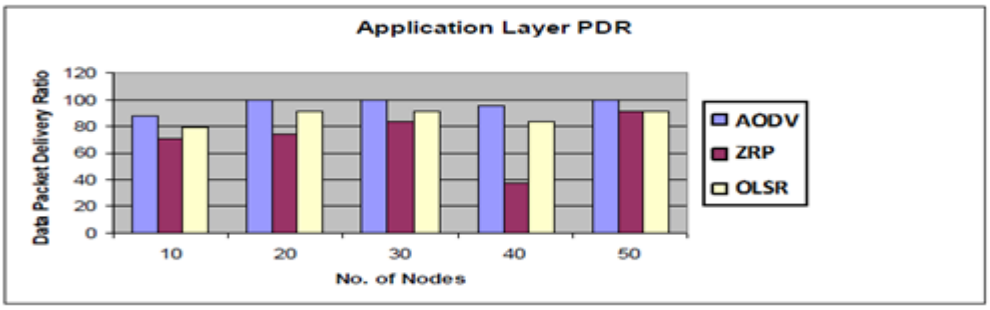

Figure 9. Data packet delivery ratio

Impact on Data packet delivery ratio: Data Packet Delivery Ratio is high for AODV when compared to ZRP and OLSR protocol. Which increases the life time of the entire network for AODV.

D. Energy consumed in transmit mode

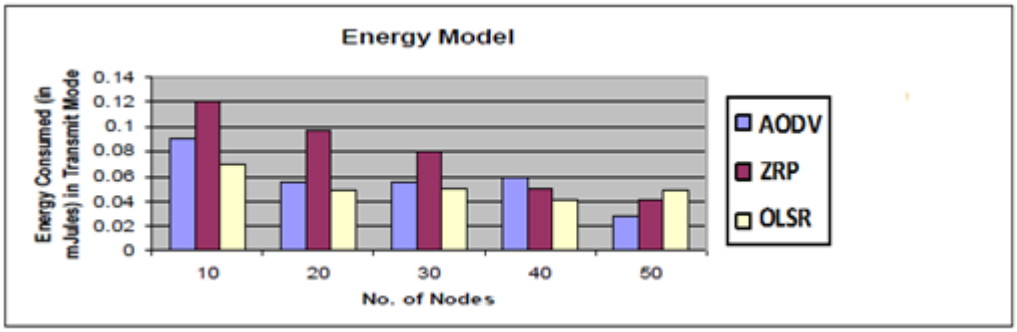

Figure 10. Energy Consumed in transmit mode

Impact on Energy consumed in transmit mode: Fig. 10 shows the total energy consumed in transmit mode is very low for OLSR protocol when compared to the other two.

E. Energy Consumed in Receive Mode

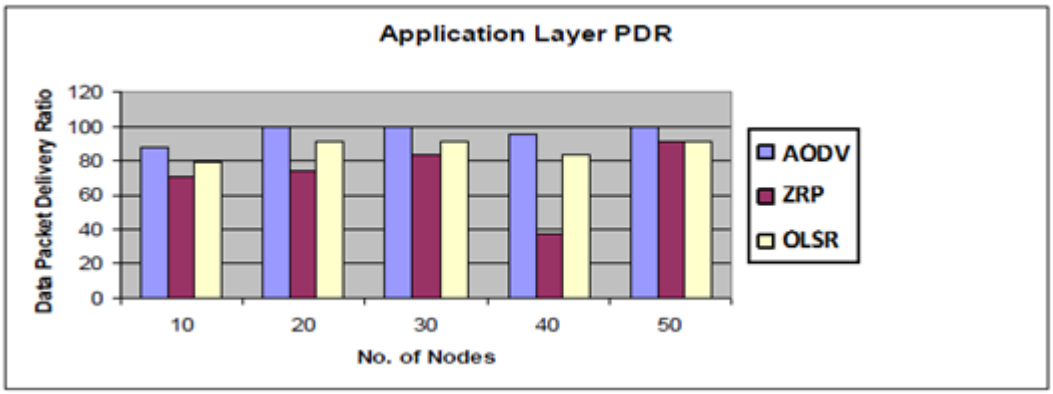

Figure 11. Energy Consumed in Receive Mode

Impact on Energy consumed in receive Mode: ZRP routing protocol consumes less power than other protocols in receive mode.

F. Routing Power

Routing Power = Throughput / Avg.End-to-End Delay

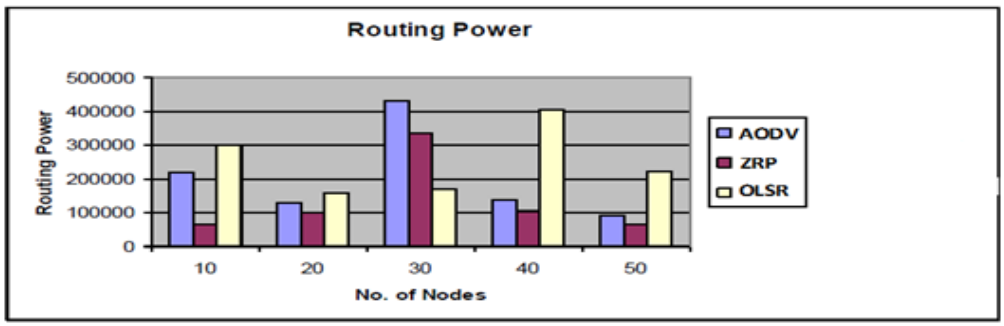

Figure 12. Energy Consumed in Receive Mode

Impact on Routing Power: The routing power effect on AODV routing protocols more as compare others, but as on average routing power of AODV protocol is reduced.

V. CONCLUSIONS

We observed that Energy saving is very important optimization objective in Manet, the energy consumed during communication is more prevailing than the energy consumed during processing because of Limited storage capacity, Communication ability, computing ability and the limited battery are main restrictions in sensor networks. By the observations we compare that the impact of energy constraints on a nodes in physical layer and application layer of the networks that AODV offers the best combination of energy consumption and throughput performance. AODV gives better throughput, packet delivery fraction, average jitter and delay performance compared to ZRP followed by OLSR. If we increased numbers of nodes also increase maximum energy consumption in OLSR followed by ZRP then AODV due to routing control packets in the network. Future work, we can reduce the waste energy consumption of the nodes by reducing the number of routing control packets and reducing the energy consumed by nodes in a large network to increase the life time of network.

REFERENCES

[1] C T. Clausen, P. Jacquet, "RFC3626: Optimized Link StateRouting Protocol (OLSR)", Experimental, http://www.ietf.org/rfc/rfc3626.txt

[2] Raffo, D., Adjih, C., Clausen, T., and Mühlethaler, P. An advanced signature system for OLSR. In Proceedings of the 2004 ACM Workshop on Security of Ad Hoc and Sensor Networks (SASN '04)

[3] Hu, Y.-C., Perrig, A., and Johnson, D. B. "Packet leashes : A defense against wormhole attacks in wireless networks" In Proceedings of INFOCOM, Twenty-Second Annual Joint Conference of the IEEE Computer and Communication Societies (April 2003).

[4] Wang, M., Lamont, L., Mason, P., and Gorlatova, M. "An effective intrusion detection approach for olsr manet protocol".

[5] T. Clausen, U.Herberg, "Security Issues in the Optimized Link State Routing Protocol Version 2 (OLSRv2)", International Journal of Network Security and its Applications, 2010.

[6] Céline Burgod, "Etude des vulnérabilités du protocole de routage OLSR" 2007.

[7] Djallel Eddine Boubiche, «Routing protocol for wireless sensor networks, "Memory Magister, University of l'Hadj Lakhdar, Batna, Algérie, 2008.

[8] Wendi Beth Heinzelman, «Application-Specific Protocol Architectures for Wireless Network », IEEE Transactions on Wireless Communications, Massachusetts Institute of Technology, June 2000.

[9] Z. J. Haas – « A new routing protocol for the reconfigurable wireless networks», dans Proc. 6th IEEE Int'l Conf. on Universal Personal Communications (ICUPC'97) (San Diego, CA, USA), vol. 2, 1997, p. 562–566.

ISSN (e): 2250 – 3005 || Vol, 04 || Issue, 4 || April – 2014 ||
International Journal of Computational Engineering Research (IJCER)

Online Cloud Based Image Capture Software for Microscope

Chetan Raga[1], Rajashekara Murthy S[2]
[1] PG Student Department of Information Science and Engineering, Rvce, Bangalore, India
[2]Assistant Professor, Department of Information Science and Engineering, Rvce, Bangalore, India

Abstract:
As it is a competitive world and very fast world, all the things are online. So we created software called Online Cloud Based Image Capture Software for Microscope. Microscope work can be very straining on both the musculoskeletal visual and systems. Workers are sit in one fixed position with their bodies conformed to the machine for extended time. Worker feel uncomfortable coupled with less advanced optical and digital technologies have made traditional microscopes limiting and ineffective in many applications. This software provides a comprehensive imaging solution. This software is aimed at providing users with the ability to view live stream captured from camera attached to a microscope .This setup is used in biomedical science field, With this application ,users can place slides under a microscope lens and view the contents on their computer screens via cloud .Time, cost and quality plays very important role to satisfy demand of the market, So the aim of this project is to create the Online Cloud Based Image Capture Software for Microscope which helps to reduce the problems of portability and storage space by making use of the concept of cloud computing which will give users various image processing options to view and manipulate images captured with the microscopic cameras.

Keywords: *Cloud computing, Microscope, Middle layer, Camera SDK, GUI, Deployment, Digital image processing, SaaS.*

I. INTRODUCTION

In today's world of fast growing technology which expects good reliability, performance, scalability, cost, agility, security and few other important characteristics, Cloud computing builds on decades of research in virtualization and more recently networking, web and software services .Cloud computing is a model for providing software, data access and storage services that do not require end-user knowledge of the physical location and configuration of the system that delivers the services. This image capture software enables microscopists to create capture effective pictures easily. The live image screen provides a preview of the image capture so you can see how the image will look before you capture it. The live image screen is ideal for panning through slides to locate areas of interest; detail magnifier and its focus gauge enable fast and precise focusing. Contrast, Color temperature and automatic white balance options create excellent color fidelity. Acquiring effective images or image sequences is as effortless as a single mouse click. After image capture, panorama, measurements, reticles, calibration marks, Z-stacking and other enhancements can be applied. Further sequences of captured images can be played back as a movie. Further Images can be saved in several different file formats for printing. This software makes effective way to enhance your professional image. Registered users who log on to the Cloud software-as-a-service (SaaS) system receive immediate access to the latest version of entire suite of image software through a centralized remote server-based account. This software will support a wide variety of research applications in fields as varied as respiratory research, oncology research, neuroscience and skeletal research. It is browser independent and easy to access. Users can pay as they go for storing data and doing analysis only for as long as they need it, with complete security and full data backup. The need for local software installation and support is eliminated, and user authentication is secure. The application can handle analysis on virtual slides that either reside locally or are uploaded to the Cloud.

Fig1.Sample Overview of microscope with camera and image capture software

II. NEED FOR PROJECT

The main advantage of cloud computing over the other non-network methods is of faster processing. Also, many processors can be used remotely, without the knowledge of the user(s), in order to expedite the processing. Thus the main reason for creating the project is to provide a centralized Image Capture Software scheme for biological medical field. Also, it will act as a centralized repository for all the captured images from microscope. The other major advantage that this system will have over the others is that it will make the users system lightweight i.e. there will be no need to maintain application at the client-side. Thus, for medical researchers this will prove to be highly efficient. The process of maintenance and distribution of dynamic usernames, passwords will be simplified and also authentication and personalized task distribution will be made possible.

Fig2. Cloud Computing

III. SOFTWARE ARCHITECTURE

Online Cloud Based Image Capture Software for Microscope is digital image processing software which enables end-users to view and process live/recorded images on the computer screen via cloud. These images are captured from a camera connected to a microscope. The GUI connects to camera using SDK (software development kit) named Camera SDK and Kernel. The camera SDK provides access to camera features like image output format (color or grayscale) exposure time, image resolution, etc. and image processing features like varying color filters manipulating brightness, contrast of image,. The Kernel is a middle layer between GUI and camera SDK. All communication between GUI and camera SDK exist through kernel.

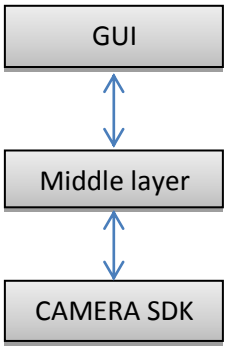

Fig3. Software Architecture

1. GUI: Graphical user interface is a type of user interface that allows users to interact with electronic devices through graphical icons and visual indicators as opposed to text-based interfaces, text navigation or typed command labels.
2. Middle layer: Middle layer is a collection of frameworks which allows quick and efficient development of 2D graphics and media processing applications. The multiple utility frameworks provided by middle layer which supports different operations of application.
3. Camera SDK: Camera SDK is a software development kit, which provides the mechanism along with required drivers to connect a microscopic camera to a computer system and helps to capture images from the camera. By means of different drivers it provides required channel between the camera and the computer system

IV. SYSTEM ARCHITECTURE

Technology is applied to generate Online Cloud Based Image Capture Software for Microscope in 3 tier architecture.
A. Data Layer (Back End): Available in the Web Server which contains account information about the user
B. Business Layer (Middle End) Decision making layer from the application layer
C. Application Layer (Front End) User Interface which shows user interface to the user and getting input from the user.
D. Login Option: Using this option user can login into the cloud for Cloud Vendor and user is provided with login id and password, by using these details he can login to that cloud from any network.
E. Display option: This would take the GUI to the server side for to display the GUI and at the server side, middle layer and camera SDK packages has been imported to communicate with the GUI.

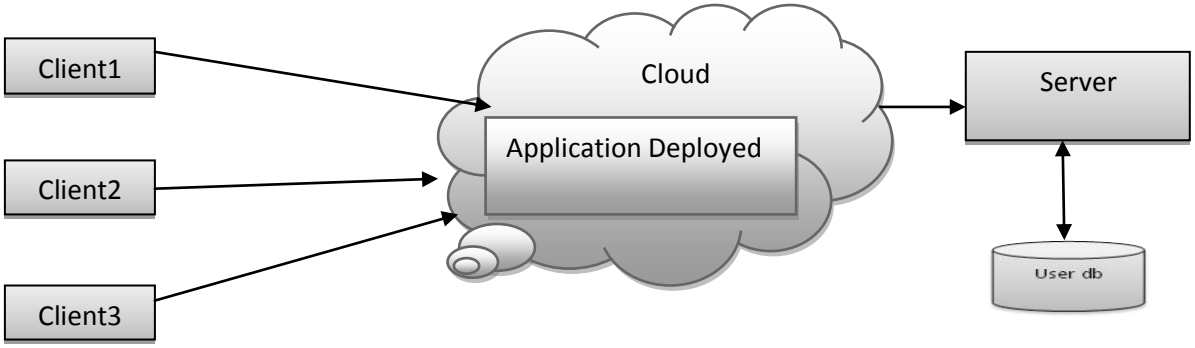

Fig4. Software Architecture

V. DEPLOYMENT DIAGRAM

A Deployment diagram shows the how the application is deployed over the private cloud to serve the users and also shows how different components are connected to each other.

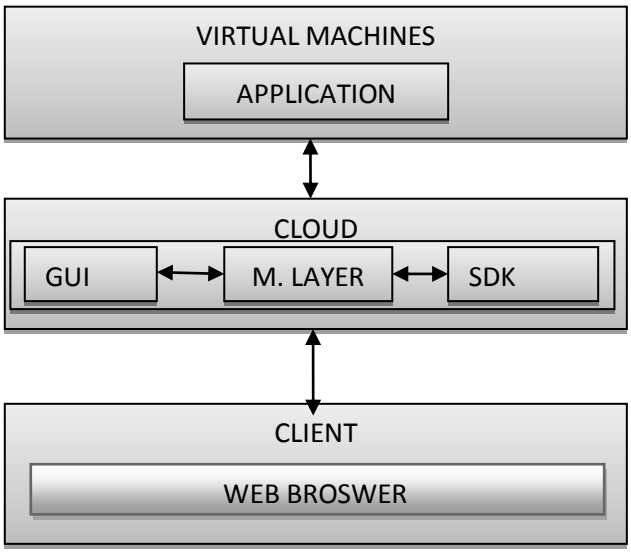

Fig5. Deployment Diagram

VI. IMPLEMENTATION

Whether you are a beginner in digital microscopy or an imaging expert, this software will guide you to reproducible results with the aid of structured workflows. With this digital image processing software, you can control essential parts of your imaging system. All of the processing steps and microscope settings are adjusted quickly and easily in a single user interface. This application allows visualizing and captured images in several dimensions. The functionality of this effective imaging toolbox expands constantly with a wide range of different modules that are tailored to specific applications or microscope accessories. Now and in the future, for your lab, you need only one microscope software.

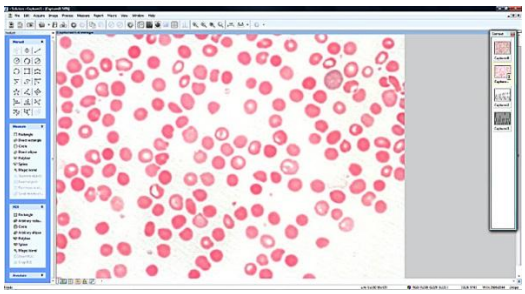

Fig6. Overview of GUI

VII. CONCLUSION

By making the use of characteristics of the Cloud computing, we have presented architecture to build an Online Cloud Based Image Capture Software for microscope. It would basically be a platform for researchers in biological science field. This would eliminate for researchers to install application separately on each computer. Currently, there are a large number of commercial software packages available, some produced by camera manufacturers or microscope, others by third parties. Unfortunately, in current automated imaging world there is no such thing as the complete solution for online and many researchers are faced with the incompatible software packages. Sometimes, due to some technical incompatibilities have to use two different software packages within the same hardware setup. Advantage of this project is that whenever the application is to be upgraded it can be done easily without installing it on each and every machine.

VIII. ACKNOWLEDGEMENT

I would like to thank Mr. Rajashekara Murthy S for guiding me in this work in RV College, Bangalore, Karnataka.

REFERENCES

[1] Online C/C++ Compiler using Cloud Computing Aamir Nizam Ansari, Siddharth Patil, Arundhati Navada, Aditya Peshave, Venkatesh Borole , Pune Institute of Computer Technology, Pune, University of Pune.

[2] Shuai Zhang Shufen Zhang Xuebin Chen XiuzhenHuo, ―Cloud Computing Research and development Trend, Future Networks, 2010.ICFN '10' Second International Conference.

[3] Cloud Documentation and Centralized Compiler for Java & Php Namrata Raut Darshana Parab Shephali Sontakke, Sukanya Hanagandi Department of Computer Engineering, JSPMs BSIOTR(W)

[4] Yogesh Bhanushali, Dwij Mistry, Shraddha Nakil, Sharmila Gaikwad, "Centralized C# Compiler Using Cloud Computing", Advanced Computing & Communication Technologies(ICACCT-2013). 7th International

[5] JunjiePengXuejun Zhang Zhou Lei Bofeng Zhang Wu Zhang Qing Li, "Comparison of Several Cloud Computing Platforms", Information Science and Engineering (ISISE), 2009 Second International Symposium "Cloud Audit,".

[6] A.RABIYATHUL BASARIYA and K.TAMIL SELVI, Computer Science and Engineering, Sudharsan Engineering College-centralized C# compiler using cloud computing, 2nd march 2012

[7] Chunye Gong Jie Liu Qiang Zhang Haitao Chen Zhenghu Gong, "The Characteristics of Cloud Computing",Parallel Processing Workshops (ICPPW), 2010 39th International Conference

[8] Grobauer, B. Walloschek, T. Stocker, E., "Understanding Cloud Computing Vulnerabilities", Security & Privacy, IEEE March-April2011

[9] Ogawa, N.; Oku, H.; Hashimoto, K.; Ishikawa, M. "Single-cell level continuous observation of microorganism galvanotaxis using high speed vision", Biomedical Imaging: Nano to Macro, 2004. IEEE International Symposium on, Vol. 2, 15-18 April 2004, Page(s): 1331 - 1334.

[10] M. Nakajima, H. Akimoto, T. Hirano, M. Kojima, N. Hisamoto, M. Homma and T. Fukuda, "Biological specimen viability analysis by hybrid microscope combined optical microscope and environmental- SEM", IEEE Int. COnf. Nanotechnology Materials and Devices, California, USA, 2010..

[11] Olympus BHS/BHT System Microscope, Olympus, pp 17. Available at: http://www.alanwood.net/downloads/olympus-bh-2-brochure.pdf, 01 Feb, 2012.

[12] R.C. Gonzaleze, and R.E. Woods, Digital Image Processing. New Delhi: Pearson Education; 3rd edition, 2009..

[13] G.J. Arjan, B.G. de Grooth, I Greve, G.J. Dolan, L.W.M.M. Terstappen, "Imaging technique implemented in cell tracks system", Cytometry, No. 7, Wiley-Liss, Inc., 2002, pp. 248-255.

[14] G. Peretti et al. "Narrow-band imaging: a new tool for evaluation of head and neck squamous cell carcinomas.Review of the literature",Acta Otorhinolaryngol Ital 2008; 28:49-54.

[15] G. Dagnino, L. S. Mattos, G. Becattini, M. Dellepiane, and D. G. Caldwell, "Comparative evaluation of user interfaces for robot- assisted laser phonomicrosurgery", EMBC 2011, Boston, MA, USA.

[16] "Imaq Vision Concepts Manual", available from: http://www.ni.com/pdf/manuals/322916b.pdf

[17] James Ambras and Vicki O'Pay, Hewiett-Packard Laboratonies, "Microscope : A Knowledge-Based Programming Environment," IEEE Software,1998,pp.50-58

ISSN (e): 2250 – 3005 || Vol, 04 || Issue, 4 || April – 2014 ||
International Journal of Computational Engineering Research (IJCER)

Finite Element Analysis of a Tubesheet with considering effective geometry properties through design methodology validated by Experiment

Ravivarma.R[1], Azhagiri. Pon[2,]
[1] M.E Thermal Engineering (Part Time), University College of Engg., BIT campus, Tiruchirappalli-24
[2] Assistant Professor, Department of Mechanical Engg., University College of Engg., BIT campus, Tiruchirappalli -24
[1, 2] Anna University: Chennai 600 025, Tamil Nadu, India

ABSTRACT
The Tubesheet, in any heat exchanger is a very important component as it provides a firm support to tubes and in the process gets exposed to thermal and pressure gradients. Various analyses required to assess integrity of Tubesheet are analysis for operating pressure loads and transient thermal analyses together with mechanical loads. The present investigation is in two parts; first one is linear Static analysis of conventional equivalent Modulus of elasticity & Poisson's ratio method, which is recommended by ASME (American Society of Mechanical Engineers) Sec. VIII, Division-1. Second is a new and realistic approach of linear Static analysis by considering the perforations of tube holes in the Tubesheet with pressure acting at inside tubes. The methodology and procedure of Finite Element (FE) method for linear Static analysis in FE method is validated through experiment. Based on the results obtained from two different approaches, the design will be validated and the optimum approach for design will be chosen.

KEYWORDS: *ANSYS, Tubesheet, Finite Element Analysis, Linear Static analysis.*

I. INTRODUCTION

The Tubesheet is a very crucial component of shell-tube type Heat Exchangers, a typical Tubesheet is shown in Fig.1. The number of tubes employed to achieve the required heat transfer is usually very large (in thousands). The tubes run either horizontally or vertically and the lengths are also quite large. The tubes, in general, belong to 'Slender' type of members and hence need firm supports at the ends. The Tubesheet provide these supports. Apart from providing support the Tubesheets also demarked two main components of Heat Exchangers which are usually called as Hot Side (Tube Side) and Cold Side (Shell Side). The basic purpose of Heat Exchanger is to extract heat from one (Hot Side) and provided to other (Cold Side). Owing to this the thermal conditions of Hot Side and Cold Side vary a great deal. Apart from thermal conditions even flow conditions (pressure, velocity) are quite different. Hence tube sheets are subjected to quite severe thermal and mechanical loads. As the Heat Exchanger tubes have to necessarily pass through the Tubesheets, the Tubesheets have very large number of perforations (equal to the number of Tube passes).

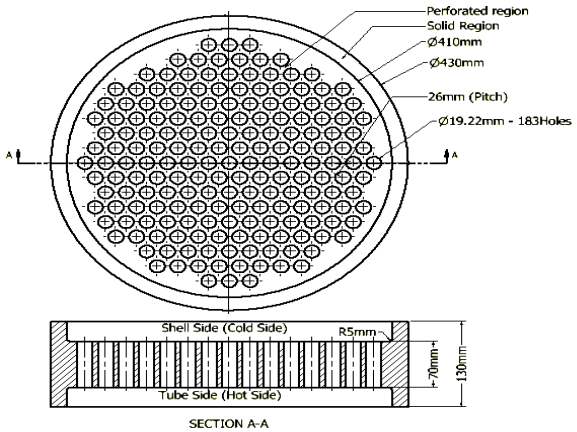

Fig. 1: A Typical Tubesheet Geometry

From these functional requirements Tubesheets are very critical structural components and their mechanical design is very crucial in the whole design of a Heat Exchanger. Tubesheets belong to a category of thick perforated plates subjected to pressure and temperature differentials. As the tubes which pass through perforations handle fluids under pressure the perforations are also subjected to internal pressure. As result, failure of a Tubesheet would result into a very big catastrophe. Hence importance of assessing structural integrity of Tubesheet against various operating conditions needs no emphasis whatsoever.

II. PRESENT INVESTIGATION:

In the mechanical sense, Tubesheet belongs to a category of perforated thick plates. Due to presence of holes in Triangular pattern, (considerable amount of material is removed) the stiffness of the tube sheet gets reduced. Reduction of stiffness in case of perforated plates is well known and analysts represent this using equivalent approach. The reduced stiffness is represented by reduction in Modulus of elasticity and Poisson's ratio. The reduction is related to hole diameter, pitch and pattern of holes. This type of approach is sufficient if the perforations are free boundaries and loading is only mechanical, i.e., say, a pressure differential.

In case of Tubesheet of large Heat Exchanger, the perforations carry tubes which have pressurized fluid. Thus the perforations are subjected to internal pressure, i.e., the boundaries are not free. Apart from this; the perforations are also subjected to thermal loads. There are gradients along the length (through tube sheet thickness) of perforations. With these two conditions, it is not sufficient to merely replace the Tubesheet by its equivalent solid plate i.e., with modified (reduced) values of Modulus of elasticity and Poisson's ratio.

The earlier practice of design of Tubesheets used to be with the help of Standard Codes [1-2] . With advent of Finite Element Method the design of Tubesheets is now possible with Finite Element Analysis. Applying Finite Element Technique to Tubesheets or rather perforated plates in general has certain issues involved. These issues are well known and have been a matter of research. Though the subject matter is available in literature [3-9] , the finer aspects of analysis are not available and the analysts would need to develop their own approaches. This precisely is the subject matter of this investigation. The present investigation is in two parts, first one is conventional equivalent Modulus of elasticity & Poisson's ratio method, which is recommended by ASME (American Society of Mechanical Engineers) Sec.VIII, Division-1. Second is a new & realistic approach of analysis by considering the perforations of tube holes in the Tube Sheet (exact model) under various operating loads like pressure differential, internal pressure at Tubes and temperature gradients. For Analysis, the Element type selection in ANSYS are based on Experimental result comparison with ANSYS output.

III. DESIGN METHODOLOGY VALIDATION BY EXPERIMENT:

3.1 Experiment

Four Carbon Steel Tensile test specimens (IS-2062), in which one specimen without holes that is shown in Fig.2a and other three specimens with holes in 14mm pitch at different diameters say 4mm, 6mm and 8mm that are shown in Fig.2b to 2d, These specimens are undergone a tensile test in Universal Testing machine. The Experimental set-up with test specimen is shown in Fig.3. The tensile tested specimens are shown in Fig.4 and Force Vs elongation plots are obtained from Universal Testing machine indicator that is shown in Fig.5. These plots are used for a reference value for Element Type (ET) selection in ANSYS-14.

a. Without Holes | b.Pitch-14mm; Hole dia.-4mm | c.Pitch-14mm; Hole dia.-6mm | d.Pitch-14mm; Hole dia.-8mm

Fig.2: Tensile test specimens -Before testing

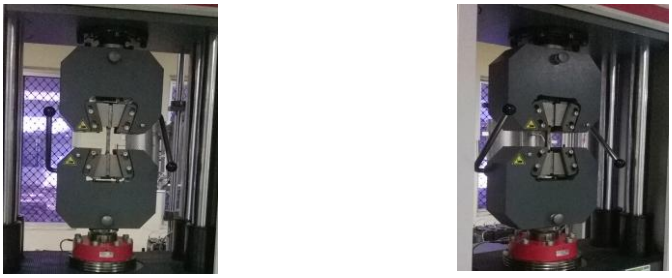

Fig.3: Experimental Set-up

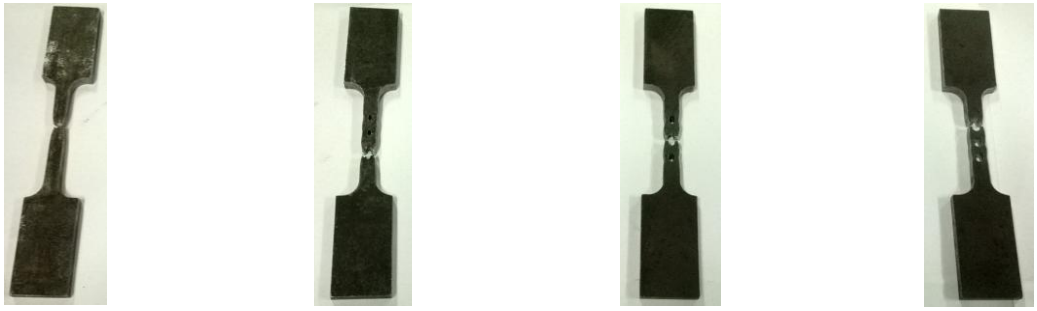

a. Without Holes | b.Pitch-14mm; Hole dia.-4mm | c.Pitch-14mm; Hole dia.-6mm | d.Pitch-14mm; Hole dia.-8mm

Fig.4: Tensile test specimens -After testing

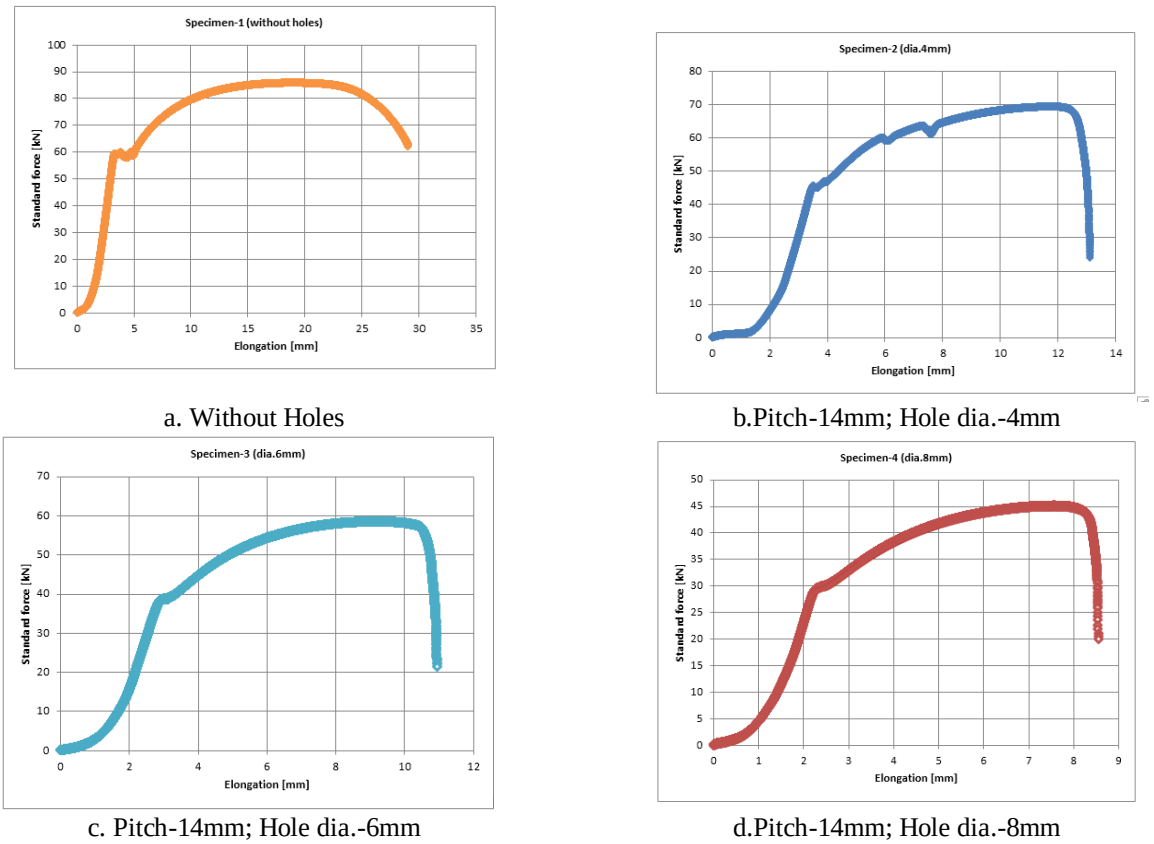

a. Without Holes | b.Pitch-14mm; Hole dia.-4mm

c. Pitch-14mm; Hole dia.-6mm | d.Pitch-14mm; Hole dia.-8mm

Fig.5: Tensile test plots for Specimens

3.2. Analytical Approach through ANSYS-14:

The Tensile test specimen with same geometry is made as volume in ANSYS-14 and meshing is done at different Element Type (ET) such as SOLID45, SOLID73, SOLID185, and SOLID186. Each Element Type have eight nodes and six degree of freedoms. The Static analysis is done in ANSYS-14 with same boundary conditions which are applied in the tensile test experiments. The predicted values of deflection for SOLID45 Element Type result for four types of specimens are shown in Fig.06. This analysis is repeated for different other Element Types of SOLID73, SOLID185, and SOLID186. The predicted values of elongations are shown in Table-I.

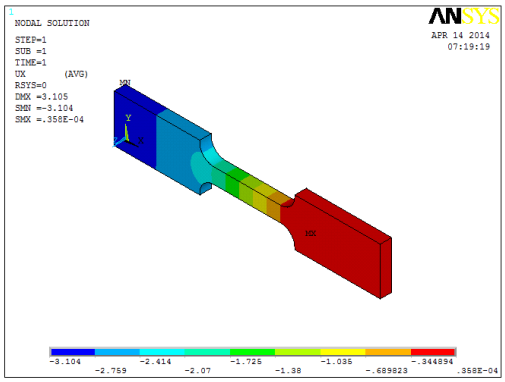

a. Elongation of specimen without holes

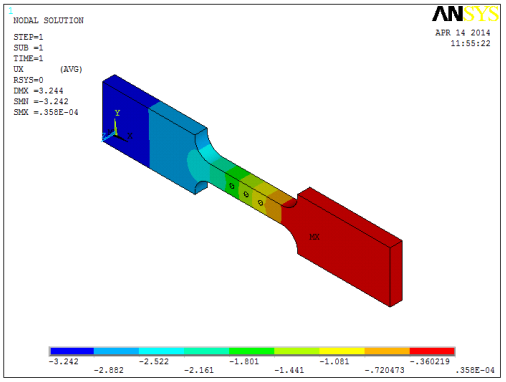

b. Elongation of specimen in 4mm diameter holes

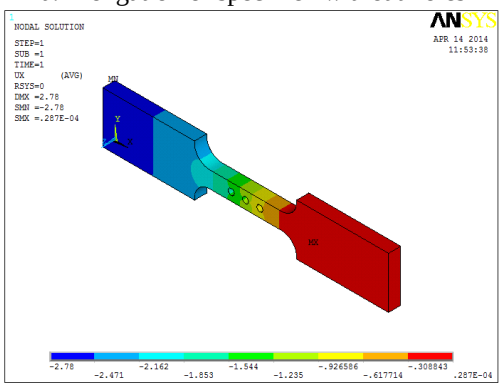

c. . Elongation of specimen in 6mm diameter holes

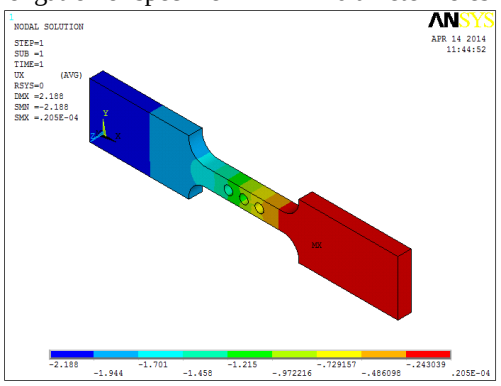

d. . Elongation of specimen in 8mm diameter holes

Fig. 6: Predicted result from SOLID45 Element Type.

3.3 Simulation of Analysis result with Experimental values:

The Finite Element values are compared with Experimental values shown in Table-I.

TABLE-I : Temsile Test Specimen Elongation

Specimens type	Elongation from Experiment value	Elongation form Analysis			
		SOLID 45	SOLID 73	SOLID185	SOLID186
Without holes	3.09 mm @ 55kN	3.105	3.105	3.105	3.111
4 mm	3.29 mm @ 40 kN	3.284	3.247	3.241	3.279
6 mm	2.72 mm @ 35kN	2.780	2.486	2.779	2.817
8 mm	2.06 mm @ 25kN	2.185	2.197	2.186	2.226

Based on the above results, SOLID 45 Element Type may be chosen as a compatible element for performing the structural analysis and the procedure and methodology followed in the analytical method through ANSYS may be extended for the static analysis of Tubesheet.

IV. FINITE ELEMENT ANALYSIS:

4.1 The FE Model:

The Tubesheet is symmetric in the parts of interest here with regard to two meridional planes, and is considered to be symmetric with regard to a cross-section in the middle between the Tubesheet. Pre-checks with a model representing one fourth of the Tubesheet is made in ANSYS-14 as per Fig.1 and same taken for linear Static analysis. The Full model of this FE model is made in ANSYS, to be too time consuming. The Tubesheet is made in two methods. The Method-1 is shows equivalent geometry properties method. In this method a model is generated in two volumes such as perforated region made as one volume and unperforated region made in another volume with 3D structural elements SOLID45, which is shown in Fig.8. This FE model consists of 36136 elements and 40327 nodes.

The Model-2, one fourth of Tubesheet (with holes) 3D model is made for analysis. This FE model consists of 237888 elements and 292323 nodes. The part of Shells, Tubesheet and a part of the tubes are modelled with 3D structural elements SOLID 45 that shown in Fig.9. All nodes at the meridional sides of the Tubesheet and Shells are assigned with symmetry boundary conditions.

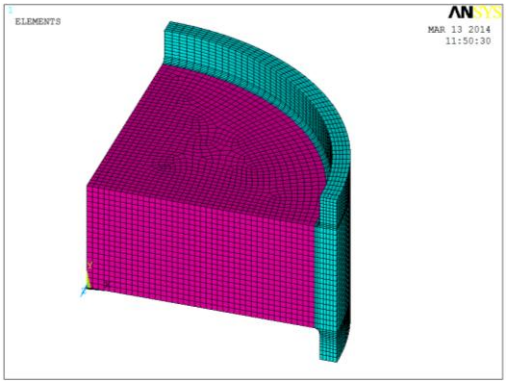

Fig.8: Equivalent of FE Model

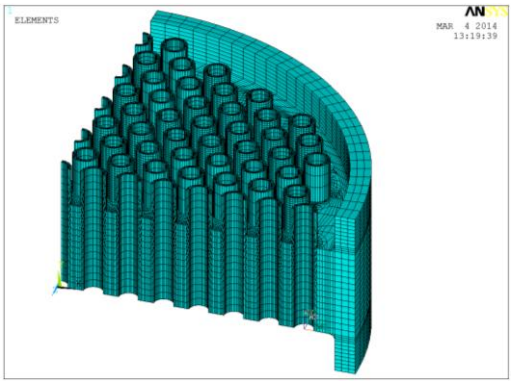

Fig.9: Tubesheet with tubes FE Model

The present investigation on Method-1 & 2 is applied for linear Static analysis approaches. The Tubesheet is subjected to three types of loads. They are; i) pressure differential across the thickness, ii) Pressure inside the holes and iii) thermal gradients which are shown in Fig.10.

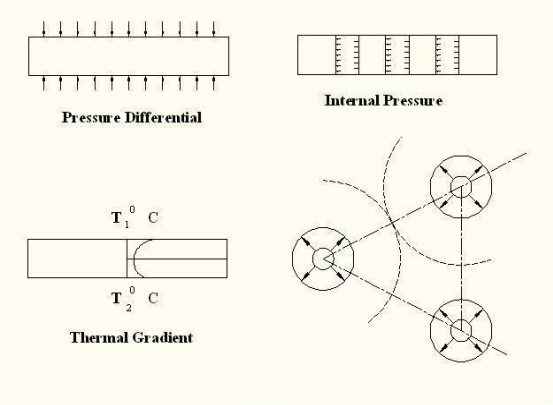

Fig.10: Types of load acting on Tubesheet

4.2 Design Parameter & Geometry Properties:

The Design parameters and Geometry Properties [10] are considered for linear Static analysis of Tubesheet is shown in Table-II and Table-III respectively.

TABLE-II: Design Parameter

Description	Values	
	Tube Side	Shell Side
Design Pressure (N/mm^2(g))	1.29	2.16
Design Temperature,T2&T1(°C)	400	200
Hydro Test Pressure(N/mm^2 (g))	1.77	3.24

TABLE-III: Geometry Properties at 25°C & 400°C [10].

Description	Values
Material for Tubesheet	SA-204 Gr.B
Moduls of elasticity, E(N/mm^2) at 25°C	202000
Poisons ratio, μ	0.3
Equivalent Modulas of elasiticity ,E*(N/mm^2) at 25°C	101000
Equivalent Poisons ratio, μ*	0.3
Moduls of elasticity, E(N/mm^2) at 400°C	171000
Equivalent Moduls of elasticity, E**(N/mm^2) at 400°C	85500

4.3 Linear Static Analysis of Tubesheet:

a. Equivalent geometry properties methods:

The linear Static analysis are done for Design conditions as well as in Hydro test condition. The differential pressure is applied on Tubesheet. The equivalent geometry properties are applied as per Table-III. The constrained are made at top and bottom of Shells. The predicted results are shown in Fig.11, 12, 13 and 14 for von Mises stress, and displacement patten for Design conditions and Hydro test condition respectively.

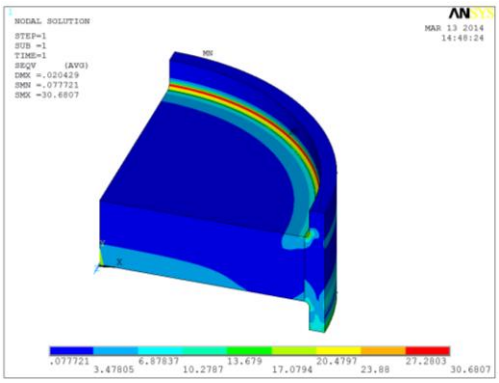

Fig.11: Von Mises Stress value at Design conditions

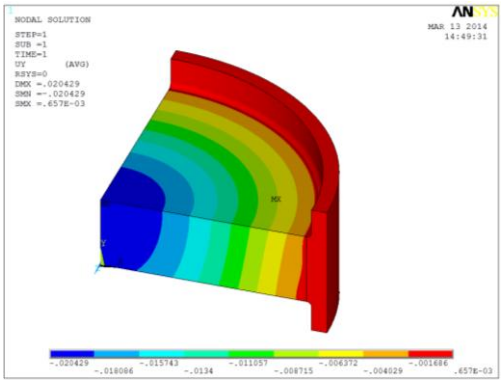

Fig.12: Displacement Patten at Design conditions

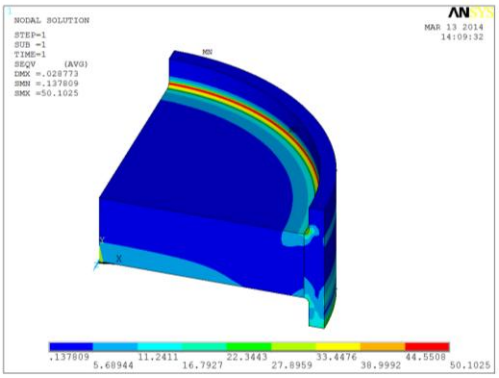

Fig.13: Von Mises Stress value at Hydro test conditions

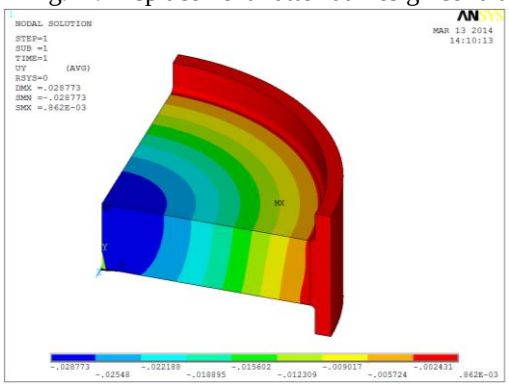

Fig.14: Displacement Patten at Hydro test conditions

b. New and realistic actual Tubesheet geometry methods:

In this method also, the linear Static analysis are done for Hydro test condition as well as in Design conditions. The differential pressure is applied on Tubesheet and tube side pressure is applied at tubes inside which same as per Table-II. The geometry properties are applied as per table-III. The predicted results are shown in Fig.14, 15, 16 and 17 for von Mises stress, and displacement patten for Design conditions and Hydro test condition respectively.

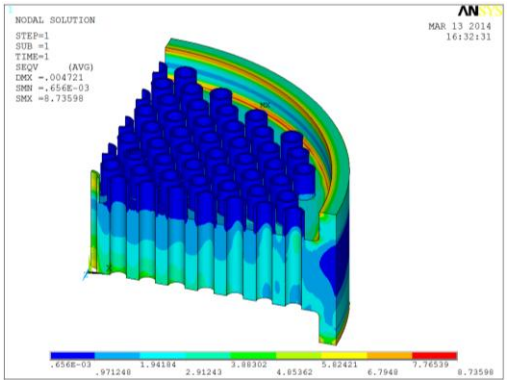

Fig.14: Von Mises Stress value at Design conditions

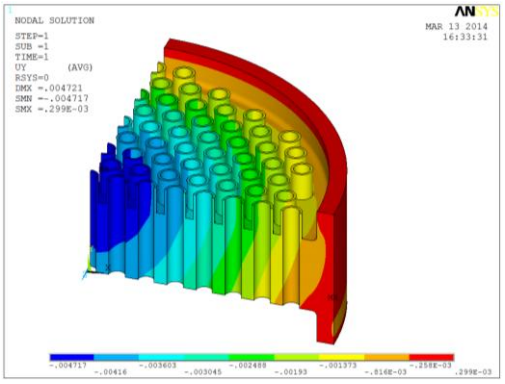

Fig.15: Displacement Patten at Design condition

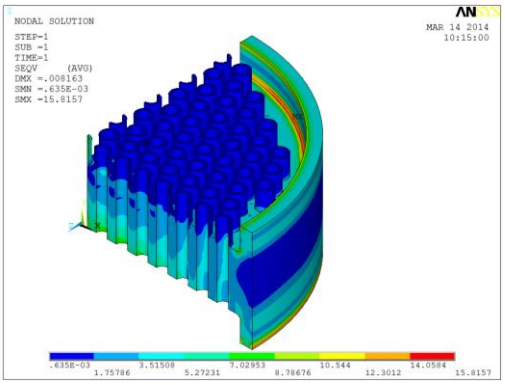

Fig.16: Von Mises Stress value at Hydro test conditions

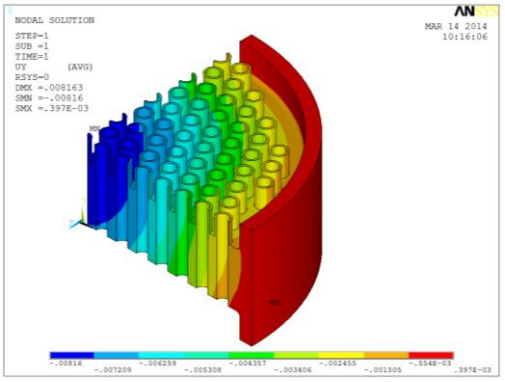

Fig.17: Displacement Patten at Hydro test conditions

V. RESULT AND DISCUSSION

The commonly followed approach for analysis is to replace the perforated part by an equivalent region and carry out axi-symmetric analysis or equivalent solid plate methods.

The axi-symmetric or equivalent solid plate results are then appropriately modified to account for the effect of holes. When loads are applied on an axi-symmetric or equivalent solid body (i.e. holes are not present in the model) the stress distribution obtained would be a continuous one. When these loads are applied on a perforated plate then the distribution would get perturbed and the ligament region, is likely to show enhanced values. This is shown schematically [11] in Fig.18.

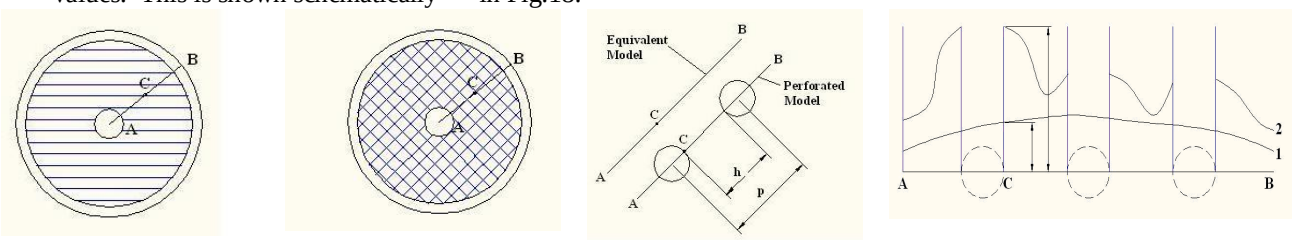

(a) Path in Equivalent model

(b) Path in Perforated Model

(c) Geometry of Two Paths

(d) Comparison of Stress Distribution

1 - Distribution in continuous plate
2 - Distribution in perforated plate

Fig. 18: Effect of Holes

At a certain point C on line AB, is the stress obtained by axi-symmetric analysis with perforated region replaced by equivalent material. At same location, would be the stress obtained at the holes boundary in the ligament region. Two types of loads are shown in Fig.10, the pressure differential can be applied on equivalent solid plate and, the pressure differential and internal pressure can be applied on perforated plate. Whereas, it is not possible to apply, pressure inside the holes in an equivalent solid plate. Its effect is computed using thickness of the tubes and the perforation attributes (p, the pitch and h, the ligament). With this, the values obtained from axi-symmetric analysis are appropriately modified.

The developed FE results for linear Static analysis from equivalent geometry properties method and new and realistic actual Tubesheet geometry methods results are generated at various Stress Categorization Lines as per Fig 19 and 22. The maximum von Mises stress, and displacement paten for Design conditions and Hydro test condition at maximum concentrated locations are shown in Fig.20, 21, 23 and 24 respectively. The predicted values at various Stress Categorization Lines which is shown in Tale-IV and V. Based on these values, the new and realistic methods von Mises stress is 36 to 75 % lesser than equivalent geometry properties method.

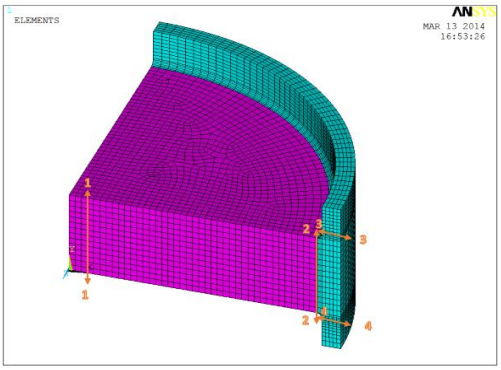

Fig. 19: Stress Categorization Lines (SCL)for equivalent geometry method

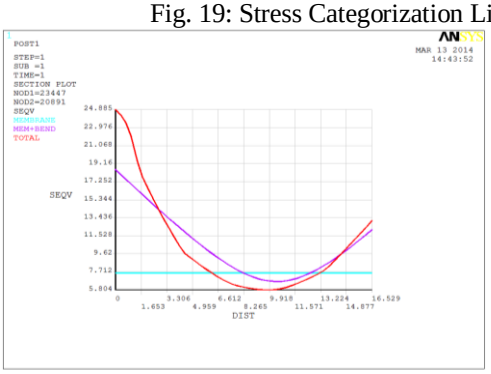

Fig. 20: von Mises plots along SCL No. 3-3 at Hydro test condition

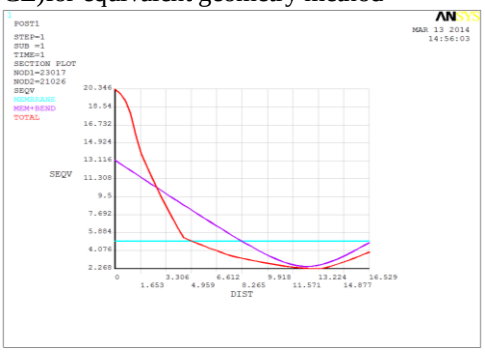

Fig. 21: von Mises plots along SCL No. 3-3 at Design Condition

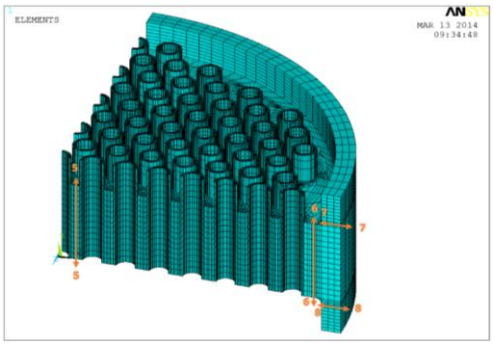

Fig. 22: Stress Categorization Lines (SCL) for actual geometry method

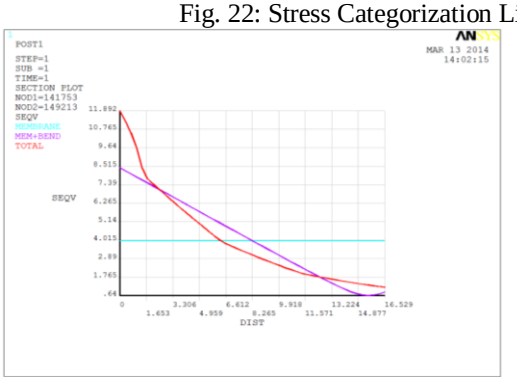

Fig. 23: von Mises plots along SCL No.7-7 at Hydro condition

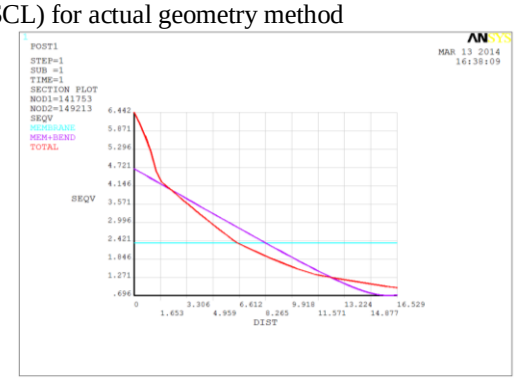

Fig. 24: von Mises plots along SCL No.7-7 at Design condition

TABLE-IV: Comparison of Max.von Mises stress (Total Stress):

SCL No	Maximum von Mises stress in N/mm^2	
	at Design condition	at Hydro test condition
Equivalent geometry method		
1-1	6.662	10.776
2-2	12.39	20.707
3-3	20.343	33.864
4-4	14.805	24.885
New and realistic actual Tubesheet geometry methods		
5-5	3.923	6.837
6-6	5.195	9.024
7-7	6.442	11.892
8-8	3.633	7.729

TABLE-V: Comparison of deflections:

Description	Deflection in mm	
	at Design condition	at Hydro test condition
Equivalent geometry method	0.0204	0.0288
New and realistic actual Tubesheet geometry methods	0.0047	0.0088

VI. CONCLUSIONS:

Various analyses required to assess integrity of Tubesheet are analysis for operating pressure loads and transient thermal analyses together with mechanical loads. The present investigation is done in two parts; first one is linear Static analysis of conventional equivalent Modulus of elasticity & Poisson's ratio method, which is recommended by ASME (American Society of Mechanical Engineers) Sec. VIII, Division-1. Second is a new and realistic approach of linear Static analysis by considering the perforations of tube holes in the Tubesheet with pressure acting at inside tubes. This linear Static Analysis, the Element Type (ET) selection in ANSYS-14 is selected based on Experimental result. Based on this investigation, the results obtained from two different approaches, design of Tubesheet for any Heat Exchanger, better to do analysis in realistic actual Tubesheet geometry methods for the selection of optimum required material.

REFERENCES

[1] ASME. ASME Boiler and Pressure Vessel Code, Section VIII Divi.1", 2013 Edition, the American Society of Mechanical Engineers - New York, 2013, 274 -283.

[2] TEMA, "Standard of Tubular Exchanger Manufactures Association" 9th Edition, Tubular Exchanger Manufactures Association, 2007, 5.7.1 – 5.7.4.

[3] Wengen Peng, Yanwei Hu, Yuanchun Liu, Guangri Jin and Yurong He "Analytical Modeling of the Strength of Tubesheet for Steam Surface Condensers", Journal of Pressure Vessel Technology, October 2013, Vol. 135 / 051206-1 to 9.

[4] Weiya Jin, Zengliang Gao, Lihua Liang, Jinsong Zheng, Kangda Zhang"Comparison of two FEA models for calculating stresses in shell-and-tube heat exchanger", International Journal of Pressure Vessels and Piping, 2004, 563–567.

[5] K. Behseta, S. Schindler, "On the design of the tubesheet and the tubesheet-to-shell junction of a fixed tubesheet heat exchanger", International Journal of Pressure Vessels and Piping, 2006, 714–720.

[6] C. F. Qian, H. J. Yu & L. Yao, "Finite Element Analysis and Experimental Investigation of Tubesheet Structure", Journal of Pressure Vessel Technology, February 2009, Vol.131/011206-1 to 4.

[7] Ricky Chana, Faris Albermanib and S. Kitipornchaic, "Stiffness and Strength of Perforated Steel Plate Shear Wall", the Twelfth East Asia-Pacific Conference on Structural Engineering and Construction; Procedia Engineering, 2011, 675–679.

[8] Masanori Ando, Hideki Takasho, Nobuchika Kawasaki & Naoto Kasahara, "Stress Mitigation Design of a Tubesheet by Considering the Thermal Stress Inducement Mechanism", Journal of Pressure Vessel Technology, December 2013, Vol. 135 / 061207-1 to 10.

[9] Khosrow Behseta, Donald Mackenzie, Robert Hamilton, "Plastic load evaluation for a fixed tube sheet heat exchanger subject to proportional loading", International Journal of Pressure Vessels and Piping, 2012, 11 – 18.

[10] ASME, "ASME Boiler and Pressure Vessel Code, Section II Part-D", 2013 Edition, the American Society of Mechanical Engineers - New York, 2013, 738 and 744.

[11] John F.Harvey,P.E, "Theory and design of pressure vessels", CBS publishers & Distributors, 4596/1A, 11 daryaganj, New Delhi-110 002 (India), 1987,136-148.

ISSN (e): 2250 – 3005 || Vol, 04 || Issue, 4 || April – 2014 ||
International Journal of Computational Engineering Research (IJCER)

Reusability of test bench of UVM for Bidirectional router and AXI bus

Manjushree.k.chavan[1,] Yogeshwary.B.H[2]
1 4th sem, M.Tech (VLSI Design & Embedded systems), RIT, Hassan,
2 Assistant professor. Dept of ECE, RIT, Hassan, Karnataka.

ABSTRACT:
The predictive analysis of the design to ensure that, it will perform the given I/O function is performed through functional verification. Verification has become the dominant cost in any of the design process. The modernization of functional verification has become necessary task in verifying a large design. The project focuses on designing the Bidirectional network on chip router through virtual channel regulator and then AXI bus and thus developing the common verification environment for both the designs to show the reusability of test bench. The bidirectional network on chip router is implemented with unified buffer structure called the dynamic virtual channel regulator. The project also aims to develop a shortest path algorithm when a packet of data is to be transmitted as many paths are available thus by designing two routers. The functionality of the design is verified by using the latest Universal verification methodologies (UVM) further with the employment of reusable test benches of UVM for both the designs. The Verification goes on with which it finds functional coverage, state coverage, code coverage and toggle coverage of the Network on Chip Router by using Questa-Sim/cadence NC simulator and the synthesis is done by using Xilinx ISE 14.3i EDA Tools.

KEYWORDS: *Universal verification methodologies, virtual channel regulator, Open verification methodology, verification methodology module, AXI interconnect.*

I. INTRODUCTION

The process of demonstrating the functionality of the design has become one of the major tasks in today's era of multi-million gate ASICs and FPGAs. Verification consumes about 70% of the design effort. The number of verification engineer is more than the design engineers so the challenge of verifying a large design is growing exponentially. There is a need to define new methods that makes functional verification easy. Several strategies in the recent years have been proposed to achieve good functional verification with less effort. The recent advancement is to develop a methodology to reduce the time taken for verification. The advancement in the verification environment should be such that it reduces the re-spin of the ASIC design due to functional bugs and thus reducing the time to market.

This project helps one to understand about the latest verification methodologies, programming concepts like Object Oriented Programming of Hardware Verification Languages for the high quality verification with automation. This project is intended in building the reusability of test bench for the designed bidirectional network on chip router through virtual channel regulator and the AXI bus using the latest UVM verification methodologies.

II. MOTIVATION FOR THE WORK

The process of modernizing the verification methodology to reduce the time taken for verification can be accomplished by using the latest universal verification methodology (UVM). UVM is a combined effort of designers and tool vendors, based on the successful OVM and VMM methodologies. Its main promise is to improve test bench reuse, make verification code more portable and thus create a new market. The reusability of this verification environment is demonstrated by designing a bidirectional network on chip router through virtual channel regulator along with the shortest path algorithm for routing and also designing the AXI bus.

III. LITERATURE SURVEY

Chow.K.W.Y., (1994) mentioned in his paper that the early stages of design was verified by design engineer only using Verilog tasks and functions due to which all the test cases was not met and also time to market was not able to reach efficiently. Lot of time was spent in verification rather than design [1].

Few years later the System Verilog language was introduced by Accellera in 2002 and as IEEE Standard 1800-2005 in 2005. In 2009, the standard was merged with the base Verilog (IEEE 1364-2005) standard, creating IEEE Standard 1800-2009. The current version is IEEE standard 1800-2012. It is the first hardware verification language.

Moorby.P., (2004) in 17th International conference proposed the several aspects of this new language and how they form a critical part in the new design for verification paradigm [2].

McMahon, Anthony , O'Keeffe, Niall, Keane Kevin ,O'Reilly, James., (2008) presented a paper on System Verilog Verification Methodology Manual (VMM) was the first successful and widely implemented set of practices for creation of reusable verification environments in System Verilog, created by Synopsys, one of the strong proponents of System Verilog[3].

S. Iman., (2008) published a paper on "Step-by-step functional verification with System Verilog and OVM", with the new verification methodology named OVM. OVM is the library of objects and procedures for stimulus generation, data collection and control of verification process. It is available in System Verilog and System C [4].

Jae-Beom Kim, Nam-Do Kim, Byeong Min., (2011) published a paper on Universal verification methodologies (UVM), which is considered to be the common verification methodology [5].

T Lakshmi Priyanka, G. Deepthi, B. Sunil Kumar., (2013) Proposed the concept of reusability of test benches with the latest verification methodology i.e. UVM with the design of a router for network on chip communication in the paper "Reusable test bench for network on chip router using advanced verification methodologies. The paper explains about the perl script to provide automation in verification [6].

M. Bechtel Brabi and Dr. A. Rajalingam., (2012) illustrated in their paper "Recent survey for Bi-Directional network on chip pipelined architecture" that bidirectional network on chip router is more efficient than the conventional architecture. The paper also evidenced about the reduced latency & buffer size, increase in bandwidth and also indicated that pipelined architecture is more useful than the parallel architecture [7].

Ying-CherngLan, Hsiao-An Lin, Shih-HsinLo , Yu Hen Hu, Sao-Jie Chen.,(2011) published paper on " A Bidirectional NOC architecture with dynamic self-reconfigurable channel", in this paper they explained the concept of dynamic self-reconfigurable channel using an (CDC) channel direction control algorithm to avoid deadlock and starvation conditions. These results exhibit consistent and significant performance advantage over conventional NoC equipped with hard-wired unidirectional channels [8].

Mr. Ashish Khodwe , Prof. C.N. Bhoyar., (2013) published a paper on Bidirectional Network on chip Router through Virtual Channel Regulator, which dynamically allocates virtual channel and buffer resources according to network traffic conditions [9].

Baoxian Zhang, JieHao, and Hussein T. Mouftah., (2012) published a paper on "Bidirectional Multi-Constrained Routing Algorithms" in order to demonstrate an algorithm to find the shortest path of transfer of packets whenever many routing paths are available or when an congestion occurs [10].

Xu Chen, Zheng Xi, and Xin-An Wang., (2013) presented a paper on "Development of verification environment for AXI Bus using system Verilog". The paper explained about the methodology of verifying an AXI bus using system Verilog [11].

Pan Guoteng, Luo Li, OuGuodong, Fu Qingchao, Bai Han., (2013) proposed a paper on " Design and verification of a MAC controller based on AXI bus" this paper explained about the verification of AXI bus using an VMM [12]. The literature survey performed in this section specifies the researches carried out on the various verification methodologies and also on the design of the router which is considered to be the fundamental unit in an NOC. The related problem definition, objectives and methodology has been explained in next section.

3.1. Problem formulation

- During the recent years modernization of verification methodologies has become major criteria in order to reduce the time taken for verification and to reduce time to market. From the literature survey it is understood that even though the System Verilog is standard hardware description language.

There should be common verification methodologies because in reality most of the procedure in the test bench will be same for different project.

- The design of a generic or conventional router with statistically allocated buffer can cause the Head-of-Line blocking problem. In order to improve the performance and thus reducing the queue blocking, the dynamic buffer allocation significantly increases buffer usage.
- The methodology for developing the verification environment for AXI bus in proposed only by using system Verilog or by VMM, it is necessary to upgrade the verification of AXI bus using UVM.

3.2. Aim of the project

The aim of this paper is the design and implementation of Bidirectional network on chip router through virtual channel regulator with the shortest path algorithm and AXI bus. The designed system is verified using the latest verification methodologies i.e., the standard is Universal verification methodologies (UVM), which supports all of Verilog, system Verilog syntax along with automation techniques and thus observing the code coverage and functional coverage and thus signifying the reusability of the test bench for the bidirectional router and AXI bus.

IV. METHODOLOGY

The need for modernized common verification environment called UVM thus used the concept of reusability of test bench. In this paper to show the reusability of test bench two stages of design is being performed. First is designing the proposed bidirectional router with virtual channel regulator and the second is designing AXI interconnect. Both of these designs are verified under common verification environment called UVM thus showing the reusability of test bench.

V. DESIGN FLOW

The design flow of the project involves two stages, first is the design and implementation of Bidirectional network on chip router through virtual channel regulator and AXI bus demonstrated in block below. The second stage is developing a common verification environment called (UVM) and thus checking the reusability of test benches for both the designs.

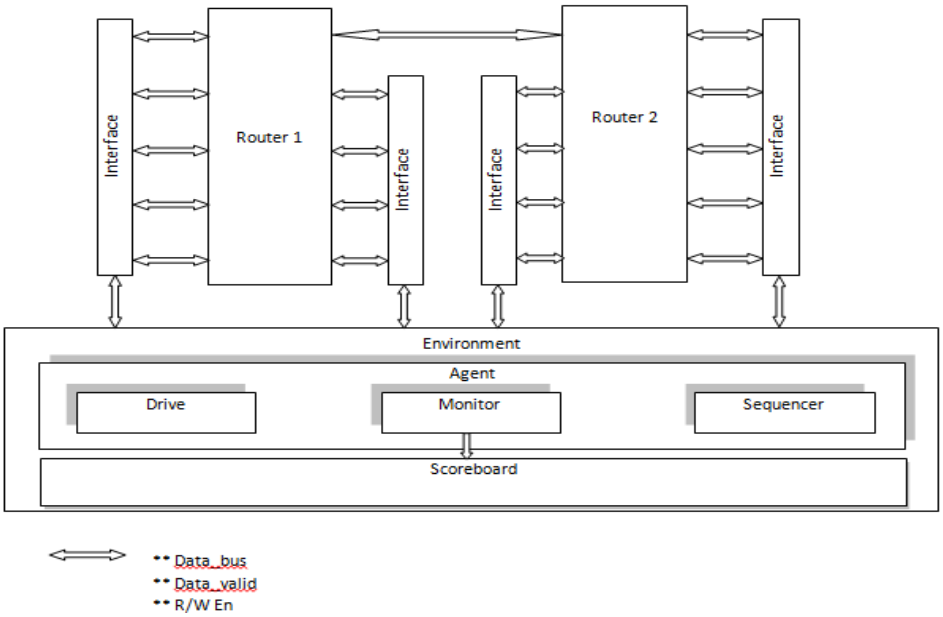

Figure 1. Flow diagram of Bidirectional routers with verification environment

The Figure.1 is the flow diagram of designing two bidirectional routers with the virtual channel regulator and the shortest path algorithm is implemented when many numbers of paths are available. The two interfaces are virtual interfaces and the packet transfer occurs through dynamic buffer allocation.

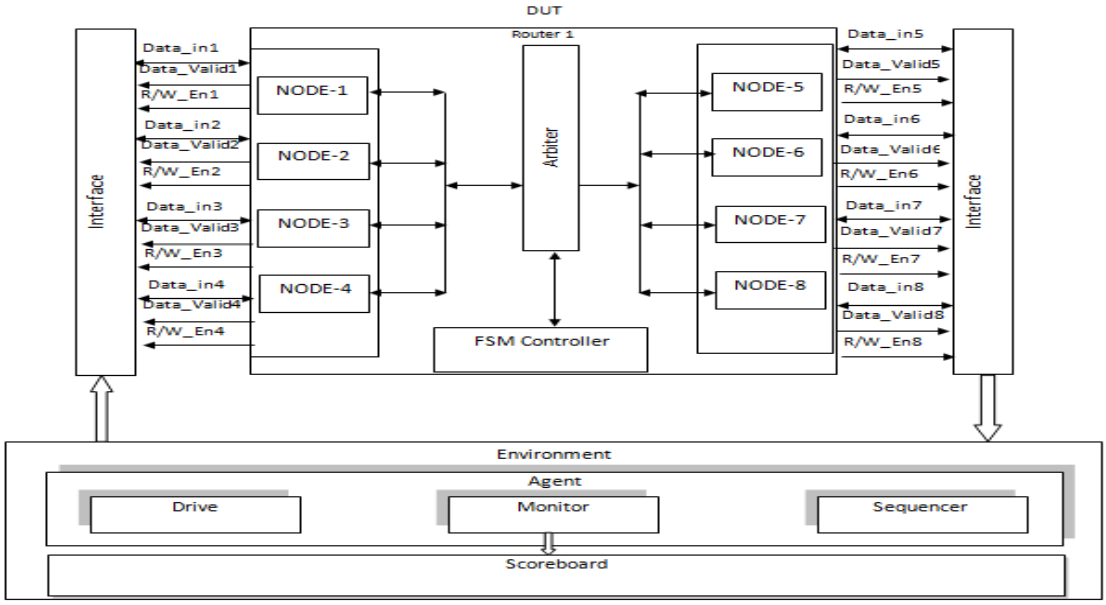

Figure 2. Flow diagram of design of each router

The Figure.2 is the flow diagram of design of each of the router. The router consists of register, FSM controller and the FIFOs where the input and output blocks are connected to the virtual interfaces. Arbiter is used in order to resolve the conflict when two or more packets of data makes a request to transmit a data in the same channel, in such case arbiter makes decision depending on the priority. The designed system is connected to the verification environment to check the functionality of the design.

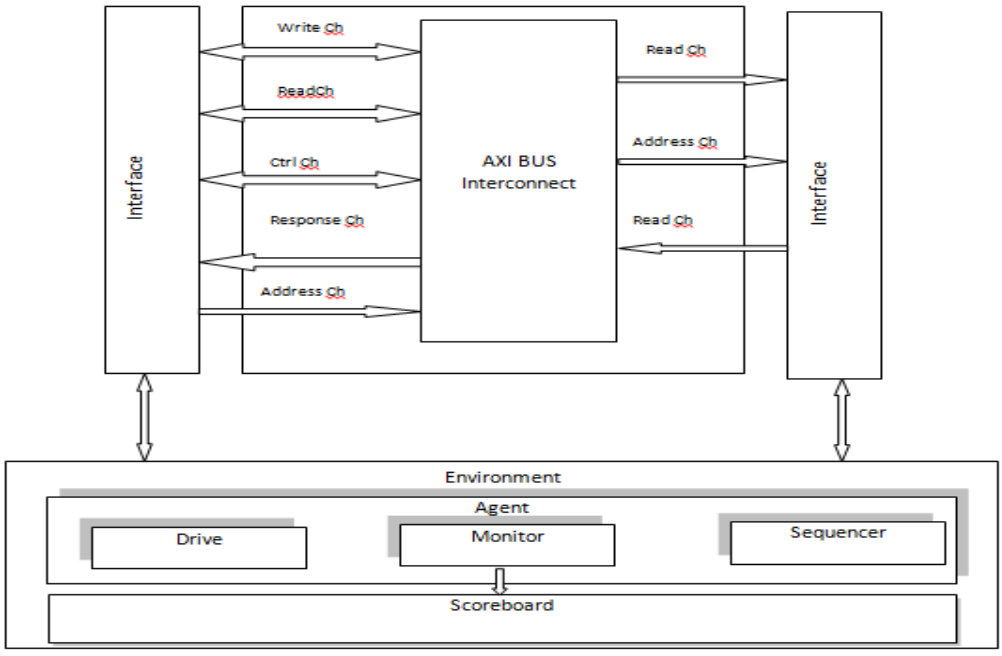

Figure 3. Flow diagram of designing AXI Bus interconnects.

The Figure.3 is the flow diagram of designing AXI Bus interconnects is the second part of the design. The AXI master and slave performs the read and write data depending on the request and grants. It is connected to the verification environment to check the intent of the design.

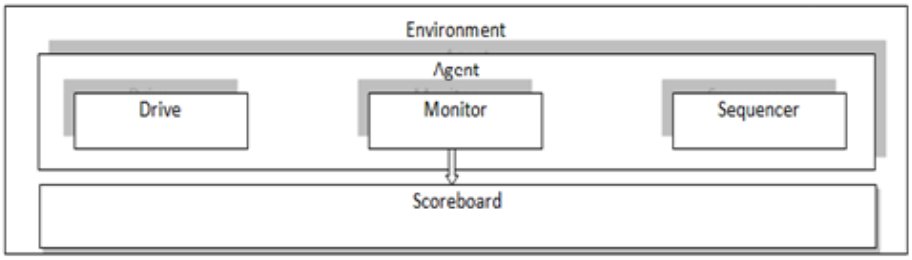

Figure 4. UVM Verification Environment

5. Results & Discussion

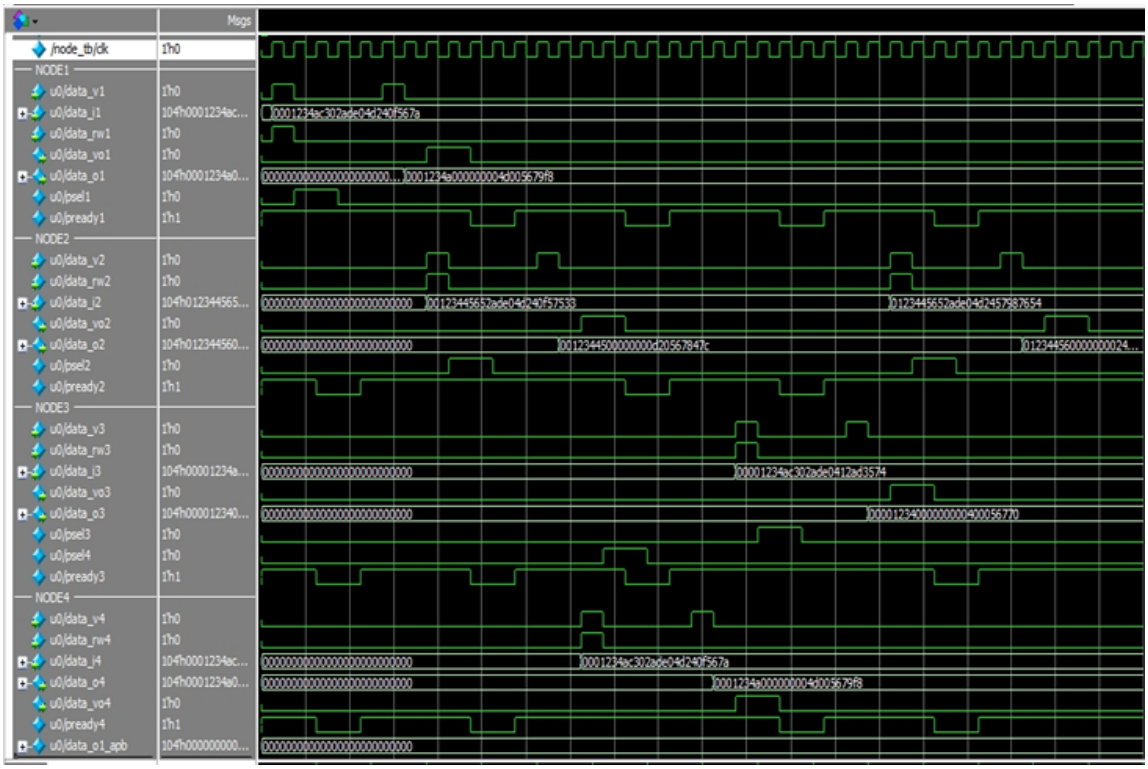

Figure.5. Simulated waveform of design of four nodes

The Figure.5 is the simulated waveform of design of the four node obtained in modelsim with the design of arbiter called round robin arbiter with APB bus. Further design is continued with the implementation of many such nodes for two routers and then designing & implementation of shortest path algorithm and then following the switch design.

VI. CONCLUSION AND FUTURE WORK

6.1. Conclusion

The result above is for generating a packet of data by creating four nodes and thus designing the round robin arbiter with APB bus. The UVM drives the input to these nodes for further verification process.

6.2. Future work

The above result is continued with the design and implementation of many such nodes with the shortest path algorithm to transmit the data packet to the other router.

The second stage is designing the AXI interconnect with the packet data transferred from AXI master and AXI slave by reading the data from the memory.

The third and the final stage is verification of these two designs by using the common verification environment with the reusable test bench and thus showing the reusability of test bench.

REFERENCES

[1] Chow.K.W.Y., "Fully specified verification simulation", Published in: Verilog HDL Conference, 1994., International, pages 22-28, Print ISBN:0-8186-5655-7.

[2] Moorby, P., "Design for verification with System Verilog", Published in: VLSI Design, 2004. Proceedings, 17th International Conference, Print ISBN: 0-7695-2072-3.

[3] McMahon, Anthony , O'Keeffe, Niall, Keane Kevin ,O'Reilly, James., "The development of advanced verification environments using System Verilog "Published in: Signals and Systems Conference, 208. (ISSC 2008). IET Irish, page(s) 325-330, print ISBN: 978-0-86341-931-7

[4] S. Iman., "Step-by-step functional verification with SystemVerilog and OVM", Hansen Brown Publishing, ISBN-10: 0-9816562-1-8, May 2008.

[5] Jae-Beom Kim, Nam-Do Kim, Byeong Min., "Beyond UVM for practical SoC verification" soc design conference (isocc), 2011 international conference, page 158-162, E-ISBN: 978-1-4577-0710-0

[6] T Lakshmi Priyanka, G .Deepthi, B. Sunil Kumar., "Reusable Test bench for Network on Chip Router using Advanced VerificationMethodologies" International Journal of Science and Modern Engineering (IJISME) ISSN: 2319-6386, Volume-1, Issue-9, August 2013.

[7] M. Bechtel Brabi and Dr. A. Rajalingam., " Recent survey for Bi-Directional network on chip pipelined architecture" International journal of Advanced Research in computer science and Software Engineering, Volume-2, issue-12.

[8] Ying-CherngLan, Hsiao-An Lin, Shih-Hsin Lo , Yu Hen Hu, Sao-Jie Chen., "A Bidirectional NOC architecture with dynamic self-reconfigurable channel", Page(s): 266 – 275, E-ISBN : 978-1-4244-4143-3, Print ISBN: 978-1-4244-4142-6

[9] Mr. Ashish Khodwe , Prof. C.N. Bhoyar., "Efficient FPGA Based Bidirectional Network on Chip Router through Virtual Channel reulator" Proceedings of 2nd International Conference on Emerging Trends in Engineering and Management , ICETEM 2013.

[10] Baoxian Zhang, JieHao, and Hussein T. Mouftah., "Bidirectional Multi-Constrained Routing Algorithms", ISSN :0018-9340, Date of Publication :07 March 2013.

[11] Xu Chen, Zheng Xi, and Xin-An Wang., "Development of verification environment for AXI Bus using system Verilog", International Journal of Electronics and Electrical Engineering, Vol. 1, No. 2, pp. 112-114, June 2013. doi: 10.12720/ijeee.1.2.112-114.

[12] Pan Guoteng, Luo Li, OuGuodong, Fu Qingchao, Bai Han., " Design and verification of a MAC controller based on AXI bus", Page(s):558 – 562, Print ISBN:978-1-4673-4893-5

ISSN (e): 2250 – 3005 || Vol, 04 || Issue, 4 || April – 2014 ||
International Journal of Computational Engineering Research (IJCER)

Quantification of Leanness in a Textile Industry

Pruthvi.H.M.[1], Sreenivasa.C.G.[2]
[1] Lecturer, Dept of Mechanical Engineering, Dr.TTIT, KGF,
[2] Associate professor. Dept of Mechanical Engineering, UBDTCE, Davangere, Karnataka.

ABSTRACT:
Right from the industrial revolution, industrial sectors are in the continuous process of improving their productivity. Researchers and practitioners working in productivity improvement area are deriving various strategies. One among these strategies is lean manufacturing. Lean manufacturing aims to identify and eliminate wastes in their working environment. The implementation of lean manufacturing has to be initiated with lean assessment. The lean assessment indicates the criteria which are not practiced for lean implementation in the industry. The scope of this paper is to carryout lean assessment in a textile industry by name Anjaneya Cotton Mill (ACM). The questionnaires for lean assessment have been developed by considering thirteen criteria grouped under four lean enablers. The assessment indicated that, ACM is practicing 51.83 % of leanness. However, a gap of 48.17% is prevailing in ACM. In order to fill this gap proposals were drawn. Most of the proposals drawn have been accepted by the management of ACM. The case study presented in this paper shall be utilized by the contemporary practitioners in implementing lean manufacturing.

KEYWORDS: *Lean manufacturing, Lean assessment, Leanness, Textile industry*.

I. INTRODUCTION

Textile manufacturers have sought to improve their manufacturing processes so that they can more readily compete with global manufacturers. Lean manufacturing techniques are the primary methods for a fair competiveness by reducing wastes. Lean manufacturing is defined as "A systematic approach to identifying and eliminating waste (non-value-added activities) through continuous improvement". Lean is concerned with eliminating all types of waste, which is much more than eliminating waste by reducing inventory. Wastes can be classified as: overproduction, time on hand, transportation, over processing, inventory, movement and defective products. All the lean tools work towards common goals of eliminating this waste in order to bring the most value to the customers. The lean tools are: visual management, policy deployment, quality methods, standardized work, just-in-time and improvement methods (5s, TPM, poka-yoke, kanban, cellular manufacturing, SMED, kaizen, value stream mapping) (Hodge et.al., 2011). One of the research agenda in lean manufacturing is the assessment of leanness (Vinodh & Vimal., 2012). The work reported in this paper was carried out to contribute a refined, exhaustive and simple leanness assessment tool. Accordingly a tool called 13 LM criteria assessment tool was designed during this work. Using this tool, the total leanness level in a textile industry was assessed. After a comprehensive analysis, the percentages of implementation of lean tools were identified. Subsequently, the success ingredients for overcoming them were evolved and suggested. These details of this work are presented in this paper.

II. LITERATURE REVIEW

Hodge et.al. (2011) determined which lean principles are appropriate for implementing in textile industry. This paper investigates the different tools and principles of lean and the use of lean manufacturing in the textile industry was examined by the researchers by considering plant tours and case studies. From this case study the researchers came to a conclusion that lean manufacturing is a strategy that does not require large investment in automation or IT and it can be implemented in both small and large companies where all employees can be involved in improving operations to meet customer needs.

Chauhan and Singh (2012) aimed to identify the measuring the associated parameters of lean. The paper provides the most important parameters to measure the status of lean manufacturing. The author concluded that, there is a broad scope to focus on the elimination of different forms of wastes from manufacturing system for the lean manufacturing in India. Green et.al (2010) wants to implement lean in a material handling system for petroleum drill bit manufacturing company. They addressed that the operational group with a tool to assist in defining the objectives of lean manufacturing has been developed by the authors. At the end, it is concluded that a special solution was developed from the process of implementing the project. The methodology was developed using lean manufacturing concepts and the material handling issues and the author identified through assessing the cells selected for the implementation of lean manufacturing in material handling operations. Review based on leanness assessment is presented in Vinodh & Vimal(2012). This paper presents the 30 criteria based leanness assessment methodology using fuzzy logic. Fuzzy logic has been used to overcome the disadvantages with scoring method such as impreciseness and ambiguity. In this paper, a conceptual model for lean assessment has been designed. Then the fuzzy lean index which indicates the lean level of the organization and fuzzy performance importance index which helps in identifying the obstacles for leanness has been analyzed. The results indicate that the model is capable of effectively assessing leanness and has practical significance. Taj (2005) presented a spreadsheet-based assessment tool to evaluate nine key areas of manufacturing namely, inventory team approach, processes, maintenance, layout/handling, suppliers, setups, quality, and scheduling/control. The results are then displayed in the score worksheet and finally a lean profile chart is created to display the current status of the plant and the gap from their specific lean targets. It is found from the results that lean assessment tool have revealed significant gap from the lean manufacturing target, and also identified opportunities for improvement. This paper provides a practical and easy way to use assessment tool to help manufacturing managers to make their manufacturing operations more productive. The literature survey presented in this section indicates that researcher have applied various tools for achieving leanness. However there is a lot of scope to implement this tool in other industrial sector for achieving leanness. In this background the scope of this paper is to quantify leanness in a textile industry.

III. METHODOLOGY

The study begins with the literature review on lean manufacturing. Based on literature review lean assessment tool has been developed which is divided in to two levels namely criteria and enablers. Then Anjaneya Cotton Mill (ACM) is selected as a case company. The questionnaire has been developed and responses were collected for the study. The leanness has been identified by scoring method and finally suitable suggestions were derived to overcome the leanness gap.

IV. CASE STUDY

4.1 About the case company

ACM is located in Davangere. In ACM yarn types of product are producted. The current turnover of ACM is 45 to 50 lakh. Presently 1500 employers are working in ACM.

4.2 Interviews

Leanness assessment was carried out using 13 criteria LM assessment tool in industry ACM. ACM is in the process of implementing LM strategy like 5s, kaizen, TPM, etc. these existed a need for organisation to measure leanness.

The case study was begun by exposing the developed 13 criteria LM assessment tool to General manager, Factory manager, Maintenance engineer of ACM. Subsequently questions concerning LM criteria were supplied to these personnel. These questions were so simple that respondent experienced no difficult in responses to these questions. As a sample, the questionnaire concerning LM criteria as shown in table 1. The marks allotted for each response of the questionnaire as shown in table 2.

Table 1: Questionnaire used to assess multifunctional team criteria

(I) Multifunctional team (MT):

1.	Cross training of workers is a regular feature?		
a.	Yes [ ]	b. Partially [ ]	c. No [ ]
2.	Empowerment of workers is enough?		
a.	Yes [ ]	b. Partially [ ]	c. No [ ]
3.	Projects are finalized with the consent of experts of various areas?		
a.	Yes [ ]	b. Partially [ ]	c. No [ ]
4.	Quality circle concept is utilized holistically?		
a.	Yes [ ]	b. Partially [ ]	c. No [ ]

Table 2: Marks allotted for each response in multifunctional team criteria

No.	CRITERIA	Q. No.	a	b	c
1	Multifunctional teams (MT)	1	15	8	0
		2	10	5	0
		3	10	5	0
		4	15	8	0

Converting responses into marks is illustrated here with the support of table 3. The first responder response against the questions 1-4 are shown in the table 3. By referring to the marks allotment given in the table 3 marks obtained against the responses of R1 (respondent 1) under LM criteria is computed. As shown in table 3 marks obtained is 23 out of 50. Similarly the computations of marks against the responses of all respondents against 13 criteria were carried out. The computed marks are present in table 4.

Table 3: Computation of marks obtained against the responses of R1 under LM criterion (multifunctional team)

LM criterian	Question no.	Responses of R1	Marks obtained
Multifunctional teams	1	b	8
	2	b	5
	3	a	10
	4	c	0
		Total	23

V. QUANTIFICATION OF LEANNESS

Table 4: Quantification of leanness under 13 criteria:

Leanness enablers	Leanness criteria	Maximum marks	Respondents			Average marks
			R_1	R_2	R_3	
Employees	Multifunctional teams	50	23	43	18	28
Technology	TPM	100	78	70	92	80
	Visual management	100	70	55	80	68.33
	SMED	100	55	100	80	78.33
	Automation	100	26	65	50	47
Manufacturing management	JIT	75	18	51	23	30.66
	Pull of raw material	25	8	20	16	14.66
	Supplier feedback	50	25	40	20	28.33
	Continuous improvement	150	84	120	56	86.66
	Elimination of waste	100	58	92	50	66.66
	Kanban	50	10	20	10	13.33
	Zero defects	50	15	40	20	25
Manufacturing strategy	Status of quality	50	22	50	22	31.33
					Total average marks	518.29
				Total leanness (TL)		0.5182 ≈51.83%

As shown in table 4 TL of ACM is 51.83%. The calculation of TL in ACM is given below

TL = total average marks/1000

TL = 518.26/1000

= 0.518 ≈ 51.83%

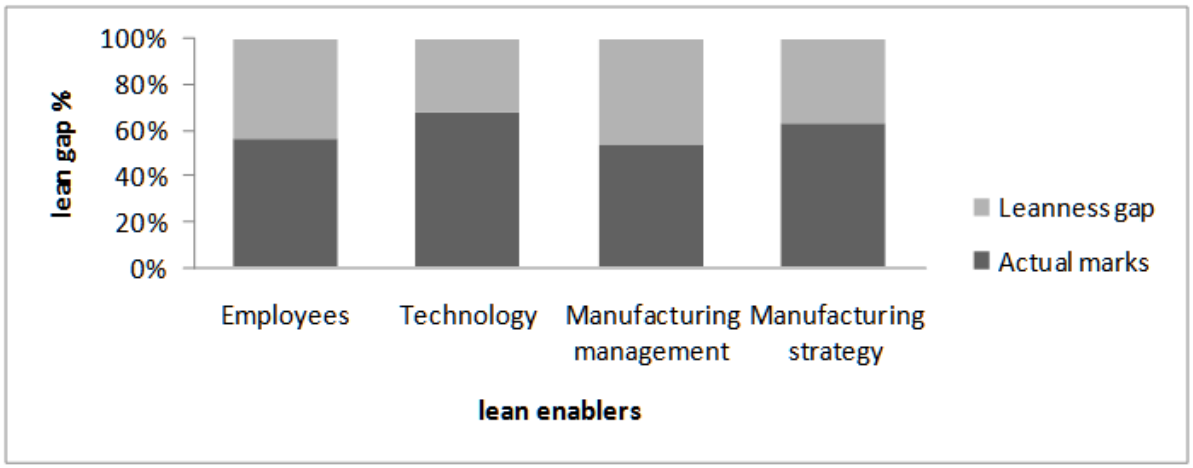

Figure 1: Gaps under LM enablers in percentage at ACM

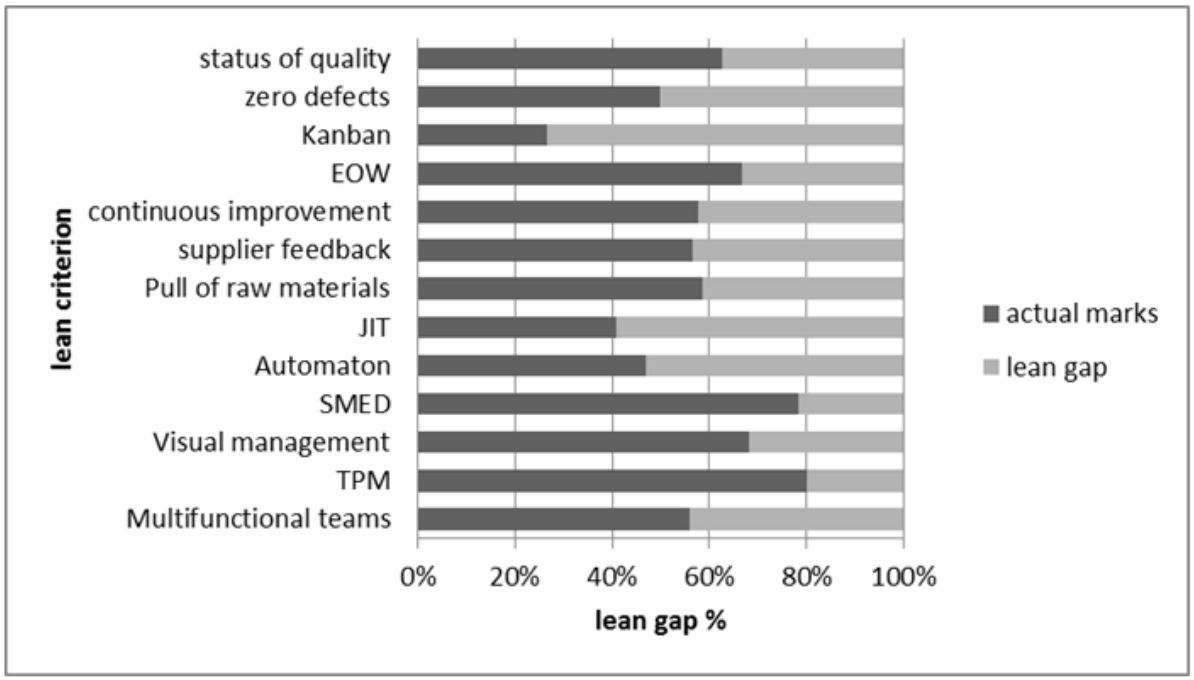

Figure 2: Gaps under LM criteria in percentage at ACM

As TL at ACM was found to be 0.518. It can be inferred that ACM has also potentials to increase its leanness level. In order to identify these potentials, the gap analysis of each LM criteria was carried out. Fig 1 shows the gaps between the actual and goal computed in terms of percentage under the four lean enablers. Fig 2 displays pictorially the gaps prevailing in each lean criterion in term of percentage. As shown in Fig 1 lean enablers such as employees and manufacturing management has more leanness gap compare to another two lean enablers. Among all criteria jit, supplier feedback, continuous improvement, kanban, automation, multi-functional teams are less than 60%. However to overcome leanness gap suitable suggestions are proposed to management.

Table 5: Identified the weak factors and suggested improvement methods

Serial No.	Weak factors	Improvement methods	Opinion/reaction of MD (in his own words)
1	Weak in Streamlining of processes	Adoption of value stream mapping	Yes we will try to adoption
2	Regular employer–employees meeting not conducted	Regular meeting will convey the company objective clearly	Always not possible
3	No job rotation system	Job rotation system make existing employee multi-skilled	Partially existed
4	Not conducting Education and cross-training employees	Regular conduction of training/ workshops will give knowledge of new manufacturing practices	Always not possible
5	Machines cannot accommodate varied jobs.	Incorporate advance technology	Lack of initial investment
6	Cross functional teams not fully successful.	Employ quality circle	ok
7	Long term manufacturing planning	Implement JIT production system	Try to implement
8	No inclusion of employee suggestion scheme	Reward scheme	ok
9	Not conducting training in continuous improvement methods and group technology	Regular conduction of training	Always not possible

VI. CONCLUSION

Despite this fact, not all companies have been able to fully acquire lean characteristics. These companies are in need of assessing the level of leanness at which they operate and the efforts that have to be exerted by them to acquire all LM capabilities. A simple and exhaustive lean assessment tool with 13 criteria has been contributed in this paper. Using this tool, leanness of ACM has been found. This quantification indicated that the TL of ACM is 51.8%. This would mean that the ACM has acquired 51.8% of LM capabilities. This quantification coincides with the assessment made at ACM. A 13 criteria LM assessment tool contribute percentage implement of lean in ACM. After that suggestions were proposed to overcome the leanness level. The company can use this leanness assessment procedure as a test kit for periodically evaluating the leanness level. This kind of leanness assessment helps to survive and grow in the competitive business environment by minimizing wastes.

ACKNOWLEDGEMENTS

The authors of this paper are thankful to the MD and employees of Anjaneya cotton mill Limited, Davangere for their permission and cooperation in conducting the case study reported in this paper.

REFERENCES

[1] S. Vinodh & K. E. K. Vimal, "Thirty criteria based leanness assessment using fuzzy logic approach", Int J Adv Manuf Technol (2012) Vol. 60, pp. 1185–1195

[2] Paul C. Hong, David D. Dobrzykowski, Mark A. Vonderembse, "Integration of supply chain IT and lean practices for mass customization Benchmarking of product and service focused manufactures", Benchmarking: An International Journal, (2010) Vol. 17, No: 4 pp. 561-592

[3] James C., Green, Jim Lee & Theodore A.Kozman "Managing Lean manufacturing in material handling operations", International Journal of Production Research, (2010) Vol.48, No:10, pp.2975-2993

[4] Stuart So, Hongyi Sun, "Supplier integration strategy for lean manufacturing adoption in electronic-enabled supply chains", Supply Chain Management: An international Journal , (2010) Vol.15, No: 6, pp. 474-487

[5] G. L. Hodge, K. G. Ross, J. A. Joines & K. Thoney "Adapting lean manufacturing principles to the textile industry" Production Planning & Control: The Management of Operations, (2011) Vol.22, No:3, pp.237-247.

[6] Todd A. Boyle, Maike Scherrer-Rathje, Ian Stuart, "Learning to be lean: the influence of external information sources in lean improvements", Journal of Manufacturing Technology Management, (2011) Vol. 22, No: 5, pp. 587-603

[7] Shahram Taj, "Applying lean assessment tools in Chinese hi-tech industries", Management Decision (2005) Vol. 43, No: 4, pp. 628-643

[8] Juan A. Marin-Garcia, Paula Carneiro, "Questionnaire validation to measure the application degree of alternative tools to mass production" International Journal of Management Science and Engineering Management, (2010) Vol. 5, No: 4, pp.268-277

[9] Gulshan Chauhan, T. P. Singh, "Measuring parameters of lean manufacturing realization", Measuring Business Excellence, (2012) Vol. 16, No: 3, pp. 57- 71.

ISSN (e): 2250 – 3005 || Vol, 04 || Issue, 4 || April – 2014 ||
International Journal of Computational Engineering Research (IJCER)

Estimating the Quality of Concrete Bridge Girder Using Ultrasonic Pulse Velocity Test

Himanshu Jaggerwal[#1], Yogesh Bajpai[#2]

[#1]*Student- M.Tech (Structural Engineering), Civil Engineering Department, GGITS Jabalpur M.P, India*
[#2]*Associate Professor- Civil Engineering Department, GGITS Jabalpur M.P, India*

ABSTRACT:

This study estimates the quality of concrete bridge girder, an attempt is also made to increase the accuracy of calculating the strength, using the nondestructive test (NDT) Ultrasonic pulse velocity tests. The aim of the present paper is to check the accuracy for assessing concrete bridges girder. This paper reviews various NDT methods available and presents a case study related to the strength evaluation of existing bridge pier. The assessment involves the Ultrasonic pulse velocity tests. Even though there are many methods for Non Destructive Test (NDT) but every method have it own boundaries and which mean the method cannot afford an accurate and consistence result for difference cases and to detect different defect. This paper is an attempt to capture the most current ideas for a very specific application of NDT: determining the condition of reinforced concrete bridges overall and bridge girders, in particular. To this end, attention is given to why NDT is needed and what aspects of concrete condition can be addressed with NDT. Some NDT methodologies that are, or may soon be, promising for concrete applications are discussed. Case studies are presented to demonstrate how NDT can be applied to concrete bridge girders and proposals are made for future areas of study and development. The use of nondestructive testing methods can help reduce the backlog of deficient bridges in two ways. First, these techniques will allow inspectors to get a more accurate view of the condition of a bridge. The second way by which NDT can help is by allowing inspectors to locate damage earlier. The data obtained from each test has been evaluated and the accurate and precise device was determined. From this research, the most accurate NDT method is Ultrasonic Pulse Velocity.

KEYWORDS: *Non Destructive Testing; Bridge Pier; Case Study.*

I. INTRODUCTION

It is often necessary to test concrete structures after the concrete has hardened to determine whether the structure is suitable for its designed use. Ideally such testing should be done without damaging the concrete. The tests available for testing concrete range from the completely non-destructive, where there is no damage to the concrete, through those where the concrete surface is slightly damaged, to partially destructive tests, such as core tests and pullout and pull off tests, where the surface has to be repaired after the test. The range of properties that can be assessed using non-destructive tests and partially destructive tests is quite large and includes such fundamental parameters as density, elastic modulus and strength as well as surface hardness and surface absorption, and reinforcement location, size and distance from the surface. In some cases it is also possible to check the quality of workmanship and structural integrity by the ability to detect voids, cracking and delamination. Non-destructive testing can be applied to both old and new structures. For new structures, the principal applications are likely to be for quality control or the resolution of doubts about the quality of materials or construction. The testing of existing structures is usually related to an assessment of structural integrity or adequacy. In either case, if destructive testing alone is used, for instance, by removing cores for compression testing, the cost of coring and testing may only allow a relatively small number of tests to be carried out on a large structure which may be misleading. Non-destructive testing can be used in those situations as a preliminary to subsequent coring.

Typical situations where non-destructive testing may be useful are, as follows:

1. Quality control of pre-cast units or construction *in situ.*
2. Removing uncertainties about the acceptability of the material supplied owing to apparent non-compliance with specification.
3. Confirming or negating doubt concerning the workmanship involved in batching., mixing, placing, compacting or curing of concrete.
4. Monitoring of strength development in relation to formwork removal, cessation of curing, prestressing, load application or similar purpose.
5. Location and determination of the extent of cracks, voids, honeycombing and similar defects within a concrete structure.
6. Determining the concrete uniformity, possibly preliminary to core cutting, load testing or other more expensive or disruptive tests.
7. Determining the position, quantity or condition of reinforcement.
8. Increasing the confidence level of a smaller number of destructive tests.
9. Determining the extent of concrete variability in order to help in the selection of sample locations representative of the quality to be assessed.
10. Confirming or locating suspected deterioration of concrete resulting from such factors as overloading, fatigue, external or internal chemical attack or change, fire, explosion, environmental effects.

II. BASIC METHODS FOR NDT OF CONCRETE STRUCTURES

The following methods, with some typical applications, have been used for the NDT of concrete:

1. Visual inspection, which is an essential precursor to any intended non-destructive test. An experienced civil or structural engineer may be able to establish the possible causes of damage to a concrete structure and hence identify which of the various NDT methods available could be most useful for any further investigation of the problem.
2. Half-cell electrical potential method, used to detect the corrosion potential of reinforcing bars in concrete.
3. Schmidt/rebound hammer test, used to evaluate the surface hardness of concrete.
4. Carbonation depth measurement test, used to determine whether moisture has reached the depth of the reinforcing bars and hence corrosion may be occurring.
5. Permeability test, used to measure the flow of water through the concrete.
6. Penetration resistance or Windsor probe test, used to measure the surface hardness and hence the strength of the surface and near surface layers of the concrete.
7. Cover meter testing, used to measure the distance of steel reinforcing bars beneath the surface of the concrete and also possibly to measure the diameter of the reinforcing bars.
8. Radiographic testing, used to detect voids in the concrete and the position of stressing ducts.
9. Ultrasonic pulse velocity testing, mainly used to measure the sound velocity of the concrete and hence the compressive strength of the concrete.
10. Sonic methods using an instrumented hammer providing both sonic echo and transmission methods.
11. Tomography modeling which uses the data from ultrasonic transmission tests in two or more directions to detect voids in concrete.
12. Impact echo testing, used to detect voids, delamination and other anomalies in concrete.
13. Ground penetrating radar or impulse radar testing, used to detect the position of reinforcing bars or stressing ducts.
14. Infrared thermography, used to detect voids, delamination and other anomalies in concrete and also detect water entry points in buildings.

2.1 Ultrasonic Pulse Velocity:-

This method is explained in IS 13311 (part 1):1992, which involves measurement of the time of travel of electronically generated mechanical pulses through the concrete. The ultrasonic pulse velocity method could be used to establish:

a) Homogeneity of concrete
b) Presence of cracks & voids
c) Changes in structures of the concrete
d) The quality of the concrete in relation to standard requirement
e) The values of dynamic elastic modulus of the concrete

The principle behind the Ultrasonic Pulse Velocity is that the pulses are generated by an electro-acoustical transducer, when pulse is induced into the concrete from a transducer, it undergoes multiple reflections at the boundaries of different material phase within the concrete. A complex system of waves is developed which include longitudinal, shear and surface waves. The receiving transducer detects the onset of longitudinal waves which is the fastest. Because the velocity of the pulses is independent of the geometry of the material through which they pass and depends only on its elastic properties. When quality of concrete in terms of density, homogeneity and uniformity is good, higher velocities are obtained. In case of poorer quality of concrete lower velocities are obtained.

The first waves to reach the receiving transducer are the longitudinal waves, which are converted into an electrical signal by a second transducer. Electronic timing circuits enable the transit time T of the pulse to be measured.

Longitudinal pulse velocity (in km/s or m/s) is given by:

$V = L/T$

(1)

Where

V is the longitudinal pulse velocity,

L is the path length,

T is the time taken by the pulse to traverse that length.

Pulse velocity measurements made on concrete structures may be used for quality control purposes. In comparison with mechanical tests on control samples such as cubes or cylinders, pulse velocity measurements have the advantage that they relate directly to the concrete in the structure rather than to samples, which may not be always truly representative of the concrete in situ. The typical classification of the quality of concrete on the basis of Ultrasonic pulse velocity is given the Table.1

Table No.1.Classification of the Quality of Concrete on the Basis of Pulse Velocity

Longitudinal pulse velocity		Quality of concrete
Km/s	Ft/s	
>4.5	>15	Excellent
3.5-4.5	12-15	Good
3.0-3.5	10-12	Medium
2.0-3.0	7-10	Poor
< 2.0	<7	Very poor

Factors affecting the pulse velocity:-

i. Surface condition and moisture content

ii. Temperature of concrete

iii. Micro cracks in concrete

iv. Water cement ratio

v. Age of concrete

vi. Presence of steel reinforcement

vii. Type of aggregate

III. CASE STUDY

3.1. General Information:-

The following case studies have been selected to demonstrate the effectiveness for NDT for detecting anomalies in reinforced concrete structures. While the cases do not all deal directly with concrete bridge girders, the methods demonstrated all can be applied readily to girders.

The NDT is applied on New Aatish Market Metro (Phase-I-East West Corridor) at Jaipur Rajasthan. The Jaipur Metro Rail Corporation has entered into an agreement (05.08.2010) with the Delhi Metro Rail Corporation (DMRC) for development of Phase-I-A from Mansarovar to Chandpole on 'deposit work' basis covering a length of 9.718 kms and Phase-I-B (Chandpole to Badi Chaupar) covering a length of 2.349 kms. The plan of New Aatish Market Metro Jaipur shown in Figure 1, below, is a reinforced concrete box girder bridge, originally constructed in 2011. It is oriented East West Corridor. This Report is prepared as study about the New Aatish Market Metro Jaipur under Phase-I-East West Corridor. The superstructure of a large part of the viaduct comprises of simply supported spans. However at major crossing over or along existing bridge, special steel or continuous unit will be provided. The standard spans c/c of piers of simply supported spans constructed by precast segmental construction technique has been proposed as 28.0m. The other spans (c/c of pier) comprises of 31.0 m, 25.0 m, 22.0 m, 19.0 m & 16.0 m, which shall be made by removing/adding usual segments of 3.0 m each from the centre of the span. The pier segment will be finalized based on simply supported span of 31.0m and the same will be also kept for all simply supported standard span. The viaduct superstructure will be supported on single cast-in-place RC pier. The shape of the pier follows the flow of forces. For the standard spans, the pier gradually widens at the top to support the bearing under the box webs. The size of pier is found to be 1.6 m diameter of circular shape and height of pier is found to be 5.5 m (from base to cap bottom).

3.2. Scope of work:-

The quality of the concrete was to be evaluated by performing Non-destructive Testing. In order to assess the quality of concrete, the following methods of testing were employed:

(i)Ultrasonic Pulse Velocity test as per IS: 13311-1992 (Part 1).

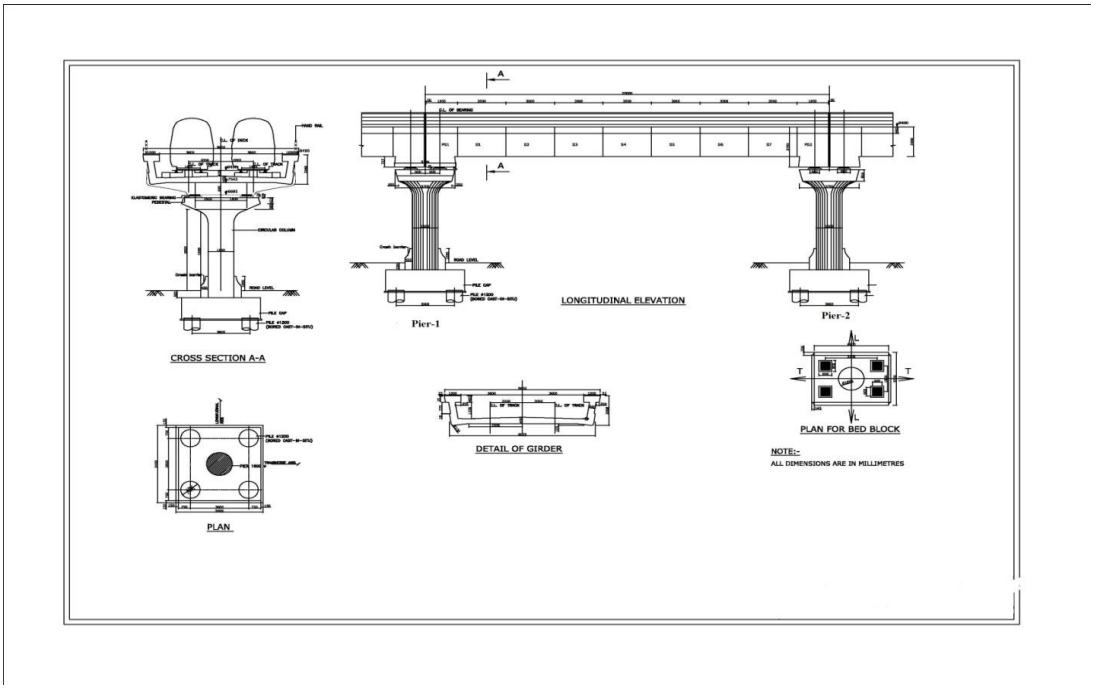

Figure 1: Plan of bridge

3.3. Analysis of Test Results:-

3.3.1. Ultrasonic Pulse Velocity Test:-

Diameter of Pier =1600mm, Height of Pier =5500mm.

Table 2: Ultrasonic pulse velocity test results

S.No.	Location	Path length (L)mm	Transit Time (T) µs	Velocity (V=L/T)km/s	Compressive Strength (f_{ck}=N/mm^2)	Arrangement
1	Pier-1.1	1273	295	4.320	46	Same Face
2	1.2	1800	462	3.90	51	Same Face
3	1.3	1273	287	4.44	61	Same Face
4	1.4	688	148	4.65	65	Same Face
5	1.5	1273	268	4.75	53	Same Face
6			**Average Pier-1**	**4.41**	**55**	
7	Pier-2.1	1663	350	4.75	67	Same Face
8	2.2	1800	371	4.85	64	Same Face
9	2.3	1663	347	4.79	62	Same Face
10	2.4	1273	266	4.79	69	Same Face
11	2.5	688	146	4.71	61	Same Face
12			**Average Pier-2**	**4.78**	**65**	
			Total Average	**4.59**	**59.5**	

Note: µs = Micro Seconds.

Average Ultrasonic Pulse (USP) Wave Velocity = (4.41+4.78)/2 = 4.59 km/sec.

3.3.2 Results:-

The Ultrasonic pulse velocity represents the quality of concrete in terms of uniformity, incidence or absence of flaws, cracks and segregation, the level of workmanship employed in concrete structure. As per the guidelines laid in IS-13311-Part 1-1992, since the USP velocity is greater than 4.5 km/sec, the concrete quality may be categorized as excellent.

3.3.3 Correlation Between compressive Strength of concrete & NDT Parameters viz. Ultrasonic Pulse Velocity test:-

In an attempt to develop correlation between compressive strength & Ultrasonic Pulse Velocity test were casted of same grades and cured and left to meet with the site conditions. A total of 2 piers each of M40 Grades concrete were obtained for testing in the sites. As per IS: 13311-1992 (part 1), the piers were tested by Ultrasonic Pulse Velocity test by holding them in compression testing machine. Ultrasonic Pulse Velocity test for same face were obtained. About 5 readings on each of piers were noted. Values of Ultrasonic Pulse Velocity test and compressive strengths of the piers are presented in table 2. Based on the procedure outlined in Is-13311-1992 (part 1) relationships between compressive strength and Rebound numbers have been developed using regression shown in figures 2 to 3. From the relevant correlation curves, most likely compressive strength of concrete has been obtained after allowing for necessary corrections.

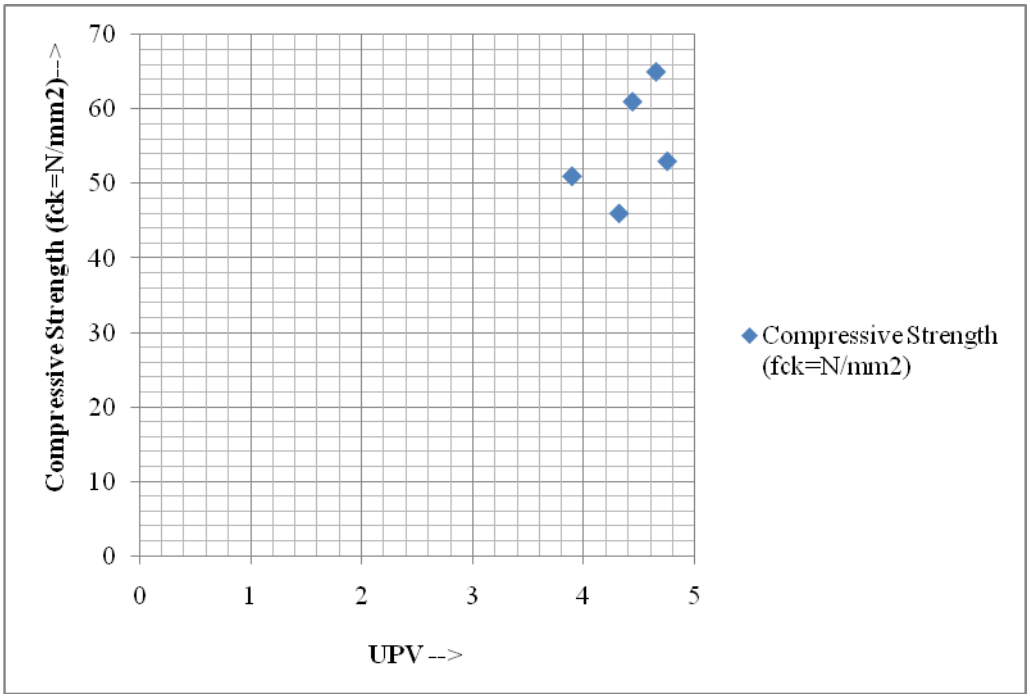

Figure 2: Correlation between Compressive Strength of Concrete & Ultrasonic Pulse Velocity Test-Pier-1

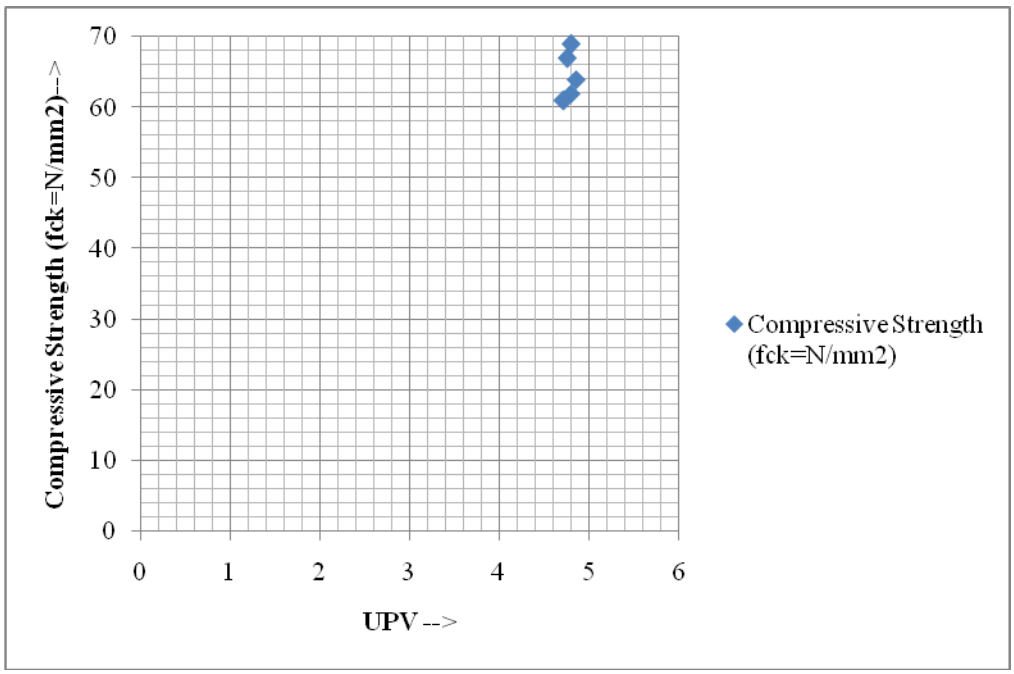

Figure 3: Correlation Between Compressive Strength Of Concrete & Ultrasonic Pulse Velocity Test-Pier-2

Using these relationships, the compressive strengths of concrete have been evaluated from the observations taken on the actual structure.

3.3.4 Compressive Strength from Ultrasonic Pulse Velocity Test:

Bridge pier-1 and pier-2, Grade adopted M40 Average value of Ultrasonic Pulse Velocity Test with same face pier-1 =4.41, pier-2=4.78.

From the correlation developed between Ultrasonic Pulse Velocity Test and compressive strength, compressive strength was obtained as pier-1= 55 MPa. , pier-2=65 MPa.

Observations on concrete on both pier. The average value of USPV for same face of both concrete pier was obtained as 4.59 km/s which as per IS:13311 (part 1) can be considered as Excellent quality concrete. From the correlation developed between USPV and compressive strength, compressive strength was obtained as 59.5 MPa.

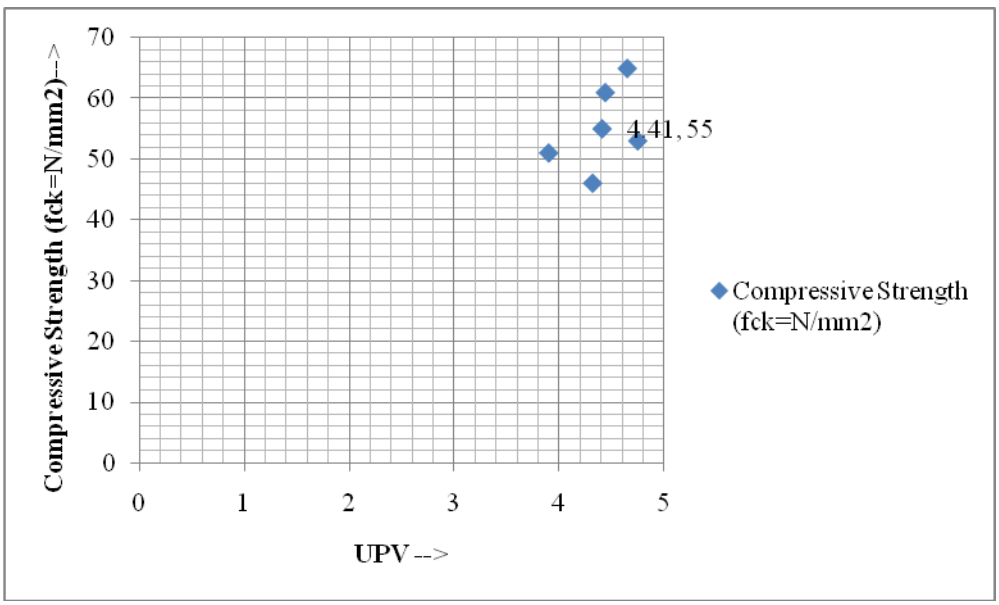

Figure 4: Correlation between Compressive Strength of Concrete & Average Ultrasonic Pulse Velocity Test-Pier-1

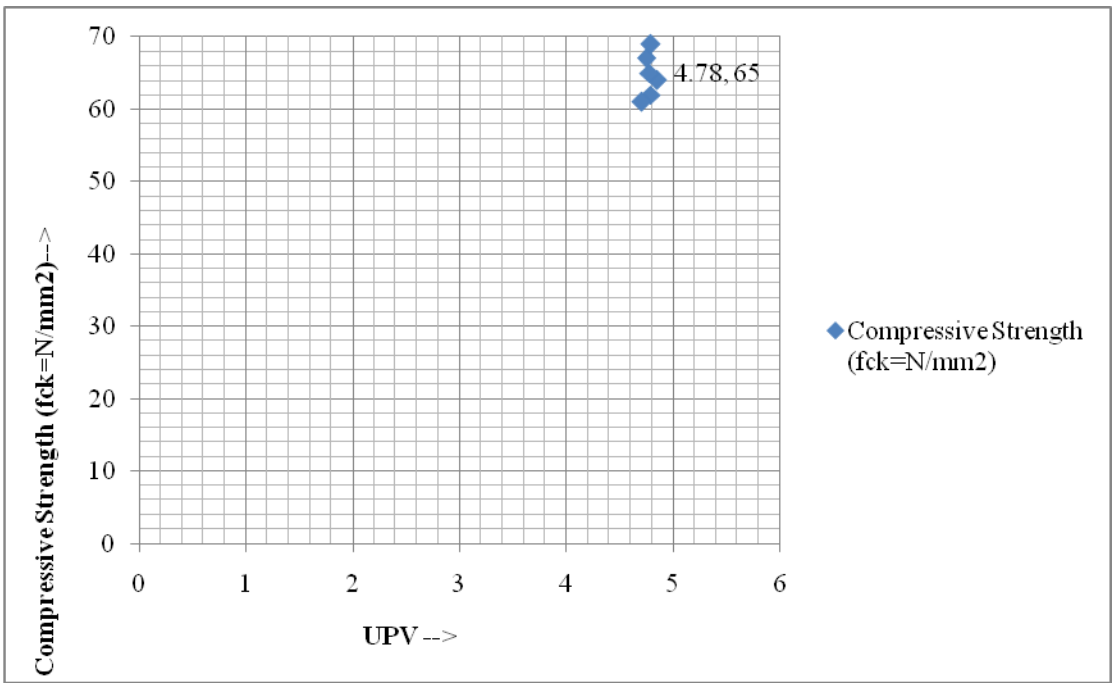

Figure 5: Correlation between Compressive Strength of Concrete & Average Ultrasonic Pulse Velocity Test-Pier-2

IV. CONCLUSION

NDT methods such as UPV very useful for predicting the service life of the structures and deterioration of the structures provided the periodical monitoring of the same member of the structures is being carried out. Since the concrete is heterogeneous and tests are affected by various factors such as age of the concrete, carbonation depth, reinforcement, cracks and voids inside the concrete, a combined test helps for assessment the strength and durability. The experimental investigation showed that a good co-relation exists between compressive strength and ultrasonic pulse velocity. Nevertheless rebound hammer should be used alone to determine the compressive strength of the structures. Ultrasonic Pulse velocity is the ideal NDT method to predict the deterioration in the structures and to determine the service life of the structures.

V. RESULTS

From the experimental data, the following conclusions can be drawn:-

1. The average of pulse velocity is 4.59 km/s far from the excellent category in concrete quality.
2. Overall of the concrete structure can be categorized as wonderful because the strength is Excellent.

REFERENCES

[1] IS 13311 (Part-1)-(1992). Methods of Non Destructive Testing of Concrete: Part-1: Ultrasonic Pulse Velocity.
[2] IS 456 2000. Code of Practice for Plain and Reinforced Concrete.
[3] Shetty.MS (2010).Concrete Technology.S.Chand& Company, New Delhi.

ISSN (e): 2250 – 3005 || Vol, 04 || Issue, 4 || April – 2014 ||
International Journal of Computational Engineering Research (IJCER)

Assessment of Characteristic Compressive Strength in Concrete Bridge Girders Using Rebound Hammer Test

Himanshu Jaggerwal[#1], Yogesh Bajpai[#2]
[#1]*Student- M.Tech (Structural Engineering), Civil Engineering Department, GGITS Jabalpur M.P, India*
[#2]*Associate Professor- Civil Engineering Department, GGITS Jabalpur M.P, India*

ABSTRACT:
The aim of the present paper is to check the compressive strength for assessing concrete bridges girder. This paper reviews various NDT methods available and presents a case study related to the evaluation of existing bridge pier. The assessment involves the Rebound hammer tests. Even though there are many methods for Non Destructive Test (NDT) but every method have it own boundaries and which mean the method cannot afford an accurate and consistence result for difference cases and to detect different defect. This paper is an attempt to capture the most current ideas for a very specific application of NDT: determining the condition of reinforced concrete bridges overall and bridge girders, in particular. To this end, attention is given to why NDT is needed and what aspects of concrete condition can be addressed with NDT. Some NDT methodologies that are, or may soon be, promising for concrete applications are discussed. Case studies are presented to demonstrate how NDT can be applied to concrete bridge girders and proposals are made for future areas of study and development. The use of non-destructive testing methods can help reduce the backlog of deficient bridges in two ways. First, these techniques will allow inspectors to get a more accurate view of the condition of a bridge. The second way by which NDT can help is by allowing inspectors to locate damage earlier. The data obtained from each test has been evaluated and the accurate and precise device was determined.

KEYWORDS: *Non Destructive Testing; Bridge Pier; Case Study.*

I. INTRODUCTION

It is often necessary to test concrete structures after the concrete has hardened to determine whether the structure is suitable for its designed use. Ideally such testing should be done without damaging the concrete. The tests available for testing concrete range from the completely non-destructive, where there is no damage to the concrete, through those where the concrete surface is slightly damaged, to partially destructive tests, such as core tests and pullout and pull off tests, where the surface has to be repaired after the test. The range of properties that can be assessed using non-destructive tests and partially destructive tests is quite large and includes such fundamental parameters as density, elastic modulus and strength as well as surface hardness and surface absorption, and reinforcement location, size and distance from the surface. In some cases it is also possible to check the quality of workmanship and structural integrity by the ability to detect voids, cracking and delamination. Non-destructive testing can be applied to both old and new structures. For new structures, the principal applications are likely to be for quality control or the resolution of doubts about the quality of materials or construction. The testing of existing structures is usually related to an assessment of structural integrity or adequacy. In either case, if destructive testing alone is used, for instance, by removing cores for compression testing, the cost of coring and testing may only allow a relatively small number of tests to be carried out on a large structure which may be misleading. Non-destructive testing can be used in those situations as a preliminary to subsequent coring.

Typical situations where non-destructive testing may be useful are, as follows:

1. Quality control of pre-cast units or construction *in situ.*
2. Removing uncertainties about the acceptability of the material supplied owing to apparent non-compliance with specification.
3. Confirming or negating doubt concerning the workmanship involved in batching., mixing, placing, compacting or curing of concrete.
4. Monitoring of strength development in relation to formwork removal, cessation of curing, prestressing, load application or similar purpose.
5. Location and determination of the extent of cracks, voids, honeycombing and similar defects within a concrete structure.
6. Determining the concrete uniformity, possibly preliminary to core cutting, load testing or other more expensive or disruptive tests.
7. Determining the position, quantity or condition of reinforcement.
8. Increasing the confidence level of a smaller number of destructive tests.
9. Determining the extent of concrete variability in order to help in the selection of sample locations representative of the quality to be assessed.
10. Confirming or locating suspected deterioration of concrete resulting from such factors as overloading, fatigue, external or internal chemical attack or change, fire, explosion, environmental effects.

II. BASIC METHODS FOR NDT OF CONCRETE STRUCTURES

The following methods, with some typical applications, have been used for the NDT of concrete:

1. Visual inspection, which is an essential precursor to any intended non-destructive test. An experienced civil or structural engineer may be able to establish the possible causes of damage to a concrete structure and hence identify which of the various NDT methods available could be most useful for any further investigation of the problem.
2. Half-cell electrical potential method, used to detect the corrosion potential of reinforcing bars in concrete.
3. Schmidt/rebound hammer test, used to evaluate the surface hardness of concrete.
4. Carbonation depth measurement test, used to determine whether moisture has reached the depth of the reinforcing bars and hence corrosion may be occurring.
5. Permeability test, used to measure the flow of water through the concrete.
6. Penetration resistance or Windsor probe test, used to measure the surface hardness and hence the strength of the surface and near surface layers of the concrete.
7. Cover meter testing, used to measure the distance of steel reinforcing bars beneath the surface of the concrete and also possibly to measure the diameter of the reinforcing bars.
8. Radiographic testing, used to detect voids in the concrete and the position of stressing ducts.
9. Ultrasonic pulse velocity testing, mainly used to measure the sound velocity of the concrete and hence the compressive strength of the concrete.
10. Sonic methods using an instrumented hammer providing both sonic echo and transmission methods.
11. Tomography modeling which uses the data from ultrasonic transmission tests in two or more directions to detect voids in concrete.
12. Impact echo testing, used to detect voids, delamination and other anomalies in concrete.
13. Ground penetrating radar or impulse radar testing, used to detect the position of reinforcing bars or stressing ducts.
14. Infrared thermography, used to detect voids, delamination and other anomalies in concrete and also detect water entry points in buildings.

2.1 Rebound Hammer Method:-

This method is explained in IS: 13311 (part2):1992.

Principle of test: When the plunger of the rebound test hammer is pressed against the surface of the concrete the spring controlled mass rebounds and the extent of such rebounds depends upon surface hardness of the concrete. The rebound is then be related to the compressive strength of concrete.

Rebound hammer is an equipment to determine the strength of material such as concrete and rock. Its measures the rebound of a spring loaded mass impacting the surface of the material. The equipment will hit the surface of material and it's dependent on the hardness of the material. When conducting the test, the equipment should be place perpendicular to the surface. The surface must clean, clear, smooth, flat and not moist.

Factors affecting the Rebound Number:-
i. Type of cement.
ii. Type of aggregate.
iii. Concrete moisture condition.
iv. Curing and age of concrete.
v. Presence of surface carbonation.

III. CASE STUDY

3.1. General Information:-

The following case studies have been selected to demonstrate the effectiveness for NDT for detecting anomalies in reinforced concrete structures. While the cases do not all deal directly with concrete bridge girders, the methods demonstrated all can be applied readily to girders.

The NDT is applied on New Aatish Market Metro (Phase-I-East West Corridor) at Jaipur Rajasthan. The Jaipur Metro Rail Corporation has entered into an agreement (05.08.2010) with the Delhi Metro Rail Corporation (DMRC) for development of Phase-I-A from Mansarovar to Chandpole on 'deposit work' basis covering a length of 9.718 kms and Phase-I-B (Chandpole to Badi Chaupar) covering a length of 2.349 kms. The plan of New Aatish Market Metro Jaipur shown in Figure 1, below, is a reinforced concrete box girder bridge, originally constructed in 2011. It is oriented East West Corridor. This Report is prepared as study about the New Aatish Market Metro Jaipur under Phase-I-East West Corridor. The superstructure of a large part of the viaduct comprises of simply supported spans. However at major crossing over or along existing bridge, special steel or continuous unit will be provided. The standard spans c/c of piers of simply supported spans constructed by precast segmental construction technique has been proposed as 28.0m. The other spans (c/c of pier) comprises of 31.0 m, 25.0 m, 22.0 m, 19.0 m & 16.0 m, which shall be made by removing/adding usual segments of 3.0 m each from the centre of the span. The pier segment will be finalized based on simply supported span of 31.0m and the same will be also kept for all simply supported standard span. The viaduct superstructure will be supported on single cast-in-place RC pier. The shape of the pier follows the flow of forces. For the standard spans, the pier gradually widens at the top to support the bearing under the box webs. The size of pier is found to be 1.6 m diameter of circular shape and height of pier is found to be 5.5 m (from base to cap bottom).

3.2. Scope of work:-

The quality of the concrete was to be evaluated by performing Non-destructive Testing. In order to assess the quality of concrete, the following methods of testing were employed:

(i) Rebound Hammer test as per IS: 13311-1992 (Part 2).

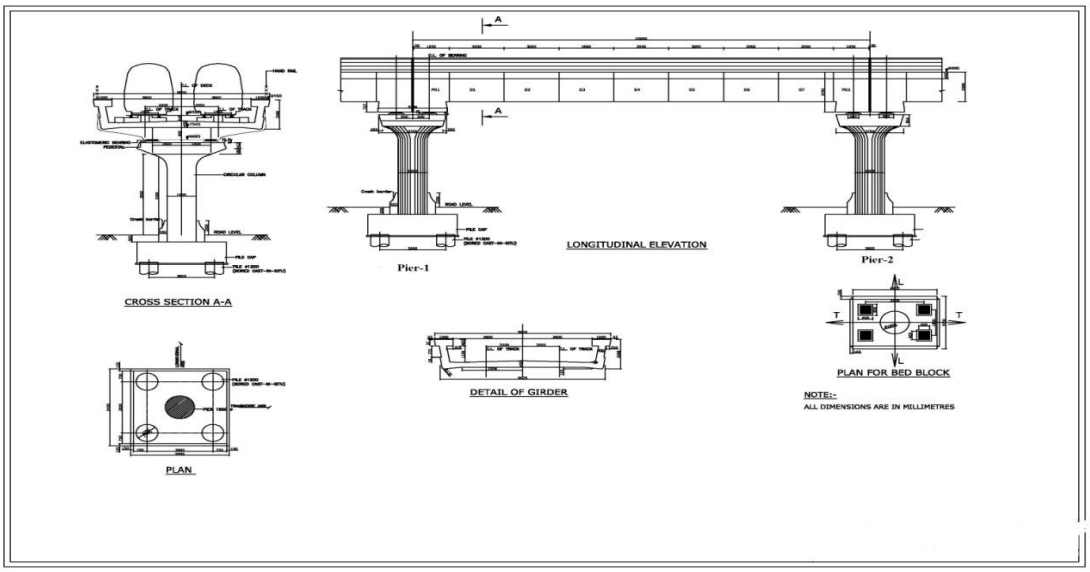

Figure 1: Plan of bridge

3.3. Analysis of Test Results:-

3.3.1. Rebound Hammer Test:-

Table 2: Rebound Hammer Test Results

S.No.	Location		Rebound value (R)	Compressive Strength (f_{ck}=N/mm^2)	Direction
1	Pier-1.1		43	46	←(Held Horizontal)
2	1.2		46	51	←(Held Horizontal)
3	1.3		51	61	←(Held Horizontal)
4	1.4		53	65	←(Held Horizontal)
5	1.5		47	53	←(Held Horizontal)
6		**Average Pier-1**	**48**	**55**	
7	Pier-2.1		54	67	←(Held Horizontal)
8	2.2		53	64	←(Held Horizontal)
9	2.3		52	62	←(Held Horizontal)
10	2.4		55	69	←(Held Horizontal)
11	2.5		51	61	←(Held Horizontal)
12		**Average Pier-2**	**53**	**65**	
		Total Average	**50.5**	**59.5**	

Combined Average Rebound Value = (48+53)/2=50.5
Combined Average Compressive Strength = (55+65)/2=59.5 MPa

3.3.2 Results:-

Compressive Strength of Concrete (as interpreted from the Rebound value) = 59.5 MPa**.** As per the guidelines laid in IS-13311-Part 2-1992, Since the compressive strength (i.e 59.5 MPa) is above 59 MPa, it can be inferred that the concrete used M40 grade concrete.

3.3.3 Correlation Between Compressive Strength of concrete & NDT Parameters viz. Rebound Index:-

In an attempt to develop correlation between compressive strength & Rebound number were casted of same grades and cured and left to meet with the site conditions. A total of 2 piers each of M40 Grades concrete were obtained for testing in the sites. As per IS:13311-1992 (part 2), the piers were tested by Rebound hammer by holding them in compression testing machine. Rebound Number or indices for horizontal position were obtained. About 5 readings on each of piers were noted. Values of Rebound indices and compressive strengths of the piers are presented in table 2. Based on the procedure outlined in IS-13311-1992 (part 2) relationships between compressive strength and Rebound numbers have been developed using regression shown in figures 2 to 3. From the relevant correlation curves, most likely compressive strength of concrete has been obtained after allowing for necessary corrections.

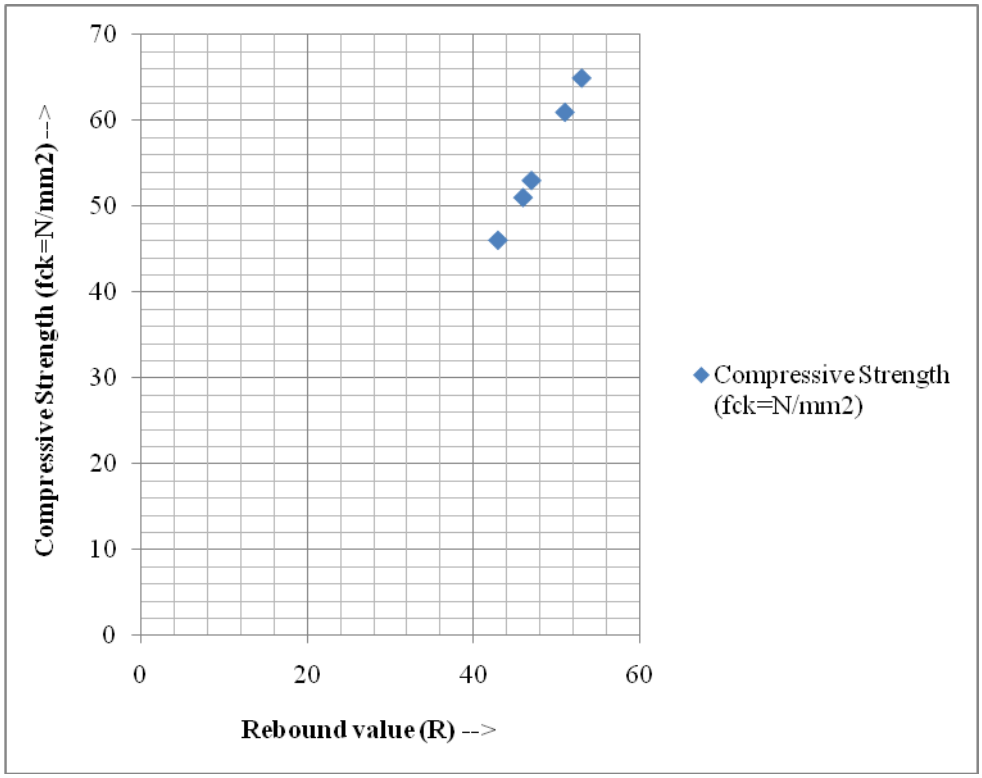

Figure 2: correlation between compressive strength & Rebound number –pier-1

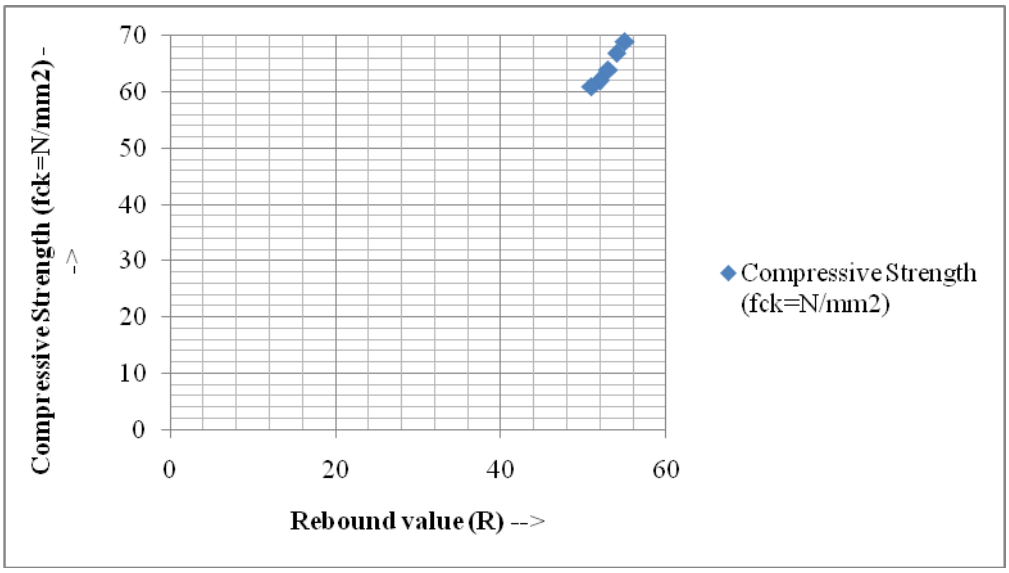

Figure 3: correlation between compressive strength & Rebound number –pier-2

Using these relationships, the compressive strengths of concrete have been evaluated from the observations taken on the actual structure.

3.3.4 Compressive Strength from Rebound indices

Bridge pier-1 and pier-2, Grade adopted M40 Average value of Rebound number with hammer held horizontal pier-1 = 48(←), pier-2=53(←).

From the correlation developed between rebound numbers and compressive strength, compressive strength was obtained as pier-1= 55 MPa. , pier-2=65 MPa.

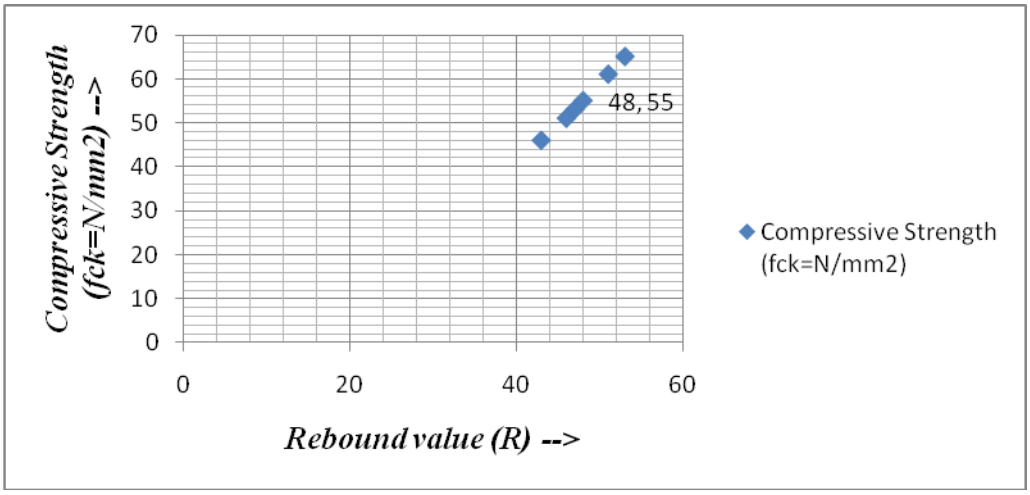

Figure 4: correlation between compressive strength & Average Rebound number –pier-1

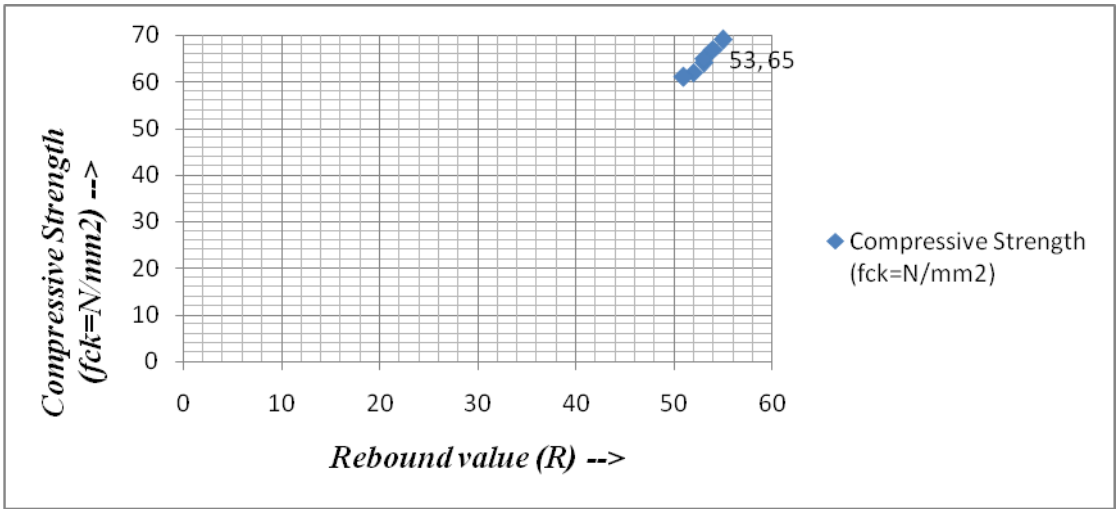

Figure 5: correlation between compressive strength & Average Rebound number –pier-2

IV. CONCLUSION

NDT methods such as Rebound hammer becomes very useful for compressive strength of the structures and structures provided the periodical monitoring of the same member of the structures is being carried out. Since the concrete is heterogeneous and tests are affected by various factors such as age of the concrete, carbonation depth, reinforcement, cracks and voids inside the concrete, a combined test helps for assessment the strength and durability. The experimental investigation showed that a good co-relation exists between compressive strength and rebound hammer. Nevertheless rebound hammer should be used alone to determine the compressive strength of the structures.

V. RESULTS

From the experimental data, the following conclusions can be drawn:-

1. The average of compressive strength on both pier is 59.5 MPa.

REFERENCES

[1] IS 13311 (Part-2) (1992) Methods of Non Destructive Testing of Concrete: Part-2: Rebound Hammer.
[2] IS 456 2000. Code of Practice for Plain and Reinforced Concrete.
[3] Shetty.MS (2010).Concrete Technology.S.Chand& Company, New Delhi.
[4] Guidebook on non-destructive testing of concrete structure, International Atomic Energy Agency, Vienna, 2002.

ISSN (e): 2250 – 3005 || Vol, 04 || Issue, 4 || April – 2014 ||
International Journal of Computational Engineering Research (IJCER)

Time Series Prediction Based on Event Driven Business Process Management

Eva Zámečníková[1], Jitka Kreslíková[2]
1 Ph.D. student at FIT BUT, Brno, Czech Republic
2 Associate professor at FIT BUT, Brno, Czech Republic

Abstract:
In this paper we would like to focus on time series prediction for building trading systems based on unification of the seemingly antagonistic concepts of Complex Events Processing (CEP) and discrete, legacy business logic. In the realm of the high frequency market-making trading systems, the incoming stream of data from multiple asset sources and venues shall be processed primarily by a real-time CEP engine till the point when the statistical characteristics of the continuous results cross into the "fat-tail" distribution region, when a set of stringent risk-management business rules kick in.

Keywords: *Business Rules, Complex Event Processing, Event-Driven Architecture, Financial Markets, High Frequency Data, Prediction, Trading.*

I. INTRODUCTION

Financial markets generate high frequency data in large quantities. The smallest data unit used for analysis is called a *tick*. In most cases, the incoming data is inhomogeneous and contains outliers and noise. For processing of this data, complex-event processing (CEP) platform can be used. Today's systems are trying to achieve the ability for the timely reaction to the occurrence of real-world situations. In the system environment this property has become a fundamental requirement. This applies to many different applications including fully automated financial trading and time series prediction. There is no ideal CEP architecture - the optimal solution requires a number of technologies, e.g. distributed computing, service oriented architecture (SOA) and high speed processing.

In the following sections we will describe both approaches – complex-event processing as business process management (BPM) and we will point out their main advantages considering the properties which can be useful for high frequency data processing. Both platforms use events and rules for data processing. Although it's possible to only focus on CEP or, alternatively, only BPM for data processing, the better way is to work with "hybrid" architecture which uses the benefits of both platforms. The systems complement each other – CEP is better for preprocessing and correlation of high volume input data and on the other hand BPM can generate automated decisions based on incoming data.

The approach of using the advantages of discrete event processing and business process management is also mentioned in [1], where the designed systems are called "Event-Driven Business Process Management". The term "Event Driven Business Process Management" was first used in June 2003 by Bruce Silver. The term was understood as a synthesis of workflow and Enterprise Application Integration (EAI). A concept of event processing and real-time business activity management (BAM) was described as single event processing without knowing anything about CEP.

II. COMPLEX-EVENT PROCESSING

Information in this section is based on [2], [3] and [4]. An *event* is a component of data and represents that something happened in the real world. It may signify a problem, an opportunity, a threshold, or a deviation. In business terms an event is composed of two elements – an event header and event body. The event header contains elements describing the event occurrence, such as the event specification ID, event type, event name, event timestamp, event occurrence number and event creator. The event body must fully describe what happened, so any interested party (subscriber to the event) can process the information without having to go back to the source system. A complex event is a composite event that is an abstraction of two or more events.

This data flows in streams. An example of event can be e.g. financial market event – a completed stock purchase (an aggregation of the events in a transaction to purchase the stock). Complex Event Processing (CEP) is a set of techniques and tools used for setting systems that react to events in real time. We find this property very useful for market data processing. By preprocessing of data we can detect a specific pattern which repeats itself in source data. Patterns are used to express situations that have to be detected. In a pattern, events are correlated with each other by means of utilizing operators. The moment we recognize a pattern, we can determine appropriate next action at the right moment in real time.

Algorithmic trading applies CEP by calculating complex algorithms that indicate when to sell or buy based on real-time processing. Market data (including the rise and fall of stock prices during the day) can be viewed as events. This data needs to be analyzed in real time in order to identify the trends in data and to react to them automatically. Financial-trading institutions could monitor worldwide stock, commodity, and other markets to recognize threats related to current holdings or potential new opportunities. For example, if a system detects a rise or fall in a stock price, it should be able to identify whether the change is a regular, periodic event or represents a fleeting market opportunity or risk [6]. Today a lot of firms participating in market trading are using event processing as their technological framework for algorithmic trading. CEP is useful in applications which deal with streaming event data and need low-latency, adaptive decisions in response to changing conditions reflected in those events. By using event pattern matching rules, CEP is able to infer causal connections between seemingly disparate events.

CEP software technology enables the complex events detection in real time. This makes the CEP challenging, because general software tools for event-analysis don't work in real time. Real-time analysis is becoming nearly a fundamental requirement – the systems process real-time data to make immediate decisions in diverse matters such as stock trading, fraud detection etc. A CEP system is a software infrastructure that typically consists of a layer of adapters that connect directly to data sources and forward the information into the analysis engine. A CEP server evaluates the business logic, then runs event-stream-analysis algorithms and delivers the results continuously to users [6]. Essentially, there are two types of CEP toolsets - stand-alone software engines or embedded CEP services. This technology allows applications to identify complex sequences of events, like specifying the order of events. These complex patterns of events can have temporal constraints (within specified short time interval) or spatial constraints (within certain given distance) or some other causal relationship. These constraints can be expressed by using Complex Event Processing Language (EPL). The data can be evaluated by using *event queries* which are evaluated continuously while the events happen. Among the application areas belong, for instance: business activity monitoring, sensor networks, market data analysis.

Data Stream Management (DSM) is something like event database. This system allows events to be stored or replayed in real time. In DSM system, the derived data can be also stored, so it's possible to use the data to simulate the behavior of new event scenario on historical data. Historically recurring event patterns can be identified in data streams. Event stream processing (ESP) refers to database techniques of processing streams that assume that events arrive in a specific order to the stream processing computing engine. ESP is considered a subset of CEP, which does not assume events arrive in a specific order.

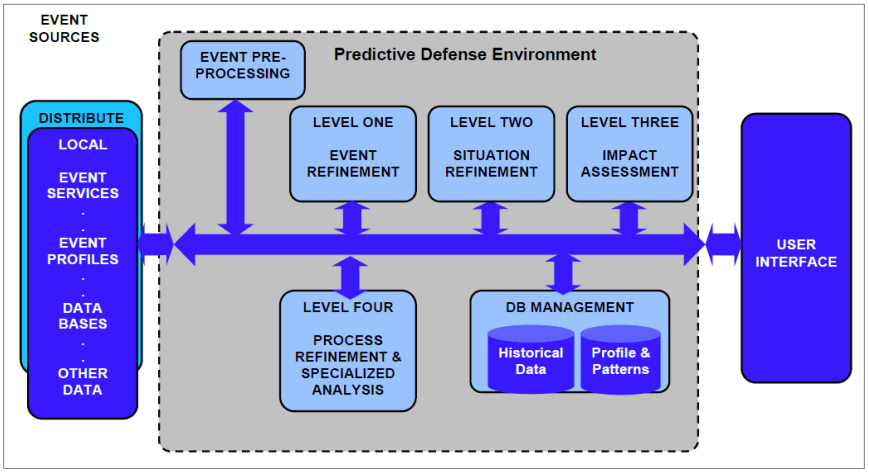

Figure 1 Complex Event Processing reference architecture - adapted from [5]

As Figure 1 shows, CEP is composed of several levels which conform to desired level of inference. At the lowest level, the event preprocessing runs – during this phase we clean the input data stream to produce some understandable data. On the next level, the events that were detected in input data are refined and subsequently initial decisions and correlations are done. The main challenge is to find relevant data. Then, situation refinement and impact assessment follows. At the level of impact assessment, we may predict the intentions of subject or to estimate potential losses or opportunities. At the end, the process refinement is done. All the results of event processing and operational visualization at all levels are summed up in a human readable format via user interface.

2.1. Differences between traditional computing and event processing

The main difference lies in the kind of data each of these two systems use. Traditional approach uses static data. Usually the data is stored in a database and a static data analysis is performed on it. So we use the data to query or to mine the information about the history.

On the other hand, event processing requires streaming data. With event processing, a business can identify patterns online and make decisions while the detected information is still relevant. The basic pattern-matching algorithm is implemented by way of looking for a potential sequence among the collected events. The algorithm then determines whether the pattern exists, what pattern it is and which events belong to it. An example might be an attempt to execute a credit card transaction from different places in a short time interval. Based on this data the decision to reject the next transaction might be made.

2.2. Event-Driven Architecture

Event-Driven Architecture (EDA) is an architecture devoted to designing and implementing systems that enable a business to respond to events in a real time. Because the events are complex, accordingly the systems have to be robust and scalable. This software infrastructure is very loosely coupled and highly distributed. The source of the event is only aware of the emergence of the event. The creator has no knowledge of the event's subsequent processing, or the interested parties (event subscribers). The traceability of an event through a dynamic multipath event network can be difficult. EDA is best used for asynchronous flows of work and information. The main idea behind EDA is that a large software system consists of many small components that all have their own function. The communication between the components is done by using events. An event can be a notification, which tells other components that a certain action is done. Because events are very important within an EDA, the handling and routing of events is very important, too. Figure 2 shows a model of EDA components.

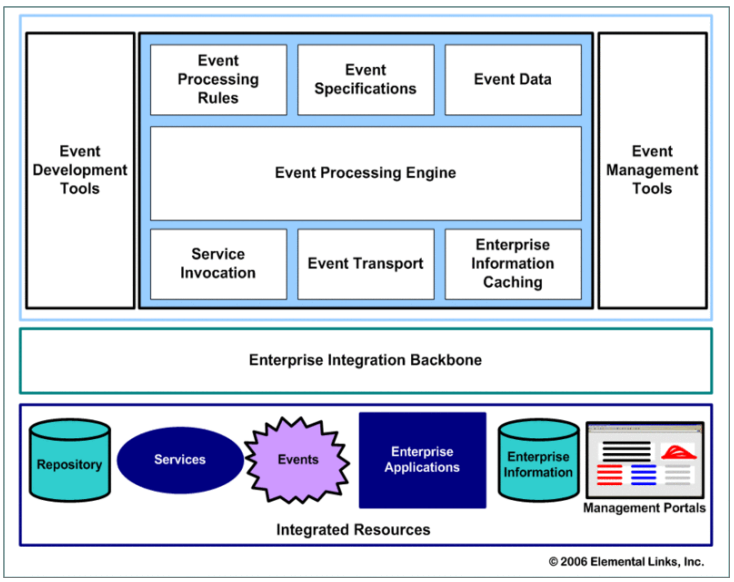

Figure 2: Event-Driven Architecture Components (taken from [4])

2.3 Business Activity Monitoring

One important aspect of CEP is business activity monitoring (BAM). What is BAM and how does it relate to event processing? BAM is defined as a process that provides a real-time access to key business performance indicators. It represents the last step in event processing as mentioned earlier in section 2. Examples of BAM applications also include algorithmic trading. End users perceive BAM by means of notifications and dashboards, but BAM systems can also trigger automated external processes. BAM applications monitor raw events as well as the real-time decisions made by event scenarios. BAM monitoring implementation is composed of three main steps:

1) gathering of data in sufficient quantity so that its processing can provide meaningful result,
2) processing of data considering relevant factor and based on this, categorizing and identifying the data,
3) clearly displaying the result of analysis in a user-friendly way.

2.4 Event scenario

An event scenario is a pattern of rules that can indicate a complex event is occurring. Event Scenario is not a standard formal notion. An example of an event scenario used in an algorithmic trading application is shown below on Figure 3. The scenario has a series of states. Each state can have one or more rules that control the flow. Let's analyze the example in Figure 3. In "start" state we begin to look for a pattern initially triggered by a rule that matches a set of filter criteria. In this case, it's looking for changes in stock prices on two ticker symbols. In the "Check Quantities" state we check for these price changes. After detecting a price change, the spread, or difference between the spreads, is calculated. If the spread does not reach a certain trading condition, the scenario returns to the "Wait for spread" state. If it does reach a buy or sell condition, the scenario transitions to the "Issue Orders" state, where it takes action — buying or selling — based on complex series of events.

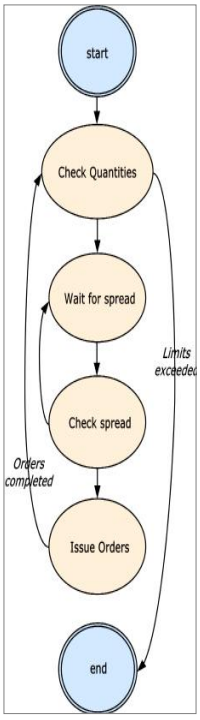

Figure 3 Example of event scenario [3]

III. BUSINESS PROCESS MANAGEMENT

Business Process Management (BPM) is a concept that intersects the fields of management and information technology. BPM covers the realm of business processes that, among other entities, consist of organizations, humans, and systems. This system is known and widely used since the early 1900's. BPM includes three activities: process design, execution, and monitoring. Business process instances are running concurrently and completely independent from each other. There are many definitions of the "business rule" term. According to [6], the business rule is a statement that defines or constrains some aspect of the business process which is intended to assert business structure, or to control or influence the behavior of the business.

A business rule cannot be decomposed further into more detailed business rules. The main characteristics of business rules include, among others, the following statements:

- Business rule classify, compute, compare and control data to direct the flow in a business process.
- Business rules can certify the data in the business forms.
- Business rules are not processes.
- Business rules provide criteria for making decisions.

A business rule may be described formally, e.g. by using the BPEL language (Business Process Execution Language) or decision trees. A business rule can also be described informally in plain language. Formalization of business rules lies in identifying the atomic statement as the definition of a term, fact, constraint, or derivation. Terms, facts, and some of the constraints can be represented as graphical models. Constraints and derivations must be translated into another formalism. One of the possible applications of business rules in CEP platforms is in event patterns description. By using the rules we can recognize certain patterns in the input events stream. Business rules might be very helpful during the decision making process. Business rules can be defined as restrictions, guidelines, computations, inferences, timings and triggers; the last two are especially fit for event processing frameworks. Business rules drive process definitions as well as the decisions made within business processes. The mapping between rules, processes and decisions is considerably easier if done from an event perspective, where the logic is defined in a precise rule set. BPM is appropriate for fairly predictable processes, while CEP is best suited for responding to events.

3.1 BPEL

BPEL (Business Process Execution Language) is an XML-based language that enables task-sharing and serves for processes automation. By using BPEL, a business process is formally described. Business processes can also be described by Business Process Modeling Notation (BPMN), but BPMN is based on graphical represenation, so for the high volume data processing, BPEL is more efficient. Smart methods exist which transform BPMN into BPEL and vice versa.

BPEL allows definition of business processes that call external services using Web Services. It provides functions for data manipulation and allows user to define process variables. Using this data, the course of the process can be influenced. This model supports business process lifecycle management. The process can be stopped, paused, resumed, etc. BPEL also supports long-running transaction model that facilitates the definition of transaction boundaries and compensatory actions in case of a failed transaction. Support for business process events (support for asynchronous call model) is also defined.

Example of a simple process in BPEL:

```
<process name="order"
  targetNamespace="http://jbpm.org/examples/hello"
  xmlns:tns="http://jbpm.org/examples/hello"
  xmlns:bpel="http://schemas.xmlsoap.org/ws/2003/03/business-process/"
  xmlns="http://schemas.xmlsoap.org/ws/2003/03/business-process/">
  <import ... > <!-- here is usually imported some external source - eg.wsdl -->
  <partnerLinks>
    <!-- establishes the relationship with the caller agent -->
    <partnerLink         name="caller"         partnerLinkType="tns:Greeter-Caller"
myRole="Greeter" />
  </partnerLinks>
  <variables>
    <variable name="request" messageType="tns:nameMessage" />
    <variable name="response" messageType="tns:greetingMessage" />
  </variables>
  <correlationSets>
    <correlationSet name="CorrelationSet1" properties="ns1:orderId">
  </correlationSets>
  <sequence name="MainSeq">
    <!-- contains the main body of the process -->
  </sequence>
</process>
```

3.2 XBRL

In relation to CEP, XBRL might be used for source events description. We might benefit from the fact that BPEL is also a XML-based language, thus we can analyze the input data in a more structured way.

Extensible Business Reporting Language (XBRL) is an XML-based markup language for electronic transmission of business and financial data. This language is an established standard for data exchange between different platforms. It provides major benefits in the preparation, analysis and communication of business information. It is an open standard and it is already utilized in a number of countries. The introduction of XBRL tags enables automated processing of business information by computer software, cutting out labour intensive

and costly processes of manual re-entry and comparison [7]. XBRL can handle data in different languages and accounting standards. It can be adapted to meet different requirements in a flexible way. Data can be transformed into XBRL by appropriate mapping tools. The benefits are clearly visible in automation, cost saving, faster, more reliable and accurate data handling, improved analysis and in better quality of information and decision-making. The last property might be very useful for financial markets' complex events processing. XBRL is a powerful and flexible version of XML which has been defined specifically to meet the requirements of business and financial information interchange.

The language dictionary is defined in XBRL Taxonomies. These are the categorization schemes which define the specific tags for individual items of data. By using XBRL, stock exchanges, investment analysts, advisers and other users can benefit from greater data transparency and robustness, clarity and consistency of company financial data and the possibility to utilize more powerful software tools for data analysis. Figure 4 shows an example of an asset, represented in XBRL (left) and in human readable form (right).

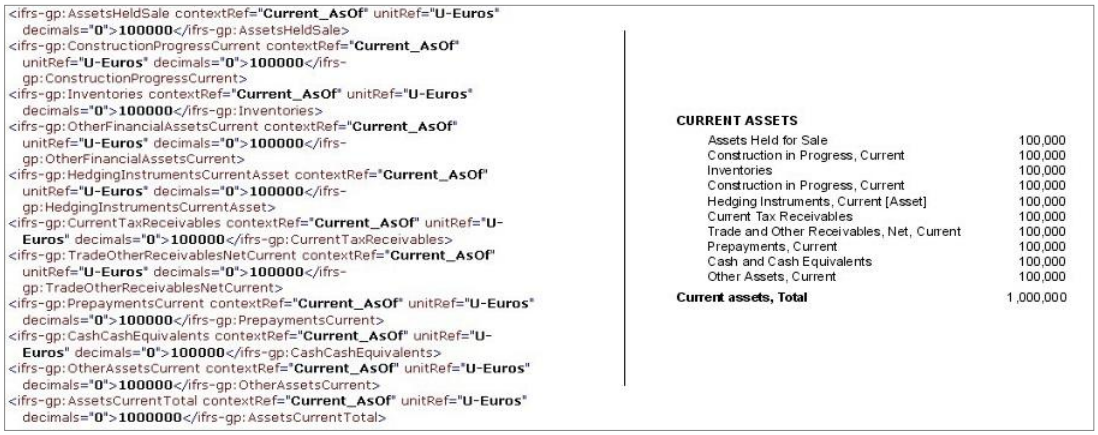

```
<ifrs-gp:AssetsHeldSale contextRef="Current_AsOf" unitRef="U-Euros"
  decimals="0">100000</ifrs-gp:AssetsHeldSale>
<ifrs-gp:ConstructionProgressCurrent contextRef="Current_AsOf"
  unitRef="U-Euros" decimals="0">100000</ifrs-
  gp:ConstructionProgressCurrent>
<ifrs-gp:Inventories contextRef="Current_AsOf" unitRef="U-Euros"
  decimals="0">100000</ifrs-gp:Inventories>
<ifrs-gp:OtherFinancialAssetsCurrent contextRef="Current_AsOf"
  unitRef="U-Euros" decimals="0">100000</ifrs-
  gp:OtherFinancialAssetsCurrent>
<ifrs-gp:HedgingInstrumentsCurrentAsset contextRef="Current_AsOf"
  unitRef="U-Euros" decimals="0">100000</ifrs-
  gp:HedgingInstrumentsCurrentAsset>
<ifrs-gp:CurrentTaxReceivables contextRef="Current_AsOf" unitRef="U-
  Euros" decimals="0">100000</ifrs-gp:CurrentTaxReceivables>
<ifrs-gp:TradeOtherReceivablesNetCurrent contextRef="Current_AsOf"
  unitRef="U-Euros" decimals="0">100000</ifrs-
  gp:TradeOtherReceivablesNetCurrent>
<ifrs-gp:PrepaymentsCurrent contextRef="Current_AsOf" unitRef="U-Euros"
  decimals="0">100000</ifrs-gp:PrepaymentsCurrent>
<ifrs-gp:CashCashEquivalents contextRef="Current_AsOf" unitRef="U-
  Euros" decimals="0">100000</ifrs-gp:CashCashEquivalents>
<ifrs-gp:OtherAssetsCurrent contextRef="Current_AsOf" unitRef="U-Euros"
  decimals="0">100000</ifrs-gp:OtherAssetsCurrent>
<ifrs-gp:AssetsCurrentTotal contextRef="Current_AsOf" unitRef="U-Euros"
  decimals="0">1000000</ifrs-gp:AssetsCurrentTotal>
```

CURRENT ASSETS

Assets Held for Sale	100,000
Construction in Progress, Current	100,000
Inventories	100,000
Construction in Progress, Current	100,000
Hedging Instruments, Current [Asset]	100,000
Current Tax Receivables	100,000
Trade and Other Receivables, Net, Current	100,000
Prepayments, Current	100,000
Cash and Cash Equivalents	100,000
Other Assets, Current	100,000
Current assets, Total	1,000,000

Figure 4 Example of asset described in XBRL and in human readable format [7]

IV. CONCLUSION

The decision making process is the key element of complex event processing. We would like to focus on this part of the process and use the rules specified by BPM for the decision making. In CEP, the decisions are made when the data stream reaches the system. If trading decisions should be made, the processing speed of the system is crucial. In this case we use data-driven decision making model which requires both historical and real time data. Using a stand–alone CEP solution is quite expensive, but if we contribute to processing with a BPM solution, we might speed up the whole process and take advantage of utilizing both the CEP and BPM domains at the same time.

The future research will be focused on design of alghoritmic models to effectively process high volume market data. We will use advantage of CEP plaform for its processing in real time and we will try to integrate business rules to control the flow of events prediction.

ACKNOWLEDGEMENT

This work was partially supported by the BUT FIT grant FIT-S-14-2299, "Research and application of advanced methods in ICT".

REFERENCES

[1] Rainer, A., Emmersberger, C., Springer, F., Wolff, C.: Event-Driven Business Process Management and its Practical Application Taking the Example of DHL. In: 1st International workshop on Complex Event Processing for the Future Internet, 28.09.-30.09.2008, Vienna, Austria.

[2] Luckham , D.: The Power of Events: An Introduction to Complex Event Processing in Distributed Enterprise Systems, Addison Wesley Professional, May 2002, ISBN: 0201727897.

[3] Palmer, M., Džmuráň, M.:An Introduction to Event Processing, Powering Real-Time, Intelligent Business Applications.

[4] Michelson, B.: Event-Driven Architecture Overview, 2006, [online, visited March 2014] <http://www.elementallinks.com/2006/02/06/event-driven-architecture-overview/#sthash.8OHnhIDm.dpbs>.

[5] Steinberg, A., & Bowman, C.: Handbook of Multisensor Data Fusion, JDL Laboratories, CRC Press, 2001.

[6] Leavitt, N.: Complex-Event processing poised for growth, Industry Trends, IEEE Computer Society, 2009.

[7] Financial Report Foundation, [online, visited March 2014] < http://www.ifrs.org/Pages/default.aspx>.